**Universidad de Valladolid**

**ESCUELA DE INGENIERÍA INDUSTRIALES**

**DEPARTAMENTO DE INGENIERÍA QUÍMICA Y TECNOLOGÍA DEL MEDIO AMBIENTE**

TESIS DOCTORAL:

# BIOPRODUCTS PROCESSING BY SFEE: APPLICATION FOR LIQUID AND SOLID QUERCETIN FORMULATIONS

Presentada por György Lévai
para optar al grado de
doctor con mención internacional por la
Universidad de Valladolid

Dirigida por:
Doctor Ángel Martín Martínez
Doctora Soraya Rodríguez Rojo

**UNIVERSIDAD DE VALLADOLID**

ESCUELA DE INGENIERÍAS INDUSTRIALES

**Secretaría**

La presente tesis doctoral queda registrada en el folio Nº_____

del correspondiente Libro de Registro con el Nº_____

Valladolid, a _____ de _____ de 2016

Fdo. El encargado del Registro

**Ángel Martín Martínez**

Profesor Contratado Doctor

Departamento de Ingeniería Química y Tecnología del Medio Ambiente

Universidad de Valladolid

y

**Soraya Rodríguez Rojo**

Investigadora Juan de la Cierva

Departamento de Ingeniería Química y Tecnología del Medio Ambiente

Universidad de Valladolid

CERTIFICAN QUE:

GYÖRGY LÉVAI ha realizado bajo su dirección el trabajo "BIOPRODUCTS PROCESSING BY SFEE: APPLICATION FOR LIQUID AND SOLID QUERCETIN FORMULATIONS", en el Departamento de Ingeniería Química y Tecnología del Medio Ambiente de la Escuela de Ingenierías Industriales de la Universidad de Valladolid. Considerando que dicho trabajo reúne los requisitos para ser presentado como Tesis Doctoral expresan su conformidad con dicha presentación.

Valladolid a _____ de_____ de 2016.

Fdo. Ángel Martín Martínez Fdo. Soraya Rodríguez Rojo

Reunido el tribunal que ha juzgado la tesis doctoral "***BIOPRODUCTS PROCESSING BY SFEE: APPLICATION FOR LIQUID AND SOLID QUERCETIN FORMULATIONS***" presentada por György Lévai y en cumplimiento con lo establecido por el Real Decreto 861/2010 (BOE 28.01.2011) ha acordado conceder por _____la calificación de___ _____.

Valladolid, a de de 2016

PRESIDENTE SECRETARIO

1er Vocal 2do Vocal 3er Vocal

# TABLE OF CONTENT

# ABSTRACT

## BIOPRODUCTS PROCESSING BY SFEE:

## APPLICATION FOR LIQUID AND SOLID

## QUERCETIN FORMULATIONS

Polyphenols are widely applied in pharmaceutic and cosmetic areas due to their beneficial effects on health, such as strong antioxidant-, antiviral- and antihistaminic capability. Quercetin is a member of flavonoids, which is the major group of the polyphenols, and is highly available in various fruits, vegetables and oils. Owing to its O-diphenol B-ring structure, it is able to donate π electrons from its benzene ring without significant stability decrease, and to scavenge reactive oxygen species and down-regulate lipid peroxidation. Moreover, it also has an anti-proliferative effect in a wide range of human cancer cell lines, and it is a highly promising active compound against a wide variety of diseases. A major limitation for the clinical application of quercetin is its low bioavailability (lower than 1% in humans), due to its low water solubility, which makes necessary to administrate it in doses, as high as 50 mg/kg.

Different approaches have been proposed in literature to increase the bioavailability of quercetin. By using chemical modification- and the synthesis of a water-soluble derivative of quercetin only 20% of bioavailability increase was reached. Production of drug loaded solid lipid nanoparticles could be also a promising alternative, and the complexation of quercetin with lecithin and cyclodextrin in aqueous solution has been tested by applying an emulsification and a low-temperature solidification method, with drug entrapment efficiency over 90% in spherical particles, with an average diameter of 155 nm.

Supercritical fluid technologies are another promising alternative in the processing of natural bioactive compounds like quercetin, because upon applying an adequate supercritical medium such as supercritical carbon-dioxide ($scCO_2$), they allow carrying out the encapsulation process at near ambient temperatures and in an inert atmosphere, thus avoiding the thermal degradation or oxidation of the product, and reducing its contamination with organic solvents. Several authors have studied the processing of quercetin by supercritical fluid technologies. Due to the low solubility of quercetin in supercritical carbon dioxide, Supercritical Antisolvent (SAS) experiments have been particularly successful. By SAS processing of pure quercetin,

crystalline particles with particle sizes in the micrometric range (1 – 6 μm) were obtained, and by a co-precipitating with an encapsulation material, such as Pluronic F127, spherical morphology of micronized particles were obtained, and the solubility of quercetin in intestinal fluid was significantly increased.

The aim of this work is to increase water solubility and hence bioavailability of quercetin, by increasing its specific surface area, precipitating it in sub-micrometric scale, and encapsulating it in biocompatible polymers, such as soy-bean lecithin and a poloxamer (Pluronic L64®). For this, Supercritical Fluid Extraction of Emulsions (SFEE) technology was used to obtain aqueous suspension product, and Particles from Gas Saturated Solutions (PGSS)-drying technology was used,to obtain dry quercetin loaded particles in controlled micrometric range.

SFEE technology presented in **Chapter I**, can be considered as an evolution of SAS technology, which is especially suitable to encapsulate poorly water soluble drugs in an aqueous suspension. The process consists of forming an oil in water (o/w) emulsion, containing the quercetin in the dispersed organic phase. The organic solvent is extracted from this emulsion using $scCO_2$, which has high affinity to the organic solvent, meanwhile low affinity to the active compound of interest. Due to the solubility differences, the supercritical solvent extracts quickly the organic solvent from the emulsion, leading to the rapid super-saturation of the active compound in the aqueous phase, and promoting its fast precipitation in nanometric scale. Quercetin is encapsulated in the aqueous suspension product by a surfactant material, which was originally added to the o/w emulsion in order to increase its stability, which is a crucial issue in SFEE process. In **Chapter I** two different biopolymers (Pluronic L64® poloxamer and soy-bean lecithin) were used as carriers and surfactant materials in the formation of o/w emulsions. Emulsions were treated by a batch SFEE equipment, at operating conditions around 100 bar and 40°C, and a part of $scCO_2$, contained by the system was renewed several times during the process, without any kind of pressure and temperature change. Optimal

number of extraction cycles and duration of each cycle was determined in these experiments, to decrease residual organic content of aqueous suspensions under the restrictions of FDA, without degradation nor agglomeration of encapsulated quercetin particles. Applying Pluronic L64® as surfactant, needle quercetin particles were obtained, with an average particle sizes around 1 μm and poor encapsulation efficiency. In case of soy-bean lecithin, quercetin loaded multivesicular liposomes were obtained, with a mean particle size around 100 nm and around 70% of encapsulation efficiency, without the presence of segregated quercetin crystals. Moreover, antioxidant activity of quercetin was enhanced by encapsulation in lecithin, in agreement with previous reports, that describe a synergistic effect of these two compounds.

The effect of the main SFEE parameters, such as pressure and temperature, initial concentration of surfactants and quercetin, organic to water ratio, and kinetics of the elimination of the organic solvent from the emulsion, is of chief importance for the optimization of the SFEE process. For that purpose, in **Chapter II** ethyl acetate and dichloromethane based o/w emulsions were prepared, using soy-bean lecithin and/or Pluronic L64® as surfactants, and they were contacted with supercritical carbon-dioxide ($scCO_2$), and mass transport properties of these systems were measured by Magnetic Suspension Balances (MSB), which provide an on-line, contactless sample weight monitoring method in a closed system. Static and dynamic measurements (applying a continuous flow of $scCO_2$ through the emulsion) were performed, and the effect on mass transport properties of the initial organic/water proportion, the concentration of surfactant materials (soy-bean lecithin and additional Pluronic L64®), and the density of $scCO_2$ atmosphere were studied. In the static system the dissolution of $scCO_2$ by the sample, and the extraction of organic phase was observed simultaneously, dominating the process in different moments. A five-parameter mass transfer model was developed for the measured results, and two parameters of them were fixed, indicating that three process steps are influencing significantly the whole behaviour of o/w emulsion – $scCO_2$ system: Dissolution

of the $scCO_2$ and the organic solvent in the water phase, and the extraction of the organic phase by the $scCO_2$ through the water phase boundary. Experimental and modelling results proved that DCM/w emulsions prepared with lecithin or with poloxamer surfactants are not adequate for SFEE processing, as phase separation occurs immediately upon pressurization, due to the high interfacial tension between the aqueous and organic phase. In the case of EtAc/w emulsion - $scCO_2$ system, only the density of $scCO_2$ was significantly influencing the speed of the mass transfer of compounds. According to dynamic measurements, the higher proportion of the organic phase is extracted with the pressurization of the system by $scCO_2$, due to the Marangoni effect, which occurs typically in $CO_2$ - $H_2O$ systems due to high density differences, or due to an intense mixing effect between o/w emulsion - $scCO_2$ during the pressurization process and phase change of $CO_2$.

As quercetin was precipitated in nanometric scale and encapsulated successfully in soy-bean lecithin (Chapter I), in **Chapter III** the combination of surfactant materials (soy-bean lecithin and Pluronic L64®) was used, in order to increase the encapsulation efficiency of quercetin, without significant morphological change of the obtained aqueous suspension product. An experimental plan using batch SFEE equipment is done in order to study the significant factors, such as the concentration of quercetin and surfactants, or the Pluronic L64® to soy-bean lecithin ratio, on the encapsulation efficiency of quercetin, and the particle size distribution of obtained aqueous suspensions. Comparing the results obtained in Chapter I in where only lecithin was used as surfactant, average encapsulation efficiency of quercetin was significantly increased. Moreover, a successful scale-up of SFEE process is done, and a semi-continuous SFEE device is designed and presented in **Chapter III**, and with a significantly shorter processing time a significantly higher amount of o/w emulsion is treated. By comparing the results of batch and scaled-up systems, robustness of scaled-up, semi-continuous SFEE process is proved.

Aqueous suspensions produced by SFEE were further treated by Particles from Gas Saturated Solutions (PGSS)-drying technology, to produce micronized, quercetin loaded dry particles, and to increase long-term stability of product. An experimental plan with PGSS-drying is done, in order to choose the applicable settings of significantly influencing process parameters, such as Gas to Liquid ratio (GLR), pre-expansion pressure and temperature, and to obtain less possible quercetin degradation and residual water content of product. A free flowing powder in micrometric scale with a residual moisture content of less than 10 w/w%, and is produced, with a maximum quercetin encapsulation efficiency of 86.4%, which is corresponding only 0.6% of quercetin loss, comparing to the aqueous suspension from which PGSS-drying experiment was performed. Lyophilization (assumed as a quercetin-degradation-free process) of two SFEE produced aqueous suspension mixtures is parallelly done with PGSS-drying, and encapsulation efficiency, and antioxidant activity of with PGSS drying and with lyophilization prepared dried products are measured and compared with each other. According to transdermal diffusion measurement, quercetin permeability of SFEE and PGSS-drying micronized dry-product through transdermal membrane into simulated intestinal fluid is increased significantly, comparing to lyophilized dry-product, which did not proved an adequate methodology, as no quercetin permeability increase was obtained, comparing to physical mixture, as micronization and encapsulation of quercetin did not take place.

Having proved the robustness of batch SFEE process in Chapter III, and as PGSS-drying obtained product characteristics are directly related to the properties of SFEE produced aqueous suspensions, a study of significant SFEE process parameters is essential, moreover assess the economic viability of the SFEE process is crucial, as the economic viability of the whole process structure relies on the SFEE process. Therefore, in **Chapter IV** an experimental plan with scaled-up, semi-continuous SFEE device is performed, in order to obtain significant process parameters, such as the concentration of quercetin in o/w emulsion, the applied $CO_2$ / emulsion ratio, the flowrate of $scCO_2$, the average density of on the emulsion bubbled thorough $scCO_2$ (influenced by the process pressure and temperature), and the duration of treatment of SFEE process. According to aqueous suspension product characteristics, pressure and temperature conditions of $CO_2$ contacted with o/w emulsion should be slightly above it's critical point, and no more than 5.5 kg $CO_2$ should be used for the treatment of 1 L emulsion, by applying an around 80-90 min of SFEE treatment time, in order to decrease the possible antioxidant activity loss of quercetin, and agglomeration effect of precipitated quercetin-loaded nanoparticles.

Based on these results, in this chapter cost evaluation of SFEE process is also done, and economically optimal process conditions are determined, considering to obtain best available process characteristics. In economic evaluation a flowsheet model of SFEE process was developed in Aspen Plus®, moreover process integration and thermo-economic evaluation was carried out using Matlab. In cost evaluation the following costs were taken into account: fixed capital investment cost, cost of utility, cost of operation labour, cost of waste treatment, cost of raw materials. According to investment cost and thermo-economic evaluation, process energy demand and cost manufacturing mainly depends on the used amount of $CO_2$, due to electricity-cooling and increased investment cost, therefore – in agreement with experimental plan results –, lowest possible $CO_2$ flow and pressure is required for optimal process operation.

# INTRODUCTION

## BIOPRODUCTS PROCESSING BY SFEE:

## APPLICATION FOR LIQUID AND SOLID

## QUERCETIN FORMULATIONS

# 1. INTRODUCTION

This PhD thesis is established in the frame of the "Training Program for the Design of Resource and Energy Efficient Products by High Pressure Processes" (DoHip) project, funded by the People Programme (Marie Curie Actions) of the European Union's Seventh Framework Programme FP7/2007-2013/ under the REA grant agreement number of 316959. The project involved universities around the European Union with proven records in high pressure technology, located in Bochum (Germany), Budapest (Hungary), Graz (Austria), Maribor (Slovenia) and Valladolid (Spain), together with one Fraunhofer institute (Essen, Germany), and supported by eight companies from seven European countries. Totally 11 master students were hired, each with an individual research project on the topic of using high pressure process technology in the design and operation of new sustainable processes and products. Each researcher had the opportunity to cooperate with each participating organisation of the DoHip project, and to do varied duration secondment and internship periods in each university, research institute and/or industrial partner involved in the project. The research topic of this PhD thesis is the Development of novel nanocarriers for drug delivery.

Production and concentration of high added value active compounds from non-usable agro-industrial residues are becoming a hot topic. Owing to huge versatility, agro-industrial waste is containing a large amount of dietary ascorbates, tocopherols and carotenoids, which are well known for their antioxidant potential [1]. Polyphenols are one of the most important bioactive compounds presents in agricultural residues, due to their strong antioxidant properties. Various epidemiological studies have shown an inverse association between the consumption of polyphenols or polyphenol-rich nutrients, and the risk of cardiovascular diseases. The so-called" French paradox" [2] also describe a relatively low incidence of cardiovascular diseases, in spite of having a high fat content diet and heavy smoker attitude, due the increased consumption of polyphenolic content alcoholic beverages, such as red wine.

## 2. POLYPHENOLIC COMPOUNDS

Polyphenols are the secondary metabolites of plants, produced as a response for stress conditions [3], such as infections, large amounts of UV rays or other factors. Polyphenols are the most versatile plant secondary metabolites, ranging from simple molecules such as phenolic acids to highly polymerized substances, such as tannins [4]. Classification of them according to the number of phenol rings contained, and the structural elements, which bind these rings are shown on **Fig 1**. Although almost all of them can be found in every kind of plants, their distribution in plant tissue, cellular and subcellular levels is not uniform. Water solubility of them is a critical distributing factor [4]. Although the results of human studies obtained for polyphenols can not be generalized due to their huge versatility and highly different bioavailability [5], clinical and epidemiological studies confirmed negative correlation between intake of polyphenols and incidence of cancer [6], [7], [8]. Moreover, polyphenols may alter lipid metabolism, inhibit low-density lipoprotein (LDL) oxidation, reduce atherosclerotic lesion formation, inhibit platelet aggregation, decrease vascular cell adhesion molecule expression, improve endothelial function and reduce blood pressure [4].

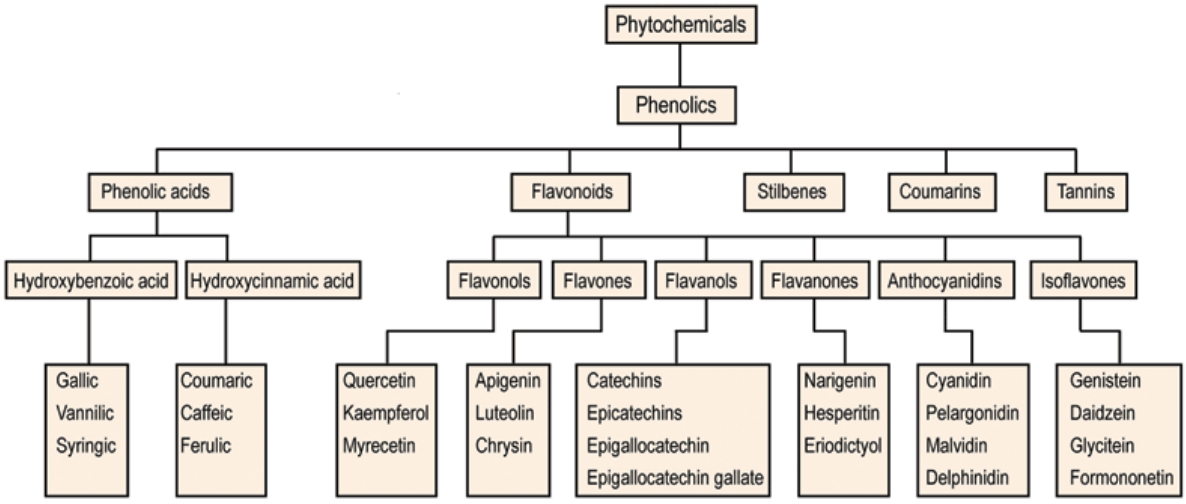


**Fig 1:** Distribution of phytochemicals [9]

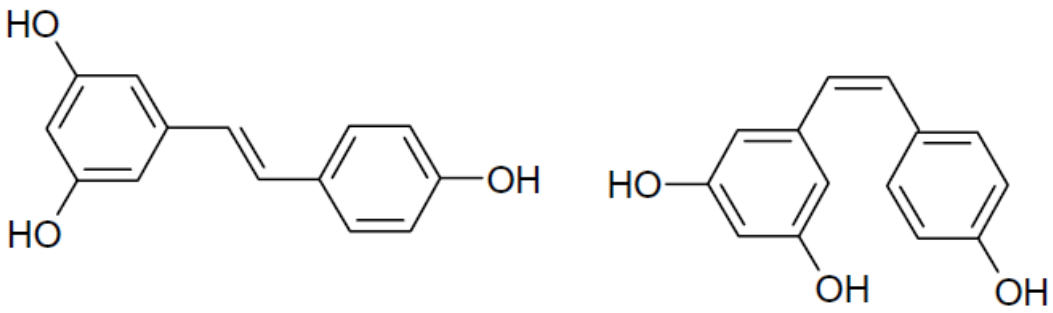


**Fig 2:** Trans - and cis- isomers of resveratrol

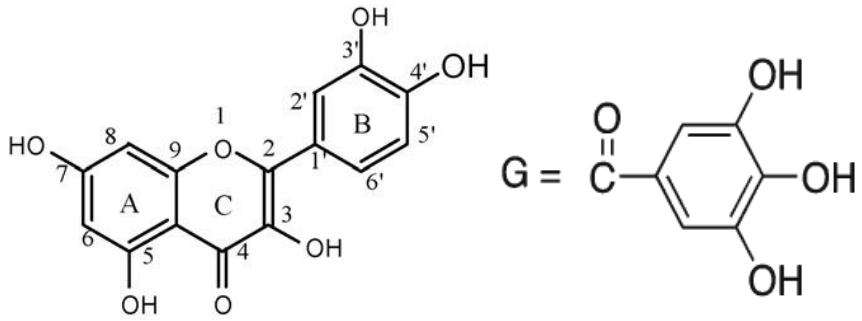


**Fig 3:** Chemical structure of quercetin [10], gallic acid (G =–OH) and gallic esters (G =–R)

[11]

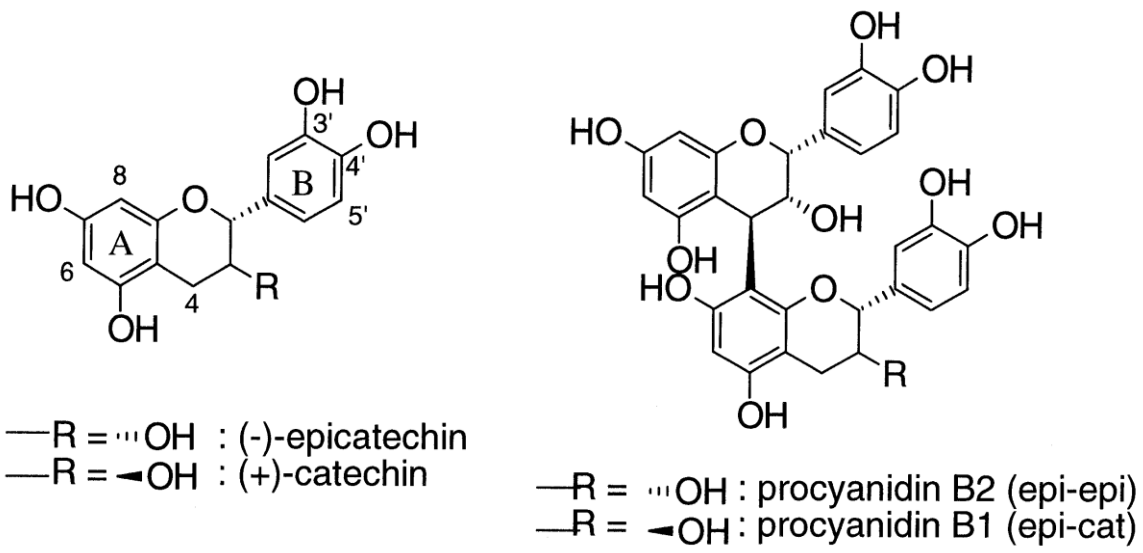


**Fig 4:** General chemical structure of catechins, epicatechins and procyanidins

Imbalance between the production of free radicals and reactive metabolites (ROS) and their elimination by protective mechanisms, defined as oxidative stress. This imbalance leads to the damage of important biomolecules and cells, lipids, proteins, carbohydrates and DNA, resulting membrane damage, fragmentation or random cross linking of molecules like DNA, enzymes and structural proteins and even lead to cell death induced by DNA fragmentation and lipid peroxidation. Consequences of oxidative stress could lead of cardiovascular diseases, cancer, neurodegenerative disorders, diabetes and autoimmune disorders. Antioxidants can delay, inhibit or prevent the oxidation of sensitive compounds detailed above, by scavenging free radicals and diminishing oxidative stress. Phytochemicals belong polyphenols can act as antioxidants by a number of potential mechanisms. The free radical scavenging, in which the polyphenols can break the free radical chain reaction, as well as suppression of the free radical formation by regulation of enzyme activity or chelating metal ions involved in free radical production, are reported to be the most important mechanisms of their antioxidant activity [12], [13]. Yilmaz Y et al. determined the peroxyl radical scavenging activities of phenolic compounds by antioxidant activity (ORAC) measurement and found the following order: resveratrol > catechin > epicatechin = gallocatechin > gallic acid = ellagic acid [14]. Moreover, resveratrol (**Fig 2**) has strong antibacterial and antifungal properties, and ability to inhibition the oxidation of low-density LDL [15].

Grape-seeds and skins contain several types and flavonoid components, occurring both in free form and as glycosides, such as quercetin (3,3’,4,4’,5,7-pentahydroxyflavone), gallic acids and esters **Fig 3**, and different isomers of catechins and epicatechins (**Fig 4**). Gallic acid is a natural agent, presents in a wide-range of fruits and vegetables, and there is a potential interest of it as an anti-cancer agent. Different type of gallate esters (B2-G2, B2-3G and B2-3′G) are significantly decreased the LNCaP cell viability, meanwhile their acid forms were ineffective in decreasing cell viability [11]. Dimeric, trimeric, oligomeric or polymeric procyanidins

(**Fig 4**) count for most of the antioxidant capacity of grape seeds [14]. Number of hydroxyl substituents is an important structural feature of flavonoids, in respect to their scavenging activity against ROS and nitric oxide, while C-2,3 double bond (presents in quercetin) might be important for the inhibition of ROS and nitric oxide production [16].

Quercetin itself proved to be a highly promising antioxidative flavonoid component owing to its o-diphenol B-ring structure [17], which has the ability of donating π electrons without significant stability loss [18], and it presents anti-proliferative effects in a wide range of human cancer cell lines [19], moreover it is widely available in various fruits, vegetable oils and many other food components. Moreover, polyphenols from apple and citrus juices, mainly quercetin are able to cross the blood-brain barrier, and present neuroprotection against hydrogen peroxide, which could indicate the oxidative damage caused by β-amyloid peptide in the pathogenesis of Arzheimer's disease [20]. Due to previously detailed health benefits of quercetin, this thesis was focusing the bioavailability- and oxidative stability increase of pure quercetin, using supercritical fluid technologies.

## 3. BIOAVAILABILITY AND FORMULATION OF POLYPHENOLIC COMPOUNDS

Bioavailabilty according to Porrini and Riso et al., is the fraction of ingested compound, that reaches the systemic circulation and the specific sites where it can exert its biological activity [21]. Health effects of polyphenols in human and in animal models depend on their absorption, distribution, metabolism and elimination. The chemical structure of polyphenols determines their rate and extent of absorption, as well as the nature of the metabolites present in the plasma and tissues. The most common polyphenols in human diet are not necessarily the most active within the body, either because they have a lower intrinsic activity or because they are poorly absorbed from the intestine, highly metabolized, or rapidly eliminated [22]. For example, different acids, like hydroxicinnamic acids are rapidly absorbed from the stomach or the small intestine, meanwhile proanthocyanidins are poorly absorbed, due to their polymeric nature and high molecular weight [23].

Polyphenols are differed in site of their absorption: quercetin-4'-glycoside is absorbed in the small intestine after hydrolysis, meanwhile quercetin-3-rutinoside is absorbed in the colon as free and metabolized forms, produced by the microflora [24]. A major limitation for the clinical application of quercetin is its low bioavailability (17% in rats [25] and lower than 1% in humans [26]), which makes it necessary to administrate in high doses (50 mg/kg) [27]. Aqueous solubility of quercetin is extremely low, 7.7 mg/L at room temperature [28] conditions, moreover it's water solubilized form in higher temperature is unstable [29], moreover antioxidant activity loss of quercetin, due to thermal degradation is also taking place [30]. Not only thermal-, but light stability of polyphenolic compounds, such as resveratrol and quercetin are also very low [31]. Light exposition could cause degradation or isomerisation of polyphenolic compound, as presented in the work of Kolouchová-Hanzlíková et al. in case of resveratrol (**Fig 5**) [15].

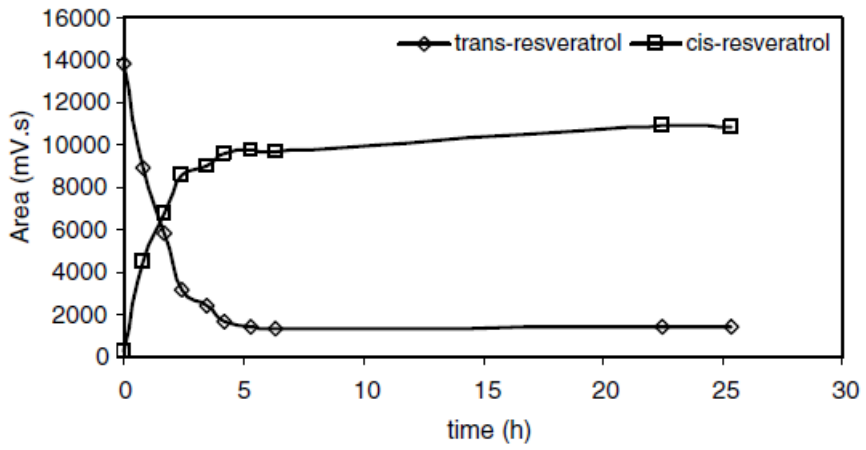


**Fig 5:** Trans-cis isomerisation of resveratrol during exposition of diffuse day light [15]

To improve the bioavailability, and long-term thermal-, heat- and chemical stability of quercetin, numerous approaches have been undertaken, involving the use of promising drug delivery systems, such as encapsulation of different types of β-cyclodextrin (including complexes as well). Other possible methods are the chemical and morphological modification of quercetin (synthetisation of a water-soluble derivative of quercetin, with 20% of bioavailability, Mulholland et al. [32]), or the formation of liposomes, solid dispersions, microparticles, nanoparticles or micelles, which appear to provide higher solubility and bioavailability [33].

Formation of drug loaded solid lipid nanoparticles is also a promising alternative to increase the bioavailability of poorly water soluble compounds, and the complexation of quercetin with lecithin and cyclodextrin in aqueous solution has been tested [34] [35]. Over 90% of drug entrapment efficiency achieved by Li et al. [36], with the production of lecithin encapsulated quercetin by emulsification and low-temperature solidification method. Spherical particles with 155 nm as average diameter was observed in heterogeneous morphologies, the with a co-existence of additional colloidal structures, like micelles, liposomes, supercooled melts, drug nanoparticles, which caused a deviation (20-500 nm) in the particle size distribution. The absorption rate in this work was studied by in-situ perfusion method in rats, obtaining a 6-fold relative increase in bioavailability, compared to unprocessed quercetin.

## 4. PROPERTIES AND APPLICATION AREAS OF SUPERCRITICAL CARBON-DIOXIDE

Thermodynamic relationship of a single-component composed closed system can be described through a p-T phase diagram (**Fig 6**), which is the graphic representation of all equilibrium phases of the currently examined component, along the whole T and p range. All single components have two characteristic points, which are the triple point, defined by the material dependent $T_t$ and $p_t$ (subscript t refers to triple), in where all the threes physical states (solid, liquid and gas phase) coexist, and the critical point, defined by the material dependent $T_c$ and $p_c$ (subscript c refers to critical). Between these characteristic p and T coordinates, the vapour-liquid equilibrium is characterized by the transition phase curve. Above the critical point ($p > p_c$, $T > T_c$) no more difference is existing between vapour and liquid state, the system becomes into the supercritical state. The supercritical fluid is not delimited from any transition phase curve, therefore the passage through the critical point occurs without the exchange of latent heat. Therefore, for a gas at $T > T_c$ but $p < pc$, every compression will produce an increase of density without formation of liquid, and without exchange of latent heat. Over the critical pressure $p > p_c$, the system passes into the supercritical state. Supercritical fluids appear as a compressed gas, therefore, supercritical fluids are similar to a liquid, with elevated density and low compressibility, and at the same time they are similar to a gas, with elevated diffusivity and low viscosity. Owing to their high penetration power inside to plant materials and their solvent power, supercritical fluids became a good solvent for solutes with chemical compatibility [37]. Critical point of $CO_2$ is: $T_c = 31.2°C$; $p_c = 73$ bar [38].

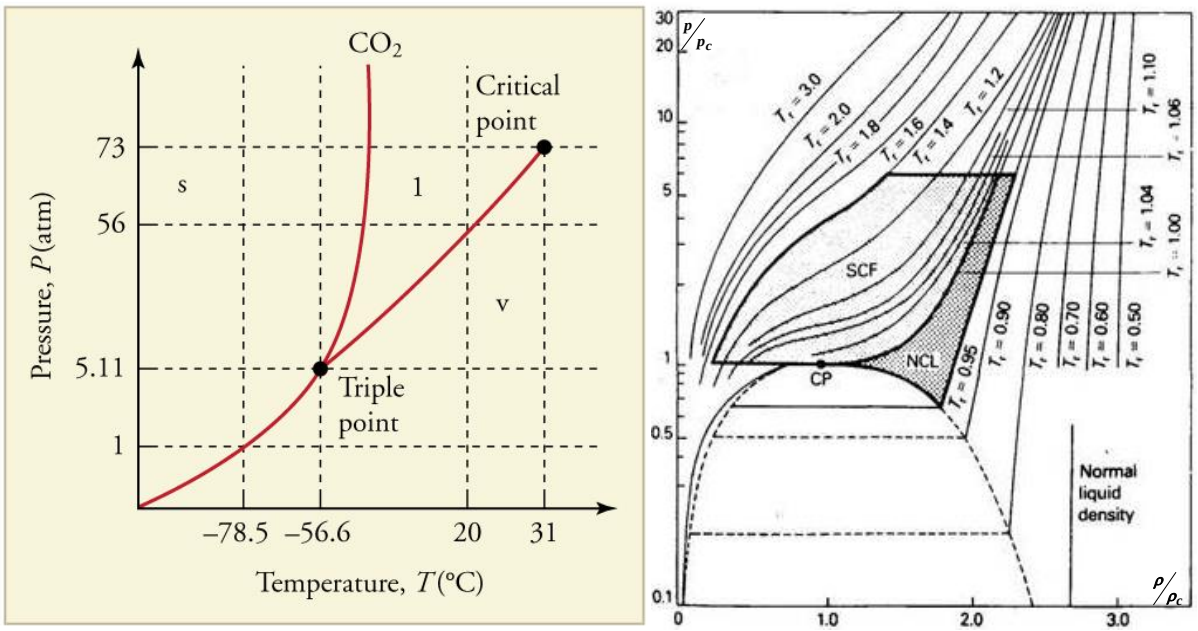


**Fig 6:** Phase diagram and reduced pressure, reduced temperature diagram of $CO_2$

$SCCO_2$ is one of the most useful supercritical fluid in the food industry, as it is non-toxic, non-explosive, available in high (food grade) purity, and can be removed from the extracted products without leaving any residue [39]. Using $scCO_2$, mainly non-polar compounds are extractable, thus the extraction of unwanted polar compounds can be avoided [40]. One of the earliest industrial application of $scCO_2$ is the decaffeination process of green coffee beans and black tea, as product quality is significantly increased upon using $scCO_2$ instead of water [41]. Supercritical fluid technologies, such as Supercritical Antisolvent- (SAS) [42], Gas Antisolvent- (GAS) [43] or Supercritical Fluid Extraction of Emulsion (SFEE) [44] methods are promising alternatives in the processing of natural bioactive compounds, such as quercetin, and to precipitate them in sub-micrometric scale, and hence increase their specific surface area and their bioavailability. Moreover, by applying an adequate supercritical medium, such as supercritical carbon-dioxide ($scCO_2$), processes can be carried out at near ambient temperatures, and in an inert atmosphere, thus avoiding the thermal degradation or oxidation of heat-sensitive bioactive compound [45], and reducing its contamination with organic solvent.

## 5. INTRODUCTION AND MODELLING REVIEW OF SFEE TECHNOLOGY

SFEE technology can be considered, as an evolution of Supercritical Anti Solvent (SAS) technology. It is especially suitable to precipitate and encapsulate poorly water soluble materials (drug, bioactive compound etc.) in sub-micrometric scale, resulting in an aqueous suspension. The process consists of forming an oil-in-water emulsion, containing the water-insoluble drug in the dispersed organic phase. In SFEE process the organic solvent is extracted from this emulsion by the supercritical solvent, which should have a high affinity to the organic solvent, and a small affinity to the active compound of interest. Due to this solubility differences, supercritical solvent quickly extracts the organic part from the emulsion, leading to the rapid super-saturation of the active compound, and hence its fast precipitation and encapsulation by surfactant materials, which originally added to the emulsion, in order to increase their long term stability, which is a crucial issue during SFEE process [46]. While in the SAS precipitation method particle nucleation and growth occur across the whole solution volume, in the case of SFEE process, the formation of particles is confined within the emulsion droplets. This restrains the size of particles obtained by SFEE, that can be one order of magnitude smaller, than particles produced by SAS solution precipitation [47]. Principles of SFEE technology is shown on **Fig 7**.

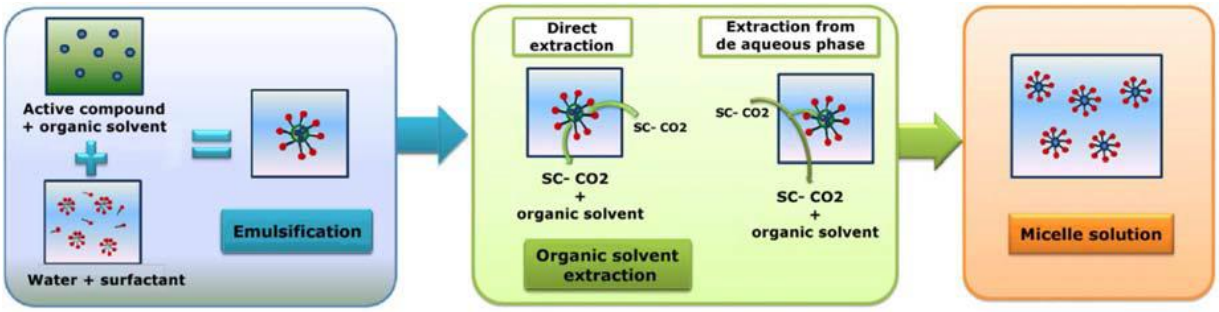


Fig 7: Principles of SFEE technology

Several experimental results are available in the literature, showing that the size and the morphology of the produced particles, as a key objective of micronization technology is influenced by several process steps, such as atomization, diffusion, precipitation, particle agglomeration etc. [48]. Therefore, modelling of supercritical processes, such as SAS, SFEE is necessary, in order to be able to optimize process conditions, and hence product specifications. Hence in SFEE process every single emulsion droplet is considered as a small Gas Antisolvent (GAS) precipitator, and precipitation occurs within the emulsion droplets [46], models for SAS process could be valid for SFEE process, too. Werling and Debenedetti et al. studied the mass transfer between a droplet of toluene and supercritical carbon-dioxide ($scCO_2$), both in subcritical- [49] and supercritical conditions [50] in SAS process. The main difference between these two conditions was, that at subcritical conditions (with a solvent-antisolvent mixture in the two-phase region), an interface always exists between the droplet and the antisolvent phases, while in supercritical conditions (where solvent and the antisolvent form a single phase), there is no well-defined interface between the droplet and its environment. These authors also found, that at subcritical conditions the droplet diameter is initially increasing, due to the condensation of $CO_2$ until the complete saturation is reached, and then the evaporation of the droplet takes place. Elvassore et al. [51] extended the model of Werling and Debenedetti, by including the solute in the calculations. They used this model to study the evolution of the precipitation front for different organic solvent-$CO_2$-solute systems. Lora et al. improved a mass transfer model based on Fick´s laws, focusing on toluene - $CO_2$ system. Their simulation showed, that initially there is always an interfacial flux into the droplet, due to the high solubility of $CO_2$ in the organic solvent [52]. Y. P. de Diego et al. also found, that initially the absorption of $CO_2$ by the liquid phase is always faster, than the evaporation of solvent phase. Dissolution of $CO_2$ in the organic phase is an exothermic process, meanwhile organic phase evaporation is an endothermic process. Initially, the temperature of the bulk of the droplet may increase, as heat of dissolution

of $CO_2$ initially is higher, than the heat of evaporation of the solvent [53]. However, the temperature of the $scCO_2$- and the continuous water phase will not change significantly, as they act as an infinite medium, comparing to the organic phase. Therefore, initially the heat transfer should take place from the bulk of the droplet to the interphase, and this heat transfer causes later on the evaporation of the organic phase.

In the work of Matte F. et al. [46], mass transfer of β-carotene contained DCM/w emulsions (using OSA-modified starch as surfactant material) - $scCO_2$ system was measured in a high pressure view cell on sub- and supercritical conditions, at 308 K, and 5 and 10 MPa, respectively. Sessile drop method was used in that work, for observing the change of the volume of an initially, – into the aqueous phase placed DCM droplet –, with different initial volumes, using a CCD camera. CCD camera was measuring the refractive index change of the droplet, which is initially higher than the surrounding $scCO_2$ medium, then becomes equal, then even lower, due to mass transport processes occurs simultaneously between the droplet and the gas phase. From refractive index change profile, the volume change, and hence the mass change of the droplet was obtained. Moreover, shape change of the drop was also observed, which is related with the change of the interfacial tension between phases, according to the fundamental pendant drop equations, presented by in the work of Bashforth and Adams [54].

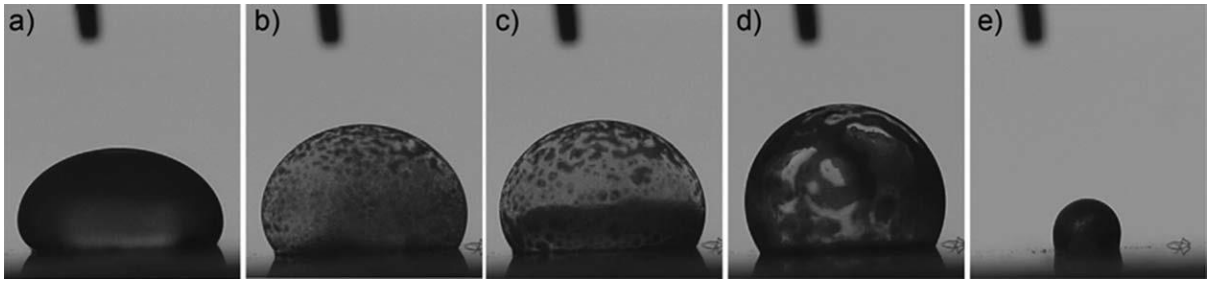


**Fig 8:** Evaluation of the observed droplet, and precipitation of β-carotene particles p = 5 MPa, T = 308 K: a) initial condition, b) beginning of particle formation, c) and d) particle agglomeration, e) final condition after the drop detachment from the cell surface [46].

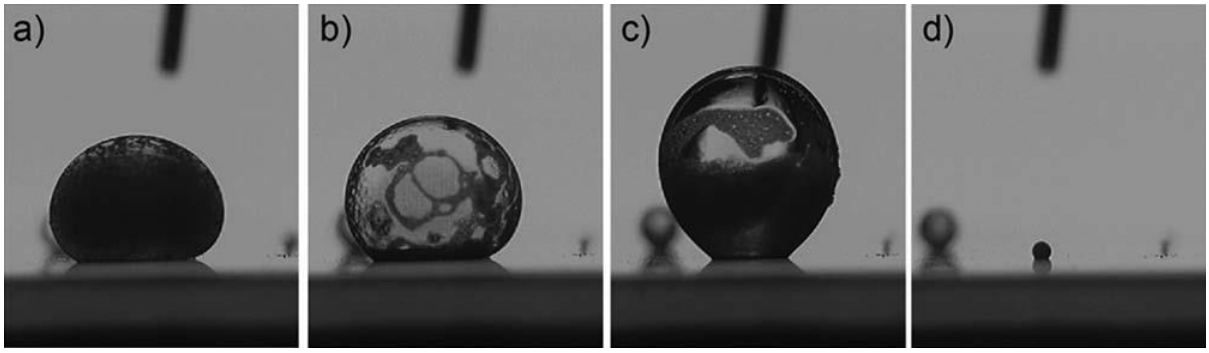


**Fig 9:** Evaluation of the observed droplet, and precipitation of β-carotene particles p = 10 MPa, T = 308 K :a) beginning of particle formation, b) and c) particle agglomeration, d) final condition after the drop detachment from the cell's surface [46].

Different behaviour of observed droplet was obtained at 5 and 10 MPa pressure, as pressure of the mixture critical point of $CO_2$ - DCM system is between these values [55]. Below the mixture critical point (p = 5 MPa, **Fig 8**), drop diameter initially increased, till reached a maximum, as the diffusion of the $CO_2$ into the DCM drop is limited by the equilibrium concentration of the DCM - $CO_2$ mixture, and the lower solubility of $CO_2$ in the water (0.0137 molar fraction [56]). On the other hand, in experimental runs performed above the mixture critical point of $CO_2$ - DCM system (p = 10 MPa, **Fig 9**), volume of drop was continuously increasing, as there is a higher solubility of $CO_2$ in water (0.0205 in molar fraction), and equilibrium conditions of the DCM - $CO_2$ mixture are not limiting the diffusion of $CO_2$ into the droplet any more. Below the mixture critical point, the volume of the droplet was decreased, after it reached a minimum, as DCM evaporation from the droplet was comparatively higher, than the absorption of $CO_2$. Meanwhile, above the mixture critical point equilibrium concentration limitations were not valid any more as detailed above, so drop volume increases, until its density is low enough to compensate the attachment effect of the surface of the cell. In the experiments of Mattea F. et al. [46], precipitation and formation of several β-carotene particles inside the drop was occurred immediately, upon pressurization of the system by $CO_2$.

During SFEE process the same behaviour of emulsion droplets is expectable, as described in the work of Mattea F. et al. [46], although more rapidly, as process conditions of SFEE are designed for obtaining the maximum available mass transport velocity of components in the o/w emulsion - $scCO_2$ system, by producing emulsions with droplet size distribution in nanometric scale, and hence, obtaining final particles size within this range, too. Results regarding the modelling of SFEE processes are more limited, as more constrains need to be taken into account, and evaporation of water phase is not taking place, and hence it persists acting as a diffusion layer. As o/w emulsion droplets – in the model presented in the work of Mattea F. et al. [43] – are taken into account as spherical droplets, convective mass transfer depends on the drop falling velocity, which is influenced by the gravity-, the buoyancy- and the drag force, acting on the drop. Moreover, as mass flow of $scCO_2$- and organic phase is simultaneously going through on the continuous water phase, in the model equations of Mattea F. et al. [43], a radial coordinate was taken into account, expressing the mass transfer change, by the variation in the thickness of the water layer. As final particle size distribution is influenced by the droplet size of the emulsion [46], process conditions of SFEE should be chosen not to destabilize the emulsion, and to avoid significant variations of emulsion droplets during the process. Mattea F. et al. [43] contacted β-carotene contained DCM/w emulsions (using n-octenyl succinic anhydride (OSA)-modified strach as surfactant material) with $scCO_2$, in order to study the evaluation of the organic content and the particle size distribution during the time of GAS process. They found, that the higher part of the organic phase was already extracted in the first hour of the process, meanwhile two additional hours were needed to decrease the residual DCM content by two orders of magnitude more, and to obtain monomodal particle size distribution by the fully precipitation of β-carotene particles. High elimination of organic solvent is necessary in SFEE process, due to the diffusion of $CO_2$ into the organic phase is increasing the interfacial tension between the aqueous and the organic phase, which leads to

phase separation. In the presented model of Mattea F. et al. [43], the saturation of organic phase by $scCO_2$ is relatively fast: after 0.3 s, the molar fraction of $CO_2$ is above 0.2 in every radial position of each emulsion droplets, so β-carotene precipitation is considered as completed already after this time. On the other hand, extraction of the organic phase is much slower: after half second, only less than half of the initial organic solvent is removed. Organic extraction in case of GAS processes are more efficient than in case of spray processes (like SAS), as liquid phase is stored inside the precipitator, and is continuously keeping contact with $scCO_2$ until the end of the treatment [43].

Rapidness of SFEE process is very important, as o/w emulsions under $scCO_2$ atmosphere are probably become much less stable than under atmospheric conditions, as found in the work of Varona et al. [57] in case of with lavandin essential oil prepared o/w emulsions. Emulsion stability in the case of SFEE process is a crucial process parameter, as experiments done in the work of Mattea F. et al. [46] demonstrate, that each emulsion droplet behaves as a miniature GAS precipitator during the SFEE process, which justifies the control of the final particle size, by the emulsion droplet size.

## 6. INTRODUCTION AND MODELLING REVIEW OF PGSS-DRYING

As previously described, the long-term stability of polyphenols and, particularly, quercetin in aqueous medium is low [33]. Thus, solid formulations with long-term stability that can be used to reconstitute the liquid formulation by addition of water are preferable to the liquid formulations that are obtained by direct application of SFEE. Different techniques are used for this purpose, such as spray-drying and lyophilisation, but these methods are limited by the application of high temperatures or by the poor control on product characteristics

Particles from Gas Saturated Solutions (PGSS)-drying technology (**Fig 10**), as an evolution of PGSS technology [58] is an alternative novel technology that can be used to remove water from the SFEE produced aqueous suspensions, operating at moderate temperatures and producing powders with small particle sizes.

In the PGSS-drying process, an aqueous solution is contacted in a static mixer with supercritical carbon-dioxide ($scCO_2$) in the pressure- and temperature range of 10-15 MPa and 373-393 K, respectively. Then this mixture is sprayed through a nozzle into a tower, which is operating at ambient pressure and smoothly elevated temperature (~70°C) conditions. As a partially water saturated gas phase is suddenly depressurized down to ambient conditions, gas phase undergoes a considerable volume expansion (from ~200 $kg/m^3$ to ~ 1.4 $kg/m^3$), and by the sudden vaporization of the liquid phase dissolved $scCO_2$, atomization effect is taking place, which promotes the formation of particles with controlled particle size distribution in micrometric range [59].

In previous works of E. de Paz- and S. Varona et al. relevant process parameters of PGSS-drying, such as $scCO_2$ to product ratio (GPR), pre-expansion pressure and pre-expansion temperature were observed by [60], [61]. Varona et al. obtained, that GPR has an important influence on the residual water content of the product: Increasing the GPR above a minimum value, appropriate moisture content could be obtained, although a compromising value need to

be found, as applying GPR above one, essential oil loss occurs, due to the possibly increased evaporation ratio in the static mixture and in the tower. GPR also influencing the particle size distribution of obtained product, as well as the pre-expansion pressure and temperature: With higher GPR and decreased pre-expansion pressure and temperature, particle size distribution of the product decreased, probably, due to upon varying the just mentioned process parameters for the just mentioned direction, higher amount of $scCO_2$ is able to dissolve into the emulsion in the static mixture, improving the atomization process, and enhancing the formation of smaller particles.

**Fig 10:** Principles of PGSS - drying technology

In PGSS-drying process two kind of atomization methods: flash-boiling- [62] and effervescent atomization [63] occur simultaneously. In case of flash-boiling atomization a superheated liquid is expanded through a nozzle, and partial evaporation of the liquid and expansion of gas bubbles leads to liquid atomization. Effervescent atomization was developed for applications, which operated with liquids which could not be superheated, or gas could not be dissolved in liquids. By an intensive mixing of gas and liquid phase at moderate pressures, a bubbly two-phase is formed and sprayed through a nozzle, and the expansion of gas bubbles promotes the atomization of the mixture. During PGSS-drying process, the biphasic $H_2O$ - $scCO_2$ flow is mixed intensively in the static mixer, as during effervescent atomization process, meanwhile flash-boiling atomization process takes place in the nozzle, during the rapid, harsh expansion of $H_2O$ - $scCO_2$ biphasic mixture. Moreover, density of $CO_2$ near the critical point varies drastically, and hence, enable a significantly higher volume expansion than gases, such as air or nitrogen, which on similar conditions are in subcritical state. Meanwhile $CO_2$ has a volume expansion rate of 370 when it is isothermally pressurized down from 10 to 0.1 MPa at T = 313 K, nitrogen or air only has a volume expansion rate of 100, when it is decompressed in similar conditions [63].

As PGSS - drying is a complete process, which could be influenced by several mechanisms: saturation of aqueous phase by $scCO_2$ and partial evaporation of water in the static mixer, atomization of aqueous suspension - $scCO_2$ biphasic mixture leaving the static mixer into the spray tower, mass transfer of water from the droplets to the gas phase, kinetics of partial formation and growth, a detailed fundamental analysis of the process is presented in the work of Á. Martín et al. [59]. As water extraction is more favourable in the tower at around ambient pressure after the micronization process than in the static mixture, temperature of the tower must be chosen to be above the dew point curve of the $CO_2$ - $H_2O$ two phase diagram, otherwise efficient water evaporation will not take place during the process [64], [65]. Moreover,

increased water extraction in the static mixture is increase the risk of obtaining dry powder in it, which could lead to the clog of the static mixture [59]. On the other hand, temperature of the tower could not exceed a limit, as thermal degradation of the product is possible. Gas to Liquid Ratio (GLR) must be chosen according to applicable temperature of the tower, in order to operate above of the dew line of $CO_2$ - $H_2O$. A PC-SAFT equation of state based model is developed in the work of Á. Martín et al., in order to calculate the limits of the mass transfer between aqueous solution and supercritical fluid in the static mixture, imposed by phase equilibrium conditions [66]. According to this model, and according to measurement details presented in the work of Á. Martín et al. [59], with the increase of pre-expansion temperature (temperature in the static mixture), GLR could be decreased, to obtain similar final moisture content in the product. Moreover, solubility of $CO_2$ in the liquid phase could be enhanced by several compounds – like poly-ethylene-glycol –, hence by applying lower GLR values, similar residual moister content results of products are obtainable [59]. As according to mass balance calculations presented in the work of Á. Martín et al. [59], at least one with order of magnitude higher GLR values are required than the experimentally detailed values, in order to reach such a low residual moister content results, which are presented. This experience proves, that drying process is influenced by kinetic factors.

Kinetics of temperature variation during the expansion process could also play an important role in water evaporation. Although by injecting the mixture into the tower, it will rapidly cool down due to the Joule–Thomson effect, water will be at a higher temperature than the bulk fluid for a short period of time [67], [68]. Meanwhile the rate of temperature change in a gas phase is in the order of $10^7$ K/s [67], Strumendo et al. [68] estimated, that this rate in a liquid – gas phase like $CO_2$ + tristearin system, is in the order of $10^4$ K/s, due to the relatively low solubility of $CO_2$ in the aqueous phase. In this longer period, water has longer time to evaporate, than expected, according to the temperature of the bulk.

## 7. APPLICABLE SUPERCRITICAL FLUID PROCESSES FOR QUERCETIN

Several authors have studied the processing of quercetin by supercritical fluid technologies. Due to the low solubility of quercetin in supercritical carbon dioxide [69], Supercritical Antisolvent (SAS) experiments have been particularly successful. By SAS processing of pure quercetin, crystalline particles with particle sizes in the micrometer range (1 – 6 μm) have been obtained [70], [71], [72]. Using SAS process, D. T. Santos et al. [71] obtained significant morphological change and particle size distribution decrease of quercetin comparing to unprocessed one (**Fig 11 A)**, meanwhile almost negligible product characteristics improvement, upon using conventional method (**Fig 11 B**).

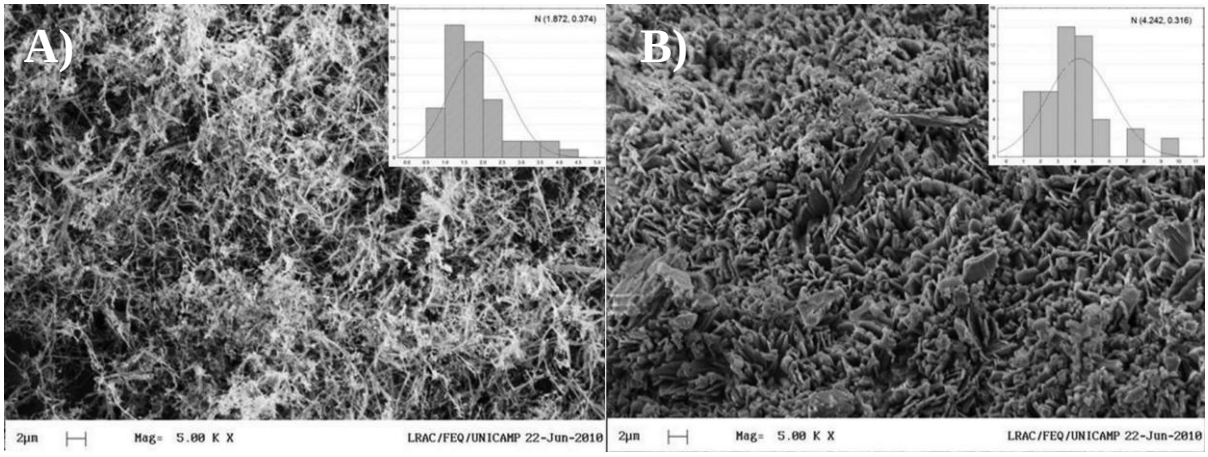


**Fig 11:** SEM pictures of micronized quercetin particles using SAS process (A) and conventional (solvent evaporation) process (B) [71]

Using SAS process, quercetin not only could be precipitated in micrometric scale to increase its very low water solubility (<0.01 mg/mL [73]), but also could be encapsulated by a kind of biopolymer, such as ethyl-cellulose, in order to avoid it from thermal- and light degradation [31]. Fernandez et al. by using SAS process obtained quasi-spherical particles in sub-micrometric range with a quercetin precipitation above 85%, and an encapsulation efficiency above 99%. Moreover, amorphous quercetin in the polymer matrix was also obtained, which is dissolved in water more rapidly, than crystalline material [31]. Fraile et al. [42] produced quercetin particles encapsulated with Pluronic F127 by SAS technology. Pure quercetin (**Fig**

**12 A**), SAS-processed crystallized quercetin as needle like particles (**Fig 12 B**), and SAS-processed with Pluronic co-precipitated quercetin (**Fig 12 C, D**) had a totally different spherical morphology, indicating that Pluronic F127 was able to successfully encapsulate the quercetin. Higher particle sizes were obtained, when the quercetin / Pluronic mass ratio was increased, due to the possible aggregation of the polymer shells (**Fig 12 C, D**). Obtained morphologies indicate, that quercetin particles acted as nucleation sites for the formation of a polymer film, and this film of polymer restrained the growth of quercetin particles, upon applied the quercetin / Pluronic mass ratio above 1. With this encapsulation method, the solubility of quercetin in simulated intestinal fluid was increased by a factor of 8.

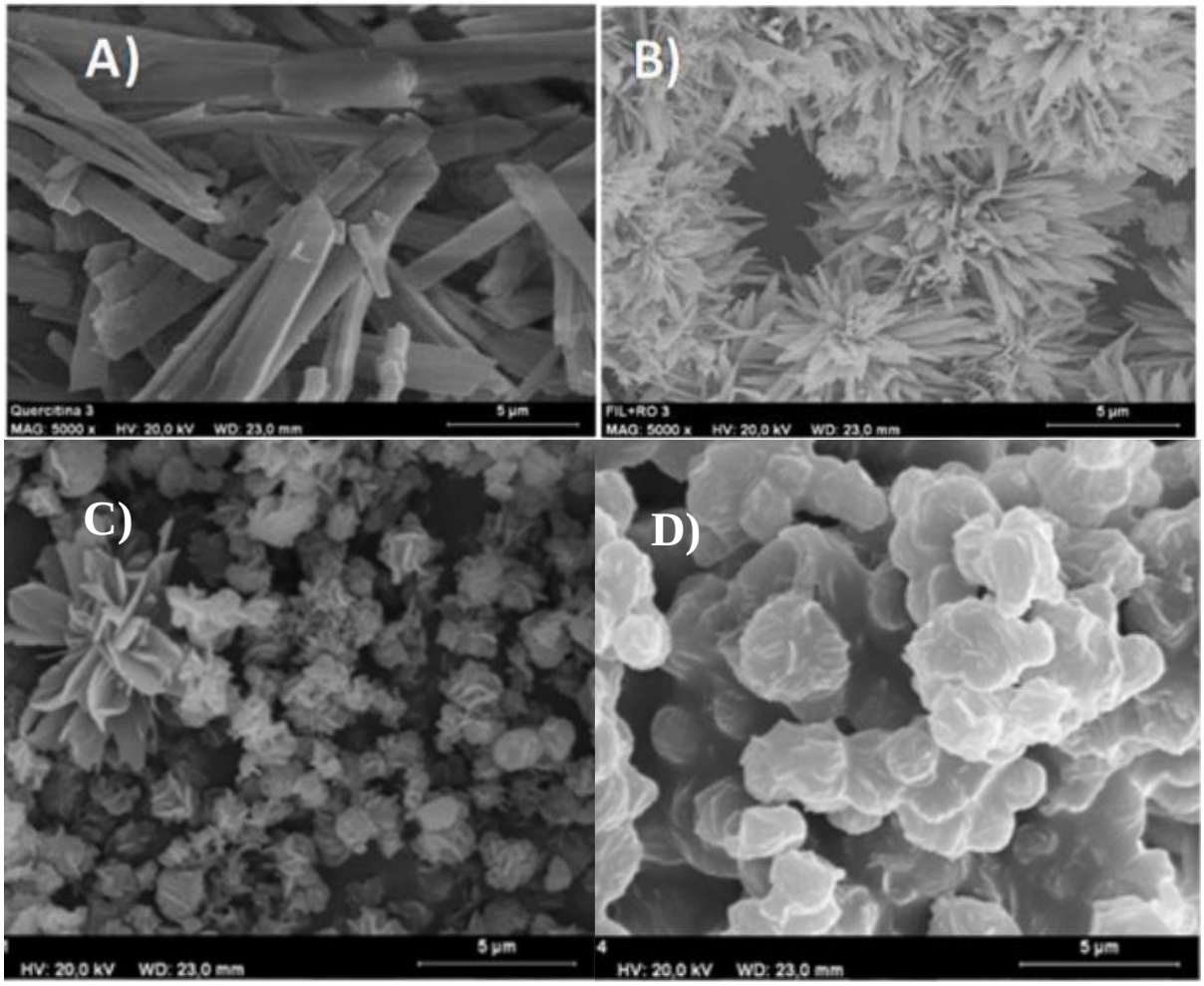


**Fig 12: A)** Raw quercetin; **B)** SAS processed quercetin from solution (0.02 g/mL) prepared in acetone; **C)** SAS processed quercetin + Pluronic F127 = 1:1 (w/w); **D)** SAS processed quercetin + Pluronic F127 = 1:1.7 (w/w) [42]

## 8. THESIS OUTLOOK

In this work supercritical technologies, such as Supercritical Fluid Extraction of Emulsion and PGSS-drying technology is used, in the production of quercetin loaded particles in nanometric scale as aqueous suspension, using SFEE technology, and in micrometric scale as dry-product, using PGSS-drying technology. Quercetin is a member of flavonoids, and it is a highly promising bioactive compound against a wide variety of diseases, owing to its high antioxidant activity. The aim of this work is to increase the bioavailability of quercetin by precipitating it in (sub)-micrometric scale (depending on the applied supercritical technology), and encapsulating it in biocompatible polymers, such as soy-bean lecithin and/or Pluronic L64®, using $scCO_2$ extraction base technologies, which leads to increase the encapsulation efficiency, owing to its mild critical temperature and hence the low degradation ratio of bioactive compounds, such as quercetin.

In **Chapter I** a batch SFEE equipment is presented, and an experimental study is done, in order to obtain optimal process conditions of SFEE and a sutaible surfactant material is selected for the total encapsulation of in nanometric scale precipitated quercetin.

In **Chapter II** mass transport processes during SFEE process are measured in static and dynamic o/w emulsion – $scCO_2$ systems are measured, using magnetic suspension balances. Moreover, a three-parameter mass transfer model is fitted on the measured results, and key steps of SFEE process are obtained.

In **Chapter III** encapsulation efficiency of quercetin was increased using the combination of surfactant materials, and a scaled-up, semi-continuous SFEE equipment was designed, in order to increase productivity. Moreover, PGSS-drying was used to extract water content of SFEE obtained aqueous suspension, and increase long-term stability of product.

In **Chapter IV** an experimental plan using scaled-up SFEE device is done, and a technical and economical feasibility study is presented.

## REFERENCES

[1] N. Babbar, H.S. Oberoi, Potential of Agro-residues as Sources of Bioactive Compounds, in: K.S. Brar, S.G. Dhillon, R.C. Soccol (Eds.), Biotransformation Waste Biomass into High Value Biochem., Springer New York, New York, NY, 2014: pp. 261–295. doi:10.1007/978-1-4614-8005-1_11.

[2] N. Ratola, J.L. Faria, A. Alves, Analysis and quantification of trans-resveratrol in wines from Alentejo region (Portugal), Food Technol. Biotechnol. 42 (2004) 125–130.

[3] R.N. Bennett, R.M. Wallsgrove, Secondary metabolites in plant defence mechanisms, New Phytol. 127 (1994) 617–633. doi:10.1111/j.1469-8137.1994.tb02968.x.

[4] S. Vladimir-Kneževi, B. Blažekovi, M.B. Stefan, M. Babac, Plant Polyphenols as Antioxidants Influencing the Human Health, print edit, InTech Europe, 2012. doi:10.5772/27843.

[5] C. Manach, A. Mazur, A. Scalbert, Polyphenols and prevention of cardiovascular diseases., Curr. Opin. Lipidol. 16 (2005) 77–84.

[6] P. Knekt, J. Kumpulainen, R. Järvinen, H. Rissanen, M. Heliövaara, A. Reunanen, T. Hakulinen, A. Aromaa, Flavonoid intake and risk of chronic diseases., Am. J. Clin. Nutr. 76 (2002) 560–568.

[7] E. De Stefani, A. Ronco, M. Mendilaharsu, H. Deneo-Pellegrini, Diet and risk of cancer of the upper aerodigestive tract - II. Nutrients, Oral Oncol. 35 (1999) 22–26. doi:10.1016/S1368-8375(98)00061-X.

[8] D.R. Ferry, A. Smith, J. Malkhandi, D.W. Fyfe, P.G. DeTakats, D. Anderson, J. Baker, D.J. Kerr, Phase I clinical trial of the flavonoid quercetin: Pharmacokinetics and evidence for in vivo tyrosine kinase inhibition, Clin. Cancer Res. 2 (1996) 659–668.

[9] Polyphenols and biochar, (2016). http://www.landesbioscience.com/curie/images/chapters/Wahle1color.gif.

[10] T.-H. Wu, F.-L. Yen, L.-T. Lin, T.-R. Tsai, C.-C. Lin, T.-M. Cham, Preparation, physicochemical characterization, and antioxidant effects of quercetin nanoparticles., Int. J. Pharm. 346 (2008) 160–8. doi:10.1016/j.ijpharm.2007.06.036.

[11] S.C. Chou, M. Kaur, J.A. Thompson, R. Agarwal, C. Agarwal, Influence of gallate esterification on the activity of procyanidin B2 in androgen-dependent human prostate carcinoma LNCaP cells, Pharm. Res. 27 (2010) 619–627. doi:10.1007/s11095-009-0037-6.

[12] C.G. Fraga, M. Galleano, S. V. Verstraeten, P.I. Oteiza, Basic biochemical mechanisms behind the health benefits of polyphenols, Mol. Aspects Med. 31 (2010) 435–445. doi:10.1016/j.mam.2010.09.006.

[13] N.R. Perron, J.L. Brumaghim, A review of the antioxidant mechanisms of polyphenol compounds related to iron binding, Cell Biochem. Biophys. 53 (2009) 75–100. doi:10.1007/s12013-009-9043-x.

[14] Y. Yilmaz, R.T. Toledo, Major Flavonoids in Grape Seeds and Skins: Antioxidant Capacity of Catechin, Epicatechin, and Gallic Acid, J. Agric. Food Chem. 52 (2004) 255–260. doi:10.1021/jf030117h.

[15] I. Kolouchová-Hanzlíková, K. Melzoch, V. Filip, J. Šmidrkal, Rapid method for resveratrol determination by HPLC with electrochemical and UV detections in wines, Food Chem. 87 (2004) 151–158. doi:10.1016/j.foodchem.2004.01.028.

[16] M. Cíz, M. Pavelková, L. Gallová, J. Králová, L. Kubala, a Lojek, The influence of wine polyphenols on reactive oxygen and nitrogen species production by murine macrophages RAW 264.7., Physiol. Res. 57 (2008) 393–402. http://www.ncbi.nlm.nih.gov/pubmed/17465695.

[17] M.F. Ramadan, Antioxidant characteristics of phenolipids (quercetin-enriched lecithin) in lipid matrices, Ind. Crops Prod. 36 (2012) 363–369. doi:10.1016/j.indcrop.2011.10.008.

[18] A. Parmar, K. Singh, A. Bahadur, G. Marangoni, P. Bahadur, Interaction and solubilization of some phenolic antioxidants in Pluronic?? micelles, Colloids Surfaces B Biointerfaces. 86 (2011) 319–326. doi:10.1016/j.colsurfb.2011.04.015.

[19] Y. Gao, Y. Wang, Y. Ma, A. Yu, F. Cai, W. Shao, G. Zhai, Formulation optimization and in situ absorption in rat intestinal tract of quercetin-loaded microemulsion, Colloids Surfaces B Biointerfaces. 71 (2009) 306–314. doi:10.1016/j.colsurfb.2009.03.005.

[20] Q. Dai, A.R. Borenstein, Y. Wu, J.C. Jackson, E.B. Larson, Fruit and Vegetable Juices and Alzheimer's Disease: The Kame Project, Am. J. Med. 119 (2006) 751–759. doi:10.1016/j.amjmed.2006.03.045.

[21] M. Porrini, P. Riso, Factors influencing the bioavailability of antioxidants in foods: A critical appraisal, Nutr. Metab. Cardiovasc. Dis. 18 (2016) 647–650. doi:10.1016/j.numecd.2008.08.004.

[22] C. Manach, Polyphenols : food sources and bioavailability . Am J Clin Nutr, Am. J. Clin. Nutr. 79 (2004) 727–747.

[23] C.G. Fraga, Plant Phenolics and Human Health: Biochemistry, Nutrition, and Pharmacology, 2009. doi:10.1002/9780470531792.

[24] A. Crozier, D. Del Rio, M.N. Clifford, Bioavailability of dietary flavonoids and phenolic compounds, Mol. Aspects Med. 31 (2010) 446–467. doi:10.1016/j.mam.2010.09.007.

[25] Khaled A. Khaled, Yousry M. El-Sayeda, Badr M. Al-Hadiyab, Disposition of the Flavonoid Quercetin in Rats After Single Intravenous and Oral Doses, Drug Dev. Ind. Pharm. 29 (2003) 397–403. doi:10.1081/DDC-120018375.

[26] R. Gugler, M. Leschik, H.J. Dengler, Disposition of quercetin in man after single oral and intravenous doses, Eur. J. Clin. Pharmacol. 9 (1975) 229–234. doi:10.1007/BF00614022.

[27] S. Chakraborty, S. Stalin, N. Das, S. Thakur Choudhury, S. Ghosh, S. Swarnakar, The use of nano-quercetin to arrest mitochondrial damage and MMP-9 upregulation during prevention of gastric inflammation induced by ethanol in rat, Biomaterials. 33 (2012) 2991–3001. doi:10.1016/j.biomaterials.2011.12.037.

[28] M.R. Lauro, M.L. Torre, L. Maggi, F. De Simone, U. Conte, R.P. Aquino, Fast- and Slow-Release Tablets for Oral Administration of Flavonoids: Rutin and Quercetin, Drug Dev. Ind. Pharm. 28 (2002) 371–379. doi:10.1081/DDC-120002998.

[29] N. Buchner, A. Krumbein, S. Rohn, L.W. Kroh, Effect of thermal processing on the flavonols rutin and quercetin, Rapid Commun. Mass Spectrom. 20 (2006) 3229–3235. doi:10.1002/rcm.2720.

[30] M. Fiol, A. Weckmüller, S. Neugart, M. Schreiner, S. Rohn, A. Krumbein, L.W. Kroh, Thermal-induced changes of kale's antioxidant activity analyzed by HPLC–UV/Vis-online-TEAC detection, Food Chem. 138 (2013) 857–865. doi:http://dx.doi.org/10.1016/j.foodchem.2012.10.101.

[31] M.T. Fernández-Ponce, Y. Masmoudi, R. Djerafi, L. Casas, C. Mantell, E.M. de la Ossa, E. Badens, Particle design applied to quercetin using supercritical anti-solvent techniques, J. Supercrit. Fluids. 105 (2014) 119–127. doi:10.1016/j.supflu.2015.04.014.

[32] P.J. Mulholland, D.R. Ferry, D. Anderson, S.A. Hussain, A.M. Young, J.E. Cook, E. Hodgkin, L.W. Seymour, D.J. Kerr, Pre-clinical and clinical study of QC12, a water-soluble, pro-drug of quercetin., Ann. Oncol. 12 (2001) 245–248.

[33] D. Althans, P. Schrader, S. Enders, Solubilisation of quercetin: Comparison of hyperbranched polymer and hydrogel, J. Mol. Liq. 196 (2014) 86–93. doi:10.1016/j.molliq.2014.03.028.

[34] T. Pralhad, K. Rajendrakumar, Study of freeze-dried quercetin-cyclodextrin binary systems by DSC, FT-IR, X-ray diffraction and SEM analysis, J. Pharm. Biomed. Anal. 34 (2004) 333–339. doi:10.1016/S0731-7085(03)00529-6.

[35] Z.P. Yuan, L.J. Chen, L.Y. Fan, M.H. Tang, G.L. Yang, H.S. Yang, X.B. Du, G.Q. Wang, W.X. Yao, Q.M. Zhao, B. Ye, R. Wang, P. Diao, W. Zhang, H. Bin Wu, X. Zhao, Y.Q. Wei, Liposomal quercetin efficiently suppresses growth of solid tumors in murine models, Clin. Cancer Res. 12 (2006) 3193–3199. doi:10.1158/1078-0432.CCR-05-2365.

[36] H. Li, X. Zhao, Y. Ma, G. Zhai, L. Li, H. Lou, Enhancement of gastrointestinal absorption of quercetin by solid lipid nanoparticles, J. Control. Release. 133 (2009) 238–244. doi:10.1016/j.jconrel.2008.10.002.

[37] A. Capuzzo, M.E. Maffei, A. Occhipinti, Supercritical fluid extraction of plant flavors and fragrances, Molecules. 18 (2013) 7194–7238. doi:10.3390/molecules18067194.

[38] B.E. Poling, J.M. Prausnitz, J.P. O apos Connell, Properties of Gases and Liquids, Exp. Therm. Fluid Sci. 1 (2007) 1–803. doi:10.1036/0070116822.

[39] D. Cossuta, T. Vatai, M. Báthori, J. Hohmann, T. Keve, B. Simándi, Extraction of hyperforin and hypericin from St. John's wort (Hypericum perforatum L.) with different solvents, J. Food Process Eng. 35 (2012) 222–235. doi:10.1111/j.1745-4530.2010.00583.x.

[40] M.B. King, T.R. Bott, Extraction of Natural Products Using Near-Critical Solvents, (1992).

[41] E. Lack, B. Simándi, 9.6 Supercritical fluid extraction and fractionation from solid materials, Ind. Chem. Libr. 9 (2001) 537–575. doi:10.1016/S0926-9614(01)80032-0.

[42] M. Fraile, R. Buratto, B. Gómez, Á. Martín, M.J. Cocero, Enhanced delivery of quercetin by encapsulation in poloxamers by supercritical antisolvent process, Ind. Eng. Chem. Res. 53 (2014) 4318–4327. doi:10.1021/ie5001136.

[43] F. Mattea, A. Martin, A. Matias-Gago, M.J. Cocero, Supercritical antisolvent precipitation from an emulsion: beta-Carotene nanoparticle formation, J. Supercrit. Fluids. 51 (2009) 238–247. doi:10.1016/j.supflu.2009.08.013.

[44] G. Lévai, Á. Martín, E. De Paz, S. Rodríguez-Rojo, M.J. Cocero, Production of stabilized quercetin aqueous suspensions by supercritical fluid extraction of emulsions, J. Supercrit. Fluids. 100 (2015) 34–45. doi:10.1016/j.supflu.2015.02.019.

[45] Y. Pérez De Diego, F.E. Wubbolts, P.J. Jansens, Modelling mass transfer in the PCA process using the Maxwell-Stefan approach, J. Supercrit. Fluids. 37 (2006) 53–62. doi:10.1016/j.supflu.2005.07.002.

[46] F. Mattea, Á. Martín, C. Schulz, P. Jaeger, R. Eggers, M.J. Cocero, Behavior of an Organic Solvent Drop During the Supercritical Extraction of Emulsions, AIChE J. 56 (2010) 1184–1195. doi:0.1002/aic.12061.

[47] B.Y. Shekunov, P. Chattopadhyay, J. Seitzinger, R. Huff, Nanoparticles of poorly water-soluble drugs prepared by supercritical fluid extraction of emulsions, Pharm. Res. 23 (2006) 196–204. doi:10.1007/s11095-005-8635-4.

[48] A. Martín, A. Bouchard, G.W. Hofland, G.-J. Witkamp, M.J. Cocero, Mathematical modeling of the mass transfer from aqueous solutions in a supercritical fluid during particle formation, J. Supercrit. Fluids. 41 (2007) 126–137. doi:10.1016/j.supflu.2006.08.015.

[49] J.O. Werling, P.G. Debenedetti, Numerical modeling of mass transfer in the supercritical antisolvent process, J. Supercrit. Fluids. 16 (1999) 167–181. doi:10.1016/S0896-8446(99)00027-3.

[50] J.O. Werling, P.G. Debenedetti, Numerical modeling of mass transfer in the supercritical antisolvent process: Miscible conditions, J. Supercrit. Fluids. 18 (2000) 11–24. doi:10.1016/S0896-8446(00)00054-1.

[51] N. Elvassore, F. Cozzi, A. Bertucco, Mass Transport Modeling in a Gas Antisolvent Process, Ind. Eng. Chem. Res. 43 (2004) 4935–4943. doi:10.1021/ie034040y.

[52] M. Lora, A. Bertucco, I. Kikic, Simulation of the Semicontinuous Supercritical Antisolvent Recrystallization Process, Society. (2000) 1487–1496. doi:10.1021/ie990685f.

[53] M. Mukhopadhyay, S. V. Dalvi, Mass and heat transfer analysis of SAS: Effects of thermodynamic states and flow rates on droplet size, J. Supercrit. Fluids. 30 (2004) 333–348. doi:10.1016/j.supflu.2003.10.001.

[54] F. Bashforth, J.C. Adams, eds., An attempt to test the theories of capillary action by comparing the theoretical and measured forms of drops of fluid. With an explanation of the method of integration employed in constucting the tables which give the theoretical forms of such drops, Cambridge [Eng.] University Press, Cambridge, 1883. https://archive.org/details/attempttest00bashrich.

[55] M. Stievano, N. Elvassore, High-pressure density and vapor-liquid equilibrium for the binary systems carbon dioxide-ethanol, carbon dioxide-acetone and carbon dioxide-dichloromethane, J. Supercrit. Fluids. 33 (2005) 7–14. doi:10.1016/j.supflu.2004.04.003.

[56] A. Bamberger, G. Sieder, G. Maurer, High-pressure (vapor+liquid) equilibrium in binary mixtures of (carbon dioxide+water or acetic acid) at temperatures from 313 to 353 K, J. Supercrit. Fluids. 17 (2000) 97–110. doi:10.1016/S0896-8446(99)00054-6.

[57] S. Varona, Á. Martín, M.J. Cocero, Formulation of a natural biocide based on lavandin essential oil by emulsification using modified starches, Chem. Eng. Process. Process Intensif. 48 (2009) 1121–1128. doi:10.1016/j.cep.2009.03.002.

[58] E. Weidner, Z. Knez, Z. Novak, A process and equipment for production and fractionation of fine particles from gas saturated solutions, World Patent, WO 95/21688, 1994.

[59] Á. Martín, E. Weidner, PGSS-drying: Mechanisms and modeling, J. Supercrit. Fluids. 55 (2010) 271–281. doi:10.1016/j.supflu.2010.08.008.

[60] E. de Paz, Á. Martín, C.M.M. Duarte, M.J. Cocero, Formulation of β-carotene with poly-(ε-caprolactones) by PGSS process, Powder Technol. 217 (2012) 77–83. doi:10.1016/j.powtec.2011.10.011.

[61] S. Varona, Á. Martín, M.J. Cocero, Liposomal incorporation of lavandin essential oil by a thin-film hydration method and by particles from gas-saturated solutions, Ind. Eng. Chem. Res. 50 (2011) 2088–2097. doi:10.1021/ie102016r.

[62] E. Sher, T. Bar-Kohany, A. Rashkovan, Flash-boiling atomization, Prog. Energy Combust. Sci. 34 (2008) 417–439. doi:10.1016/j.pecs.2007.05.001.

[63] S.D. Sovani, P.E. Sojka, A.H. Lefebvre, Effervescent atomization, Prog. Energy Combust. Sci. 27 (2001) 483–521. doi:10.1016/S0360-1285(00)00029-0.

[64] Á. Martín, H.M. Pham, A. Kilzer, S. Kareth, E. Weidner, Micronization of polyethylene glycol by PGSS (Particles from Gas Saturated Solutions)-drying of aqueous solutions, Chem. Eng. Process. Process Intensif. 49 (2010) 1259–1266. doi:10.1016/j.cep.2010.09.014.

[65] E. Badens, C. Magnan, G. Charbit, Microparticles of soy lecithin formed by supercritical processes, Biotechnol. Bioeng. 72 (2001) 194–204. doi:10.1002/1097-0290(20000120)72:2<194::AID-BIT8>3.0.CO;2-L.

[66] Á. Martín, H.M. Pham, A. Kilzer, S. Kareth, E. Weidner, Phase equilibria of carbon dioxide+poly ethylene glycol+water mixtures at high pressure: Measurements and modelling, Fluid Phase Equilib. 286 (2009) 162–169. doi:http://dx.doi.org/10.1016/j.fluid.2009.08.010.

[67] J. Li, H.A. Matos, E.G. De Azevedo, Two-phase homogeneous model for particle formation from gas-saturated solution processes, J. Supercrit. Fluids. 32 (2004) 275–286. doi:10.1016/j.supflu.2004.01.004.

[68] M. Strumendo, A. Bertucco, N. Elvassore, Modeling of particle formation processes using gas saturated solution atomization, J. Supercrit. Fluids. 41 (2007) 115–125. doi:10.1016/j.supflu.2006.09.003.

[69] A. Chafer, T. Fornari, A. Berna, R.P. Stateva, Solubility of quercetin in supercritical CO2 + ethanol as a modifier: Measurements and thermodynamic modelling, J. Supercrit. Fluids. 32 (2004) 89–96. doi:10.1016/j.supflu.2004.02.005.

[70] X. Liu, Z. Li, B. Han, T. Yuan, Supercritical Antisolvent Precipitation of Microparticles of Quercetin, Chinese J. Chem. Eng. 13 (2005) 128–130. http://www.cjche.com.cn/EN/abstract/abstract474.shtml#.

[71] D.T. Santos, M.A.A. Meireles, Micronization and encapsulation of functional pigments using supercritical carbon dioxide, J. Food Process Eng. 36 (2013) 36–49. doi:10.1111/j.1745-4530.2011.00651.x.

[72] P. Alessi, A. Cortesi, N. De Zordi, T. Gamse, I. Kikic, M. Moneghini, D. Solinas, Supercritical Antisolvent Precipitation of Quercetin Systems: Preliminary Experiments, Chem. Biochem. Eng. Q. 26 (2012) 391–398. <Go to ISI>://WOS:000314256800010.

[73] L. Chebil, C. Humeau, J. Anthony, F. Dehez, J.M. Engasser, M. Ghoul, Solubility of flavonoids in organic solvents, J. Chem. Eng. Data. 52 (2007) 1552–1556. doi:10.1021/je7001094.

# OBJECTIVES

## BIOPRODUCTS PROCESSING BY SFEE:

## APPLICATION FOR LIQUID AND SOLID

## QUERCETIN FORMULATIONS

Global aim of this work is to increase bioavailability of quercetin, using supercritical fluid technologies, such as Supercritical Fluid Extraction of Emulsions (SFEE) to obtain quercetin-loaded nanoparticles contained aqueous suspension product, and Particles from Gas Saturated Solutions (PGSS)-drying technology to obtain micronized, dry quercetin-loaded particles.

- SFEE technology will be used to produce highly loaded quercetin nanoparticles in aqueous suspension, encapsulated by biocompatible surfactants, in order to increase thermal- and light stability of the active compound.
    - Process parameters such as p, T, concentration of surfactants, quercetin and organic phase will be tested, in order to optimize SFEE as a batch process.
    - Various surfactant materials and the combination of them will be tested, in order to upgrade their encapsulation efficiency and protection capacity for the active compound.
- Mass transfer properties in o/w emulsion - $scCO_2$ system will be studied in a static system using Magnetic Suspension Balances, to obtain the key process steps of SFEE.
    - Based on measurement results, diffusion processes of compounds during SFEE process will be modelled.
- Mass transfer measurements in dynamic system – applying continuous $scCO_2$ flow through the emulsion – will be performed as well, to obtain critical scaling-up factors of SFEE process.
    - Based on static- and dynamic measurement results SFEE process will be scaled up.

- SFEE process will be modified to a semi-continuous manner, performing a continuous $scCO_2$ flow through the emulsion in order to increase the production rate of aqueous suspensions.
    - Process parameters of scaled-up SFEE will be optimized using an experimental plan.
- PGSS-drying technology will be used to produce encapsulated quercetin loaded dry particles, in controlled particle size distribution.
    - Critical process parameters of PGSS-drying, such as Gas to Liquid Ratio, pre-expansion pressure and temperature will be obtained.
- Supercritical micronization processes obtained product characteristics, such as morphology, antioxidant activity quercetin aqueous solubility and transdermal permeability will be compared with lyophilization (as non-supercritical) technology obtained product characteristics.
    - Feasibility of the application of supercritical technologies based on product characteristics and process economic studies will be observed.

# CHAPTER I

## PRODUCTION OF STABILIZED QUERCETIN AQUEOUS SUSPENSIONS BY SUPERCRITICAL FLUID EXTRACTION OF EMULSIONS

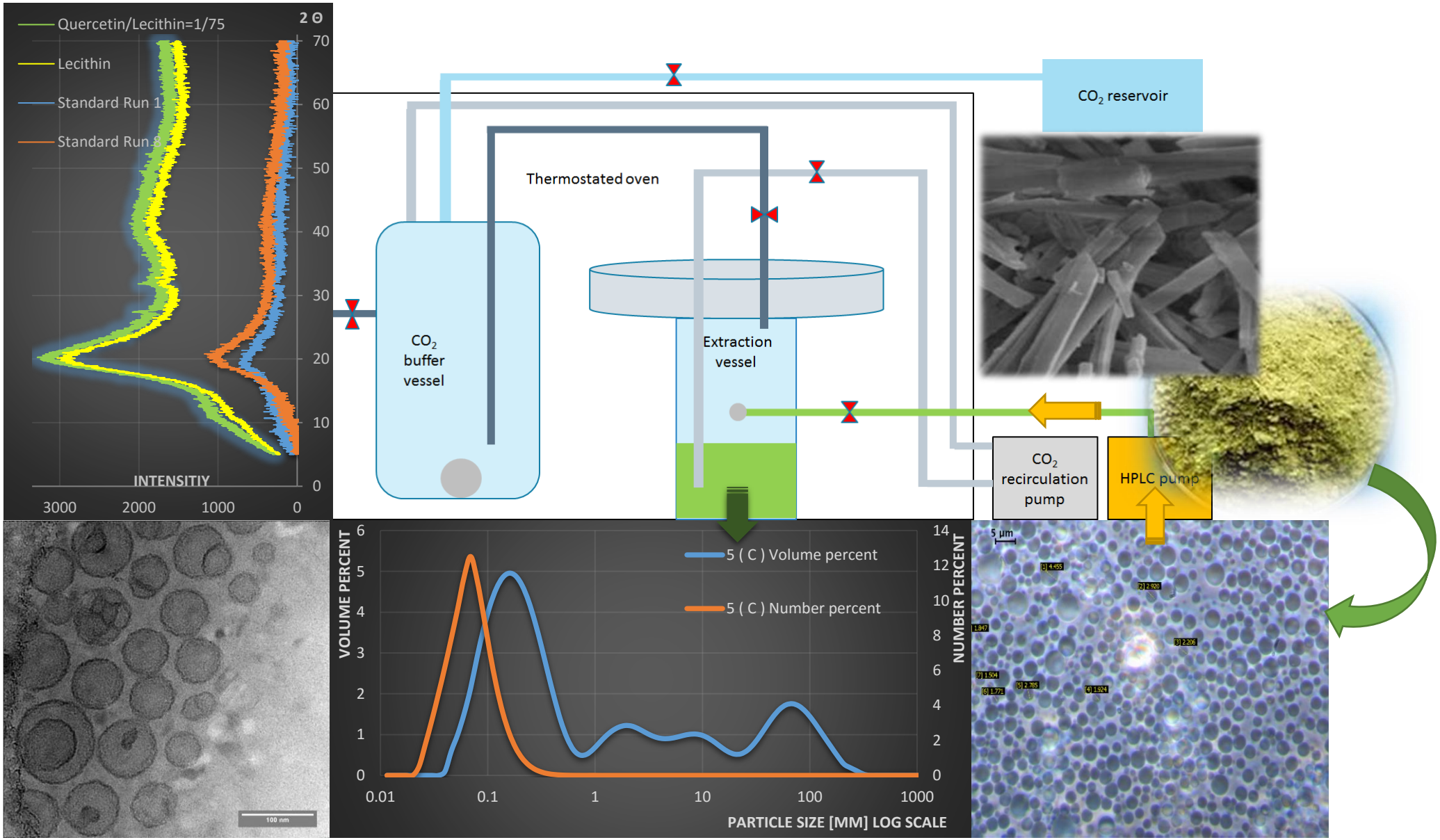
Quercetin/Lecithin=1/75
Lecithin
Standard Run 1
Standard Run 8
2 Θ
70
60
50
40
30
20
10
0
INTENSITIY
3000
2000
1000
0
CO2 reservoir
Thermostated oven
CO2 buffer vessel
Extraction vessel
CO2 recirculation pump
HPLC pump
100 nm
VOLUME PERCENT
NUMBER PERCENT
5 ( C ) Volume percent
5 ( C ) Number percent
0.01
0.1
1
10
100
1000
PARTICLE SIZE [MM] LOG SCALE
5 µm

**ABSTRACT**

Quercetin is a flavonoid with highly promising bioactivity against a variety of diseases, due to its strong antioxidant, antiviral and antihistaminic effect, but these applications are limited by the low solubility of quercetin in gastrointestinal fluids and the correspondingly low bioavailability. The objective of this work is to produce encapsulated quercetin particles in sub-micrometric scale, in order to increase their low bioavailability. These particles were produced by extraction of organic solvent from oil in water emulsions by Supercritical Fluid Extraction of Emulsions (SFEE). Due to the rapid extraction of organic solvent by this method, the continuous aqueous phase becomes rapidly supersaturated for the active compound, causing the precipitation of quercetin particles in sub-micrometric scale, encapsulated by the surfactant material. Two different biopolymers (Pluronic L64® poloxamers and soy bean lecithin) were used as carriers and surfactant materials. In experiments with Pluronic, needle quercetin particles were obtained after SFEE treatment, with particle sizes around 1 μm and poor encapsulation efficiency. In case of soy lecithin, quercetin-loaded multivesicular liposomes were obtained, with a mean particle size around 100 nm and around 70% encapsulation efficiency of quercetin, without presence of segregated quercetin crystals.

**Keywords:** encapsulated quercetin, sub-micrometric scale, multivesicular system, supercritical fluid extraction of emulsion, antioxidant activity

## 1. INTRODUCTION

Quercetin (3,3',4,4',5,7-pentahydroxyflavone, chemical structure presented on **Fig 1**) is a bioflavonoid, available in various fruits, vegetables and oils. It can scavenge reactive oxygen species, and down-regulate lipid peroxidation due to its ion chelating and iron stabilizing effect [1]. Furthermore it can promote the oxidation of $Fe^{2+}$ to $Fe^{3+}$, which is less effective in generating free radicals. These effects of quercetin may be explained by its o-diphenol B-ring structure [2] and the ability of donating π electrons from the benzene ring, while it is remaining relatively stable [3]. It also has anti-proliferative effects in a wide range of human cancer cell lines [4]. Due to these properties, quercetin is a highly promising active compound against a wide variety of diseases.

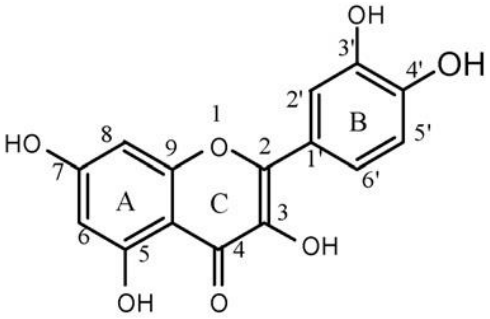


**Fig 1:** Chemical structure of quercetin [5]

A major limitation for the clinical application of quercetin is its low bioavailability, that makes it necessary to administrate high doses (50 mg/kg) [6]. Due to the low water solubility of quercetin, it has a minimal absorption rate in the gastrointestinal tract, and its oral bioavailability is lower than 17% in rats [7] and lower than 1% in humans [8]. Different approaches have been proposed in literature to increase the bioavailability of quercetin. Mulholland et al. [9] synthesized a water-soluble derivative of quercetin, but its bioavailability was only 20%. Also, to increase the bioavailability of this poorly water soluble compound, drug loaded solid lipid nanoparticles could be a promising alternative, and the complexation of quercetin with lecithin and cyclodextrin in aqueous solution has been tested [10] [11]. Li et al.

[12] produced lecithin encapsulated quercetin by emulsification and low-temperature solidification, with over 90% drug entrapment efficiency in spherical particles of an average diameter of 155 nm was observed. Heterogeneous morphologies were obtained with a co-existence of additional colloidal structures, like micelles, liposomes, supercooled melts, drug nanoparticles, which caused a certain scatter in the particle size distribution, with particle sizes spanning the range from 20 nm to 500 nm. The absorption rate of quercetin loaded solid lipid nanoparticles was studied by in-situ perfusion method in rats, obtaining a 6-fold relative increase in bioavailability, compared to unprocessed quercetin.

Supercritical fluids are another promising alternative in the processing of natural bioactive compounds such as quercetin, because they allow carrying out the encapsulation process at near ambient temperatures, and in an inert atmosphere, thus avoiding the thermal degradation or oxidation of the product and reducing its contamination with organic solvents. Several authors have studied the processing of quercetin by supercritical fluid technologies. Due to the low solubility of quercetin in supercritical carbon dioxide [13], Supercritical Antisolvent (SAS) experiments have been particularly successful. By SAS processing of pure quercetin, crystalline particles with particle sizes in the micrometer range (1 – 6 μm) have been obtained [14], [15], [16]. Fraile et al. [17] produced quercetin particles encapsulated with Pluronic F127 by SAS technology. As in previous works, SAS-processed pure quercetin crystallized as needle like particles, meanwhile quercetin co-precipitated with Pluronic had a totally different spherical morphology, indicating that Pluronic F127 was able to successfully encapsulate quercetin. Higher particle sizes were obtained when the quercetin / Pluronic mass ratio was increased, due to the possible aggregation of the polymer shells. Obtained morphologies indicate, that quercetin particles acted as nucleation sites for the formation of a polymer film, and this film of polymer restrained the growth of quercetin particles above the mass ratio of

1/1 = quercetin / Pluronic. With this encapsulation method, the solubility of quercetin in simulated intestinal fluid was increased by a factor of 8.

Supercritical Fluid Extraction of Emulsions (SFEE) technology can be considered as an evolution of SAS technology, which is especially suitable to encapsulate poorly water soluble drugs in an aqueous suspension. The process consists of forming an oil-in-water emulsion, containing the water-insoluble drug in the dispersed organic phase. By SFEE, the organic solvent is extracted from this emulsion by the supercritical solvent, which should have high affinity to the organic solvent and a low affinity to the active compound of interest. Due to the solubility differences, the supercritical solvent quickly extracts the organic solvent from the emulsion, leading to the rapid super-saturation of the aqueous phase by the active compound, and hence a fast precipitation of it. Meanwhile in the SAS antisolvent precipitation method particle nucleation and growth occur across the whole solution volume, in the case of SFEE the formation of particles is confined within the emulsion droplets. This restrains the size of the particles obtained, that can be one order of magnitude smaller than particles produced by solution precipitation [18].

F. Mattea et al. studied the precipitation of β-carotene by continuous SFEE in order to model the process [19]. In this study submicro- and nano-particles were obtained with a residual organic content as low as 1 ppm. The obtained particle size distribution was directly related with the droplet size distribution of the initial emulsion, while residual organic content depended on the process parameters, such as the pressure and the temperature. Model results showed that the saturation of organic phase droplets with $CO_2$ caused a rapid antisolvent effect, which in the continuous implementation of the process can take place during the drop fly time, while the elimination of the residual organic solvent was much slower. Based on experimental and model results, a two-step process strategy can be proposed. The first step would involve contact between emulsion and $CO_2$, to ensure the saturation of the disperse phase, in order to

achieve precipitation by antisolvent effect. A second step would involve an extended contact between $CO_2$ and emulsion, in order to eliminate the remaining organic solvent. This step might be slower than the first, because once the particles are formed, emulsion destabilization is no longer a problem. In a subsequent work, Santos et al. extended this approach to the precipitation of lycopene [20].

The aim of this study is to apply the Supercritical Fluid Extraction of Emulsion process to the encapsulation of quercetin. Based on the available information, two different carrier materials have been found to increase the water solubility and the bioavailability of quercetin have been tested: Pluronic block copolymers, and soybean lecithin. The influence of the main process parameters has been studied, including properties of the initial emulsion, extraction time and extraction conditions. The performance of the process has been evaluated analysing the encapsulation efficiency and particle size and morphology of the final aqueous suspensions.

## 2. EXPERIMENTAL SECTION

### 2.1 Materials

Quercetin Hydrate ($C_{15}H_{10}O7xH_2O$, 95% purity, CAS: 849061-97-8) was obtained from Acros Organics (New Jersey, USA). The surfactant material poly-(ethylene glycol)- block –poly-(propylene glycol)- block -poly-(ethylene glycol) (Pluronic L64®, CAS: 9003-11-6) was obtained from Sigma Aldrich (St Louis, USA). Soy-bean lecithin was obtained from Glama-Sot (SOTYA, Madrid, Spain). Ethyl Acetate (EtAc, CAS: 141-78-6) and methanol (MeOH, CAS: 67-56-1), with a purity of 99% and 99.9 %, respectively, were obtained from Panreac Química (Barcelona, Spain). Acetonitrile (CAS: 75-05-8); acetic acid (reference number: 211008.1211) with a purity of 99.9% and 99.5 %, respectively, were obtained from Panreac Química (Barcelona, Spain). Carbon dioxide was provided by Carburos Metálicos (Barcelona, Spain).

## 2.2 Emulsion preparation and supercritical extraction of the emulsion

The initial emulsion was prepared using an Ultraturrax IKA LABOR-PILOT 2000/4 (IKA-WERKE GMBH&CO.KG) high frequency mixing device with a cooling jacket. The required amount of quercetin was dissolved in an organic solvent (ethyl acetate), and a required amount of surfactant material (Pluronic L64 or lecithin) was dissolved in water, purified by Millipore Elix. Then these two solutions were mixed together by a magnetic stirring for 5 minutes, in order to obtain a homogeneous dispersion. Afterwards, the dispersion was mixed by the Ultraturrax emulsifier at 70 Hz frequency for a predefined time.

To extract the organic solvent from the initially prepared emulsion, a batch SFEE equipment – presented on **Fig 2** – was used. The equipment consists of two vessels: an extractor vessel with a volume of 85 mL, and a buffer vessel with a volume of 100 mL. The vessels are located in a thermostated oven, and are separable from each other by two valves.

Firstly, the equipment was pressurized with $scCO_2$ and thermostated (typically, at 110 bar and 40ºC). Afterwards 25 mL of the initially prepared emulsion was injected by an HPLC pump (Jasco PU-2080) into the extraction vessel. The emulsion was loaded after the pressurization of the system, as otherwise the disturbances caused by the addition of $CO_2$ can spill the emulsion out from the extraction vessel into the recirculation circuit, making it difficult to recollect the treated emulsion after the experiment. Then the HPLC pump was isolated from the circuit by closing the valve in its impulsion, and the $CO_2$ recirculation pump was switched on, starting the circulation of the $scCO_2$ between the $CO_2$ buffer vessel and the extraction vessel. During this process, $scCO_2$ was bubbled through the emulsion, in order to extract the organic solvent from it. As the $scCO_2$ gradually became saturated with organic solvent during this batch extraction process, it was partially renewed several times in each experiment, in order to increase the efficiency of the extraction. To do so, the extraction vessel was isolated from the recirculation circuit by closing the valves in its inlet and outlet connections, in order to

maintain the extraction vessel at a constant pressure, meanwhile the $CO_2$ was renewed in the rest of the circuit, thus minimizing the disturbances and losses of emulsion by entrapment in $CO_2$ during the repeated depressurization processes needed for each $CO_2$ renewal. Considering that the volume of the extraction vessel is 85 mL and it contains 25 mL of liquid emulsion, meanwhile the volume of the buffer vessel is 100 mL, it is estimated that approximately 60% of $CO_2$ in the circuit was renewed with this procedure. After several cycles, the complete system was slowly depressurized, and the aqueous suspension – got from the emulsion by SFEE treatment – was retrieved from the extraction vessel and stored for analysis.

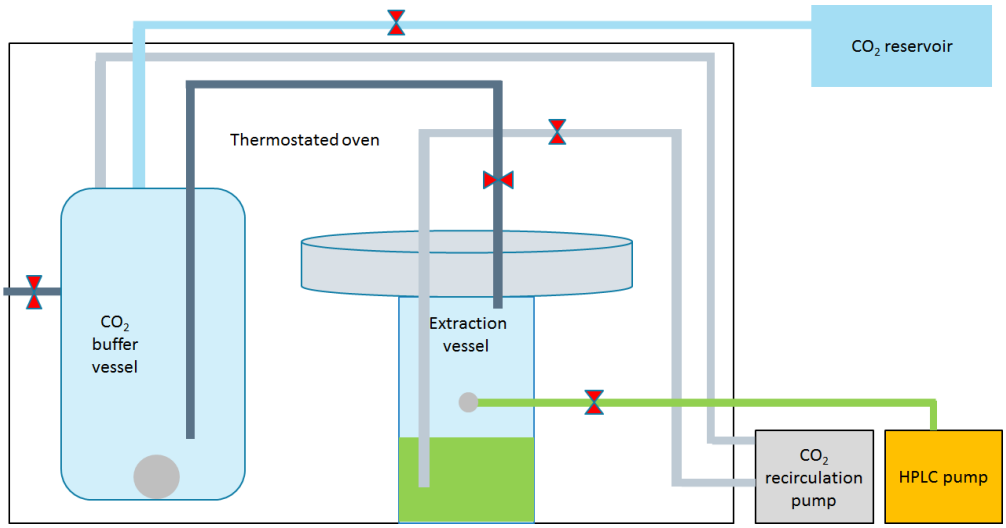


**Fig 2:** Schematic diagram of batch Supercritical Extraction of Emulsions (SFEE) equipment

## 2.3 Analytical methods

### 2.3.1 Initial emulsion stability measurement by laser diffraction

A TurbiScan Classic laser scattering device (Formulaction, France) was used in order to determine the average droplet size in the initial emulsion and to characterize its possible destabilization by creaming processes [21], due to the lower viscosity of organic droplets with respect to the continuous aqueous phase. For this, a glass vial was filled at 5.5 cm height with the sample, and inserted into the device, and the delta back scattering (ΔBS%) was recorded every 10 minutes for 8 hours. Observations for creaming were made, and the data were computed using Migration Software Version 1.3, equipped in the TurbiScan [22]. Typically the slope of the cream peak thickness kinetics was first identified. The linear portion of this slope was zoomed and copied into the Migration Software, from where the migration rate (equivalent to the creaming index), which characterizes the breakage velocity and therefore the instability of the emulsion, is computed. The software calculates the hydrodynamic mean particle diameter (equivalent diameter) from particle migration velocity V [m/s], continuous phase viscosity and density, dispersed phase density and volume fraction, using the General Settling Law [23].

### 2.3.2 Particle size distribution measurement and morphological characterization

A Malvern Mastersizer 2000 Light Scattering device from Malvern Instruments was used in order to define the particle size distribution in the final aqueous suspension after SFEE treatment. This equipment is able to measure particle size between 0.02 – 2000 μm, using a diode laser 4 mW with a dual – wavelength detection system (red light 633 nm, blue light 436 nm). The sample was diluted by deionized water in the dispersion unit (Hydro SM) to obtain an adequate level of laser obscuration and prevent multiple scattering effects. The refractive index of the dispersed phase (water) is 1.331, meanwhile for quercetin particles is 1.823. Each measurement was performed triplicate.

Additionally, visual observations of the initial emulsions, and SFEE-treated aqueous suspensions were done by microscopy in order to obtain information about the morphology of the initial emulsion and the final suspension, and to confirm the size measurements, obtained by laser diffraction. Two different techniques were used depending on the particle size of the analysed samples: optical microscopy, using a Leica microscope for initial emulsion, and Cryo - TEM technology using a GATAN PB3 Cryoplunge equipment to freeze and carbon coat the sample. The carbon coated samples were analysed by a JEOL JEM-FS2200 HRP 200 kV TEM equipment with electron filtering, to obtain micrographs of the frozen samples of the final suspensions after the SFEE treatment, when lecithin was used as surfactant material, due to the too low particle size of samples for optical microscopy.

Fourier Transform Infrared Spectroscopy (FTIR) measurements were done by ALPHA PLATINUM – ATR device equipped with a high throughput ZnSe ATR crystal, produced by BRUKER. Before FTIR measurement, samples were dried in a thermostated oven under 0,1 bar vacuum for two days at 35°C, in order to remove the adsorbed water and solvents, while avoid the degradation of quercetin.

X-Ray diffraction (XRD) patterns of dried samples were determined by a BRUKER D8 DISCOVER A25 device, Generator 3KW, Ceramic cupper tube 2.2 KW type FFF, in order to determine the crystallinity of lecithin encapsulated quercetin samples. Samples were prepared similar way than in case of FTIR measurements.

### 2.3.3 Residual organic content

The remaining organic solvent concentration after SFEE treatment was measured by Head Space Gas Chromatography. Measurements were done three times in different days, in order to determine the reliability of measurements and to evaluate the standard deviations of measurements.

In order to perform the chromatographic analysis, 4 mL of sample were introduced in a 10 mL vial, and this vial was hermetically closed with a septum. The vial was heated for 1 hour in an oven at 40º C, and after that time, a sample of the vapour of the upper part of the vial (headspace) was taken with a 1000 µL syringe and introduced into the chromatograph. The syringe must be filled 3 times with that same vapour in order to homogenize its content.

The apparatus used for this analysis was an Agilent Technologies 7890A gas chromatograph with a flame ionization detector (FID), with a HP-5 5% phenyl-methyl-silicone 30 m x 32 m x 25 µm column. The operating conditions for the analysis were: injector temperature 200º C, detector temperature 200º C, column temperature 80 ºC, injector flow rate 24 mL/min, column flow rate 1 mL/min (He) and split (sample dilution) 70:1.

### 2.3.4 Quercetin concentration

Quercetin concentration after SFEE treatment was determined by two different methods, depending on the surfactant material used in the experiments. In case of Pluronic L64, quercetin content in the aqueous suspension was determined by UV-VIS spectroscopy using a Shimadzu UV-2550 spectrophotometer. Measurements were done at a wavelength of 373 nm. Samples were diluted in 20 volumes of acetone before measurement. In addition, long term stability measurements of remained quercetin were also done, keeping the samples in fridge at 4ºC at least one month after the experiment.

In samples with lecithin as carrier material, it was not possible to determine the concentration of quercetin by UV-VIS spectroscopy due to the interference of lecithin in the absorption spectra [24]. In this case, quercetin concentration was determined by HPLC using a Waters 2487 chromatography system, consisting of a Waters In-Line degasser, Waters 515 HPLC pump and Waters 717 Plus Autosampler device. The injection volume of samples was 20 µL. The mobile phase was acetonitrile / milliQ water containing acetic acid in 5 V/V% concentration with a flowrate of 1 mL/minute. The method used a Pre-column, Guard cartridge

package 2 from BIO-RAD: Bio-Sil C18 HL90-5 30 X 4.6 mm with a pore size 5 µm. The column was Waters Symmetry ® C18 150 X 4.6 mm with a pore size 5 µm, thermostated at 30°C. The detector was Waters 2784 Dual λ absorbance detector set on wavelength of 373 nm in order to determine the quercetin concentration with a retention time 8.32 min. Each sample was measured twice: one without centrifugation, and one with 30 min 2.3 g centrifugation (Spectrafuge 240, Labnet International Inc., NJ, USA) in order to separate sedimented crystals. Furthermore samples were diluted 5 times in volume by MeOH and filtered by 2.2 µm pore size PTFE filters. To quantify the concentration of quercetin, a calibration line was developed from analysis of standard solutions of quercetin dissolved in a solution of methanol / water = 70 / 30 (V/V%), in the concentration range from 25 to 200 µg/mL.

2.3.5 Antioxidant activity

Oxygen radical absorbance capacity (ORAC) measurements were also made in order to measure the ability of the antioxidant species, present in the sample to inhibit the oxidation of disodium fluorescein (FL) catalysed by peroxyl radicals generated from α, α'-Azodiisobutyramidine Dihydrochloride porum (AAPH). In a 96-well micro plate 25 µL of the appropriate sample dilution were added together with 150 µL of disodium fluorescein (10 nM). The micro plate was put in a fluorescent reader that allowed incubating the samples at 37ºC for 30 minutes. The reaction was started with 25 µL of AAPH (240 mM). Fluorescence emitted by the reduced form FL was measured in an BMG LABTECH Fluostar OPTIMA fluorescent reader, recorded every 1 min at the emission wavelength of 530±25 nm and excitation wavelength of 485±20 nm for a period of 90 min. Phosphate buffer (75 mM, pH=7.4) was used to prepare AAPH and FL solutions, and was also used as blank. Standards went from 13 till 200 µM Trolox, and additionally one independent control sample was also prepared. Samples and an independent control sample were analysed six times, blank and standards three times. Final ORAC values were calculated by a regression equation between the Trolox concentration

and the net area under the FL decay curve and expressed as µM Trolox Equivalents per gram of quercetin (µM TE/g quercetin). Samples were centrifuged by 2.3 g, diluted 50 times by milliQ water and filtered by 2.2 µm pore size PTFE filters [25].

## 2.4 Experimental plans and statistical analysis of results

A design of experiments was established in order to determine the significant factors influencing the final particle size distribution and quercetin recovery ratio in the SFEE treated aqueous suspensions. The design of experiments involved an analysis of process parameters changed in two levels with a full resolution plan together with three centrum point measurements, in order to determine the reproducibility of experiments and the linearity of the influencing factors. Experimental plans were analysed by the Statistica software using the DOE experimental analyses tool.

According to several articles, regarding to supercritical fluid extraction of emulsion technology, there is a significant correlation between the droplet size in initial emulsion and the final particle size distribution [18], [20]. Thus, as a preliminary study, in the first set of the experiments the main process parameters analysed were those expected to influence the properties of the initial emulsion: quercetin concentration (0.02 – 0.04 w/w%), Pluronic L64 concentration (0.6 – 1 w/w%), organic/water ratio (0.2 – 0.3) and emulsifying time ( 2 – 6 min). In five cases SFEE treatment of the emulsion was completed as well, in order to determine the required number of cycles and duration of cycles of SFEE treatment according to the final particle size distribution and residual organic content.

According to the results of the first experimental plan, a second experimental plan (three factors varied in two levels, full resolution with three centrum point measurements) was performed to study the effect of Pluronic L64 concentration (0.8 – 1.2 w/w%), quercetin concentration (0.02

– 0.03 w/w%) and organic/water ratio (0.25 – 0.35), in the remaining organic solvent, average final particle size in aqueous suspension and quercetin recovery ratio after SFEE treatment. Finally, a similar experimental plan (three factors varied in two levels with three centrum point measurements, not full resolution), was completed using lecithin as carrier material instead of Pluronic L64, in order to determine the significant factors influencing the average droplet size in initial emulsion, particle size distribution in SFEE treated aqueous suspensions, and quercetin recovery ratio. Varied factors were: concentration of lecithin (1.6 – 2 w/w%), concentration of quercetin (0.020 – 0.028 w/w%) and organic/water ratio (0.25 – 0.3).

## 3. RESULTS AND DISCUSSION

### 3.1 Extraction efficiency of organic solvent

As a preliminary study, ethyl acetate-on-water emulsions stabilized by Pluronic L64 were treated by SFEE applying different extraction times, in order to optimize the requested treatment time decreasing the residual organic content under 100 ppm. This value is well below the restriction of FDA: 5000 ppm, corresponding with 50 mg/day [26]. Five drying cycles were applied with varying cycle times, with an extraction pressure of 10 MPa and an extraction temperature of 40ºC. The results are reported in **Table 1**. In order to decrease the remained organic solvent below 100 ppm, treatment time should be around 575 min. A further increase in SFEE treatment time is not advisable since particles could aggregate or degrade due to the longer treatment time, and there is no significant reduction in the residual ethyl acetate content. Considering this, in all further SFEE experiments, five extraction cycles with a total extraction time of 575 min were used, with the following extraction times in each cycle: 20 min in the 1$^{st}$ cycle, 90 min in the 2$^{nd}$ cycle, 120 min in the 3$^{rd}$ cycle, 135 min for in 4$^{th}$ cycle and 210 min in the 5$^{th}$ and last cycle, with longer extraction times in the last cycles, because as the

concentration of solvent in the initial emulsion becomes smaller, more time is required for saturation of the carbon dioxide used for the extraction.

**Table 1:** Variation of the residual organic content after SFEE treatment as a function of the total extraction time

| Total Extraction Time [min] | Residual organic content [ppm] |
|---|---|
| 581 | 14 |
| 529 | 48 |
| 496 | 113 |
| 577 | 200 |
| 572 | 18 |

### 3.2 Emulsification of ethyl acetate in water using Pluronic L64 as surfactant: variation of emulsion properties with emulsification conditions

As presented in **Table 2**, an experimental plan was completed in order to determine the significant factors influencing the average emulsion droplet size in the initial emulsion. **Fig 3** shows an optical microscopy picture of a typical initial emulsion, whose average droplet size, according to TurbiScan Classic laser diffraction device, was 2.5 µm. As shown in this figure, a homogeneous droplet size was obtained, demonstrating that the conditions employed were appropriate for producing an emulsion with the required characteristics of a small droplet size and a high homogeneity. Furthermore, droplet sizes determined by an image analysis technique are equivalent to the average droplet sizes measured by TurbiScan, confirming the reliability of the TurbiScan size measurements.

**Table 2:** Experimental plan for studying the effect of factors influencing initial emulsion droplet size

| Standard run | Ethyl acetate/water ratio [mL/mL] | Quercetin concentration [w/w%] | Pluronic concentration [w/w%] | Emulsifying time [min] | Average droplet size in initial emulsion [µm] |
|---|---|---|---|---|---|
| 1 | 0.2 | 0.02 | 0.6 | 6 | 2.6 |
| 2 | 0.2 | 0.04 | 0.6 | 6 | 2.3 |
| 3 | 0.2 | 0.02 | 1.0 | 6 | 3.9 |
| 4 | 0.2 | 0.04 | 1.0 | 6 | 5.1 |
| 5 | 0.3 | 0.02 | 0.6 | 6 | 4.1 |
| 6 | 0.3 | 0.04 | 0.6 | 6 | 4.0 |
| 7 | 0.3 | 0.02 | 1.0 | 6 | 2.9 |
| 8 | 0.3 | 0.04 | 1.0 | 6 | 2.8 |
| 9 | 0.2 | 0.02 | 0.6 | 2 | 4.1 |
| 10 | 0.2 | 0.04 | 0.6 | 2 | 2.2 |
| 11 | 0.2 | 0.02 | 1.0 | 2 | 4.0 |
| 12 | 0.2 | 0.04 | 1.0 | 2 | 4.9 |
| 13 | 0.3 | 0.02 | 0.6 | 2 | 4.5 |
| 14 | 0.3 | 0.04 | 0.6 | 2 | 4.4 |
| 15 | 0.3 | 0.02 | 1.0 | 2 | 3.6 |
| 16 | 0.3 | 0.04 | 1.0 | 2 | 3.3 |
| 17 (C) | 0.25 | 0.03 | 0.8 | 4 | 2.9 |
| 18 (C) | 0.25 | 0.03 | 0.8 | 4 | 2.4 |
| 19 (C) | 0.25 | 0.03 | 0.8 | 4 | 1.9 |

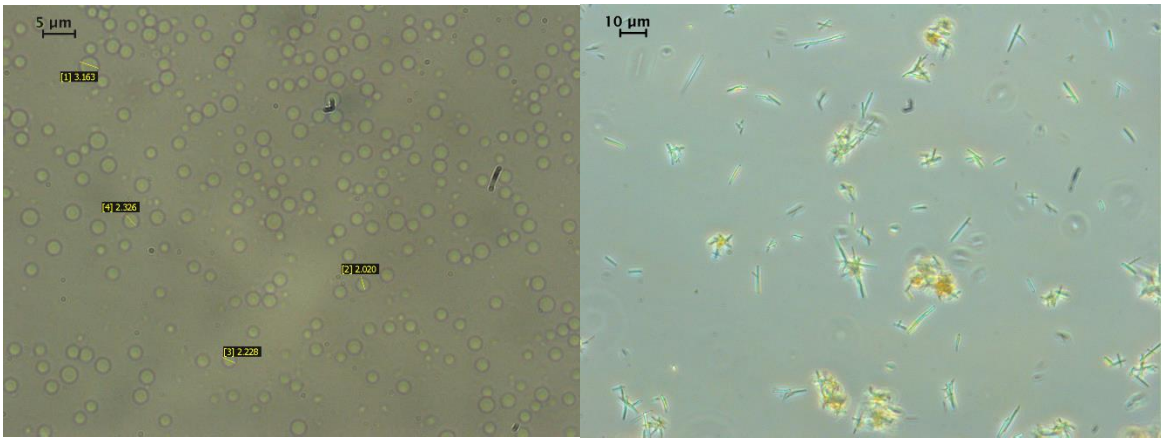


**Fig 3:** Experiments with Pluronic L64 surfactant: Optical microscopy picture of the initially prepared emulsion (left) and of aqueous suspension of quercetin particles obtained by SFEE treatment of the emulsion (right). Inserts show sizes measured by an image analysis technique

**Fig 4** presents the results obtained from the statistical analysis of the results of the experimental plan presented in Table 2 as surface response plots. According to centrum point measurements, a linear model is not suitable for all of the factors, so it is necessary to use a quadratic model as well. Significant factors in 95% confidence level are the combination of the concentration of Pluronic L64 and EtAc. With higher concentrations of both compounds, smaller droplet diameters could be obtained in the initial emulsion (Figure 4). Another significant factor, according to a quadratic model, is the emulsification time. The optimum emulsification time was 4 minutes (Figure 4), with larger emulsion droplet sizes when either the emulsification time was too short for a complete homogenization of the system, or too high leading to an increased droplet size probably due to coalescence and temperature effects. According to these results and S. Varona et al. [27], a fixed emulsification time of 4 minutes was employed in all remaining experiments. Concentration of quercetin was not a significant factor on the average droplet size of initial emulsion.

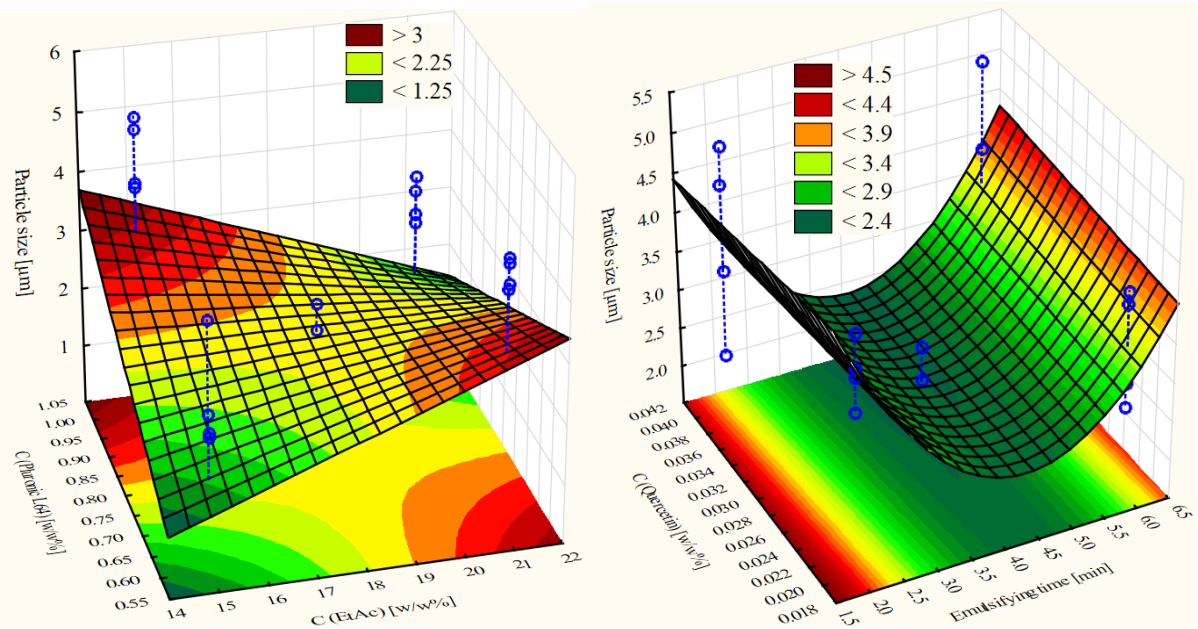


**Fig 4:** Surface plot of influencing factors on average droplet size of initial emulsion

### 3.3 Supercritical Fluid Extraction of Emulsions stabilized with Pluronic L64

**Table 3** shows the experimental plan completed in order to study the Supercritical Extraction of Emulsions using Pluronic L64 as surfactant. **Fig 3** shows a micrograph of quercetin particles obtained after SFEE treatment. As presented in this figure, long needle-like particles were obtained showing some agglomeration. Furthermore, **Fig 5** presents typical particle size distributions. Probably due to the needle morphology of crystals obtained in experiments in every cases, the particle size distributions were multimodal. However, it must be noted, that due to the needle-like morphology, the accuracy of particle size measurements probably is not high, because the measured dimensions of the crystals depend on the spatial orientation of crystals in the measurement cells during measurement. As reported in **Table 3**, in the experiments with the best results according to the mean particle size marked bold, the residual EtAc content was under 300 ppm and the proportion of particles with a size below 10 µm was higher than 30% (V/V%). According to UV-VIS measurements, in every case around 70% of the initially added quercetin was recovered in the SFEE treated aqueous suspension,

corresponding to quercetin concentrations in the range of 0.160 – 0.245 g/L, and in every cases the quercetin content was stable up to two months, with samples stored in glass vials at ~4°C.

**Table 3:** Experimental plan for studying the effect of factors of Supercritical Fluid Extraction of Emulsions prepared with Pluronic L64 on final particle size, quercetin recovery and residual organic solvent concentration (Best results according to final particle size and residual organic content marked by Bold)

| **Experi-ment** | **Solvent/ water ratio [ml/ml]** | **Quercetin concent-ration [w/w%]** | **Pluronic concent-ration [w/w%]** | **Quer-cetin recovery [%]** | **Average droplet size in initial emulsion [µm]** | **D(0.5) [µm]** | **Under 10 µm [V/V%]** | **Residu-al EtAc [ppm]** |
|---|---|---|---|---|---|---|---|---|
| 1 (C) | 0.30 | 0.02 | 1.0 | 64.7 | 2.3 | 778.6 | 10.2 | 259 |
| 2 (C) | 0.30 | 0.02 | 1.0 | 70.0 | 2.4 | 150.6 | 15.0 | 354 |
| 3 (C) | 0.30 | 0.02 | 1.0 | 72.8 | 2.9 | 462.2 | 5.0 | 233 |
| 4 | 0.25 | 0.02 | 0.8 | 64.7 | 3.0 | 389.1 | 15.0 | 134 |
| **5** | **0.25** | **0.03** | **0.8** | **66.6** | **2.1** | **13.4** | **37.5** | **170** |
| **6** | **0.25** | **0.03** | **0.8** | **65.6** | **2.1** | **0.9** | **79.5** | **140** |
| 7 | 0.25 | 0.02 | 1.2 | 70.8 | 2.7 | 163.9 | 15.7 | 107 |
| 8 | 0.25 | 0.03 | 1.2 | 71.1 | 1.9 | 108.4 | 22.2 | 1684 |
| 9 | 0.35 | 0.02 | 0.8 | 69.1 | 3.4 | 126.2 | 26.1 | 2317 |
| 10 | 0.35 | 0.03 | 0.8 | 73.1 | 3.6 | 93.6 | 25.6 | 2361 |
| 11 | 0.35 | 0.02 | 1.2 | 73.0 | 2.6 | 87.3 | 23.2 | 2608 |
| 12 | 0.35 | 0.03 | 1.2 | 69.7 | 2.5 | 7.8 | 52.6 | 1436 |
| 13 | 0.35 | 0.03 | 1.2 | 68.0 | 3.1 | 3.2 | 64.6 | 1623 |

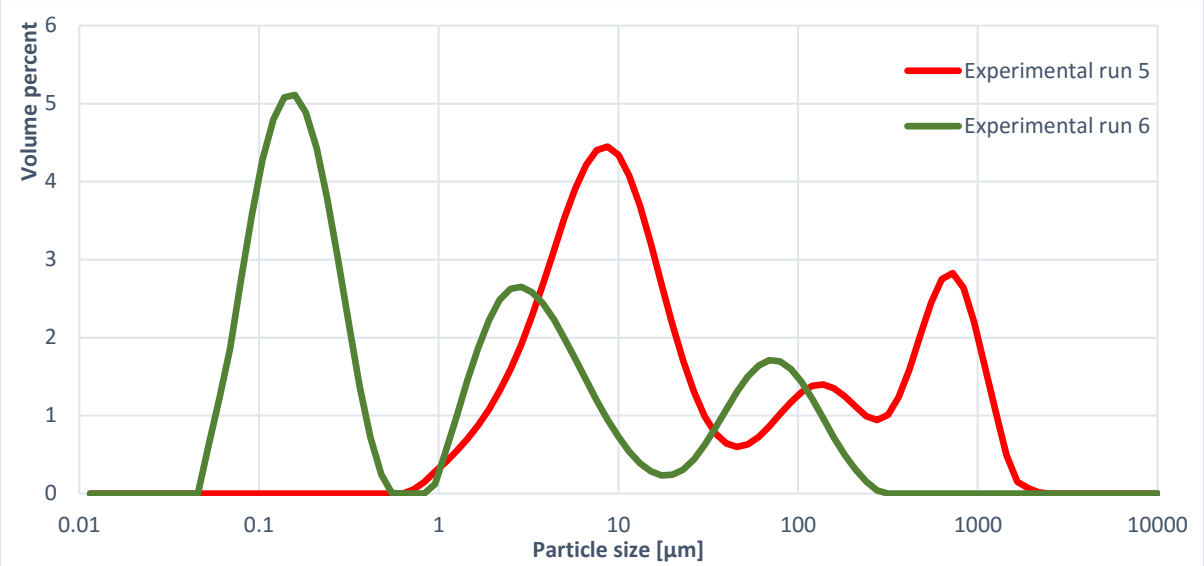


**Fig 5:** Example for multimodal particle size distribution with Pluronic L64: experimental run 5 indicated by red, experimental run 5 indicated by green.

According to the statistical analysis of results, presented in the Pareto chart shown in **Fig 6**, final particle size distribution were influenced by the concentration of quercetin, according to linear model, and concentration of EtAc, according to a quadratic model. In order to decrease the particle size, it is necessary to increase the concentration of quercetin, and to choose an optimal concentration of EtAc. If the initial concentration of EtAc is high, high residual organic solvent concentrations are observed in the final product, which can also influence the formation of particles, meanwhile if the concentration of EtAc is too low, it is possible that solvent is removed and particles formed already in the first cycles of the extraction, and particles start to aggregate or degrade along the remaining treatment time. On the other hand, there is no significant factor influencing the quercetin recovery ratio.

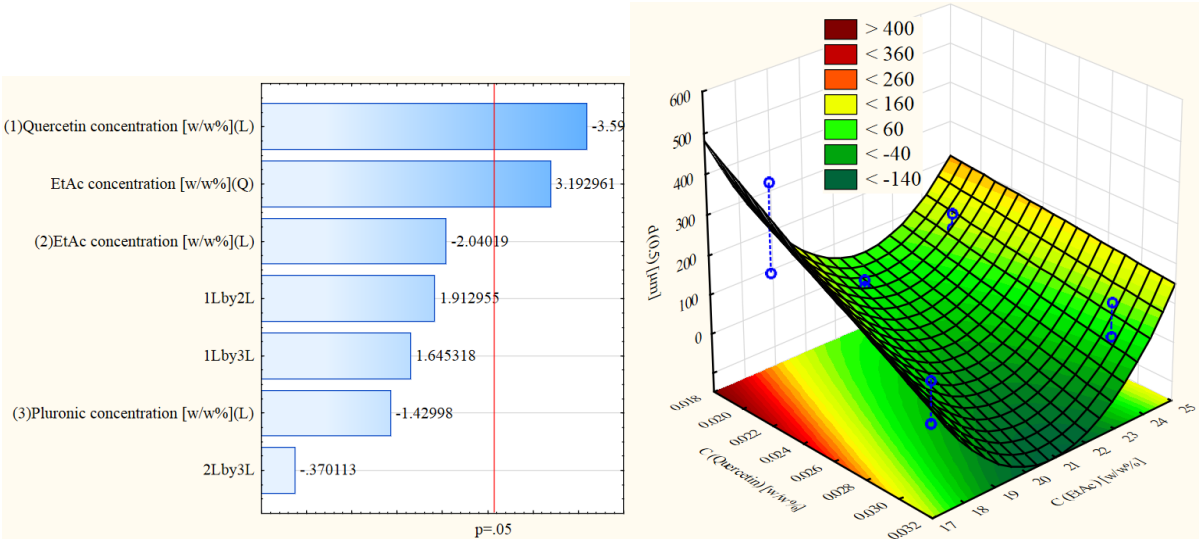


**Fig 6:** Influencing factors for particle size distribution in SFEE treated aqueous suspension

The results of the statistical analysis indicate, that the outcome of the precipitation mainly depended on the initial concentration of quercetin in the original solution, which is a determinant factor for an antisolvent precipitation from a homogeneous solution, and it was not influenced by the parameters, that significantly influenced the droplet size of the emulsion, such as the concentration of surfactant, or the organic/water ratio. These results of the statistical analysis agree with the morphology presented in the micrograph of **Fig 3**, which as previously described, showed large crystalline particles of quercetin, which apparently were not encapsulated or dispersed by the surfactant material. Indeed, the morphologies and sizes – obtained and shown in this Figure – are similar to the results reported by Fraile et al. by precipitation of quercetin by SAS process from quercetin – acetone homogenous solutions, changing the initial concentration of quercetin. In the work of Fraile et al., morphology and particle size depended on the initial concentration of quercetin: with increasing quercetin concentration, particle size decreased. Precipitated quercetin crystals also showed needle-like morphology, agglomerated in flocks of about 1 µm scale [17]. Considering these results, it can be concluded, that Pluronic L64 is not a suitable material to encapsulate quercetin, as the

precipitation occurred as in a normal anti-solvent process, and the surfactant did not provide any additional control over particle size through the formation of an emulsion template.

### 3.4 Preparation of emulsions using lecithin as surfactant

In this section, an experimental plan was completed, using lecithin as surfactant material, as reported in **Table 4**, analysing the process parameters (solvent/water ratio, quercetin concentration and lecithin concentration) with a significant influence regarding the average droplet size in initial emulsion, as well as final particle size distribution and quercetin recovery in SFEE treated aqueous suspensions.

As presented in **Table 5**, the droplet size of the initial emulsions prepared with lecithin, showed smaller variations with process conditions than those observed in experiments with Pluronic L64 and reported in **Table 2**. According to the statistical analysis of the results presented in **Table 4**, factors influencing the average droplet size in initial emulsion were the concentration of lecithin and the concentration of EtAc. The concentration of lecithin should be increased in order to decrease the droplet size in initial emulsion, while the concentration of EtAc should be decreased.

In addition, to a smaller droplet size and smaller variability of this size (**Table 4** and **Table 5**), the use of lecithin as surfactant provided a better stability of the emulsion. This is shown in the results presented in **Table 5**, that summarize the measurements of emulsion stability, performed with the Turbiscan apparatus. As presented in this table, the migration rate which is related to the emulsion destabilization by the creaming effect, was less than half in emulsions prepared with lecithin, than in emulsions prepared with Pluronic L64®.

**Table 4** Experimental plan for studying the effect of factors on emulsion droplet size, final particle size, quercetin recovery and residual organic solvent concentration (Centrum point measurements marked by (C), best result according to final particle size distribution marked by Bold)

| Experiment | Solvent/ /water ratio [ml/ml] | Quercetin concent-ration [w/w%] | Lecithin concent-ration [w/w%] | Quercet-in recove-ry [%] | Droplet size in initial emulsion [μm] | D (0.5) [μm] | Under 1 μm [V/V%] | Mode [μm] | Resi-dual EtAc [ppm] |
|---|---|---|---|---|---|---|---|---|---|
| **1** | **0.20** | **0.020** | **2.0** | **74.1** | **1.3** | **0.19** | **77.7** | **0.127-0.172** | **24** |
| 2 | 0.20 | 0.028 | 1.6 | 49.3 | 1.4 | 6.384 | 36.6 | 0.134-0.181 | 18 |
| 3 | 0.30 | 0.020 | 1.6 | 67.3 | 1.9 | 0.257 | 65.4 | 0.140-0.191 | 23 |
| 4 | 0.30 | 0.028 | 2.0 | 66.9 | 1.6 | 0.548 | 52.8 | 0.137-0.186 | 26 |
| 5 (C) | 0.25 | 0.024 | 1.8 | 57.7 | 1.9 | 0.3 | 60.0 | 0.130-0.177 | 177 |
| 6 (C) | 0.25 | 0.024 | 1.8 | 74.0 | 1.9 | 0.426 | 55.1 | 0.130-0.177 | 7 |
| 7 (C) | 0.25 | 0.024 | 1.8 | 68.2 | 1.9 | 0.426 | 55.4 | 0.138-0.158 | 82 |
| 8 | 0.20 | 0.020 | 2.0 | 37.1 | 1.5 | 1.229 | 47.1 | 0.138-0.158 | 10 |
| 9 | 0.20 | 0.02 | 3.3 | 34.8 | 1.1 | 0.631 | 54.8 | 0.138-0.158 | 62 |

**Table 5:** Stability of ethyl acetate-on-water emulsions prepared with Pluronic L64 and lecithin surfactants

| **Surfactant material** | **Pluronic L64** | **Lecithin** |
|---|---|---|
| **Range of solvent/water ratio [mL/mL]** | 0.25 – 0.35 | 0.2 – 0.23 |
| **Surfactant concentration range [w/w%]** | 0.8 – 1.2 | 1.6 – 2.0 |
| **Migration rate between [mm/min]** | $3.37 \cdot 10^{-3}$ – $8.60 \cdot 10^{-3}$ | $1.58 \cdot 10^{-3}$ – $3.63 \cdot 10^{-3}$ |
| **Standard deviation of migration rate** | $1.67 \cdot 10^{-3}$ | $6.40 \cdot 10^{-4}$ |
| **Average droplet size [µm]** | 2.6 | 1.6 |
| **Droplet size changing between [µm]** | 1.9 – 3.4 | 1.1 – 1.9 |
| **Standard deviance of droplet size [µm]** | 0.48 | 0.27 |

### 3.5 Supercritical Fluid Extraction of Emulsions stabilized with Lecithin

**Table 4** reports the main results obtained after SFEE treatment of emulsions prepared with lecithin. As shown in **Fig 7**, after SFEE treatment, multimodal particle size distributions were obtained, with a main peak in the sub-micrometer size range, and additional peaks at larger sizes, that probably corresponded to a small number of large quercetin crystals that were not encapsulated in lecithin, in some cases visible for the naked eye.

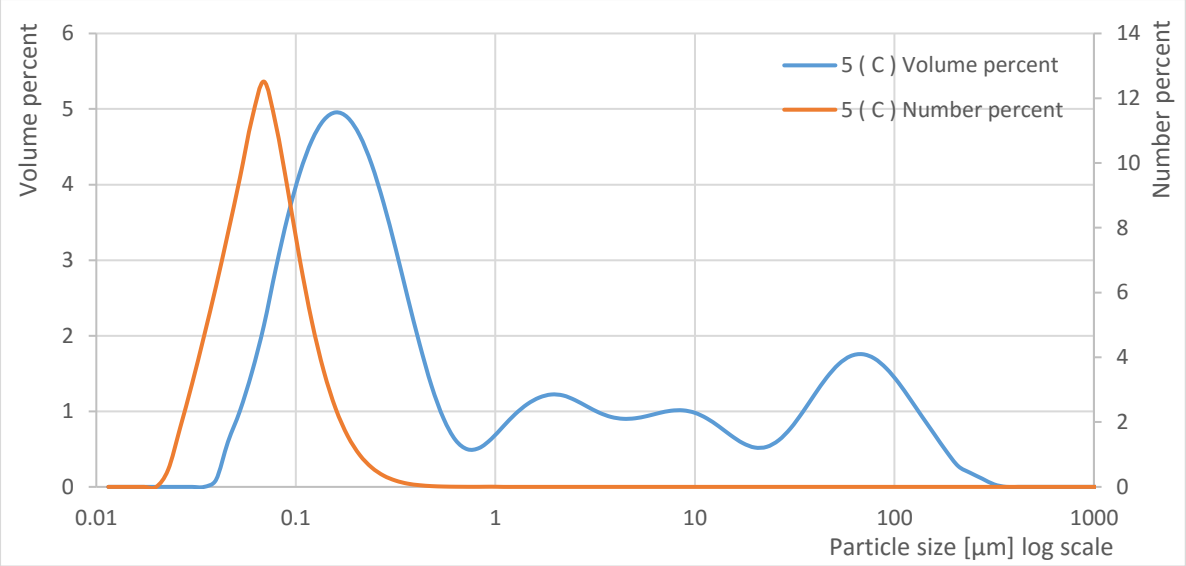


**Fig 7:** Final particle size distribution of SFEE treated emulsions prepared with lecithin, according to volume percent and number percent

The morphology of particles obtained after SFEE treatment can be observed in the TEM micrographs presented in **Fig 8**. The micrographs showed vesicles of lecithin formed in the aqueous media, without presence of segregated quercetin crystals. The size observed, correspond well with the measurements obtained by laser diffraction, reported in **Table 4**. In experiments performed with higher lecithin concentration, TEM micrographs showed bigger particles due to the formation of multi-layered vesicles (**Fig 8** C). One experimental run was done without quercetin (other settings are the same as in the case of centrum point runs), in order to can compare by TEM the structure of the system with and without quercetin (**Fig 8** D). Multivesicular system is observed in all cases (expect of the one with higher lecithin concentration, **Fig 8** C), without any variation in the morphology due to the presence of quercetin, which further indicates that segregated crystals of quercetin were not formed, and therefore did not alter the morphology of the vesicles.

Regarding the influence of process parameters, if experimental results are analysed considering the average particle size D(0.5), inconclusive results with weak dependencies in all process parameters are obtained, due to the low reproducibility of the tail of the particle size

distribution, that probably corresponds to the fraction of quercetin that was not encapsulated inside the lecithin (**Fig 7**). In contrast, analysing the fraction of particles with a size below 1 µm, which can be considered as a quantitative estimation of the proportion of particles that showed an appropriate encapsulation in lecithin, a far less sensitive dependency on varied factors was observed, and only the concentration of quercetin and lecithin proved to be significant. As presented in **Fig 9**, in order to get more particles under 1 µm according to a linear model, the concentration of quercetin should be decreased, while the concentration of lecithin should be increased. Furthermore, as presented in **Table 4**, the mode of the particle size distribution which corresponds to the mean particle size of the sub-micrometric particles (**Fig 7**), practically does not show any variations between experiments, with values in a range between 130 and 190 nm. The very small correlation between this size and the initial emulsion properties observed in this work, is in contrast with the correspondence between these two values reported in previous works [12], [20]. This is probably due to the small variation of the properties of emulsions prepared with lecithin, with process conditions described in section 3.4.

The average of recovered quercetin after SFEE is 65.4 %, corresponding to concentrations in the range of 0.16 – 0.2 g/L, depending on the initially added quercetin. This result is approximately 16 – 20 times higher than the solubility of quercetin in pure water (0.01 g/l) [28], indicating that it was possible to substantially increase the amount of quercetin, that could be stabilized in the aqueous suspension by encapsulation in lecithin liposomes. No significant factor was found to influence the quercetin recovery. According to **Figure 10**, lecithin encapsulated quercetin was stable up to 14 days. This means, that the degradation of quercetin, the crystallization process of quercetin out of lyposomes, or growing of already existing quercetin crystals are very slow.

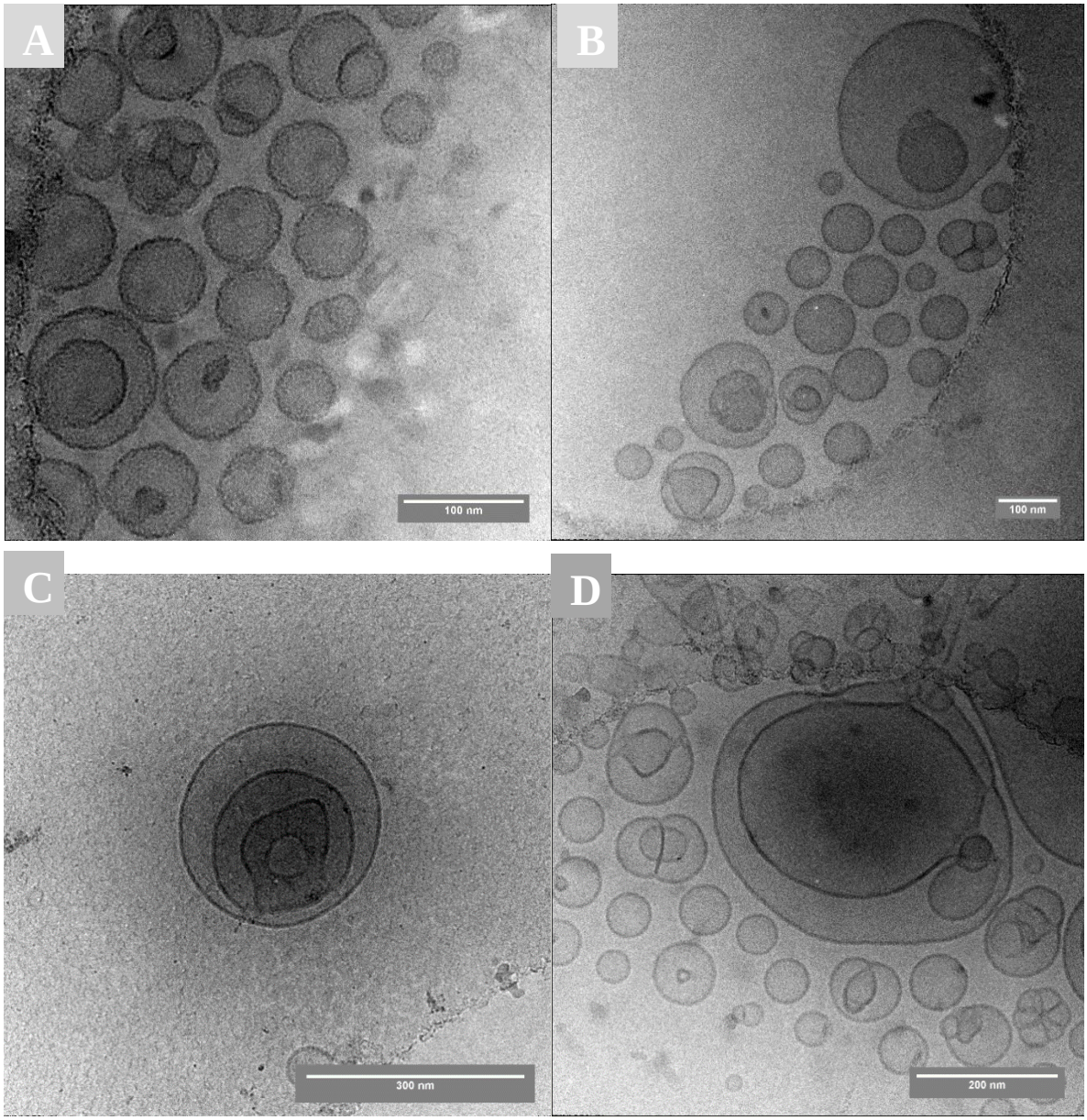


**Fig 8:** TEM micrographs of particles obtained after SFEE treatment of quercetin emulsion prepared with lecithin: Experimental run 1 of **Table 4** (A), Experimental run 8 (B), Experimental run 9 (C) and centrum point run without quercetin (D).

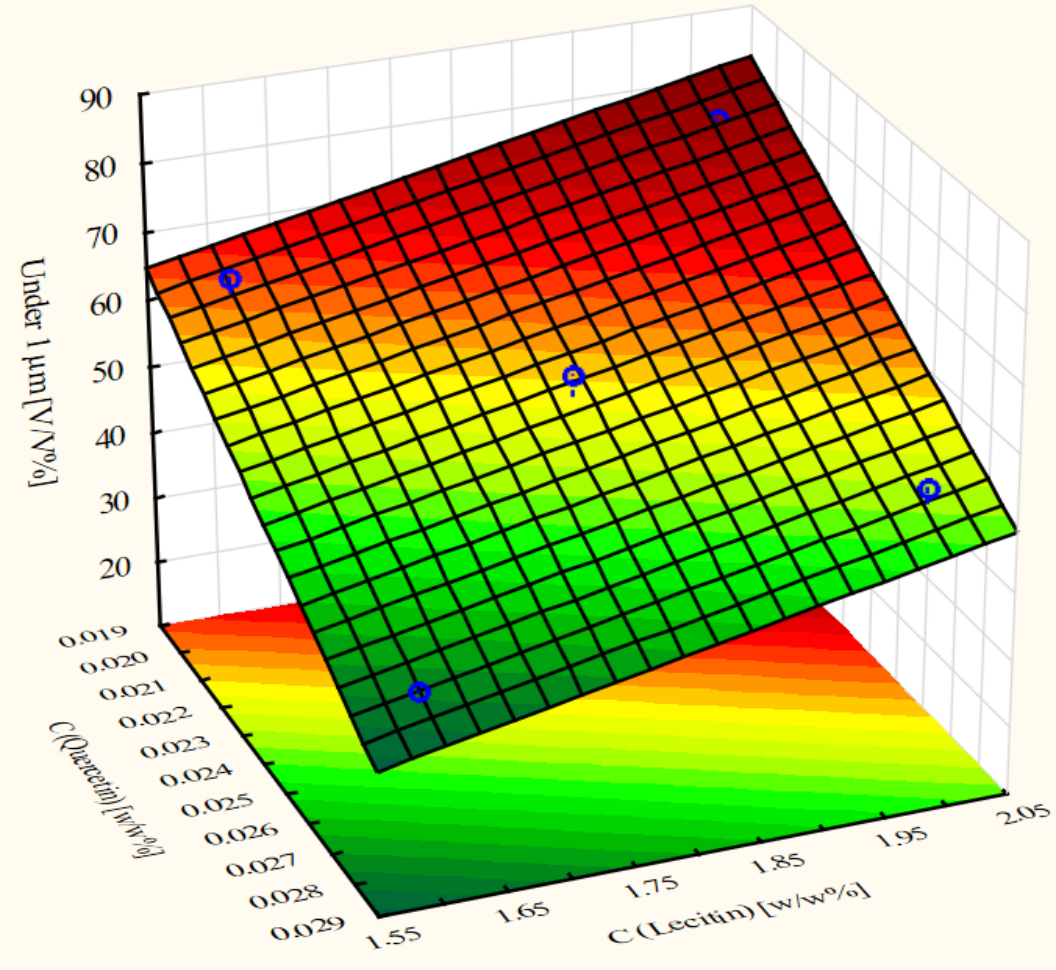


**Fig 9:** Surface diagram of influencing factors to final particle size distribution according to volume percent of particles under 1 µm

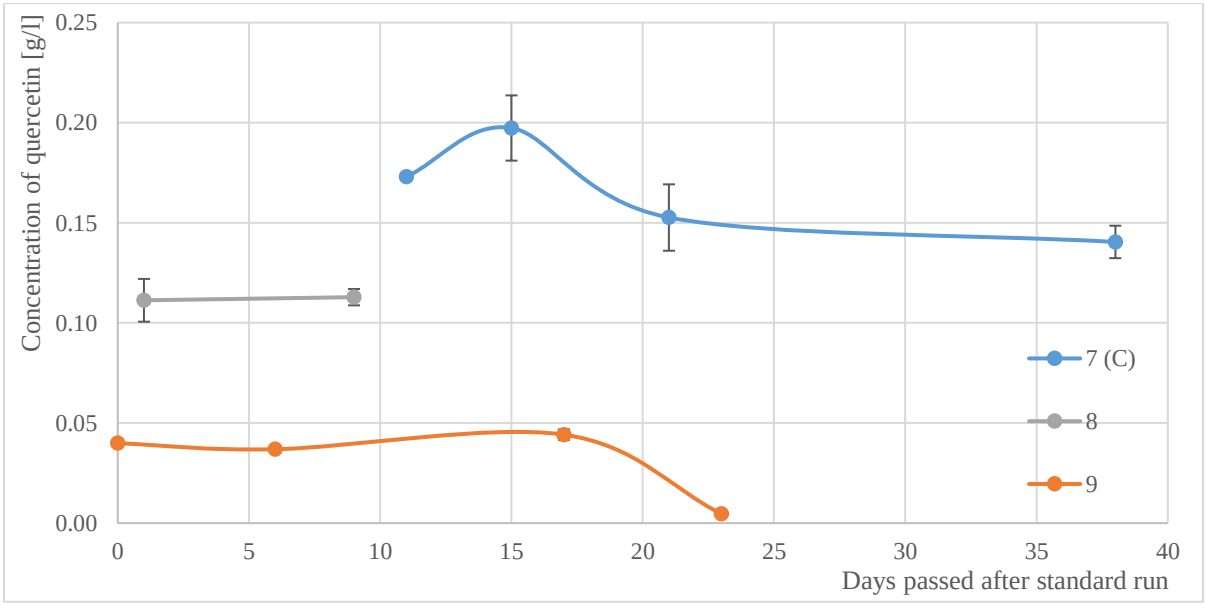


**Figure 10:** Stability of quercetin after experimental run

### 3.6 Structural characterization

Several SFEE treated aqueous suspensions where characterized by FT-IR spectroscopy in order to determine the mechanism of encapsulation of quercetin by lecithin. As presented in **Fig 11**, pure quercetin show its characteristics peaks in the range of 1600 – 1100 $cm^{-1}$, and OH – phenolic bending: 1400 – 1200 $cm^{-1}$ [29]. Lecithin shows characteristic peaks in the range of 1765 – 970 (at 1765-1720 $cm^{-1}$ corresponding to C=O, 1200-1145 $cm^{-1}$ corresponding to P=O, 1145-970 $cm^{-1}$ corresponding to P-O-C, and 1200-970 $cm^{-1}$ corresponding to P-O-C + $PO_2$) [30].

According to FTIR spectra's presented on **Fig 11**, it can be observed that the characteristic peaks of quercetin are not present in the spectra of the SFEE treated sample. In contrast, a quercetin – lecithin physical mixture's spectra shows characteristic peaks of quercetin around 1625 $cm^{-1}$ and 1170 $cm^{-1}$. This result indicates, that in the SFEE treated sample quercetin is encapsulated by the lecithin, and it not presents as segregated crystals.

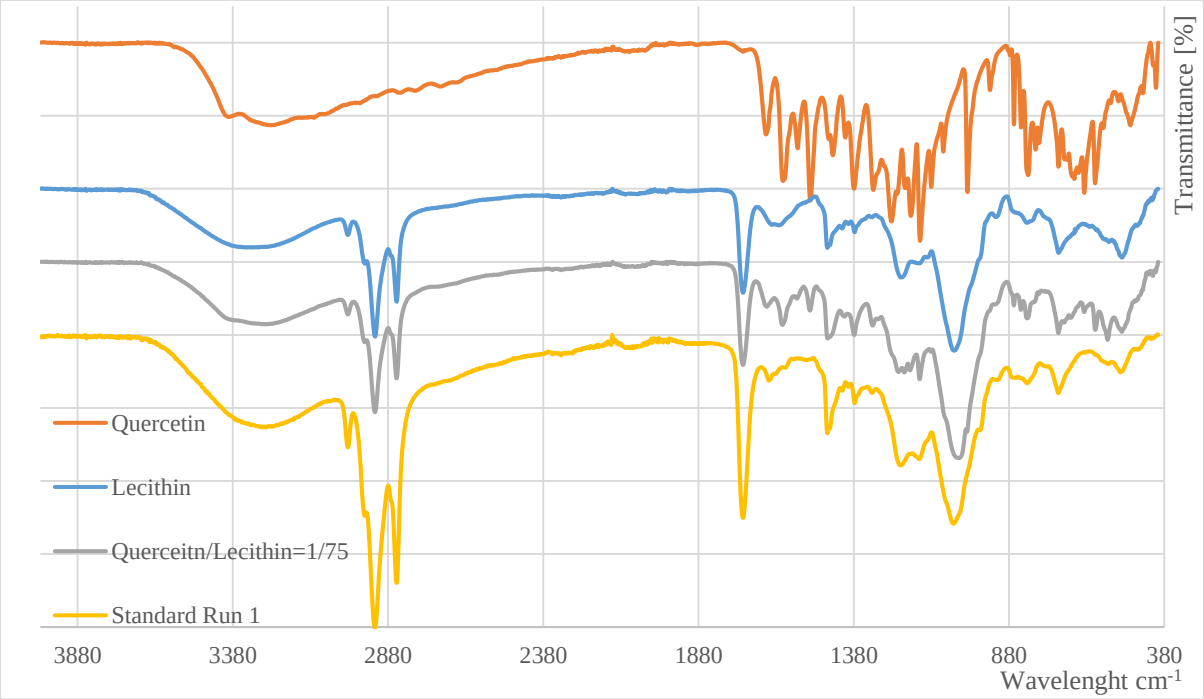


**Fig 11:** FTIR spectra of pure quercetin, pure lecithin, quercetin – lecithin physical mixture, Standard Run 1

An XRD spectra of physical mixture of quercetin/lecithin = 1/75 in mass and experimental run 1 and 8 were measured also by XRD, in order to examine the encapsulation of quercetin by lecithin. In order to directly analyse the aqueous suspensions without drying, samples from experimental runs were disposed on the surface of a silica slide, and their spectra was corrected as well of the spectra of the pure silica slide. As visible on the spectra presented on **Fig 12**, lecithin presents a peak at 20°, meanwhile pure quercetin has high crystallinity and presents its characteristics peaks at 2θ values: 10.78°, 12.46°, 15.88°, and two more prominent peaks at 25.66°, and 27.4° [31], [32]. According to the XRD spectra, physical mixture and the experimental runs have similar spectra than pure lecithin has, conforming that encapsulation of quercetin is performed without the formation of segregated crystals.

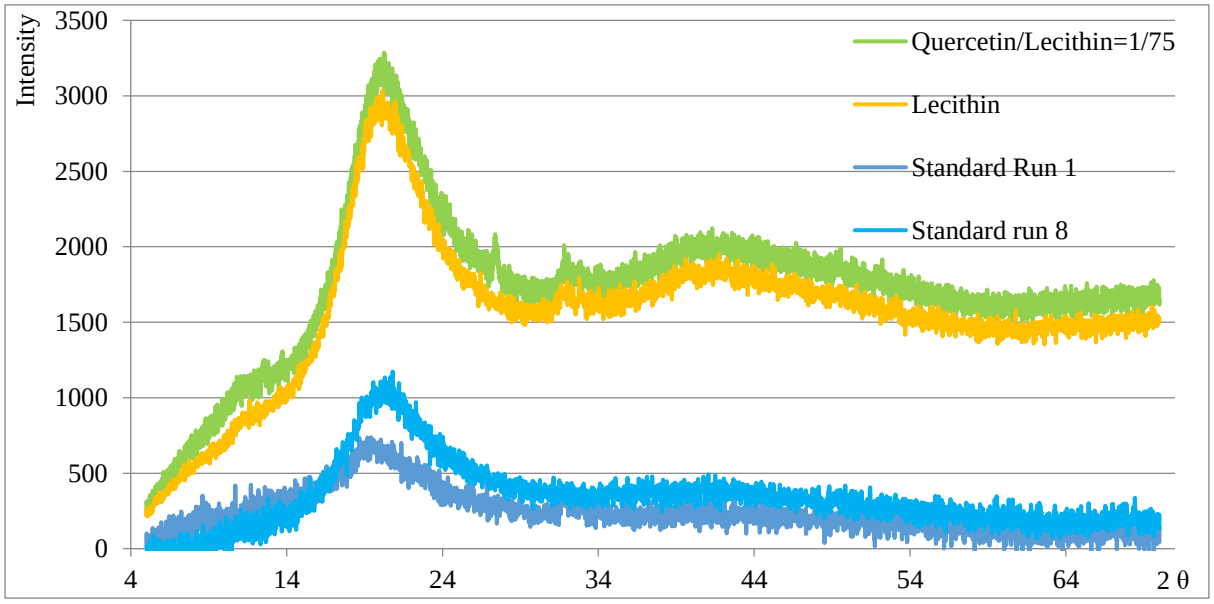


**Fig 12:** X-Ray diffraction spectra of pure lecithin, quercetin – lecithin physical mixture, Experimental run 1 and 8

### 3.7 Antioxidant activity

The antioxidant activity of some of the SFEE treated samples was measured by ORAC as well. In agreement with Fraile et al. [17], the antioxidant activity of unprocessed crystalline quercetin (prepared in EtOH (abs.) / water milliQ = 1 / 1 in volume) determined in this work is 6300 ± 300 µM Trolox equivalent / g of quercetin. The antioxidant activity of soy-bean lecithin samples are also presented in **Fig 13**, reported as µM Trolox equivalent / g of lecithin. SFEE treated lecithin sample (experimental run without quercetin, other settings are the same as in the case of centrum point runs) has a non-measurable and negligible antioxidant activity comparing to lecithin only dissolved in water milliQ. This drastic reduction of the antioxidant activity can be due to a partial extraction of low molecular weight antioxidant compounds of lecithin during the supercritical $CO_2$ treatment, such as sterols.

Furthermore, quercetin – lecithin physical mixtures in different mass ratios (quercetin / lecithin = 1 / 36; quercetin / lecithin = 1 / 75 and the same as the centrum point standard runs; quercetin / lecithin = 1 / 160 and an equal mass ratio as experimental run 9) were also prepared in a solution EtOH (abs.) / water milliQ = 1 / 1 in volume, in order to compare the antioxidant activity of pure physical mixtures (without SFEE treatment) with antioxidant activities of treated samples. As shown on **Fig 13**, quercetin – lecithin physical mixtures have an increased antioxidant activity, comparing to pure, unprocessed quercetin, due to an antioxidant synergism effect: there are chain structures formation between quercetin and phosphatidyl-choline, linked by hydrogen bonds [2]. The antioxidant activity of physical mixtures (reported as a function of the amount of quercetin in the sample) is independent on the mass ratio of quercetin / lecithin. Quercetin encapsulated in lecithin by SFEE treatment also shows a higher antioxidant activity than pure quercetin. However, as in the case of pure lecithin, SFEE treated quercetin-lecithin samples show lower antioxidant activity than physical mixtures of the two compounds, again probably due to the loss of low molecular weight antioxidant compounds of lecithin, or due to

destruction of previously mentioned chain structures between soy-bean lecithin and quercetin during the $CO_2$ extraction process.

Analyzing the results of SFEE treated samples, in case of experimental run 8, the antioxidant activity is not changing significantly in the following 10 days after the experiment. Furthermore, antioxidant activity of experimental run 7 (C) also did not change significantly after 10 days. Moreover, an increased antioxidant activity is obtained in experimental run 9 (with an increased lecithin concentration, quercetin / lecithin ~ 1 / 160 in mass ratio) comparing with the other SFEE treated samples.

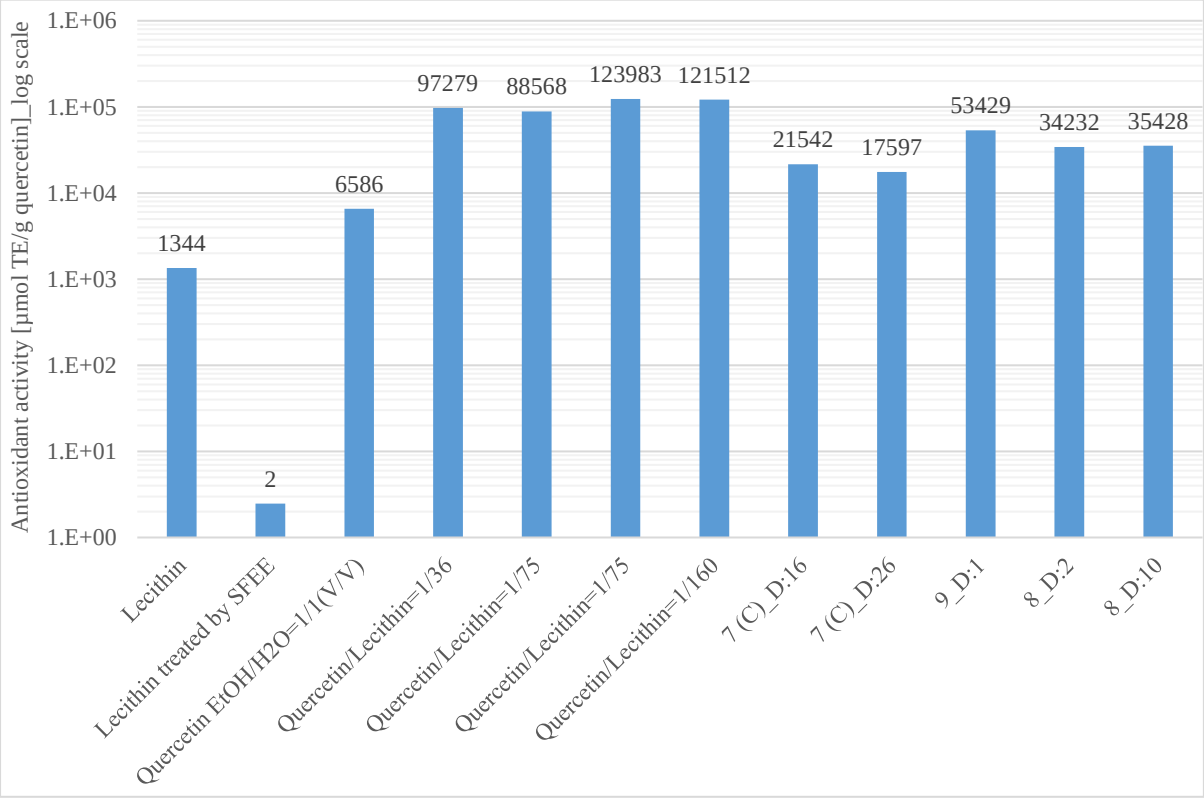


**Fig 13:** ORAC measurement results, "D" indicate the days passed between SFEE treatment and ORAC measurement

## 4. CONCLUSION

In this work encapsulated quercetin microparticles were produced by SFEE from an initially prepared oil in water emulsion. Two types of surfactant material were tried: Pluronic L64® and soy-bean lecithin. Pluronic is not a suitable material to encapsulate quercetin, because micrometric crystalline particles of quercetin were obtained without encapsulation, meanwhile with soy-bean lecithin, multivesicular system was obtained in sub-micrometric scale, with an encapsulation efficiency around 70%, encapsulated quercetin stable up to two weeks and residual organic content below 300 ppm, and without presence of crystalline quercetin particles. The antioxidant activity of quercetin was enhanced by encapsulation in lecithin, in agreement with previous reports that describe a synergistic effect of these two compounds, but the antioxidant activity decreased by SFEE treatment, perhaps due to a partial extraction of low molecular weight fractions of soy-bean lecithin by supercritical $CO_2$.

**Acknowledgements**

This research has been funded by the European Initial Training Network FP7-PEOPLE 2012 ITN 316959, "DoHip", and by Junta de Castilla y León with project VA225U14. Á. Martín thanks the Spanish Ministry of Economy and Competitiveness for a Ramón y Cajal research fellowship. S. Rodríguez-Rojo thanks the Spanish Ministry of Economy and Competitiveness for a Juan de la Cierva research fellowship.

**REREFENCES**

[1] S. Das, A.K. Mandal, A. Ghosh, S. Panda, N. Das, S. Sarkar, Nanoparticulated quercetin in combating age related cerebral oxidative injury, Curr Aging Sci. 1 (2008) 169–174. http://www.ncbi.nlm.nih.gov/entrez/query.fcgi?cmd=Retrieve&db=PubMed&dopt=Citation&list_uids=20021389.

[2] M.F. Ramadan, Antioxidant characteristics of phenolipids (quercetin-enriched lecithin) in lipid matrices, Ind. Crops Prod. 36 (2012) 363–369. doi:10.1016/j.indcrop.2011.10.008.

[3] A. Parmar, K. Singh, A. Bahadur, G. Marangoni, P. Bahadur, Interaction and solubilization of some phenolic antioxidants in Pluronic?? micelles, Colloids Surfaces B Biointerfaces. 86 (2011) 319–326. doi:10.1016/j.colsurfb.2011.04.015.

[4] Y. Gao, Y. Wang, Y. Ma, A. Yu, F. Cai, W. Shao, G. Zhai, Formulation optimization and in situ absorption in rat intestinal tract of quercetin-loaded microemulsion, Colloids Surfaces B Biointerfaces. 71 (2009) 306–314. doi:10.1016/j.colsurfb.2009.03.005.

[5] T.-H. Wu, F.-L. Yen, L.-T. Lin, T.-R. Tsai, C.-C. Lin, T.-M. Cham, Preparation, physicochemical characterization, and antioxidant effects of quercetin nanoparticles., Int. J. Pharm. 346 (2008) 160–8. doi:10.1016/j.ijpharm.2007.06.036.

[6] S. Chakraborty, S. Stalin, N. Das, S. Thakur Choudhury, S. Ghosh, S. Swarnakar, The use of nano-quercetin to arrest mitochondrial damage and MMP-9 upregulation during prevention of gastric inflammation induced by ethanol in rat, Biomaterials. 33 (2012) 2991–3001. doi:10.1016/j.biomaterials.2011.12.037.

[7] Khaled A. Khaled, Yousry M. El-Sayeda, Badr M. Al-Hadiyab, Disposition of the Flavonoid Quercetin in Rats After Single Intravenous and Oral Doses, Drug Dev. Ind. Pharm. 29 (2003) 397–403. doi:10.1081/DDC-120018375.

[8] R. Gugler, M. Leschik, H.J. Dengler, Disposition of quercetin in man after single oral and intravenous doses, Eur. J. Clin. Pharmacol. 9 (1975) 229–234. doi:10.1007/BF00614022.

[9] P.J. Mulholland, D.R. Ferry, D. Anderson, S.A. Hussain, A.M. Young, J.E. Cook, E. Hodgkin, L.W. Seymour, D.J. Kerr, Pre-clinical and clinical study of QC12, a water-soluble, pro-drug of quercetin., Ann. Oncol. 12 (2001) 245–248.

[10] T. Pralhad, K. Rajendrakumar, Study of freeze-dried quercetin-cyclodextrin binary systems by DSC, FT-IR, X-ray diffraction and SEM analysis, J. Pharm. Biomed. Anal. 34 (2004) 333–339. doi:10.1016/S0731-7085(03)00529-6.

[11] Z.P. Yuan, L.J. Chen, L.Y. Fan, M.H. Tang, G.L. Yang, H.S. Yang, X.B. Du, G.Q. Wang, W.X. Yao, Q.M. Zhao, B. Ye, R. Wang, P. Diao, W. Zhang, H. Bin Wu, X. Zhao, Y.Q. Wei, Liposomal quercetin efficiently suppresses growth of solid tumors in murine models, Clin. Cancer Res. 12 (2006) 3193–3199. doi:10.1158/1078-0432.CCR-05-2365.

[12] H. Li, X. Zhao, Y. Ma, G. Zhai, L. Li, H. Lou, Enhancement of gastrointestinal absorption of quercetin by solid lipid nanoparticles, J. Control. Release. 133 (2009) 238–244. doi:10.1016/j.jconrel.2008.10.002.

[13] A. Chafer, T. Fornari, A. Berna, R.P. Stateva, Solubility of quercetin in supercritical CO2 + ethanol as a modifier: Measurements and thermodynamic modelling, J. Supercrit. Fluids. 32 (2004) 89–96. doi:10.1016/j.supflu.2004.02.005.

[14] X. Liu, Z. Li, B. Han, T. Yuan, Supercritical Antisolvent Precipitation of Microparticles of Quercetin, Chinese J. Chem. Eng. 13 (2005) 128–130. http://www.cjche.com.cn/EN/abstract/abstract474.shtml#.

[15] D.T. Santos, M.A.A. Meireles, Micronization and encapsulation of functional pigments using supercritical carbon dioxide, J. Food Process Eng. 36 (2013) 36–49. doi:10.1111/j.1745-4530.2011.00651.x.

[16] P. Alessi, A. Cortesi, N. De Zordi, T. Gamse, I. Kikic, M. Moneghini, D. Solinas, Supercritical Antisolvent Precipitation of Quercetin Systems: Preliminary Experiments, Chem. Biochem. Eng. Q. 26 (2012) 391–398. <Go to ISI>://WOS:000314256800010.

[17] M. Fraile, R. Buratto, B. Gómez, Á. Martín, M.J. Cocero, Enhanced delivery of quercetin by encapsulation in poloxamers by supercritical antisolvent process, Ind. Eng. Chem. Res. 53 (2014) 4318–4327. doi:10.1021/ie5001136.

[18] B.Y. Shekunov, P. Chattopadhyay, J. Seitzinger, R. Huff, Nanoparticles of poorly water-soluble drugs prepared by supercritical fluid extraction of emulsions, Pharm. Res. 23 (2006) 196–204. doi:10.1007/s11095-005-8635-4.

[19] F. Mattea, A. Martin, A. Matias-Gago, M.J. Cocero, Supercritical antisolvent precipitation from an emulsion: beta-Carotene nanoparticle formation, J. Supercrit. Fluids. 51 (2009) 238–247. doi:10.1016/j.supflu.2009.08.013.

[20] D.T. Santos, Á. Martín, M.A.A. Meireles, M.J. Cocero, Production of stabilized sub-micrometric particles of carotenoids using supercritical fluid extraction of emulsions, J. Supercrit. Fluids. 61 (2012) 167–174. doi:10.1016/j.supflu.2011.09.011.

[21] E. Dickinson, Milk protein interfacial layers and the relationship to emulsion stability and rheology, Colloids Surfaces B Biointerfaces. 20 (2001) 197–210. doi:10.1016/S0927-7765(00)00204-6.

[22] O. Mengual, G. Meunier, I. Cayre, K. Puech, P. Snabre, Characterisation of instability of concentrated dispersions by a new optical analyser: The TURBISCAN MA 1000, Colloids Surfaces A Physicochem. Eng. Asp. 152 (1999) 111–123. doi:10.1016/S0927-7757(98)00680-3.

[23] P. Mills, P. Snabre, Settling of a Suspension of Hard Spheres, Europhys. Lett. 25 (1994) 651–656. doi:10.1209/0295-5075/25/9/003.

[24] N.S. Acharya, G. V. Parihar, S.R. Acharay, PHYTOSOMES: NOVEL APPROACH FOR DELIVERING HERBAL EXTRACT WITH IMPROVED BIOAVAILABILITY, Pharma Sci. Monit. An Int. J. Pharm. Sci. 2 (2011) 144–160.

[25] F. Ganske, B. Labtech, G.E.J. Offenburg, ORAC Assay on the FLUOstar OPTIMA to Determine Antioxidant Capacity, Bmglabtech.Com. (2006). http://www.bmglabtech.com/application-notes/fluorescence-intensity/orac-148.cfm.

[26] Purdief, Guidance for Industry Q3C — Tables and List Guidance for Industry Q3C — Tables and List Guidance for Industry Q3C — Tables and List, 9765 (2012) 301–827. http://www.fda.gov/Drugs/GuidanceComplianceRegulatoryInformation/Guidances/default.htm\nhttp://www.fda.gov/BiologicsBloodVaccines/GuidanceComplianceRegulatoryInformation/Guidances/default.htm.

[27] S. Varona, Á. Martín, M.J. Cocero, Formulation of a natural biocide based on lavandin essential oil by emulsification using modified starches, Chem. Eng. Process. Process Intensif. 48 (2009) 1121–1128. doi:10.1016/j.cep.2009.03.002.

[28] L. Chebil, C. Humeau, J. Anthony, F. Dehez, J.M. Engasser, M. Ghoul, Solubility of flavonoids in organic solvents, J. Chem. Eng. Data. 52 (2007) 1552–1556. doi:10.1021/je7001094.

[29] D. Bennet, M. Marimuthu, S. Kim, J. An, Dual drug-loaded nanoparticles on self-integrated scaffold for controlled delivery, Int. J. Nanomedicine. 7 (2012) 3399–3419. doi:10.2147/IJN.S32800.

[30] J.M. Nzai, a. Proctor, Soy lecithin phospholipid determination by fourier transform infrared spectroscopy and the acid digest/arseno-molybdate method: A comparative study, J. Am. Oil Chem. Soc. 76 (1999) 61–66. doi:10.1007/s11746-999-0048-9.

[31] A. Shawky, M. Ghanem, H. Saleh, M. Ali, S.M. El-shanawany, E.A. Ibrahim, Solubility and dissolution enhancement of quercetin via preparation of spray dried microstructured solid dispersions Abstract :, 37 (2013) 12–24.

[32] S. Scalia, M. Haghi, V. Losi, V. Trotta, P.M. Young, D. Traini, Quercetin solid lipid microparticles: A flavonoid for inhalation lung delivery, Eur. J. Pharm. Sci. 49 (2013) 278–285. doi:10.1016/j.ejps.2013.03.009.

# CHAPTER II

## MEASUREMENT AND MODELLING OF MASS TRANSPORT PROPERTIES IN SUPERCRITICAL CARBON-DIOXIDE – (ETAC/DCM BASED) OIL IN WATER EMULSION SYSTEMS

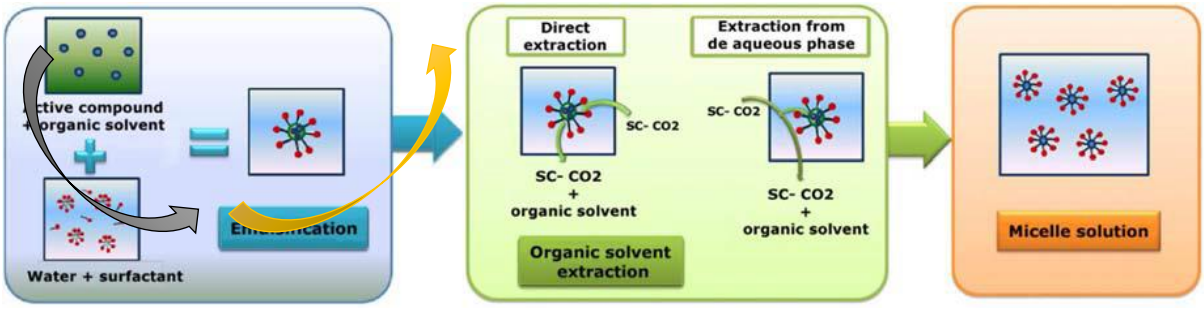


Supercritical Fluid Extraction of Emulsion (SFEE) process

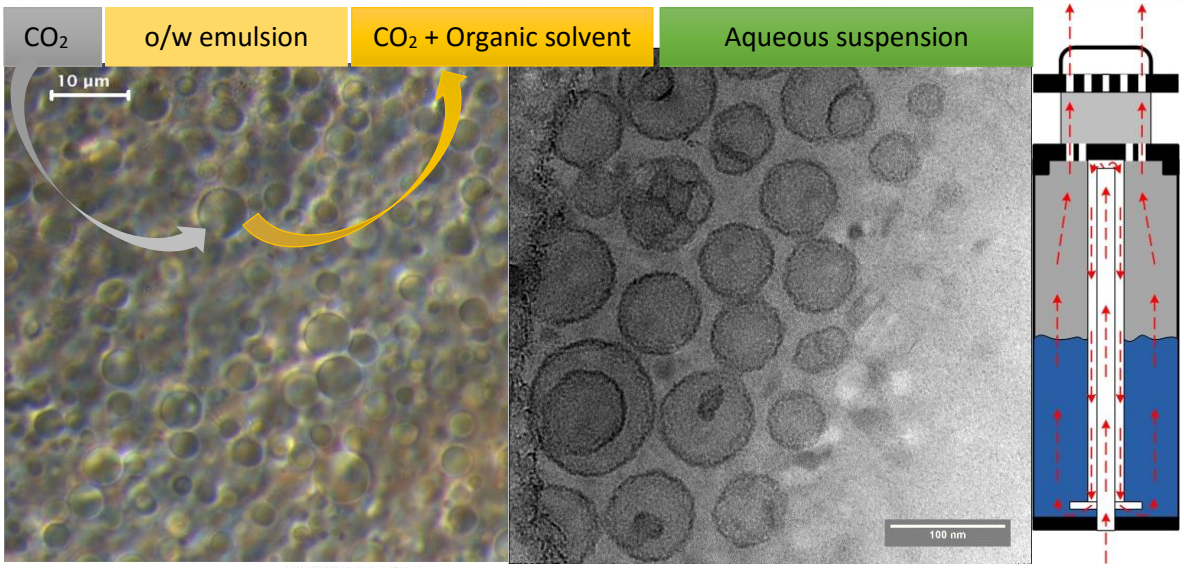


Sample holder with continuous $scCO_2$ flow through the o/w emulsion

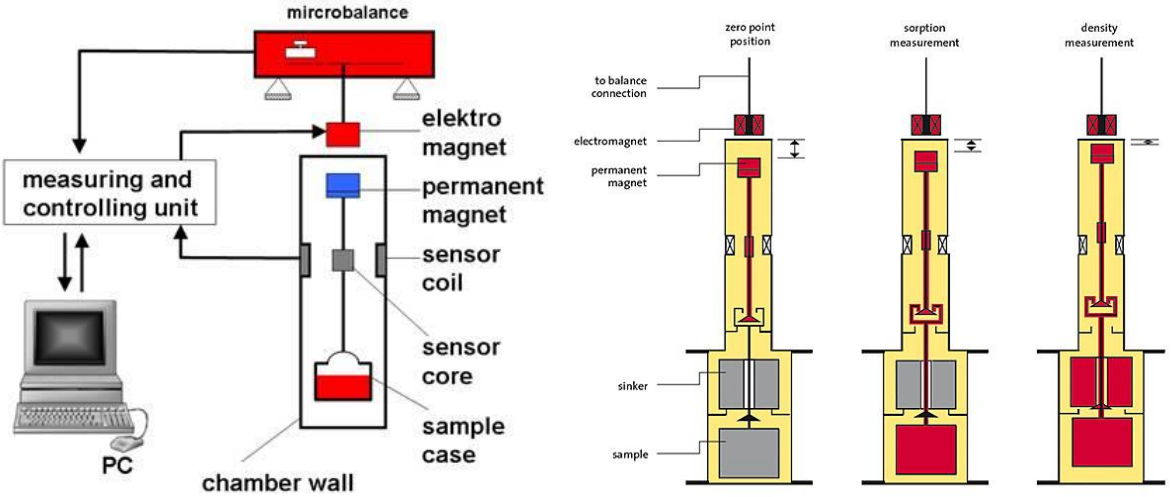


Magnetic Suspension Balance (MSB) device for static- and dynamic measurement

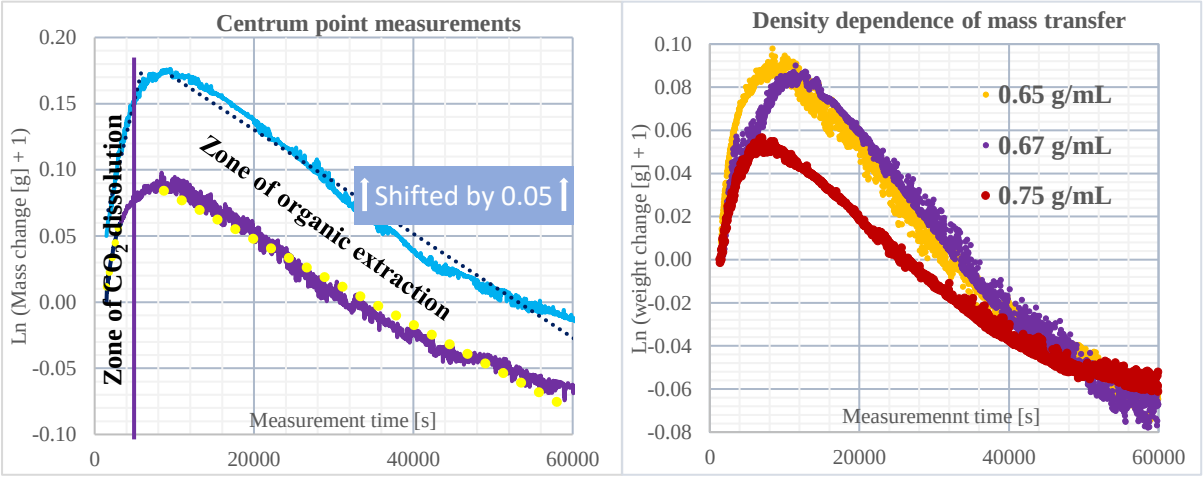


Results obtained in static measurements: EtAc/w – $scCO_2$ system

**ABSTRACT**

Supercritical Fluid Extraction of Emulsion (SFEE) technology is used for producing aqueous suspensions, containing encapsulated particles in nanometric scale. In SFEE technology a supercritical fluid is used for the rapid extraction of an organic phase from an initially prepared oil in water (o/w) emulsion, resulting the rapid supersaturation of the aqueous phase with the material of interest, and hence the precipitation of it in sub-micrometric range. Optimization of process conditions (pressure, temperature, initial concentration of surfactants, organic- and water phase and material of interest) is a key factor in SFEE process, as these conditions influence several process steps, such as atomization, diffusion, particle precipitation and agglomeration. In this work ethyl acetate and dichloromethane based o/w emulsions were prepared using soy-bean lecithin and/or Pluronic L64® as surfactant material, and contacted with supercritical carbon-dioxide ($scCO_2$). Mass transport properties of these systems were measured by magnetic suspension balances (MSB), which provide an on-line, contactless weight measurement method. Static and dynamic measurements with a continuous flow of $scCO_2$ through the emulsion were done, and a five parameters mass transfer model – based on the experimental results – was developed. According to the experimental results, the initial concentration of the surfactant materials and the organic phases are not influencing significantly the mass transport properties. Moreover, parameters with significant influence on the residual organic content were not found. Experimental and modelling results proved, that dichloromethane/w emulsion is not an adequate material for SFEE process, as phase separation occurs immediately upon pressurization, due to high interfacial tension between aqueous and organic phase.

**Keywords:** SFEE process; magnetic suspension balance; oil/water emulsion; supercritical carbon dioxide; mass transfer modelling; interfacial tension

## 1. INTRODUCTION

Technologies applying a certain kind of supercritical fluids are promising alternatives in the processing of natural bioactive compounds, as they allow to carry out the encapsulation and micronization process at near-ambient temperatures and in an inert atmosphere, and thus avoiding the thermal degradation or oxidation of the product, and reducing its contamination by organic solvents. The Supercritical Fluid Extraction of Emulsion (SFEE) technology is an alternative to precipitate and encapsulate bioactive compounds in nanometric scale, resulting in a higher specific surface area, and hence a higher solubility and bioavailability of these compounds.

SFEE technology can be considered as an evolution of Supercritical Anti Solvent (SAS) technology. It is especially suitable to encapsulate poorly water soluble drugs in an aqueous suspension. The process consists of forming an oil-in-water emulsion, containing the water-insoluble drug in the dispersed organic phase. In SFEE process the organic solvent is extracted from this emulsion by the supercritical solvent, which should have a high affinity to the organic solvent, and a small affinity to the active compound of interest. Due to this solubility differences, supercritical solvent quickly extracts the organic solvent from the emulsion, leading to the rapid super-saturation of the active compound, and hence its fast precipitation. While in the SAS precipitation method particle nucleation and growth occur across the whole solution volume, in the case of SFEE process, the formation of particles is confined within the emulsion droplets. This restrains the size of particles obtained by SFEE, that can be one order of magnitude smaller, than particles produced by SAS solution precipitation [1].

Several experimental results are available in the literature, showing that the size and the morphology of the produced particles as a key objective of micronization technology, is influenced by several parameters. However, optimization of process conditions its complex, as

these conditions influence several process steps, such as atomization, diffusion, precipitation, particle agglomeration etc. [2]. Therefore, modelling of supercritical processes, such as SAS, PGSS, SFEE is necessary, in order to be able to optimize process conditions, and hence product specifications.

Regarding SAS process, Werling and Debenedetti et al. studied the mass transfer between a droplet of toluene and supercritical carbon-dioxide ($scCO_2$), both in subcritical- [3] and supercritical conditions [4]. The main difference between these two conditions was, that at subcritical conditions (with a solvent-antisolvent mixture in the two-phase region), an interface always exists between the droplet and the antisolvent phases, while in supercritical conditions (where solvent and the antisolvent form a sinlge phase), there is no well-defined interface between the droplet and its environment. These authors also found, that at subcritical conditions the droplet diameter is initially increasing due to the condensation of $CO_2$ until the complete saturation is reached, and then evaporation of the droplet takes place. Elvassore et al. [5] extended the model of Werling and Debenedetti by including the solute in the calculations. They used this model to study the evolution of the precipitation front for different organic solvent-$CO_2$-solute systems. Lora et al. improved a mass transfer model based on Fick´s laws focusing on toluene - $CO_2$ system. Their simulation showed, that initially there is always an interfacial flux into the droplet due to the high solubility of $CO_2$ in the organic solvent [6]. Y. P. de Diego et al. also found, that initially the absorption of $CO_2$ by the liquid phase is always faster than the evaporation of solvent phase. Moreover, pressure and temperature have a complex effect on the mass transfer, as higher pressures enhance the atomization process, meanwhile temperature should be a compromised value, as it enhances the evaporation of organic phase, but also could be enhance the degradation of biologically active compounds [7]. Shekunov et al. [8] studied the paracetamol - ethanol - $CO_2$ system, and they attributed the swelling or shrinking of the droplets to the total molar flux to or from the droplet surface. Mukhopadhyay M. et al. [9]

presented a two-way mass transfer model between $CO_2$ and organic systems based on the SAS mechanism, which is taking into account the convective mass and heat transfer. As $CO_2$ dissolution in the organic phase is an exothermic process, meanwhile organic phase evaporation is an endothermic process, initially the temperature of the bulk of the droplet may increase, as heat of dissolution of $CO_2$ initially is higher, than the heat of evaporation of the solvent. However, the temperature of the $scCO_2$- and continuous water phase will not change significantly, as they act as an infinite medium, comparing to the organic phase. Therefore, initially the heat transfer should take place from the bulk of the droplet to the interphase, and this heat transfer causes later on the evaporation of the organic phase.

Results regarding the modelling of SFEE processes are more limited, as more constrains need to be taken into account, and evaporation of water phase is not taking place, and hence it persists acting as a diffusion layer. As o/w emulsion droplets in the model presented in the work of Mattea F. et al. [10] are taken into account as spherical droplets, convective mass transfer depends on the drop falling velocity, which is influenced by the gravity-, buoyancy- and drag force, acting on the drop. Moreover, as mass flow of $scCO_2$- and organic phase is simultaneously going through on the continuous water phase, in the model equations of Mattea F. et al. [10], a radial coordinate was taken into account, expressing the mass transfer change by the variation in the thickness of the water layer. Hence in SFEE process every single emulsion droplet is considered as a small Gas Antisolvent (GAS) precipitator [11], the final particle size distribution is influenced by the droplet size of the emulsion, hence process conditions of SFEE should be chosen not to destabilize the emulsion, and to avoid significant variations of emulsion droplets during the process. Mattea F. et al. [10] contacted β-carotene contained DCM/w emulsions (using n-octenyl succinic anhydride (OSA)-modified strach as surfactant material) with $scCO_2$, in order to study the evaluation of the organic content and the particle size distribution during the time of GAS process. They found, that the higher part of the organic phase was already

extracted in the first hour of the process, meanwhile two additional hours were needed to decrease the residual DCM content by two orders of magnitude more, and to obtain monomodal particle size distribution, by the fully precipitation of β-carotene particles. High elimination of organic solvent is necessary in SFEE process, due to the diffusion of $CO_2$ into the organic phase is increasing the interfacial tension between the aqueous and the organic phase, which leads to phase separation [11]. In the beginning of the process bimodal particle size distribution was obtained by Mattea F. et al. [10], due to the formation of empty starch micelles. In the presented model of Mattea F. et al. [10], the saturation of organic phase by $scCO_2$ is relatively fast: after 0.3 s the molar fraction of $CO_2$ is above 0.2 in every radial position of each emulsion droplets, so β-carotene precipitation is considered as completed already after this time. On the other hand, extraction of the organic phase is much slower: after half second only less than half of the initial organic solvent is removed. Organic extraction in case of GAS processes are more efficient than in case of spray processes (like SAS), as liquid phase is stored inside the precipitator, and is continuously keeping contact with $scCO_2$ until the end of the treatment [10].

In the work of Matte F. et al. [11], mass transfer of β-carotene contained DCM/w emulsions (using OSA-modified starch as surfactant material) - $scCO_2$ system was measured in a high pressure view cell on sub- and supercritical conditions, at 308 K, and 5 and 10 MPa, respectively. Sessile drop method was used in that work for observing the change of the volume of an initially, – into the aqueous phase placed DCM droplet –, with different initial volumes, using a CCD camera. CCD camera was measuring the refractive index change of the droplet, which is initially higher than the surrounding $scCO_2$ medium, then becomes equal, then even lower, due to mass transport processes occurs simultaneously between the droplet and the gas phase. From refractive index change profile the volume change, and hence the mass change of the droplet was obtained. Moreover, shape change of the drop was also observed, which is related with the change of interfacial tension between phases, according to the fundamental

pendant drop equations, presented by in the work of Bashforth and Adams [12]. Different behaviour of observed droplet was obtained at 5 and 10 MPa pressures, as pressure of the mixture critical point of $CO_2$ - DCM system is between these values [13]. Below the mixture critical point (p = 5 MPa), drop diameter initially increased, till reached a maximum, as the diffusion of the $CO_2$ into the DCM drop is limited by the equilibrium concentration of the DCM - $CO_2$ mixture, and the lower solubility of $CO_2$ in the water (0.0137 molar fraction [14]). On the other hand, in experimental runs performed above the mixture critical point of $CO_2$ - DCM system (p = 10 MPa), volume of drop was continuously increasing, as there is a higher solubility of $CO_2$ in water (0.0205 in molar fraction) and equilibrium conditions of the DCM - $CO_2$ mixture are not limiting the diffusion of $CO_2$ into the droplet any more. Below the mixture critical point, the volume of the droplet was decreased, after it reached a minimum, as DCM evaporation from the droplet was comparatively higher, than the absorption of $CO_2$. Meanwhile above the mixture critical point, equilibrium concentration limitations were not valid any more as detailed above, so drop volume increases, until its density is low enough to compensate the attachment effect of the surface of the cell. In the experiments of Matte F. et al. [11], precipitation and formation of several β-carotene particles inside the drop was occurred immediately, upon pressurization of the system by $CO_2$. During SFEE process, the same behaviour of emulsion droplets is expectable as described in the work of Mattea F. et al. [11], although more rapidly, as process conditions of SFEE are designed for obtaining the maximum available mass transport velocity of components in the o/w emulsion - $scCO_2$ system, by producing emulsions with droplet size distribution in nanometric scale, and hence, obtaining final particles size within this range, too. Rapidness of SFEE process is very important, as o/w emulsions under $scCO_2$ atmosphere are probably become much less stable than under atmospheric conditions, as found in the work of Varona et al. [15] in case of with lavandin prepared o/w emulsions. Emulsion stability in the case of SFEE process is a crucial process

parameter, as experiments done in the work of Mattea F. et al. [11] demonstrate, that each emulsion droplet behaves as a miniature GAS precipitator during the SFEE process, which justifies the control of the final particle size, by the emulsion droplet size.

In this work mass transfer properties were measured in the system of $scCO_2$ - oil in water (o/w) emulsions, using magnetic suspension balances. Emulsions prepared with ethyl acetate, EtAc, and with dichloromethane, DCM, as organic solvents, and Pluronic L64® and soy-bean lecithin as surfactants. Obtained results were used to optimize the process conditions of SFEE technology, in order to decrease the residual organic content under the restrictions of FDAA, applying the shortest processing time as possible, and hence decrease the possible degradation effect of quercetin, and to avoid the aggregation effect of encapsulated particles. Model equations were fit to the obtained results in order to study which parameters have significant influence on the mass transport. Extraction of organic part from o/w emulsions using continuous $scCO_2$ flow was measured as well.

## 2. EXPERIMENTAL

### 2.1 Materials

Surfactant materials: poly-(ethyleneglycol)-block–poly-(propyleneglycol)-block-poly-(ethyleneglycol) (Pluronic L64, CAS: 9003-11-6) was obtained from Sigma–Aldrich (St. Louis, USA), soy-bean lecithin was obtained from Aurica® (Vital Lecithin Granulat 250 g; PZN 07519389). Ethyl acetate (EtAc, CAS: 141-78-6; LOT: 1409303; EC: 205-500-4; Code: E/0900/15) was obtained from Fisher Chemical, Fisher Scientific UK, Bishop Meadow Road, Loughborough. Dichloromethane (DCM, CAS: 75-09-2; LOT: SZBE3490V) was obtained from Sigma–Aldrich (St. Louis, USA).

### 2.2 Preparation of oil in water emulsions

Initial oil in water emulsions were prepared using an IKA®-WERKE ULTRA-TURRAX® T 50 basic device. Emulsions did not contain any active compound, considering that the typically low amounts of active compound present in the emulsion are not have a significant influence on the transport properties. Emulsions were prepared using EtAc or DCM as dispersed organic phase, and water, containing soy-ben lecithin or a mixture of soy-bean lecithin and Pluronic L64® as surfactant material, as continuous phase. The continuous water phase of the emulsion was prepared by adding a determined amount of surfactant material, homogenized using a magnetic stirrer. Afterwards a determined amount of organic phase was added into the continuous aqueous phase, and emulsified using the ULTRA-TURRAX® device at 4000 rpm for 4 min duration. These emulsifying conditions were determined and optimized in a previous work [16].

## 2.3 Interfacial tension measurements

Interfacial tension of water – EtAc and water – DCM system was measured using an EasyDyne U2-03 tensiometer produced by Krüss, Hamburg. Wilhelmy plate method is applied by using a Platinum plate, as it can be optimally wetted due to its high surface free energy, which helps it to form a contact angle of 0° with liquids. Area of wetted length is 40.2 mm.

## 2.4 Magnetic suspension balance device for static measurements

Magnetic suspension balance (MSB) is a state of the art device, which let us accurately measure the weight or weight change of a sample, under harsh conditions. As it can be seen on **Fig 1**, the sample is placed in a closed cell, and instead of hanging directly beneath a balance, it is linked via a measuring load decoupling to a magnetic suspension clutch, which consists of a permanent magnet, an electro magnet, and a position sensor. A PID controller unit maintain the suspension magnet in a constant floating position, by controlling the electromagnet. Herewith, the measuring weight force is transmitted to the microbalance, which is located under ambient conditions, out of the closed measuring cell, containing the sample.

This system let us study the mass transport properties in oil in water emulsions, by real time monitoring the weight of the sample under $scCO_2$ atmosphere. During all measurements, temperature and pressure of the system were monitored online and kept constant. As an indication of the stability of measurements, **Fig 7** and **Fig 8** show the evolution of pressure and temperature during a typical experimental run. Static MSB device was tempered using an outer jacket, heated by a Julabo FP 50 oil thermostat. The MSB device during the whole measurement period can be tared and calibrated automatically, by lowering the suspension magnet in a controlled way, and placing the sample-hanger on a small support. Different positions of coupling magnet and sample-holder can be seen on **Fig 2**. In a state so-called zero-

point (ZP) position, the sample is decoupled from the balance, and the suspension magnet alone is in a freely suspended state, and only its weight is transmitted to the magnet. This ZP position setting of the MSB let us correct the measured sample weight detail by the changing atmosphere, that can cause sensitivity drifts of the unloaded balance. During the measurement period, in every five minutes a ZP position is recorded, and used for the correction of the sample weight data, measured during the following five minutes. Weight data were taken every 30 seconds.

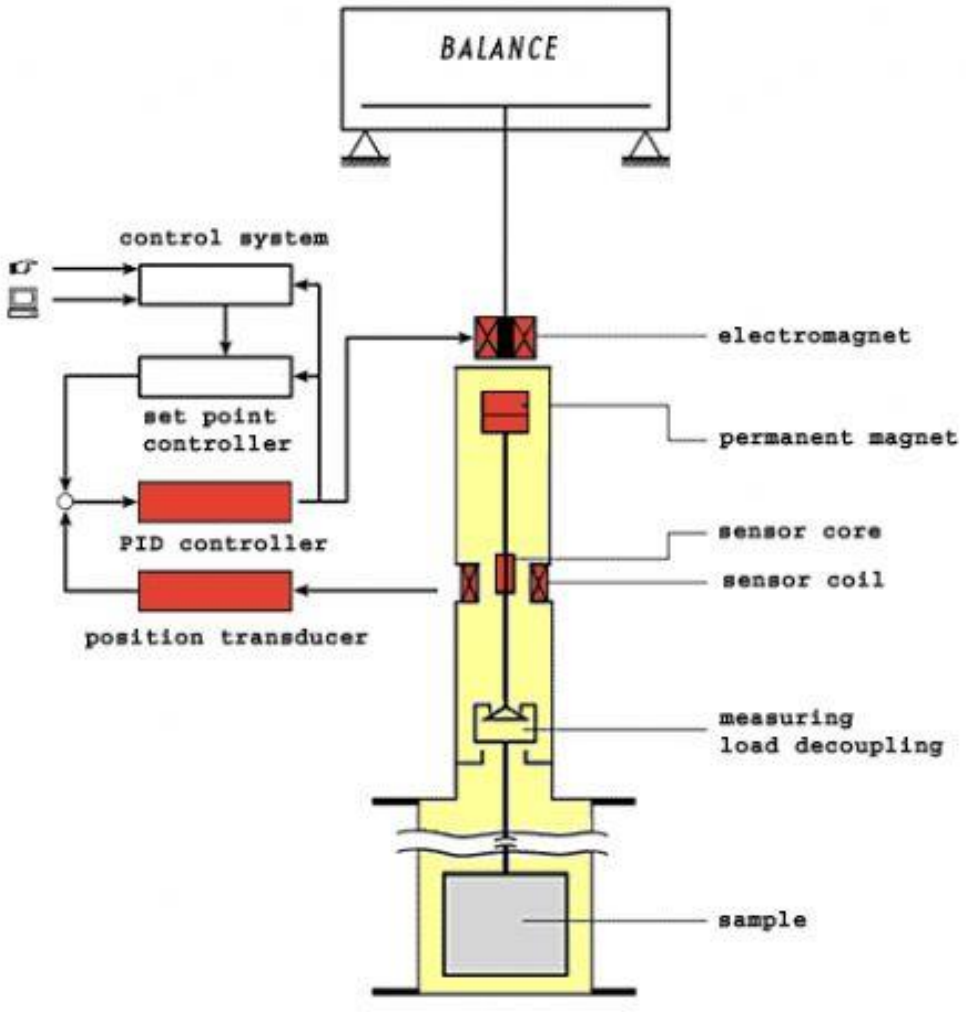


**Fig 1:** Static magnetic suspension balance device

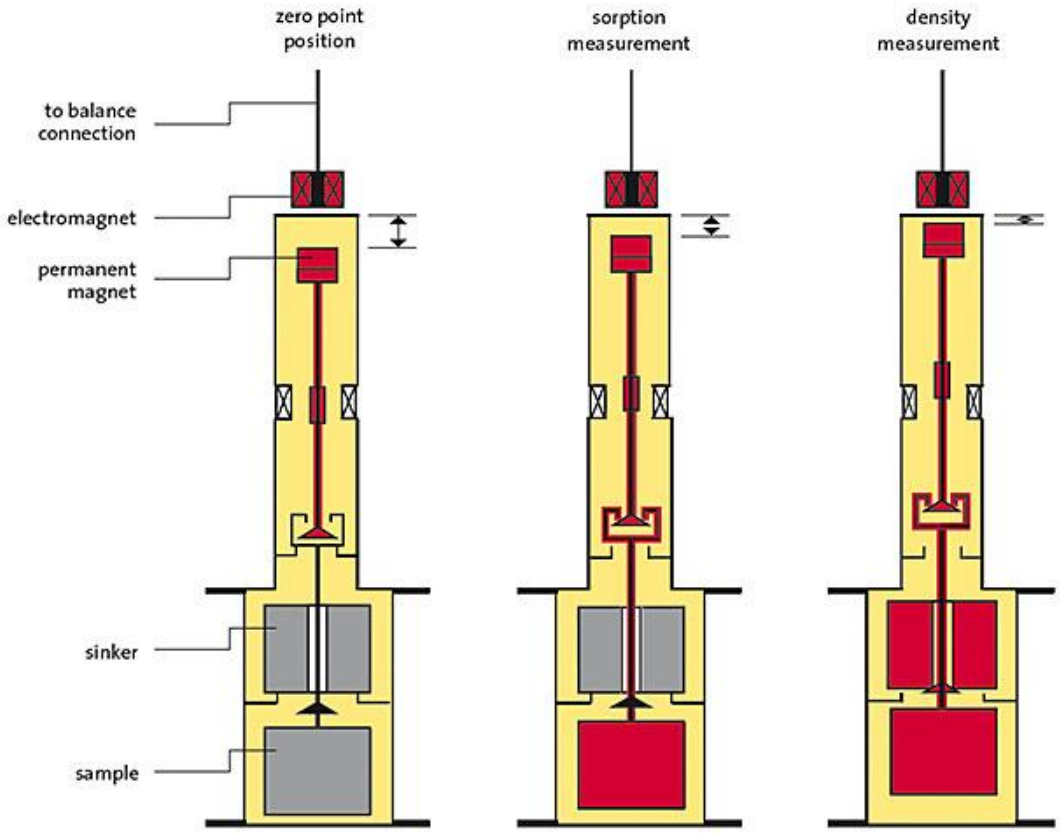


**Fig 2:** MSB device for dynamic measurement with positions of 1.: zp; 2.: MP2; 3.: MP3

Usually ~1.5 mL of the initially prepared emulsion was placed in a glass cell, which was then hanged on the sample-hanger, which is linked directly to the permanent magnet of the static MSB device. In every experiment, the volume of the measured sample was calculated accurately, from the initial mass of the inserted sample, using an average density data, which was weighted by the mass fraction of the added compounds. Afterwards, the cell was closed, and recording of sample weight was started. The cell was preheated, in order to reach constant temperature conditions of the sample and the sample area as early as possible. Then pressure was slowly increased until the desired pressure was reached, using a Maximator ® Compressor device. Automated pressure regulator valve for on-line pressure regulation was used during the whole measurement period, in order to avoid changes in transport properties, caused by the changing temperature conditions of the $scCO_2$ atmosphere. Measurement was continued until a constant sample weight was observed.

## 2.5 Magnetic suspension balance device for dynamic measurements

A MSB device was redesigned, in order to be able to do mass transport properties measurement in dynamic conditions, in which a continuous flow of $scCO_2$ was maintained. A specific sample holder was designed and presented in the work of Fieback T. et al. [17], where a $scCO_2$ flow passes through the emulsion. The applied $scCO_2$ flow scheme through the emulsion is shown on **Fig 3**.

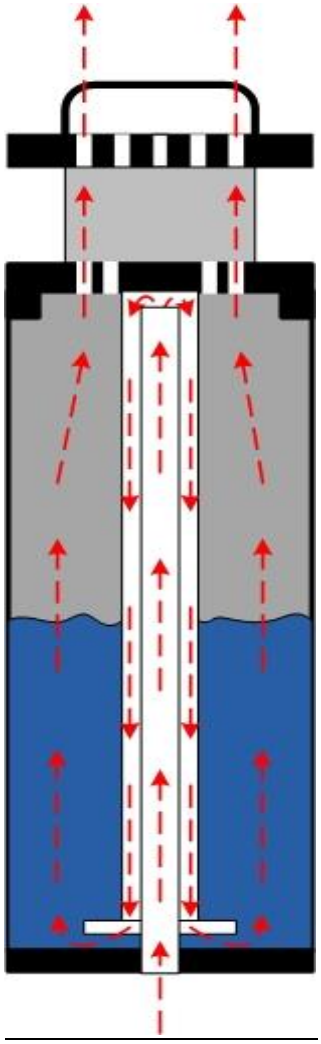

**Fig 3:** Sample-holder of dynamic measurements: arrows indicates the flow direction of $scCO_2$

This further developed MSB device which let us measure simultaneously the weight of two samples, using three different vertical positions of the suspension magnet, corresponding to three different measuring positions (**Fig 2**). The first position is the ZP, which let us to tare the balance during the measurement period, for reasons described in section 2.4. In the position of Measuring Point 1 (MP1), the weight of the first sample is monitored during the measurement period. In this work, the weight of a sinker (an inert sample of known volume and vacuum weight to determine the surrounding fluid density by Archimeded principle) was continuously monitored in MP1, in order measure the density change of the $scCO_2$ atmosphere in the sample area. In positon of Measuring Point 2 (MP2), the weight of the sample and the weight of the sinker were monitored together, and with a simple subtraction of these measurements the weight of the sample was obtained.

Around 5 mL of the initially prepared emulsion was placed into the sample holder. Then the cell was closed and the initial weight of sample and sinker was recoded. Cell was tempered using electrical heating, controlled by a PID controller. Liquid $CO_2$ was pumped into the cell, using an HPLC pump with a constant flowrate of 6.5 mL/min. Once the desired pressure was reached, constant $CO_2$ flow was further maintained by the HPLC pump, and the pressure regulation valve was slightly opened. The weight of the sample and the sinker was monitored continuously during the whole measurement period. As pressure was kept constant manually using a basic ballcock valve, pressure deviation was +/- 2 bar. Due to pressure fluctuations, measured weight data was slightly fluctuated as well. By correcting the sample weight with the buoyancy effect of the $scCO_2$ atmosphere, fluctuations were attenuated, and a basic trend of how the sample weight is decreasing during the measurement process was obtained. Once the basic trend line was obtained, pumping of $CO_2$ was stopped, and during the depressurization process sample weight was continuously monitored, until the phase change of $CO_2$ from supercritical to subcritical took place (at about 70 bar).

## 3. RESULTS AND DISCUSSION

### 3.1 Results of interfacial tension measurements

As interfacial tension is a crucial issue in the SFEE process as the increase of interfacial tension has a destabilizing effect on the emulsion, application of surfactant materials has a huge benefit on SFEE process [10].

**Table 1:** Interfacial tensions in water – EtAc system

| $C_{Lecithin}$ [w/w%] | $C_{Pluronic\ L64}$ [w/w%] | Surface tension [mN/m] | Temperature [°C] |
|---|---|---|---|
| 0.0 | 0.0 | 6.70 | 19.0 |
| 2.4 | 0.0 | 1.05 | |
| 2.9 | 0.0 | 1.05 | |
| 2.4 | 0.5 | 0.55 | |
| 2.4 | 1.0 | 0.60 | |

Experimental results about water – EtAc system are detailed in **Table 1**. As experimental results show, using soy bean lecithin as surfactant material in a proportion of only 2.4 w/w% is sufficient to achieve a six times reduction of the interfacial tension between water and EtAc. By increasing the concentration of lecithin, interfacial tension is not decreased any more, as the critical micelle concentration (CMC) of lecithin is already reached. Using 0.5 w/w% of Pluronic L64® as an additional surfactant material, an additional reduction of interfacial tension was obtained. As CMC of Pluronic L64® is already achieved [18], further increase of its concentration has no effect on interfacial tension. As a dependency of interfacial tension in the concentration of lecithin and additional Pluronic L64® is obtained, in transport properties measurements the effect of these factors were also studied.

**Table 2**: Interfacial tensions in water – DCM system

| $C_{lecithin}$ [w/w%] | $C_{Pluronic\ L64}$ [w/w%] | Surface tension [mN/m] | Temperature [°C] |
|---|---|---|---|
| 0.0 | 0.0 | - | 18.5 |
| 2.4 | 0.0 | 9.95 | |
| 2.9 | 0.0 | 8.45 | |
| 2.4 | 0.5 | 8.10 | 18.0 |
| 2.9 | 0.5 | 7.50 | |
| 2.4 | 0.5 | 7.45 | |
| 2.9 | 0.6 | 7.60 | |

Interfacial tension in the case of water – DCM system was much higher than in the case of water – EtAc system, as miscibility of water - DCM is negligible comparing to water – EtAc. The interfacial tension between water – DCM without applying surfactant material was above the measurable limit of the device employed and therefore interfacial tensions could not be accurately measured in this solvent-surfactant system. However, result suggested a similar trend of variation and similar limiting CMC concentrations as in water-EtAc systems.

### 3.2 Results obtained by static MSB device

Typical weight-change profiles during the measurement are plotted on **Fig 4** in case of o/w emulsions prepared by EtAc. The measured weight was corrected with the buoyancy effect of the $scCO_2$ atmosphere, which depends on the density of $scCO_2$ and the volume of the sample. Volume correction of emulsions was not necessary, as the volume of o/w emulsions (EtAc and DCM based as well) were practically constant during the whole measurement period according to visual observations done by view cell.

The weight detail collected from the first 30 min of experimental run were not usable, due to fluctuations of measured weight occurred, caused by the pressurization, and slow temperature homogenization of the system. After that period, in the beginning of the process a weight increase took place, as $CO_2$ absorption by the emulsion is much faster than organic extraction,

due the high solubility of $scCO_2$ in the organic phase [4][6][7]. Afterwards EtAc extraction became a dominant process, resulting in negative weight changes of the o/w emulsions. In the end of the process a nearly constant weight ($\Delta m = 0$) was obtained, marking that equilibrium conditions of the system are achieved. As shown in **Fig 4**, from the results of replicated experiments it can be concluded, that measurements were highly reproducible.

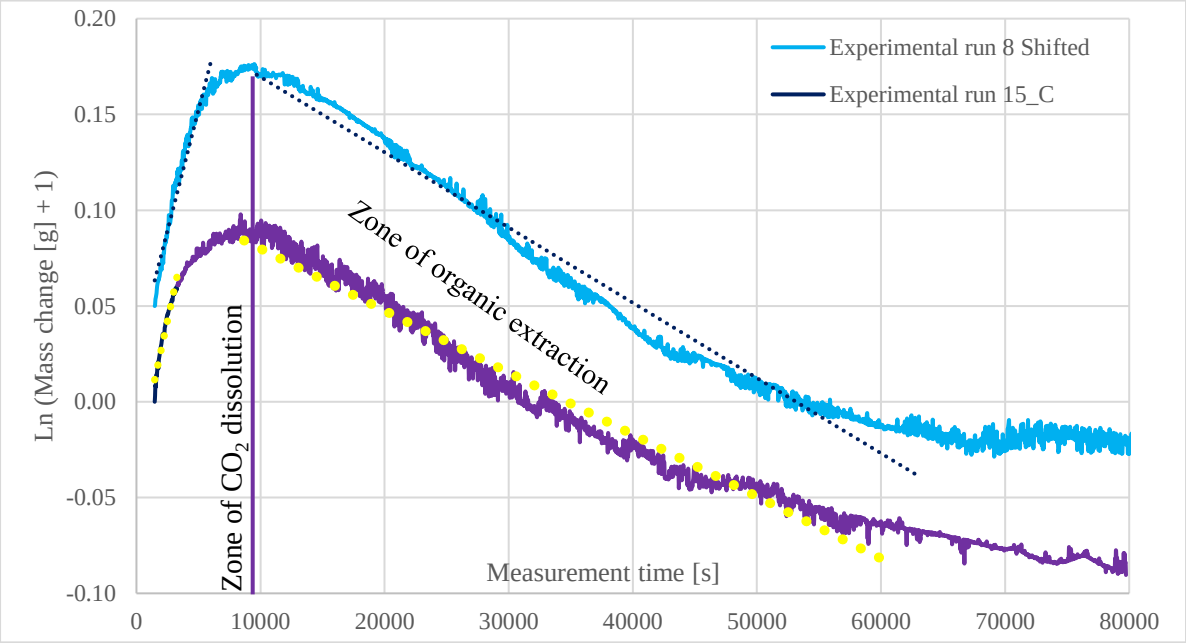


**Fig 4:** Ln(Δm+1) curves of o/w emulsions prepared with EtAc, contacted with $scCO_2$ with similar p and T settings to prove reproducibility of measurements. Experimental run 29.06.2015 is shifted on axis y by 0.05 to positive direction.

In case of emulsions prepared with DCM and contacted with $scCO_2$, a faster process is obtained (~14 hours instead of ~19 hours), as plotted on **Fig 18**. The absorption period of $scCO_2$ in the case of DCM/w emulsions is three times faster than in the case of EtAc/w emulsions. The extraction of the organic phase is also much faster in case of DCM/w emulsions. This result is probably a consequence of the approximately 5.4 times lower mutual solubility of DCM and water (1.6 V/V%), than EtAc and water (8.7 V/V%) [19]. While EtAc shows a comparatively high miscibility in water (8.7 V/V%), which means that a considerable amount of EtAc has to

be extracted from the aqueous phase by a diffusion process, in the case of DCM/w emulsions, practically all the organic solvent is restricted in the organic-rich phase. Moreover, the lower polarity of DCM – compared to EtAc –, which increases the mutual miscibility of $scCO_2$ and DCM, can also justify this result. This result is consistent with the observations of the SFEE process, that indicate that much longer extraction times are needed to reach similar residual organic solvent concentration results in the case of EtAc/w emulsions, than in the case of DCM/w emulsions [10] [16]. In several cases the $CO_2$ dissolution process was not even measurable in DCM/w emulsions, because the absorption process of $scCO_2$ was much faster, than the total homogenization of pressure and temperature characteristics in the sample surrounding $scCO_2$ medium (**Fig 18**). As density fluctuations were taking place during the homogenization of temperature of $scCO_2$ medium, buoyancy effect was not exactly countable, and hence the measured weight was not exactly correctable. Moreover, as the thermal conductivity of $scCO_2$ is sharply changing with its density [20], the temperature homogenization process was even slower.

As the two reverse process: $scCO_2$ absorption and organic phase extraction are taking place simultaneously during the process, but they were dominating it in different periods along the whole measurement, for the analysis of results, the obtained curves were divided into two different zones: "$CO_2$ dissolution-" and "Extraction" zone as shown on **Fig 4**, and magnified on **Fig 5** and **Fig 6**. Linear equations were fitted on the natural logarithm of weight change profiles, and the characteristics of the obtained curves were compared, in order to analyse the transport properties in $scCO_2$ – o/w emulsion system. As buoyancy correction is influenced by the density of the surrounding $scCO_2$ medium, in all sampling points the bouncy effect was recalculated, as smooth density fluctuations occurred, due to small fluctuations of temperature and pressure. As the mass change of the emulsion in the extraction part is rapidly become negative, curves are shifted to positive direction along the axes Y (equation 4), in order to

maintain mathematically possible, the natural logarithmic calculation. In order to determine the weight-change-profile of the o/w emulsions more accurately, obtained mass results were not corrected by the mass of the empty sample holder. The fitting to a logarithmic equation is justified by the fact, that a single diffusion process (i.e., comprising only $CO_2$ dissolution or only solvent extraction) is mathematically represented by such a logarithmic function (ln C ~ t), as presented in equations (1-3). In these equations, the slopes marked by K characterize the rapidity of the diffusion processes (of $CO_2$ into the droplet and solvent out of the droplet). On the other hand, due to reasons detailed in the beginning of this section, curves are shifted in time, and the intercept of axis Y has no relevant physical meaning in $CO_2$ dissolution zone, hence it will not be further analysed in this work. Meanwhile intercept of axis Y in the zone of organic extraction is corresponding with the maximum absorption capacity of $CO_2$ by the sample.

$$\frac{dc}{dt} = K * c \tag{1}$$

$$\int\left(\frac{dc}{c}\right) = \int K dt \tag{2}$$

$$\ln(c) = Kt + Y \tag{3}$$

$$c = (\Delta m + 1) \tag{4}$$

Where:

K is the mass transfer coefficient

t is the elapsed time

Δm is the weight change of the sample

Y is a constant

Although in the current case characterizing equations 1 - 4 are simplifications, as the two processes are occurring simultaneously, this simplification is justified by the difference of rates of these two processes (being the extraction much slower than the $CO_2$ dissolution), and as it will be shown in the following sections this approximation provides a valuable interpretation of the obtained results.

### 3.2.1 Evaluation of transport properties in EtAc/w emulsions

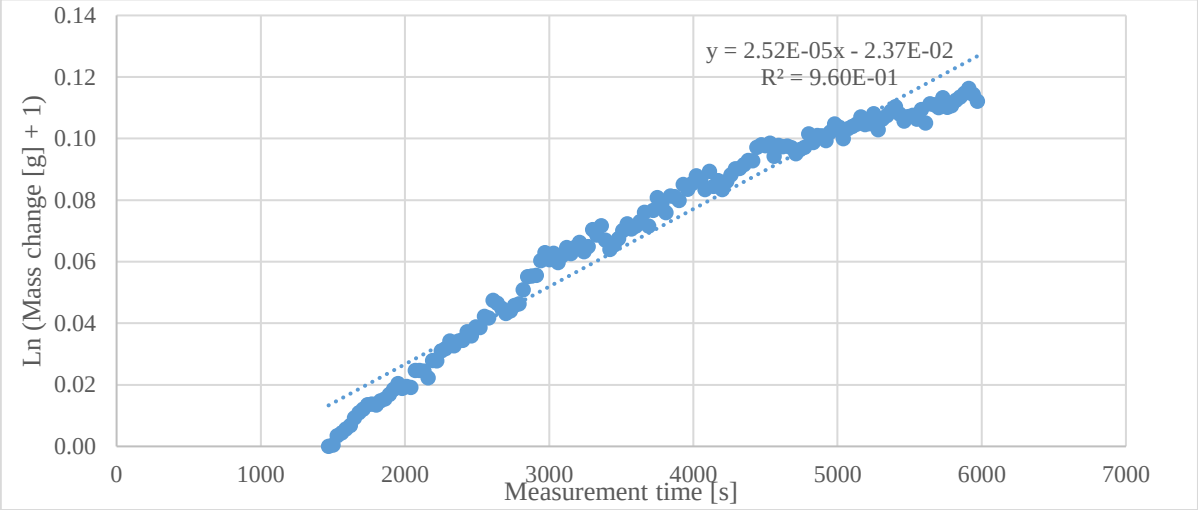


**Fig 5:** Ln(Δm+1) curve with fitted equation in "$CO_2$ dissolution zone" of Experimental run 8

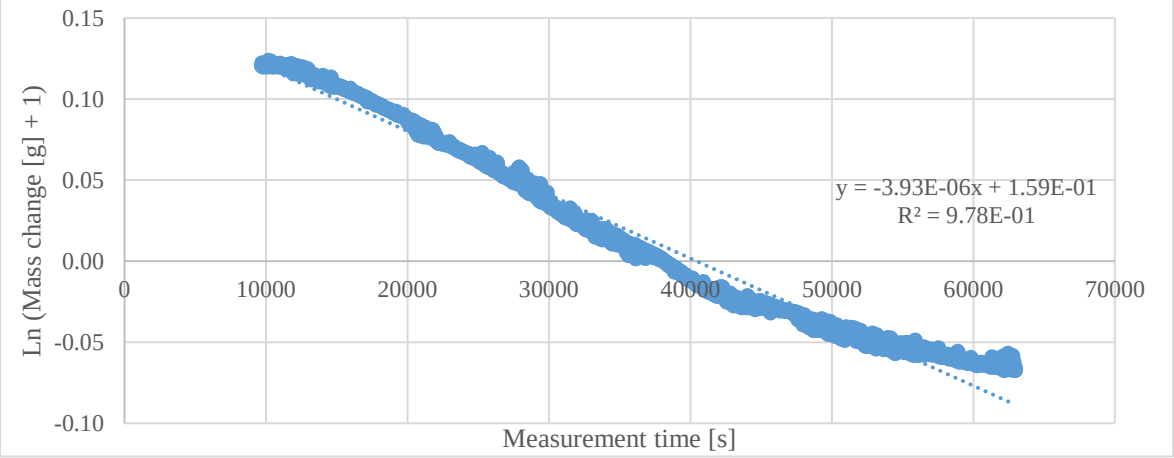


**Fig 6:** Ln(Δm+1) curve with fitted equation in "extraction zone" of Experimental run 8

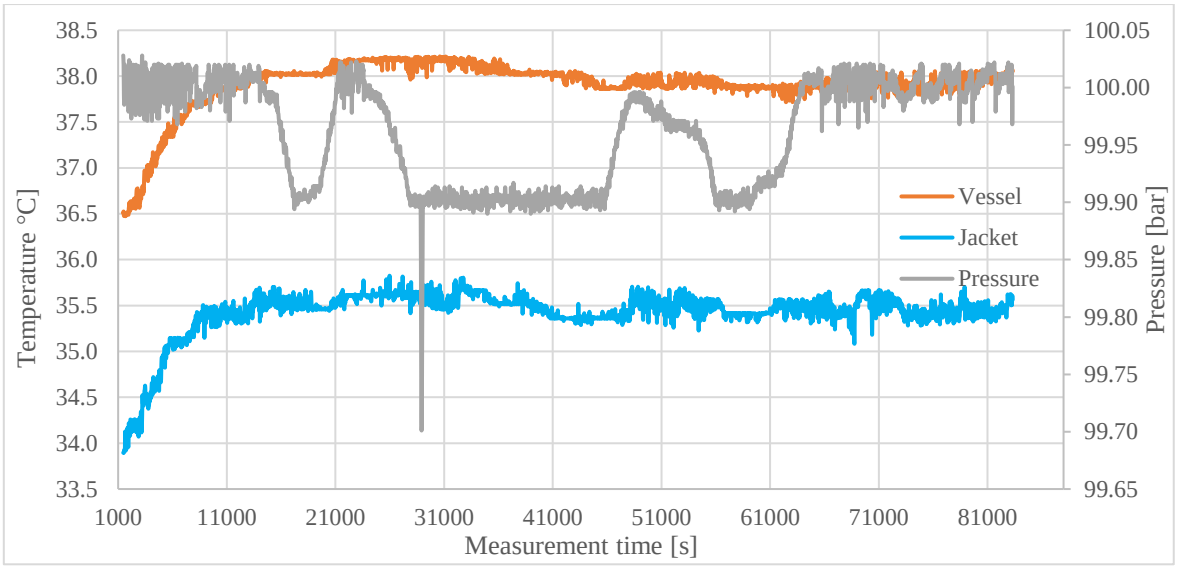


**Fig 7:** Temperature- and pressure monitoring during measurement time in case of Experimental run 8

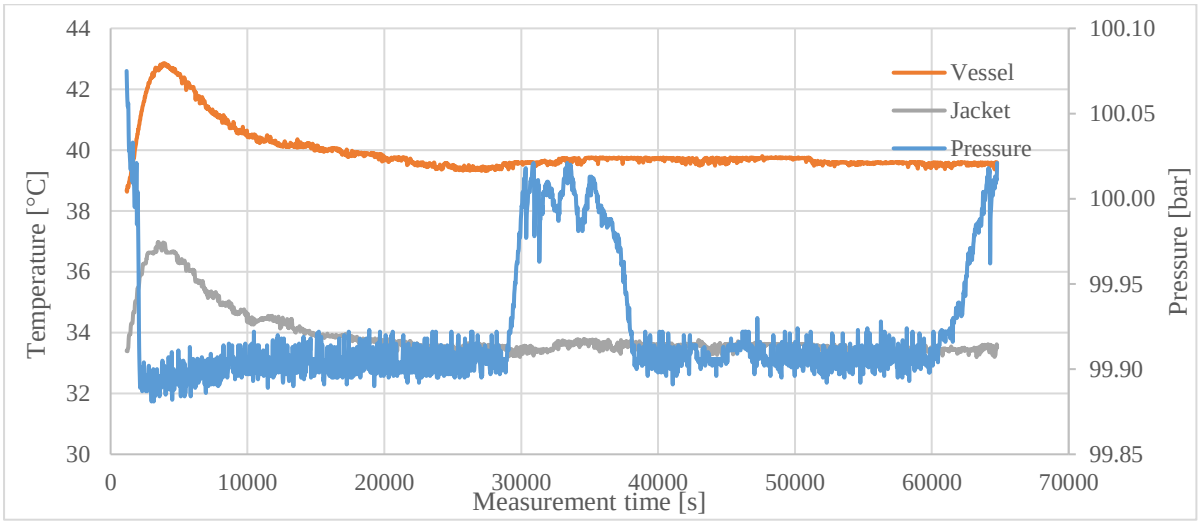


**Fig 8:** Temperature- and pressure monitoring during measurement time in case of Experimental run 2

An experimental plan with several centrum point measurements (detailed in **Table 3**) was done, in order to study the effect of factors, such as solvent to water ratio (varied between 1/3 – 1/5 in volume ratio), concentration of the surfactant material lecithin (1.5 – 2.5 w/w%), concentration of additional surfactant material Pluronic L64® (0.4 – 0.8 w/w%), temperature (34.7 – 44.1°C), and pressure (85.0 – 110.0 bar). Obtained profiles of two centrum point measurements are plotted on **Fig 4**, in order to prove the reproducibility of the measurements. Residual EtAc content was determined from the weight difference of the sample, measured before and after the experimental run at ambient conditions. According to the experimental runs, done at p = 100 bar and T = 40°C, marked by font type Italic in **Table 3**, the concentration of EtAc and soy-bean lecithin has no significant influence on the transport properties: the characteristic equation values of the curves just varied by the measurement deviation values (**Fig 9, Fig 10, Fig 11**). As visible on that figures, addition of Pluronic L64® neither has significant influence on the transport properties. This result is in agreement with the result of Mattea F. et al [11]. However, they found, that for the injection of $CO_2$ into DCM/w emulsion, in the organic phase dissolved surfactant material (OSA modified starch) was precipitated as large particles due to the solubilisation and antisolvent effect of $CO_2$ in DCM, and particles were migrating to the interface of the drop and to the medium.

**Table 3:** Experimental plan with EtAc/w emulsions: Runs for study the *effect of concentration of EtAc, Lecithin, Plurnic L64®* marked by font type Italic; runs for study the **effect of temperature and pressure (full resolution)** marked by font type Bold; Centrum point runs marked by "_C"; repetitions of previous experiments marked by "_rep"

| Number of experimental run | $C_{L64}$ [w/w%] | $C_{Lecithin}$ [w/w%] | $C_{EtAc}$ [w/w%] | Solvent/ /water ratio [ml/ml] | p [bar] | T [°C] | Density of $scCO_2$ medium [g/mL] | $CO_2$ dissolution slope | Organic extraction slope | Y intercept in organic extraction zone | Residual EtAc [w/w%] |
|---|---|---|---|---|---|---|---|---|---|---|---|
| 1 | - | *1.5* | *14.9* | *1/5* | *98.8* | *40.3* | *0.60* | *2.54E-05* | *-4.16E-06* | *8.73E-02* | *0.6* |
| 2_rep | - | *1.5* | *14.9* | *1/5* | *99.9* | *39.5* | *0.64* | *3.05E-04* | *-3.21E-06* | *5.02E-02* | *3.5* |
| 3 | - | *2.5* | *14.8* | *1/5* | *103.7* | *38.9* | *0.65* | *4.33E-05* | *-2.10E-06* | *6.45E-02* | *2.4* |
| 4_rep | - | *2.5* | *14.8* | *1/5* | *100.0* | *39.2* | *0.63* | *3.77E-05* | *-3.08E-06* | *9.22E-02* | *3.3* |
| 5 | - | *1.5* | *22.8* | *1/3* | *101.8* | *42.9* | *0.56* | *1.88E-05* | *-4.83E-06* | *5.71E-02* | *0.6* |
| 6 | - | *2.5* | *22.6* | *1/3* | *99.3* | *39.1* | *0.63* | *3.74E-05* | *-3.86E-06* | *1.15E-01* | *2.5* |
| 8 | - | *2.5* | *22.6* | *1/3* | *100.0* | *36.3* | *0.67* | *2.52E-05* | *-3.93E-06* | *1.59E-01* | - |
| 9 | - | *4.9* | *22.0* | *1/3* | *99.9* | *37.3* | *0.67* | *2.71E-05* | *-3.27E-06* | *1.18E-01* | *0.5* |
| 10 | *0.4* | *2.0* | *18.9* | *1/4* | *99.9* | *40.1* | *0.63* | *1.91E-05* | *-3.08E-06* | *1.07E-01* | *1.1* |
| 11 | *0.8* | *2.0* | *18.8* | *1/4* | *99.7* | *42.2* | *0.57* | - | *-1.81E-06* | *1.65E-03* | - |
| **12_C** | **-** | ***2.0*** | ***19.0*** | ***1/4*** | ***99.9*** | ***40.0*** | ***0.63*** | **-** | ***-8.94E-07*** | ***-1.42E-01*** | |
| **13_C** | **-** | ***2.0*** | ***19.0*** | ***1/4*** | ***101.6*** | ***40.0*** | ***0.64*** | ***3.27E-05*** | ***-3.94E-06*** | ***1.24E-01*** | **-** |
| **14_C** | **-** | ***2.0*** | ***19.0*** | ***1/4*** | ***103.0*** | ***41.2*** | ***0.62*** | ***3.09E-05*** | ***-2.13E-06*** | ***7.12E-02*** | ***1.6*** |
| **15_C** | **-** | ***2.0*** | ***19.0*** | ***1/4*** | ***98.0*** | ***38.0*** | ***0.65*** | ***2.99E-05*** | ***-2.55E-06*** | ***9.26E-02*** | ***3.5*** |
| **16** | **-** | **2.0** | **19.0** | **1/4** | ***85.0*** | ***40.6*** | **0.33** | **5.06E-05** | **-1.11E-05** | **5.17E-01** | **0.4** |
| **17** | **-** | **2.5** | **19.0** | **1/4** | ***110.0*** | ***39.1*** | **0.66** | **2.24E-05** | **-2.96E-06** | **1.26E-01** | **3.3** |
| **18** | **-** | **2.5** | **19.0** | **1/4** | ***100.0*** | ***44.1*** | **0.50** | **3.03E-05** | **-3.08E-02** | **1.60E-01** | **-** |
| **19** | **-** | **2.5** | **19.0** | **1/4** | ***99.9*** | ***36.0*** | **0.70** | **2.04E-05** | **-2.29E-06** | **5.41E-02** | **2.6** |
| 20 | - | 1.5 | 22.8 | 1/3 | 110.6 | 40.7 | 0.67 | 3.20E-05 | -3.73E-06 | 1.26E-01 | 3.1 |
| 21 | - | 2.5 | 22.6 | 1/3 | 109.5 | 38.5 | 0.70 | 1.51E-05 | -3.55E-06 | 9.15E-02 | 1.5 |
| 22 | 0.4 | 2.0 | 18.9 | 1/4 | 99.9 | 42.0 | 0.60 | - | -4.70E-06 | 1.69E-01 | 2.1 |
| 23 | 0.4 | 2.0 | 18.9 | 1/4 | 85.0 | 37.8 | 0.43 | - | -1.17E-05 | 6.29E-02 | 3.2 |
| 24 | 0.4 | 2.0 | 18.9 | 1/4 | 94.9 | 34.7 | 0.75 | 1.48E-05 | -2.64E-06 | 7.21E-02 | 4.0 |
| 25 | 0.8 | 2.0 | 18.8 | 1/4 | 97.1 | 40.5 | 0.59 | 2.75E-05 | -4.18E-06 | 9.57E-02 | - |
| 26 | 0.8 | 2.0 | 18.8 | 1/4 | 99.9 | 35.9 | 0.70 | 6.22E-06 | -4.32E-06 | 6.02E-02 | 14.5 |

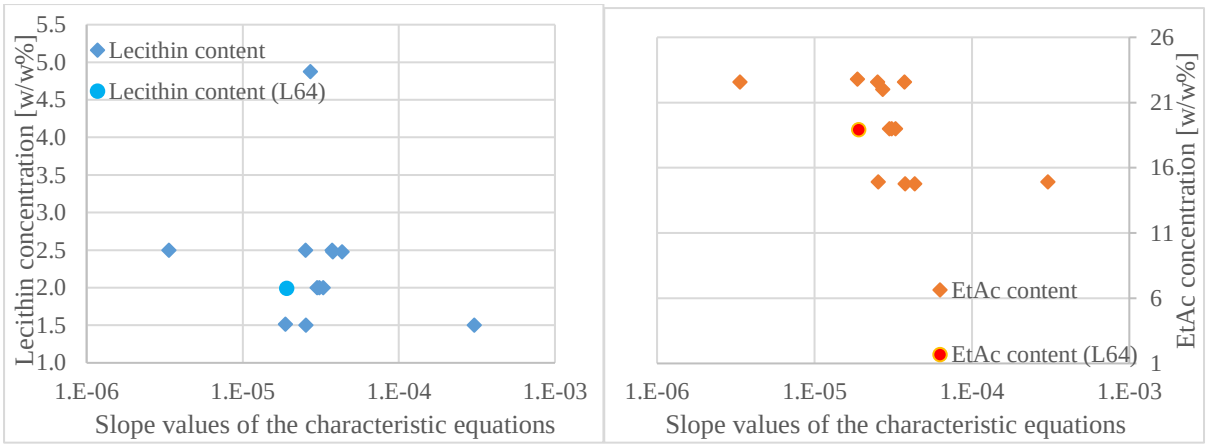


**Fig 9:** Dependency of slope values of the characteristics equations in the "$CO_2$ dissolution zone" about lecithin- and EtAc content – log scale

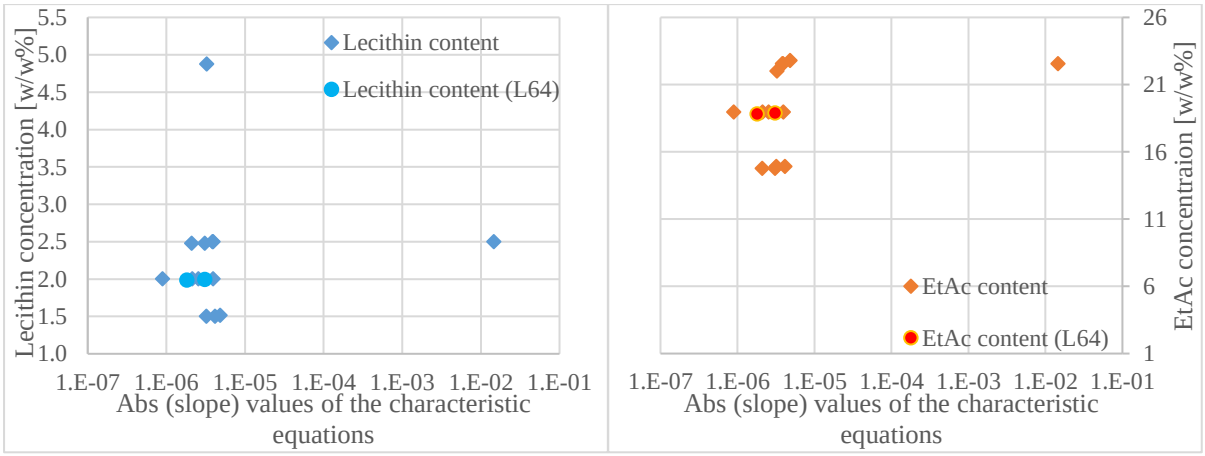


**Fig 10:** Dependency of slope values of the characteristics equations in the "extraction zone" about lecithin- and EtAc content – log scale

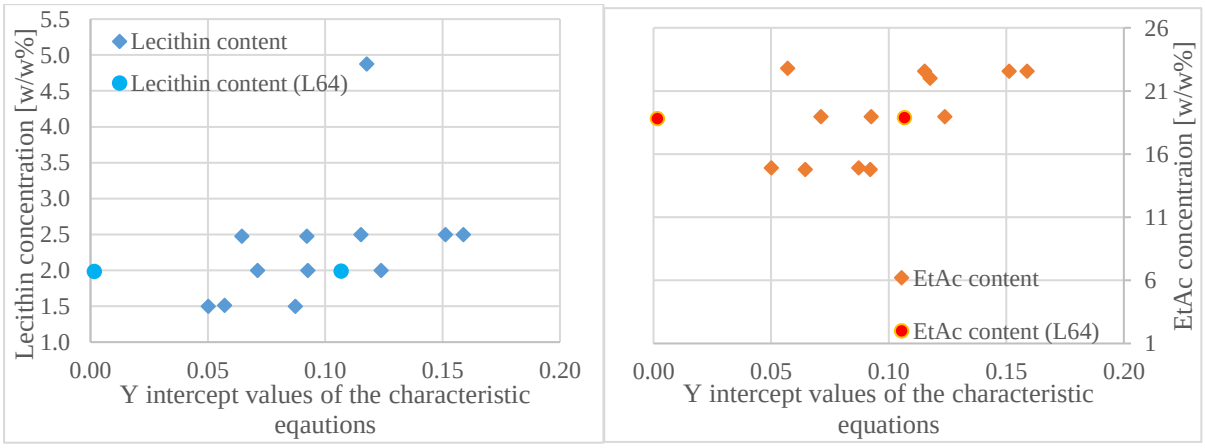


**Fig 11:** Dependency of Y intercept values of the characteristics equations in the "organic phase extraction zone" about lecithin- and EtAc content

On the other hand, results show a significant dependence on the density of the supercritical fluid. Slope values of the characteristics equations in $CO_2$ dissolution part are only influenced by the density of the $scCO_2$ medium, as visible on **Fig 12**. As the density of the extraction medium decrease, the slope part of the equation is increasing, which means a faster $CO_2$ dissolution by the emulsion This result could be, due to the viscosity of $scCO_2$ is decreasing at lower density [20], resulting a faster diffusion rate in lower density region. Increasing of diffusion coefficient with decreasing density was measured by Sassait P. R. et al. [21]. Results indicate, that $CO_2$ mass transfer is governed by this parameter and not by the phase equilibrium limitations, which is consistent, considering that all experiments were carried out at a pressure above the mixture critical point of the solvent-$CO_2$ system.

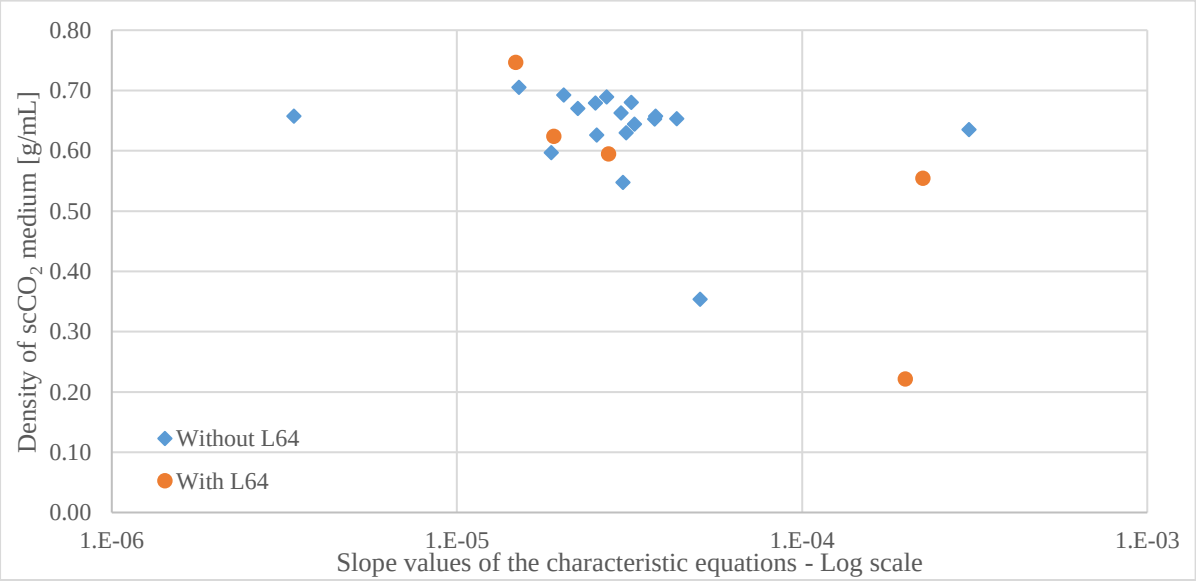


**Fig 12:** Dependency of slope values of the characteristics equations in the "$CO_2$ dissolution zone" about $scCO_2$ density

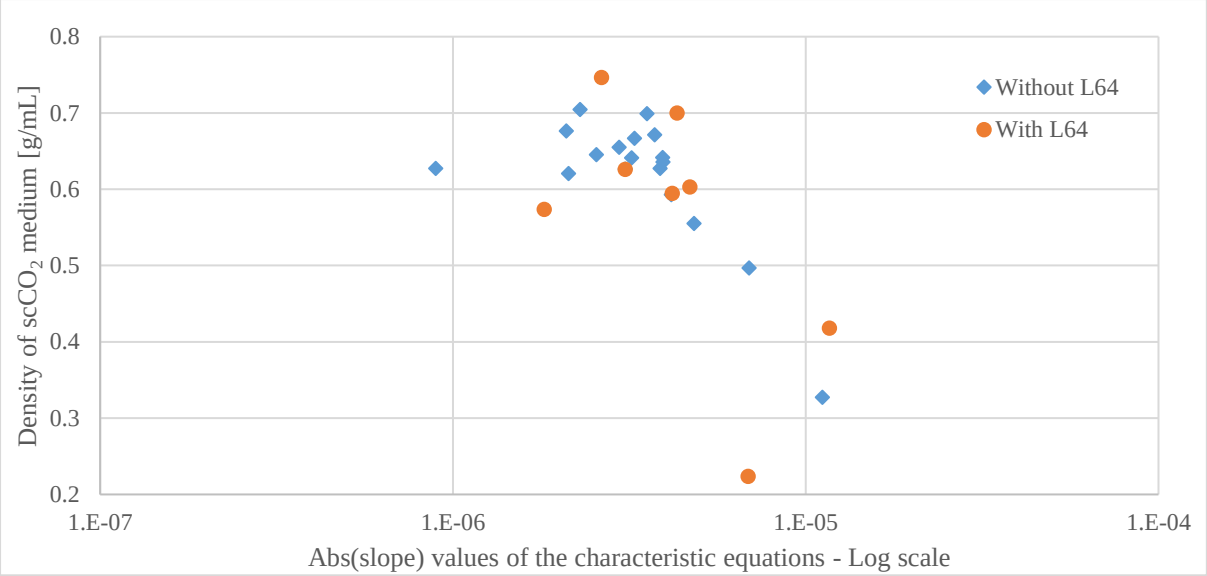


**Fig 13:** Dependency abs(slope) values of the characteristics equations in the "organic extraction zone" about $scCO_2$ density

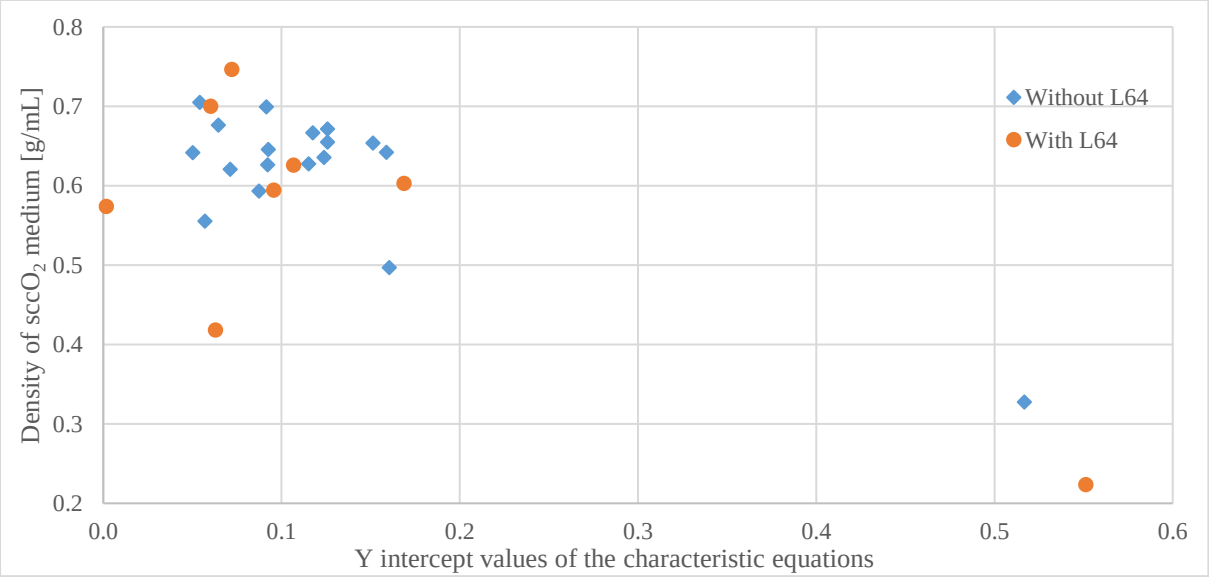


**Fig 14:** Dependency of Y intercept values of the characteristics equations in the "organic extraction zone" about $scCO_2$ density

Dependency of the natural logarithmic values of the characteristic equations on the density of $scCO_2$ in the organic phase extraction part is visible on **Fig 13**. With the density decrease of $scCO_2$ the slopes of the curves tend to higher negative values, which mean a faster organic extraction from the o/w emulsions, due to the higher diffusivity in a lower density region [21].

Meanwhile in the $CO_2$ saturation zone the process is not limited by the phase equilibrium conditions.

Density of $scCO_2$ has no significant influence on the maximum dissolve capacity of $CO_2$ by the sample (**Fig 14**), as the composition of o/w emulsions were not changed significantly, as main part of them was water. This result is consistent with the lack of dependency on phase equilibrium conditions due to the operation above the mixture critical point, discussed above. However, in the lower density region higher Y intercepts values are obtained, due to higher weight of sample holder was measured, as the buoyancy effect caused by the $scCO_2$ medium is lower in lower density region, than in higher density region. As visible on **Fig 12**, **Fig 13** and **Fig 14**, Pluronic L64® has no significant influence on the transport properties.

In order to verify, that pressure and temperature are influencing together the transport properties by changing the density of the $scCO_2$ extraction medium, results of experiments marked by font type Bold in **Table 3** and were plotted on **Fig 15** and **Fig 16**. The dissolution of $scCO_2$ and the extraction of EtAc are influenced by both of the temperature and the pressure together: with pressure decrease and temperature increase (density decrease) transport becomes faster, as concluded above.

Density of the $scCO_2$ medium and the additional Pluronic L64® neither has effect on the residual EtAc content of o/w emulsions, as presented on **Fig 17**. This result confirms again, that the process is not limited by phase equilibrium. Plotted curves on **Fig 4** also confirm, that weight change profiles, and hence mass transfer is only influenced by the density of the o/w emulsion surrounding medium.

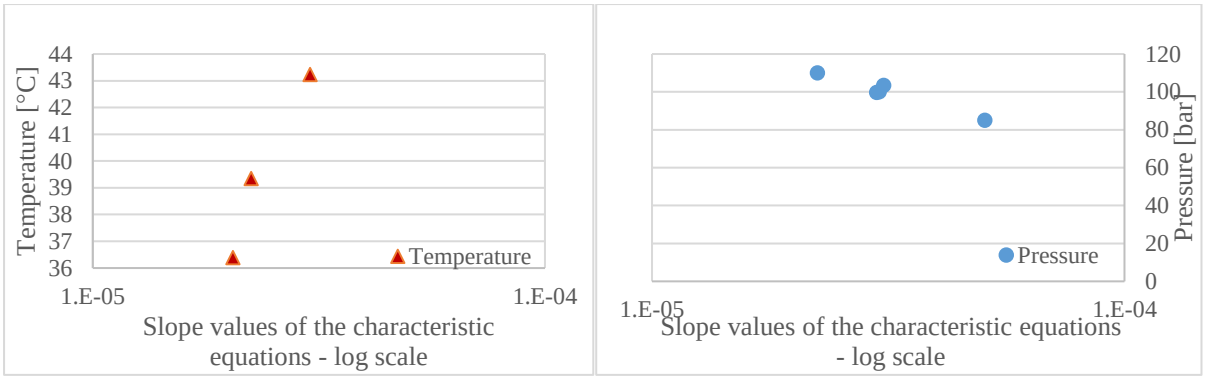


**Fig 15:** Dependency of slope values of the characteristics equations in the "$CO_2$ dissolution zone" about temperature and pressure of $scCO_2$

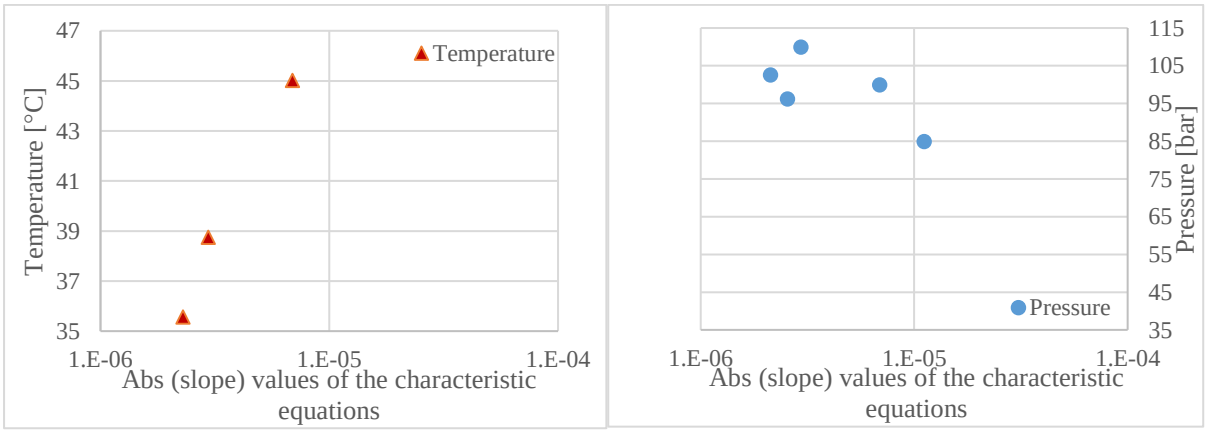


**Fig 16:** Dependency of abs(slope) values of the characteristics equations in the "organic extraction zone" about temperature and pressure of $scCO_2$

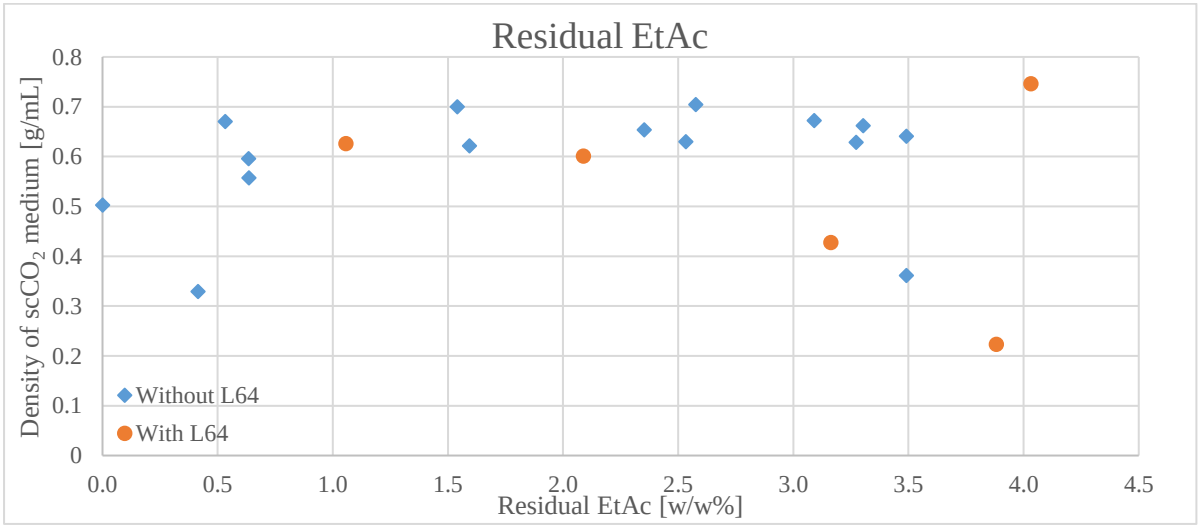


**Fig 17:** Residual EtAc content depending on the density of $scCO_2$

### 3.2.2 Evaluation of transport properties in DCM o/w emulsions

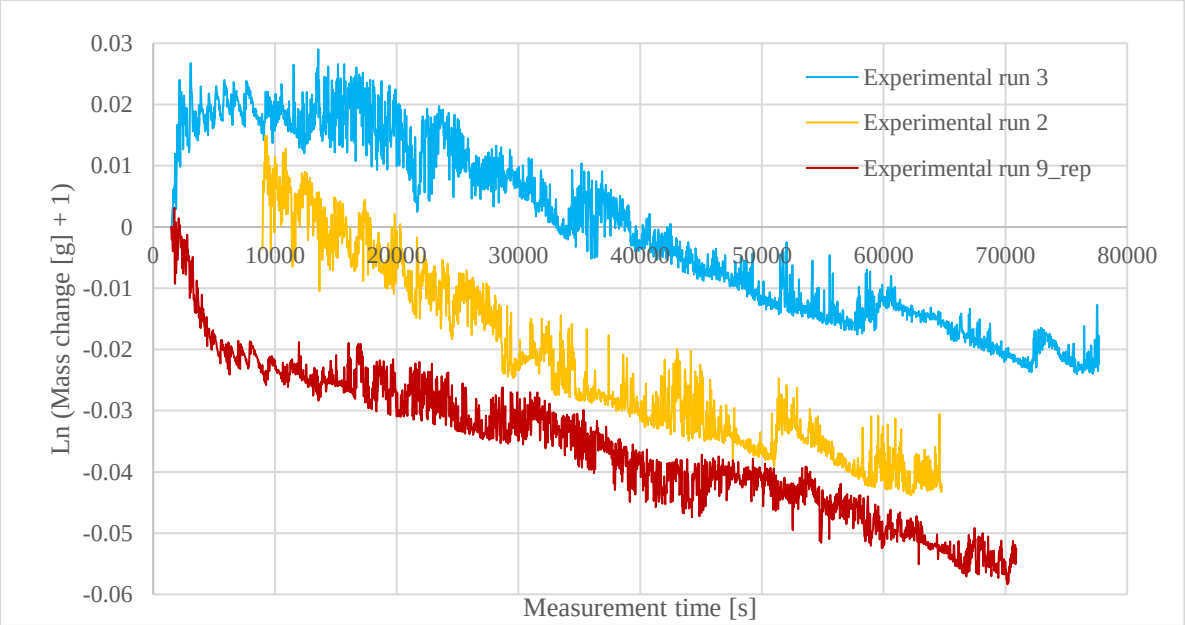


**Fig 18:** Ln(Δm+1) curves of o/w emulsions prepared with DCM, contacted by $scCO_2$

Transport properties of $scCO_2$ – DCM based o/w emulsions were measured by static MSB device as well, in order to compare the characteristics of transport processes with EtAc based o/w emulsion – $scCO_2$ system. Results obtained in section 3.2.1 were used to create the experimental plan for DCM based o/w emulsions. As in case of with EtAc prepared o/w emulsion, only density dependency of transport properties was obtained, experimental plan was created mainly to explore the effect of density on mass transport properties (in the density range of $scCO_2$ 0.5 – 0.7 g/mL), and by neglecting any effects of concentration of surfactant materials and DCM. However, a few experimental run in the centrum point p and T settings of $scCO_2$ medium is done (detailed in **Table 4** by font type Bold), in order to verify, that by neglecting the concentration effect of surfactant materials and the initial water to organic ratio, is not leading us to experimental errors.

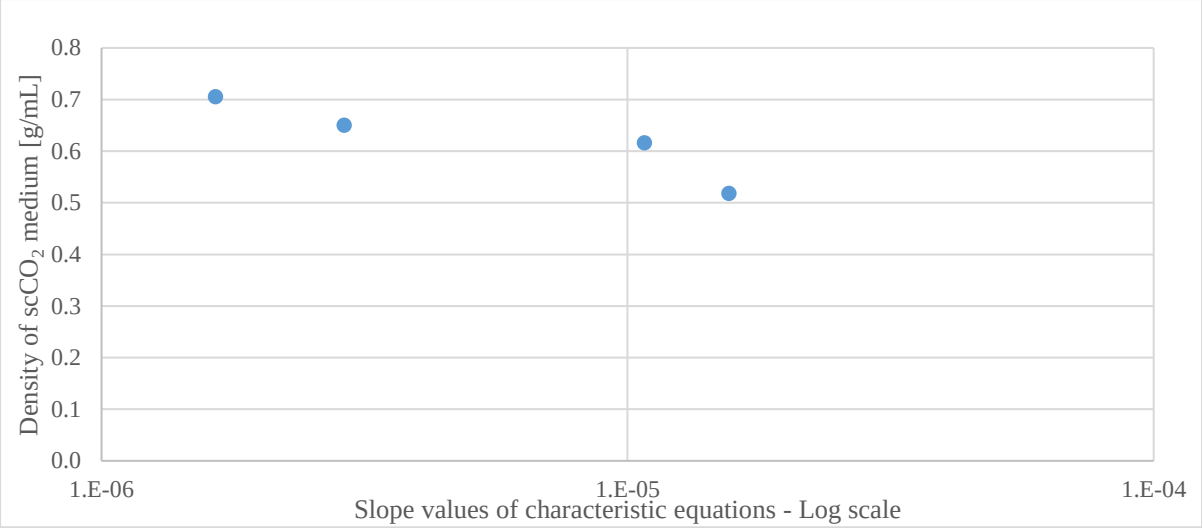


**Fig 19:** Dependency of slope values of the characteristics equations in the "$CO_2$ dissolution zone" about $scCO_2$ density

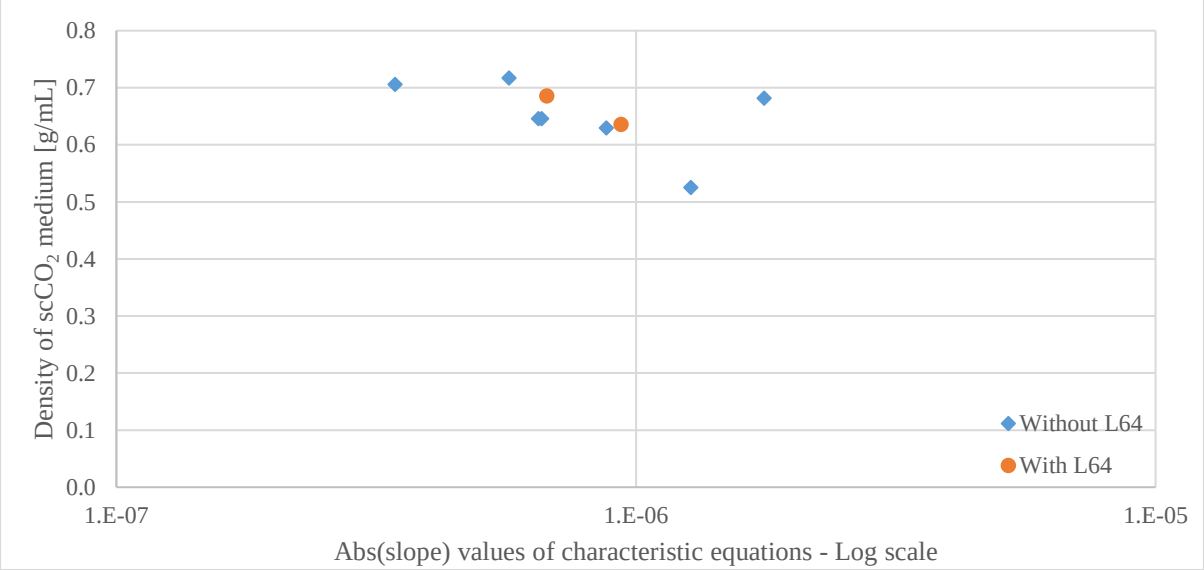


**Fig 20:** Dependency of abs(slope) values of the characteristics equations in the "organic extraction zone" about $scCO_2$ density

As mentioned before in section 3.1, in several experimental runs with DCM prepared o/w emulsions, $CO_2$ dissolution took place faster, than the stabilization of accurately measurable conditions, as visible on **Fig 18**. Therefore, it was only possible to measure the $CO_2$ dissolution part in a few experimental runs (**Fig 19**). However, – as visible on **Fig 18** –, by applying $scCO_2$

as extraction medium in lower density, $CO_2$ dissolution process is not measurable at all due to its rapidity, and due to the lack of exact starting point, reproducibility of measurements is worse, than the reproducibility of measurements in case of EtAc o/w emulsions - $scCO_2$ systems. However, it is possible to conclude, that – similarly to the o/w emulsions prepared with EtAc, – with decreasing $scCO_2$ density, the dissolution of $scCO_2$ into the o/w emulsion tends to be faster. However, the extraction of organic solvent part also tends to be faster with decreasing $scCO_2$ density (**Fig 20**), and according to visual observations, the use of DCM-o/w emulsions on SFEE process can be unfavourable, because emulsion destabilization and phase separation occurs immediately during the pressurization of the system with $scCO_2$, as visible on **Fig 21**. Rapid emulsion destabilizing effect is caused by the low miscibility and high interfacial tension of water – DCM system, detailed in section 3.1. Similarly, as described with EtAc based o/w emulsions, the density of $scCO_2$ has no significant effect on the maximum $CO_2$ absorption capacity by the sample (**Fig 22**).

**Fig 21:** Phase separation of DCM/w emulsion upon pressurizing by $CO_2$

In order to verify, that transport properties in case of with DCM prepared o/w emulsion are not influenced by the concentration of DCM or surfactant materials, results of experimental runs marked by font type Bold in **Table 4** are plotted on **Fig 23**, **Fig 24** and **Fig 25**. Effect of additional Pluronic L64® was also studied and plotted separately on figures, marked by "(L64)". Transport properties are neither influenced by the concentration of DCM and lecithin, nor by the concentration of Pluronic L64® as additional surfactant material. All experiments plotted on **Fig 23**, **Fig 24** and **Fig 25** are done at about 100 bar and different temperatures. As shown in these figures, only temperature change neither has no significant effect on the mass transport properties.

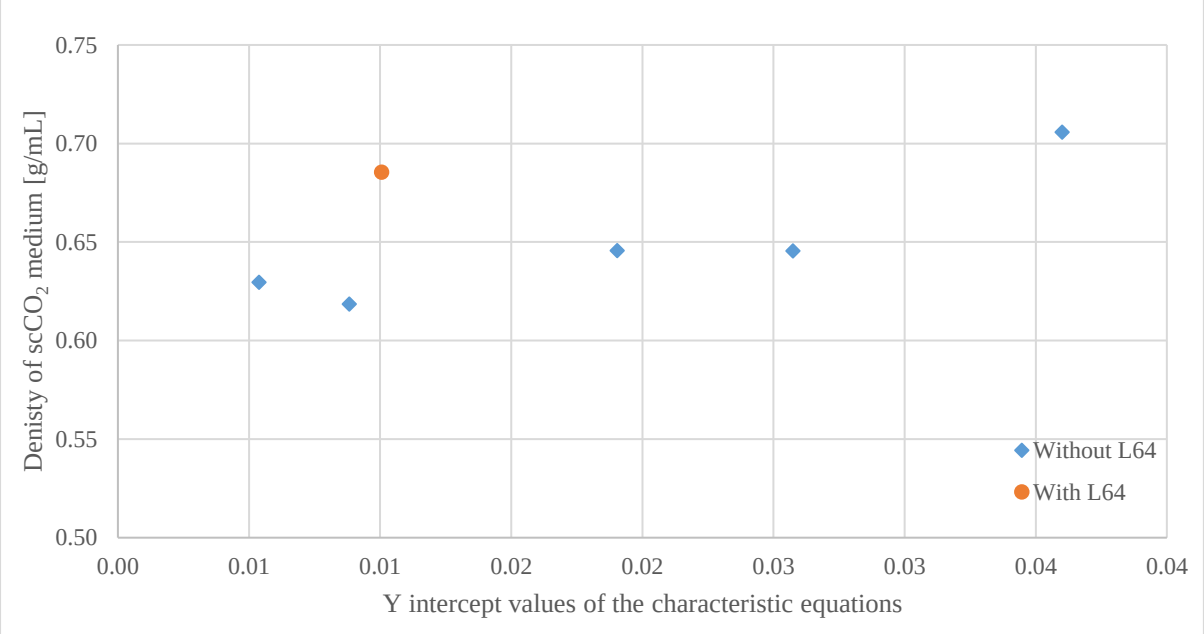


**Fig 22:** Dependency of Y intercept values of the characteristics equations in the "organic extraction zone" about $scCO_2$ density

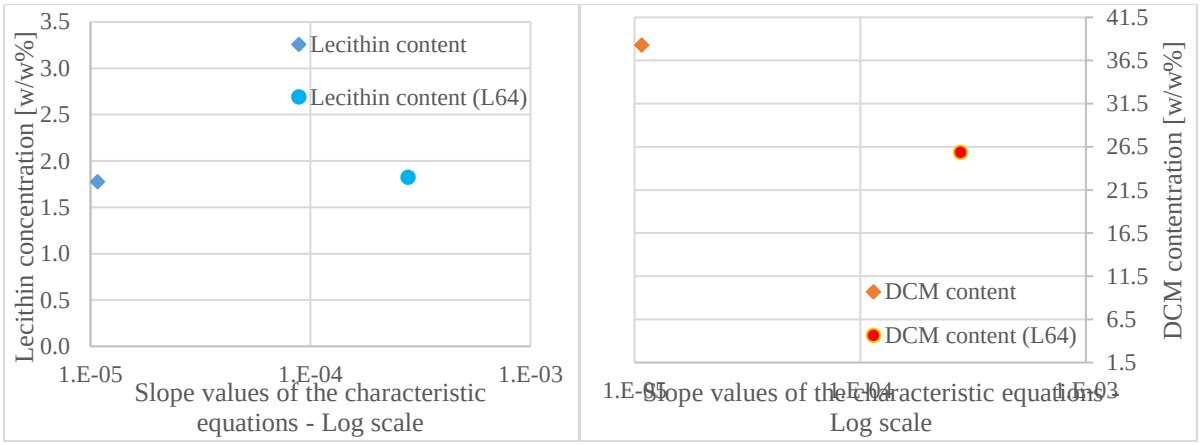


**Fig 23:** Dependency of slope values of the characteristics equations in the "$CO_2$ dissolution zone" about lecithin- and DCM content in case of static measurements

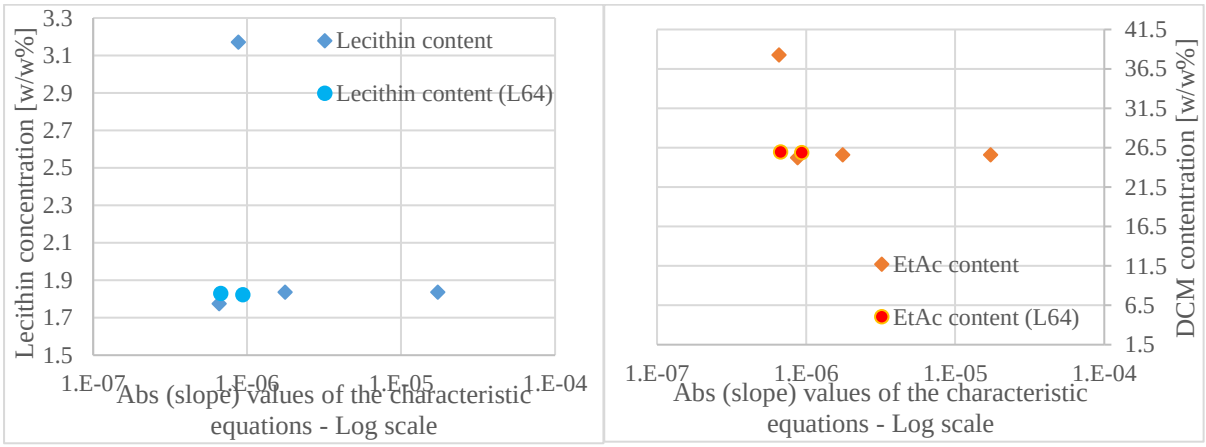


**Fig 24:** Dependency abs(slope) values of the characteristics equations in the "organic extraction zone" about lecithin- and DCM content in case of static measurements

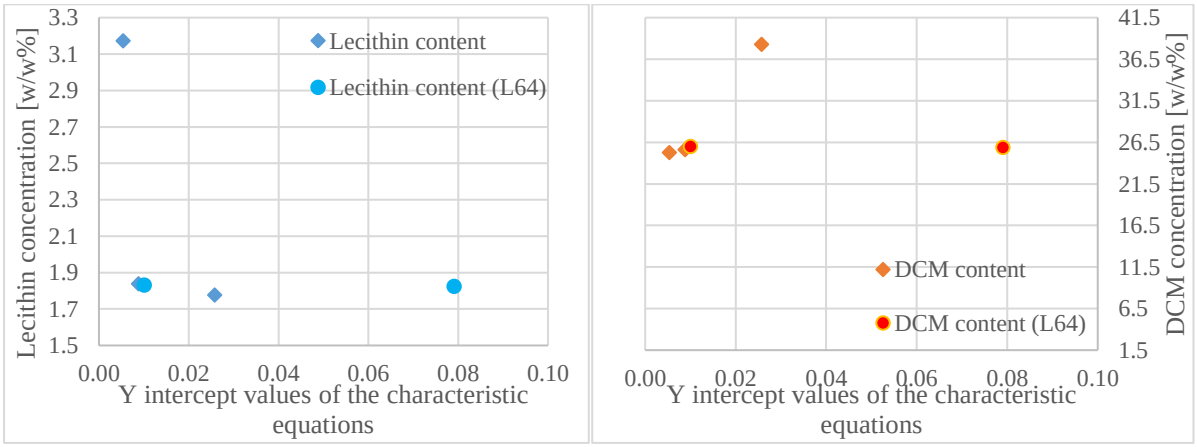


**Fig 25:** Dependency of Y intercept values of the characteristics equations in the "organic extraction zone" about lecithin- and DCM content in case of static measurements

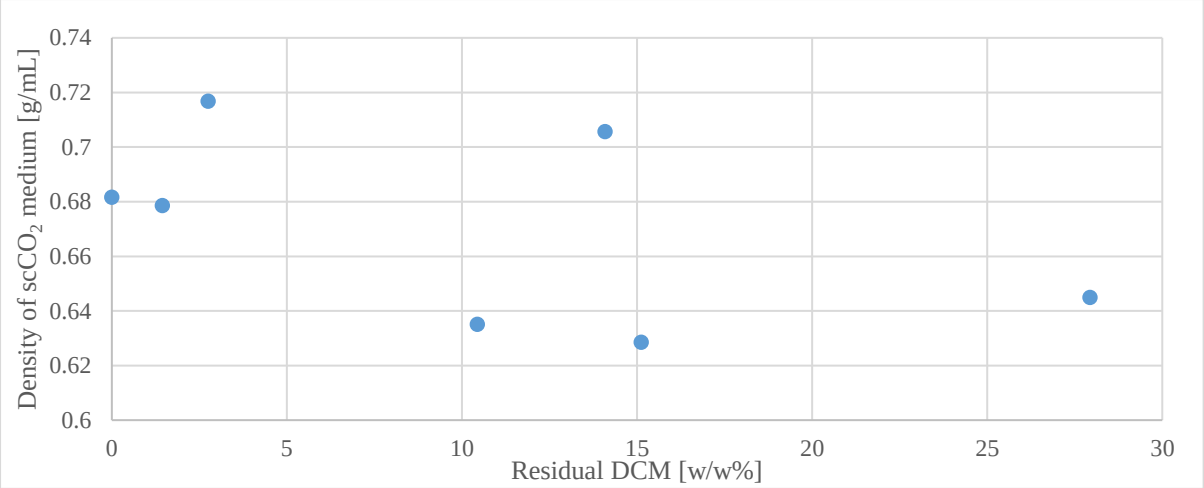


**Fig 26:** Residual DCM content depending on the density of $scCO_2$ in case of static measurements

Residual DCM content after the extraction process is independent of the density of $scCO_2$ extraction medium (**Fig 26**), and significantly higher, than the residual organic content in experiments with EtAc prepared o/w emulsions. This result is due to the rapid destabilization and phase separation of o/w emulsions, with the formation of thick water layer on top of the DCM phase, which separates the $scCO_2$ from the DCM, and acts as an extra border and limitation for the mass transport.

**Table 4**: Experimental plan with DCM prepared o/w emulsions: Runs for study the **effect of concentration of lecithin and DCM** marked by font type Bold; runs for study the *effect of temperature change only* marked by font type Italic; Centrum point runs marked by "_C"; repetitions of previous experiments marked by "_rep

| **Number of experimental run** | **$C_{L64}$ [w/w%]** | **$C_{Lecithin}$ [w/w%]** | **$C_{DCM}$ [w/w%]** | **Solvent/ /water ratio [ml/ml]** | **p [bar]** | **T [°C]** | **Density of $scCO_2$ medium [g/mL]** | **$CO_2$ dissolution slope** | **Organic extraction slope** | **Y intercept in organic extraction zone** | **Residual EtAc [w/w%]** |
|---|---|---|---|---|---|---|---|---|---|---|---|
| **1_C** | **-** | **1.8** | **25.6** | **1/4** | **99.9** | **40.4** | **0.62** | **-** | **-1.73E-05** | **8.82E-03** | **-** |
| **2** | **-** | **3.2** | **25.2** | **1/4** | **99.9** | **40.5** | **0.63** | **-** | **-8.77E-07** | **5.38E-03** | **15.1** |
| **3** | **-** | ***1.8*** | ***38.3*** | ***1/2*** | ***99.9*** | ***39.8*** | ***0.64*** | **1.08E-05** | **-6.58E-07** | **2.57E-02** | ***27.9*** |
| **4** | **-** | ***1.8*** | ***25.6*** | ***1/4*** | ***99.3*** | ***36.9*** | ***0.68*** | **-** | **-1.76E-06** | **-1.96E-02** | **-** |
| ***5*** | ***0.4*** | ***1.8*** | ***26.0*** | ***1/4*** | ***99.9*** | ***36.9*** | ***0.68*** | **-** | **-6.74E-07** | **1.01E-02** | ***1.4*** |
| ***6*** | ***0.7*** | ***1.8*** | ***25.9*** | ***1/4*** | ***99.9*** | ***39.7*** | ***0.64*** | **2.78E-04** | **-9.36E-07** | **7.91E-02** | ***10.4*** |
| 7 | - | 1.8 | 25.6 | 1/4 | 99.9 | 38.9 | 0.52 | 1.56E-05 | 1.28E-06 | 5.39E-02 | - |
| 8 | - | 1.8 | 25.6 | 1/4 | 109.9 | 38.3 | 0.71 | 1.65E-06 | -3.44E-07 | 3.60E-02 | 14.1 |
| 9_rep | - | 1.8 | 25.6 | 1/4 | 109.9 | 37.4 | 0.72 | - | -5.70E-07 | -1.49E-02 | 2.7 |

### 3.3 Mass transport model fitting on results, obtained in static MSB experiments

Mass transport properties of both, with EtAc and with DCM prepared o/w emulsions were modelled, using the following model equations:

$$\frac{\partial xw_{CO_2}}{\partial t} = k(1) * \left[ \frac{\partial xw_{eq,ini}}{\partial t} - \frac{\partial y_{CO_2}}{\partial t} \right] - k(4) * \max \frac{n_{org}}{n_{org,ini}} * \left( \frac{\partial xw_{CO_2}}{\partial t} - 0 \right) \quad (5)$$

$$\frac{\partial xw_{org}}{\partial t} = k(2) * \left[ \frac{\partial xw_{eq,ini}}{\partial t} - \frac{\partial x_{org}}{\partial t} \right] + k(3) * \max \frac{n_{org}}{n_{org,ini}} * \left( \frac{\partial xw_{org}}{\partial t} - x_{orgw} \right) \quad (6)$$

$$\frac{\partial x_{org}}{\partial t} = -k(3) * \max \frac{n_{org}}{n_{org,ini}} * \left( \frac{\partial xw_{org}}{\partial t} - x_{orgw} \right) \quad (7)$$

$$\frac{\partial xorg_{CO_2}}{\partial t} = k(4) * \max \frac{n_{org}}{n_{org,ini}} * \left( \frac{\partial xw_{CO_2}}{\partial t} - 0 \right) - k(5) * \max \frac{n_{CO_2}}{n_{CO_2} + n_{org}} * \max\left(n_{CO_2,ini}\right) \quad (8)$$

In Equaitions detailed above, in subscripts written “org”,”w” and “$CO_2$” mean the mass flow of organic-, water- and $CO_2$ compounds, respectively.

“Org” = organic phase

“w” = aqueous phase

“ini” = in initial conditions

“eq” = in equilibrium

Equation 5 represents the $CO_2$ flow into the aqueous phase, from the $scCO_2$ phase and from the organic phase. The “ $\max \frac{n_{org}}{n_{org,ini}}$ ” part is characterizing the decreasing interphase between the aqueous and the organic phase, due to the decreasing organic concentration in the organic phase, due to extraction of the organic solvent. Equation 6 is characterizing the organic flow into the aqueous phase, from the $scCO_2$-, and from the organic phase. Multiplication with the last part in Equation 5 and in Equation 6 is, in order to avoid negative values of mass. Equitation

7 is characterizing the organic flow into the aqueous phase, and hence the residual organic concentration. Equation 8 is characterizing the $CO_2$ transfer from the aqueous phase into the organic phase. In this equation, parameter k(5) is characterizing the behaviour of $scCO_2$ – organic phase when their density become equal, due to the extraction ,and hence density decrease of the organic phase [11]. All calculations were done considering molar values of composition and density.

The constants k(1), k(2), k(3), k(4), k(5) are the parameters, which correspond with the experimentally obtained slope values, and the aim of the modelling is to fit these parameters to the experimentally obtained mass transfer results. Accurate phase equilibrium calculations are essential to provide an accurate initial component estimation for the three-phase- system at a given pressure and temperature, which was not measurable, due to reasons detailed in section 3.2. For the initial estimation of $H_2O$ - EtAc - $scCO_2$ and $H_2O$ - DCM - $scCO_2$ system the flash calculation codes presented by Á. Martín et al. [22] were used, applying the Peng-Robinson Equation of state with Stryjek-Vera alpha function [23], and with Wong-Sandler mixing rules (PRWEoS) [24]. Requested parameters for the pure components were determined using the group contribution methods [25]. Similarly, to the work of Á. Martín et al. [2], first the conditions of equilibrium at the interface were solved, then partial differential equations (PDE) are simultaneously solved by using the ODE23 function of MATLAB® R2013b software. Objective function was to minimalize the residual difference – shown on Equation 9 – between the fitted and the measured data. Accurateness of fitting was determined according to Equation 10.

$$\text{Residuum} = \sum_{i=1}^{n}\left(x_{i,\text{model}} - x_{i,\text{data}}\right)^2 \qquad 9$$

$$\text{Accurateness of fitting} = {}^{1}\!/_{n} * \text{Residuum} \qquad 10$$

A continuous water layer was assumed between the $scCO_2$ and the organic phase. This assumption is justified by visual observations in case of EtAc/w emulsions, which were stable in $scCO_2$ atmosphere. However, in case of DCM/w emulsions, rapid destabilization upon pressurization with $CO_2$ took place, and due to immiscibility of the two phases and density differences, formulation of separated water layer on DCM layer occurred.

Further assumptions were applied in the model:

- Isobaric and isothermal conditions
- Organic phase droplets are homogeneously distributed within the emulsion drop.
- The influence of the surfactant on the diffusion and mass transfer is not considered. Indeed experimental results demonstrate that the surfactant has no influence on the mass transfer (sections 3.2.1, 3.2.2).
- For all physical properties calculations, it is considered that the continuous phase of the emulsion is pure water. This simplification is justified by the small solubility of DCM, EtAc and $CO_2$ in water.
- Equilibrium at the liquid–supercritical $CO_2$ interface as well as at the organic phase–aqueous phase interface is assumed by initial calculations with PRWEoS.
- The concentration of water in the $scCO_2$ rich phase has been considered as zero, since the water solubility in the experimental conditions is very low [26] [14] [27].

**Table 5:** Modelling results of parameters: results of EtAc based emulsions marked by font type Underlined, *results of DCM based emulsion* marked by font type Italic

| | **k1*10$^{-4}$** | **k2*10$^{-4}$** | **k3*10$^{-4}$** | **k4*10$^{-4}$** | **k5*10$^{-4}$** |
|---|---|---|---|---|---|
| **Range of change** | 0.39-81.52 | 0.16-716.47 | 0.13-7.86 | 0.55-4791.12 | 0.07-0.61 |
| **Difference** | 81.14 | 716.32 | 7.73 | 4790.57 | 0.54 |
| ***Range of change*** | *0.10-42.84* | *0.92-25.86* | *0.45-7.30* | *0.28-2.89* | *0.02-0.08* |
| ***Difference*** | *42.74* | *24.93* | *6.85* | *2.60* | *0.06* |

Initially, the values of all the five parameters were changed, in order to optimize the fitting of model to the experimental results, and to minimize the deviance between them. The maximum and minimum values, and the difference between them of both (with EtAc and with DCM prepared) o/w emulsions are visible in **Table 5**. Difference between minimum and maximum values of the coefficients is the smallest in case of parameters k(3) and k(5), as k(5) is only a correction for the decrease of density difference between $scCO_2$ and organic phase during the process, meanwhile parameter k(3) is characterizing the residual organic content of o/w emulsions, which is nearly independent in the studied density region of the density of $scCO_2$, as obtained in section 3.2.1 and 3.2.2. In case of DCM/w emulsions, parameter k(4) also has a small difference between its fitted minimum and maximum value, as it is related to mass transfers occurred in the aqueous phase, which is become separated immediately upon pressurization with $CO_2$, due to emulsion destabilization and phase separation, as mentioned in section 3.2.2. Due to these reasons, in the final correlation of parameter values of k(3) and k(5) were fixed, and further modelling runs were done, in order to obtain the influence of $scCO_2$ extraction medium density on parameters k(1), k(2) and k(4).

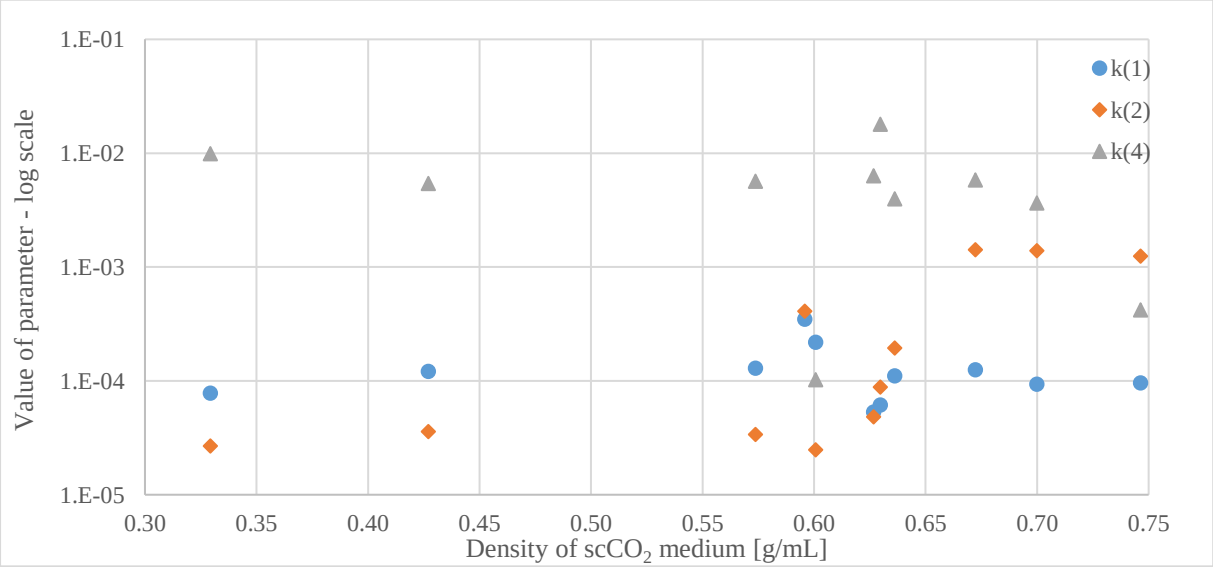


**Fig 27:** Density dependency of model parameters k(1), k(2), k(4) in EtAc based o/w emulsions

Values of parameters k(1), k(2), k(4) in case of $scCO_2$ - EtAc based o/w emulsions – obtained by the model with fixed parameter values of k(3) and k(5) –, are plotted on **Fig 27**. Values of parameter k(1) are in a low order of magnitude, due to the low solubility of $scCO_2$ in water, but values are slightly increasing with the density of $scCO_2$. Values of parameter k(2) are in the same order of magnitude as the parameter values of k(1), as the solubility of organic solvent in water is also very low. Values of parameter k(2) are increasing with the density increase of $scCO_2$, as more $CO_2$ is dissolved into the water phase, and hence the driving force for the extraction of organic solvent contained by the water phase is higher, so the mass transfer of the organic phase to the $scCO_2$ phase becomes faster [9]. Modelling results show, that parameter k(4) is at least one order of magnitude higher than the other two parameters, as the organic phase and the $scCO_2$ are highly miscible, and hence this process is faster than $CO_2$- or organic flow into the aqueous phase.

As mentioned in section 3.2.2, SFEE process is unfavourable in case of DCM based o/w emulsions, as phase separation occurs immediately upon the pressurization by $CO_2$, due to high interfacial tension value between water and DCM phase. This result is proved by the modelling results of $scCO_2$ – DCM o/w emulsion system as well, as the parameters k(1), k(2), k(4) are randomly chancing, as shown on **Fig 28**. Moreover, the characteristic value of model accurateness is changing in a significantly wider range in DCM/w – $scCO_2$ system, than in EtAc/w – $scCO_2$ system, as shown in **Table 7**.

**Table 6**: Accurateness characterizing values of modelling

| $\frac{1}{n}$ * Residuum | EtAc/w – $scCO_2$ system | DCM/w – $scCO_2$ system |
|---|---|---|
| **Average** | $1.02*10^{-4}$ | $7.43*10^{-4}$ |
| **Range of change** | $1.30*10^{-4}$ - $3.87*10^{-3}$ | $8.20*10^{-6}$ - $3.91*10^{-3}$ |

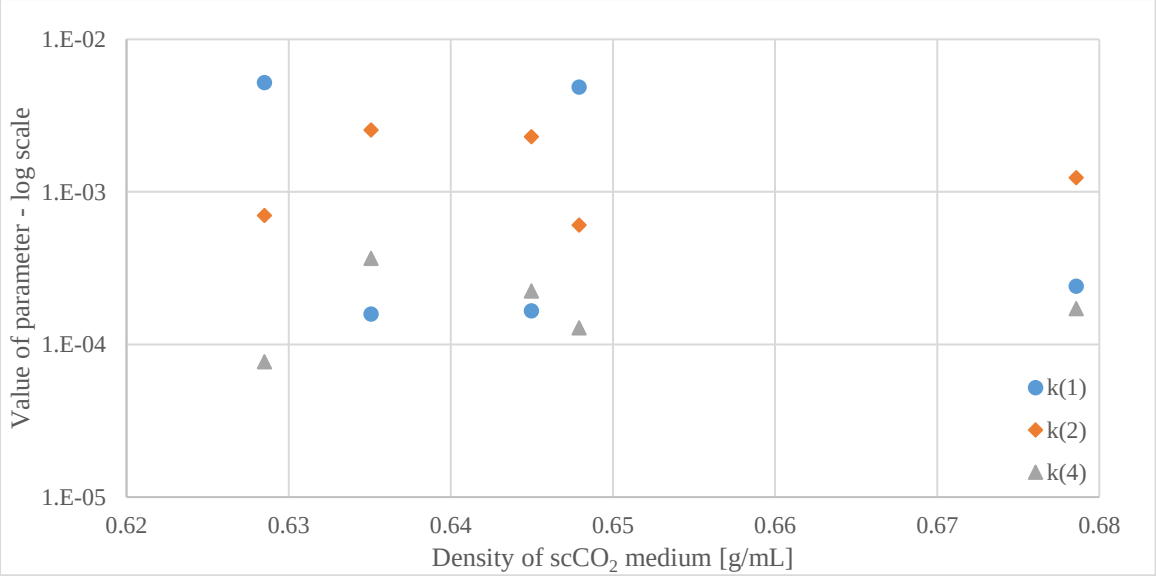


**Fig 28:** Density dependency of model parameters k(1), k(2), k(4) in DCM based o/w emulsions

### 3.4 Results obtained by dynamic MSB device

A usual weight-change-profile measured by dynamic MSB device shown on **Fig 29**. Measured weight is the sum of the weight of the holder, the sinker and the sample. Strong initial weight decrease is taking place in the beginning of the process, associated to the pressurization of the cell by $CO_2$, as visible on **Fig 31**. For this reason, the evaluation of the measured results was only possible after the desired pressure and temperature was reached (about 30 min). Cell was preheated, and temperature controlling was maintained after phase change of $CO_2$ had been occurred, in order to reach constant, homogenous temperature conditions in the cell, as early as possible. A usual way to analyse the weight change results is shown on **Fig 30**. The measured weight has to be corrected by the buoyancy effect of the $scCO_2$ atmosphere, whose effect depends on the density of $scCO_2$ and the volume of the sample. The volume of o/w emulsions was assumed constant during the whole measurement period, according to visual observations detailed in section 3.1.

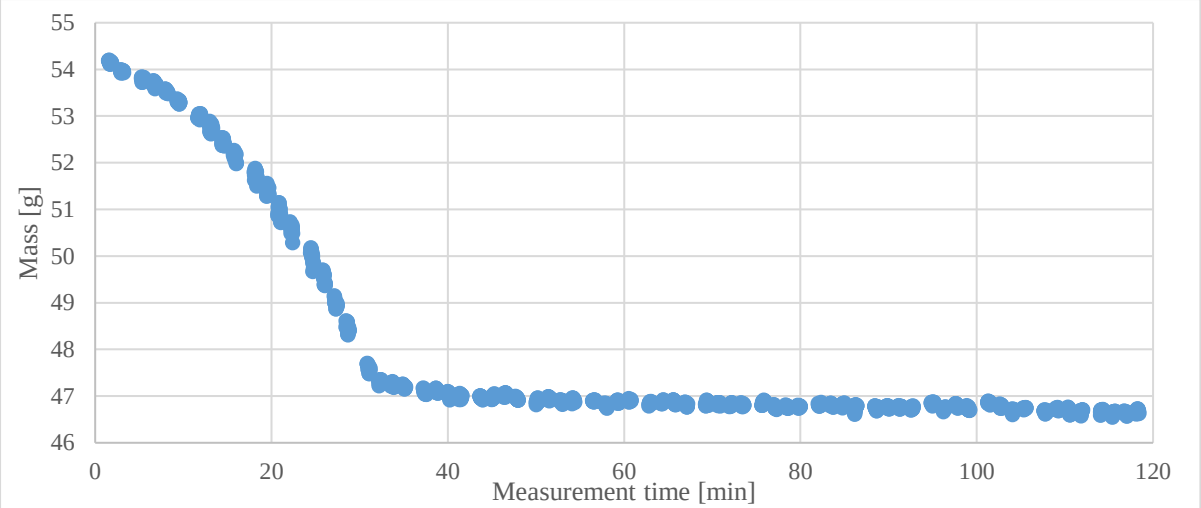


**Fig 29:** General weight evolution of emulsion prepared with EtAc contacted by $scCO_2$: experimental run 7

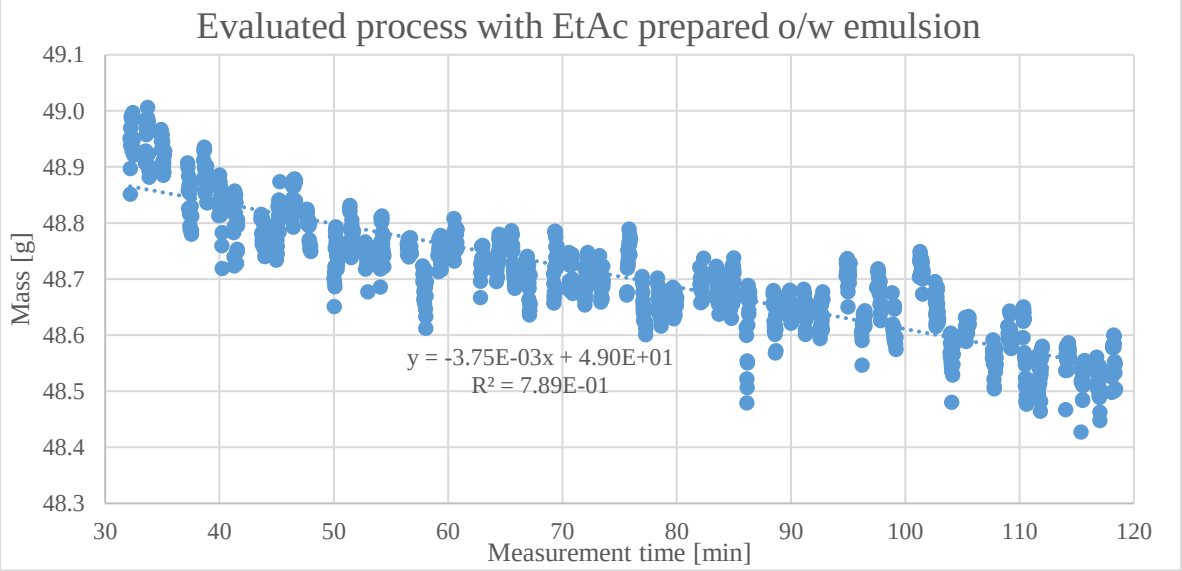


**Fig 30:** Process evaluation in case of experimental run 7 (with EtAc prepared o/w emulsion)

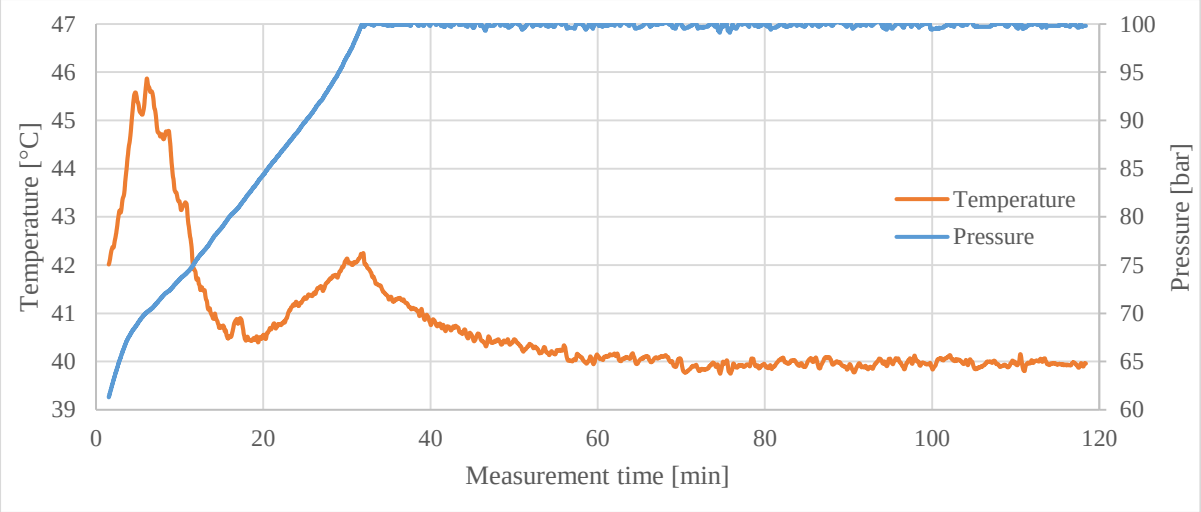


**Fig 31:** Temperature- and pressure monitoring during measurement time in experimental run 7 (with EtAc prepared o/w emulsion) in case of dynamic measurement

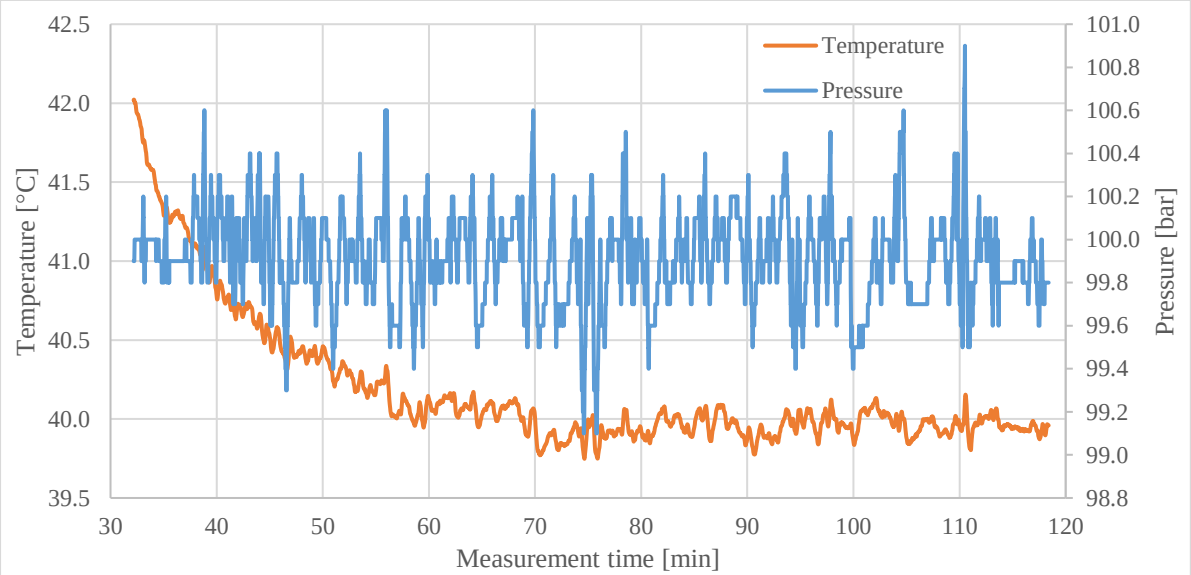


**Fig 32:** Temperature- and pressure monitoring in the evaluation period in case of experimental run 7 (with EtAc prepared o/w emulsion)

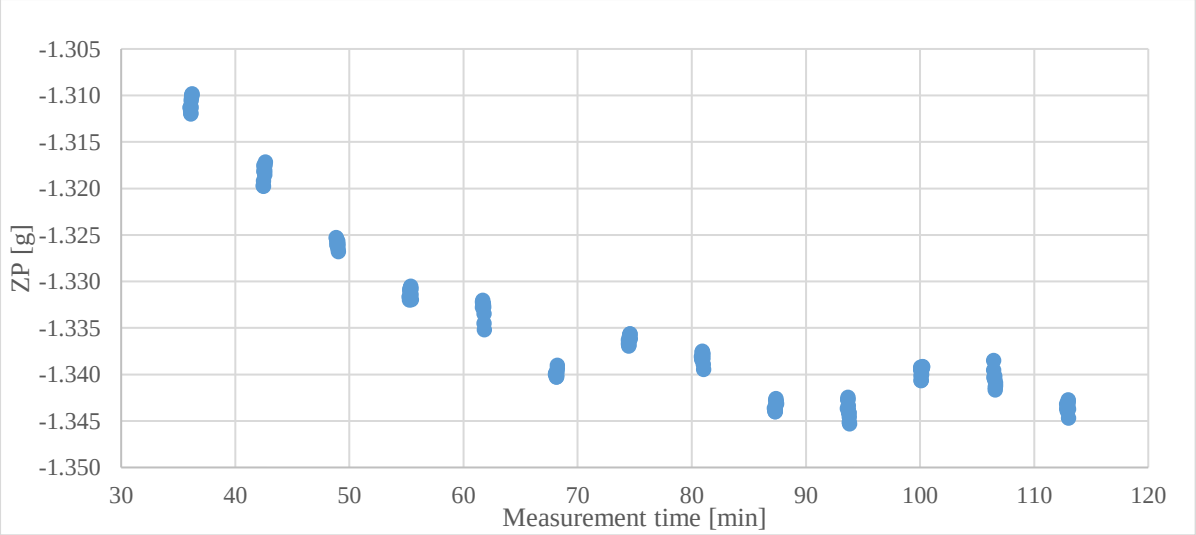


**Fig 33:** Change of ZP in evaluation period in case of experimental run 7 (with EtAc prepared o/w emulsion)

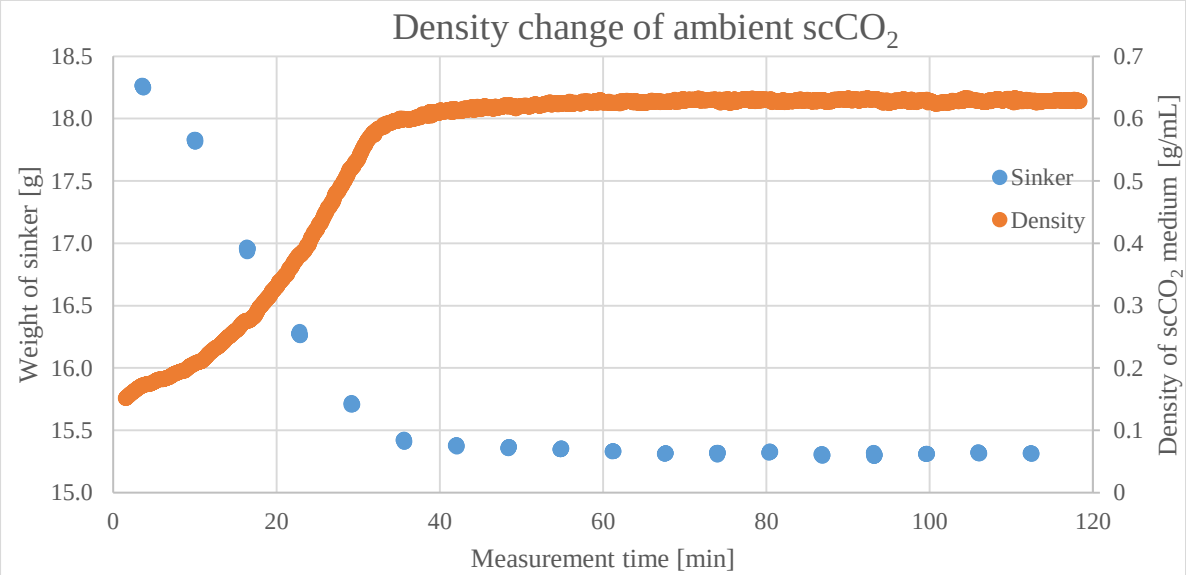


**Fig 34:** Weight change of sinker during measurement time and evaluation of ambient density in case of experimental run 7 (with EtAc prepared o/w emulsion)

On **Fig 32** the average fluctuation of temperature and pressure in the measuring period is plotted. Due to reasons detailed in section 2.5, compared to the experiments done by the static MSB device, bigger fluctuations of pressure and temperature occurred, which lead to less accurate results, even after the correction with the buoyancy effect. Weight results plotted on **Fig 30** are already corrected by the bouncy effect, and by the average of ZP (recorded during the measurement and plotted on **Fig 33**), but not corrected with the weight of the sample holder and the sinker, in order to obtain the most accurate results as possible. The value of ZP remains nearly constant during the whole measurement period, therefore simply using its average for the weight correction is not leading to significant errors. Measured weight of sinker (**Fig 34**) is characterizing the density change of the $scCO_2$ atmosphere which is surrounding the sample. In order to evaluate the mass change result of o/w emulsions contacting continuously with $scCO_2$, a linear equation was fitted on the weight profile, obtained by the dynamic MSB device, plotted on **Fig 30**. Slope of the equation is characterizing the rate of the extraction of the organic solvent, meanwhile the intercept of the equation is the addition of the initial weight of the sample, the sample-holder, and the sinker. As this intercept has no relevant physical meaning in terms of the transport processes playing roll in the o/w emulsions contacted by $scCO_2$, in further evaluation it was not used. Generally, the slopes of the obtained mass-change curves are around two orders of magnitude higher, than the slopes of the static process, meaning that the extraction of organic phase from the o/w emulsions is much faster in the dynamic SFEE process than in the static SFEE process, due to the continuous $scCO_2$ flow through the sample.

### 3.4.1 Dynamic measurement of transport properties in o/w emulsions prepared by EtAc

As detailed in **Table 7**, an experimental plan was done in order to determine the significant factors for mass transport properties in with EtAc prepared o/w emulsions contacted continuously with $scCO_2$. Effect of the concentrations of surfactant materials and EtAc, and the effect of the pressure- and the temperature, was studied. According to **Fig 35**, neither the concentration of EtAc, nor the concentration of lecithin and additional Pluronic L64® as surfactants have effect on the EtAc extraction rate from the o/w emulsions.

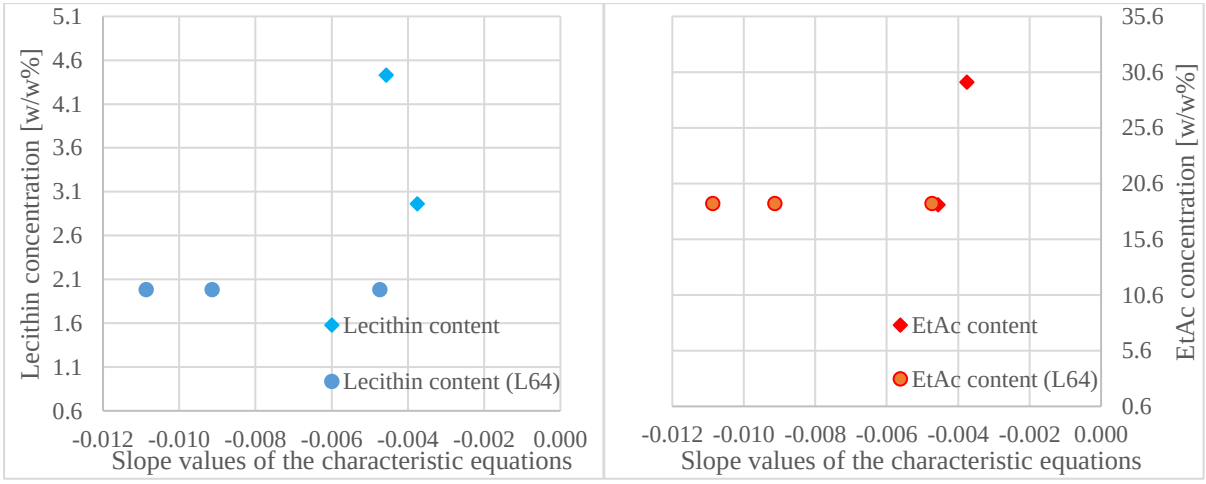


**Fig 35:** Dependency of slopes of the characteristics equations about lecithin- and EtAc content in case of dynamic measurement

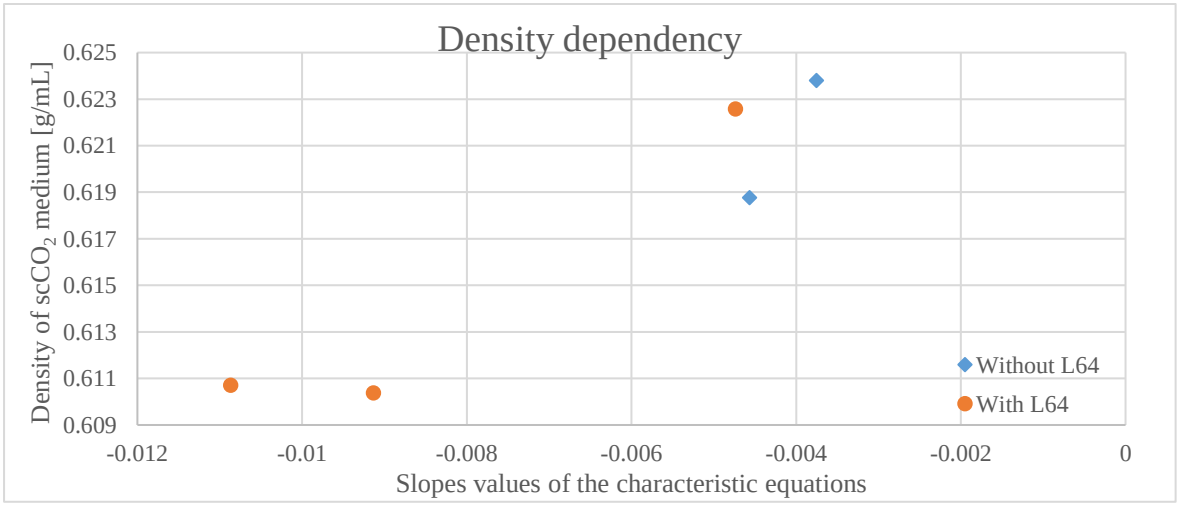


**Fig 36:** Dependency of slopes of the characteristics equations about density of $scCO_2$

Density dependency of mass transport might be visible on **Fig 36** – which is comparable with the results obtained in section 3.2.1 by static MSB device –, with decreasing density of the $scCO_2$ extraction medium, a faster extraction of EtAc occurs, due to the diffusivity increase of $scCO_2$ [21], detailed in section 3.2.1. Effect of the temperature and the pressure was measured separately (**Fig 37**) in order to verify, that these parameters need to be changed together by changing the density of $scCO_2$, which has influence on the transport properties in o/w emulsions, as in case of results obtained by static MSB device, and detailed in section 3.2.1. Although a density dependency of transport properties is visible in case of dynamic measurements, generally the slopes of obtained mass-change curves are very low, meaning that the extraction of organic phase from the o/w emulsions is very slow. Despite of the slow organic extraction, usually a low amount of residual EtAc is determined after a relatively short extraction process comparing with the static process: usual measurement time was around 1 – 1.5 hour, as plotted on **Fig 30**. Respecting this observation an additional measurement was done, in which the sample was only pressurized till 100 bar, then immediately depressurized, in order to measure the loss of EtAc in case of this method. By only pressurizing and depressurizing the sample, almost as much EtAc is removed, as with longer measurement processes, indicating that extraction of the organic phase is more efficient during the pressurization, as the pressurization process causes an efficient mixing effect between the o/w emulsion and the $CO_2$. Moreover, the phase change of $CO_2$ from liquid to supercritical might produce an extra mixing effect, which makes the solubilisation and extraction of organic phase even more effective. According to that observation, the pressurization process of o/w emulsions might be an important process issue of SFEE process. Similar conclusion is obtained in the work of Mattea F et al. [11], as experimental results indicated an immediate volume increase of the drops upon by pressurizing the system, as water phase became rapidly saturated by $scCO_2$, due to the pressurization caused an extra stirring effect. Moreover, model results were

more comparable with experimental results, if the diffusion of $CO_2$ in the water layer was neglected, indicating that the mass transfer of $CO_2$- and DCM phase throughout the water layer, is much faster, than a simple molecular diffusion. Natural convection of streams and interfacial turbulence caused by the Marangoni effect, which occurs in $CO_2$ - $H_2O$ system as its density is much lower than density of pure $H_2O$, is also could be a possible reason for the faster mass transfer process of $scCO_2$- and low molecular weight organic phases [28] [29].

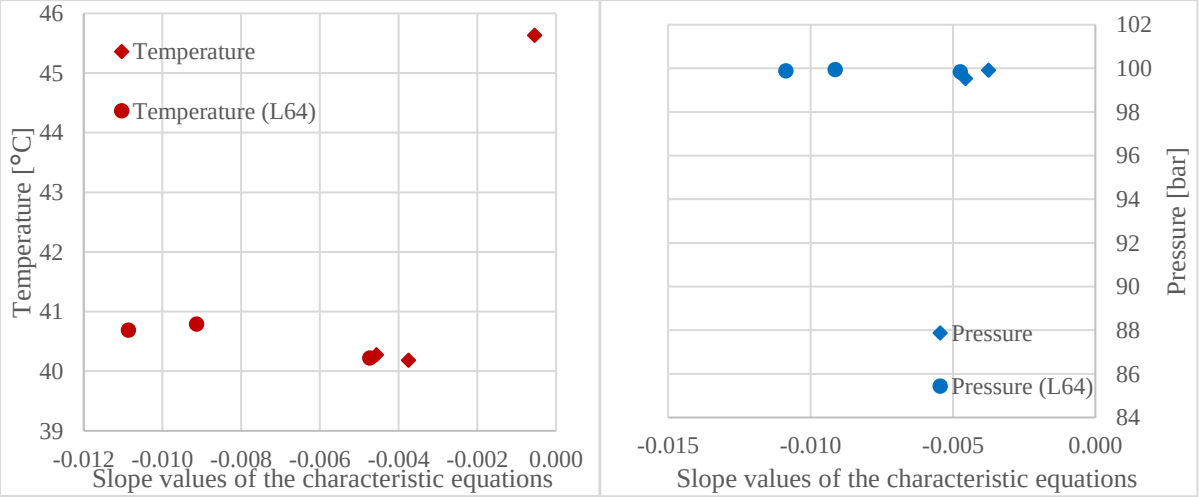


**Fig 37:** Dependency of slopes of the characteristics equations about temperature and pressure of $scCO_2$ in $scCO_2$ – EtAc o/w emulsion systems in case of dynamic measurements

### 3.4.2 Dynamic measurement of transport properties in o/w emulsions prepared by DCM

An experimental plan detailed in **Table 8** was done, in order to determine the significant factors, which are influencing the transport properties in with DCM prepared o/w emulsions. Similarly, to EtAc based o/w emulsions, neither the concentration of DCM, nor the concentration of surfactant materials or additional Pluronic L64® have significant influence on the mass transport properties **Fig 38**). Density-, pressure- and temperature dependency is neither visible on **Fig 39** and **Fig 40**, due to the reason detailed in section 3.4.1. Highest part of the organic phase is already extracted by a simple pressurization and depressurization process as well, as proved by the last experiment, detailed in **Table 8**.

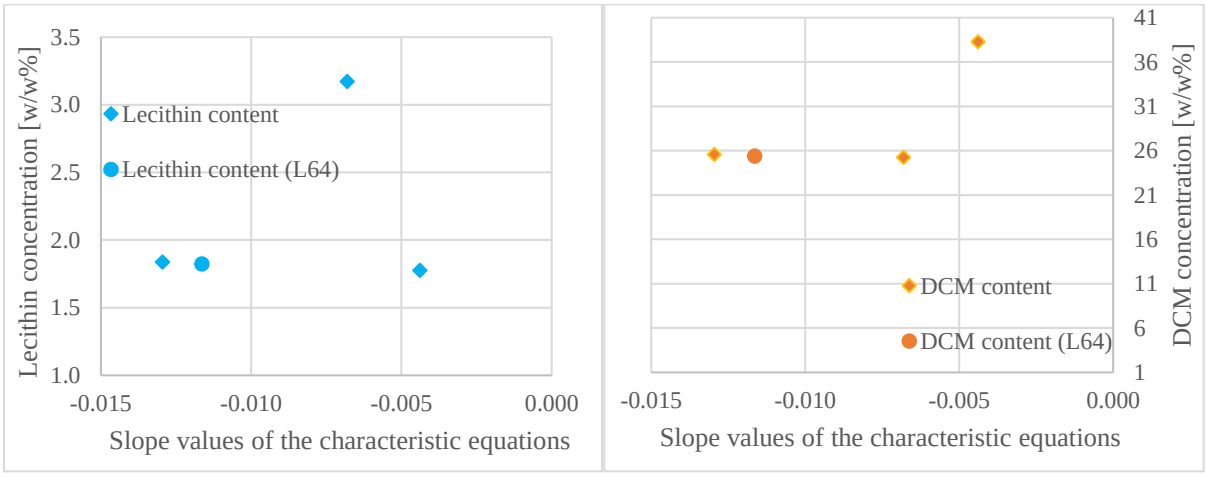


**Fig 38:** Dependency of slopes of the characteristics equations about lecithin- and DCM content in case of dynamic measurements

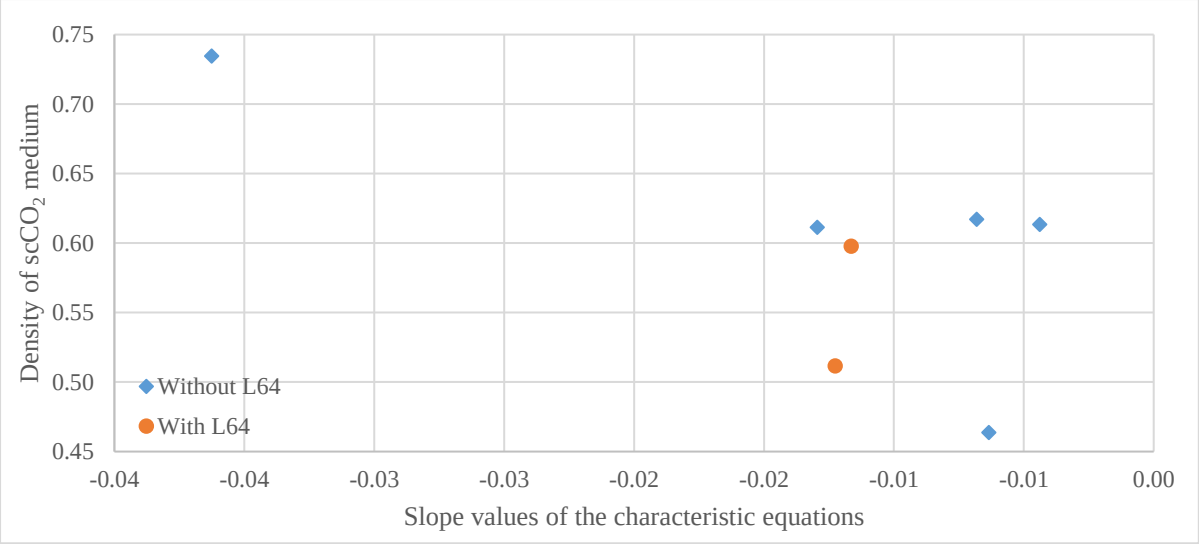


**Fig 39:** Dependency of slopes of the characteristics equations about density of $scCO_2$ in $scCO_2$ – DCM o/w emulsion systems in case of dynamic measurements

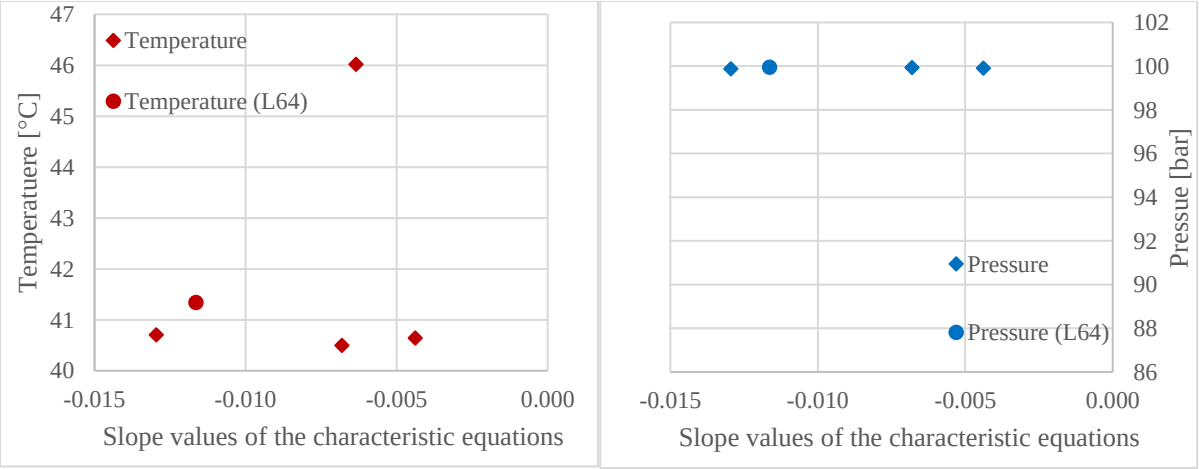


**Fig 40:** Dependency of slopes of the characteristics equations about temperature and pressure of $scCO_2$ in $scCO_2$ – DCM o/w emulsion systems in case of dynamic measurements

Table 7: Experimental plan for dynamic measurement with EtAc prepared o/w emulsions: Runs for study the **effect of concentration of lecithin and DCM** marked by font type Bold; runs for study the *effect of temperature- and pressure change only* marked by font type Italic; Centrum point runs marked by "_C"; "Only pressurized": After sample was pressurize till 100 bar at 40°C, immediately depressurized

| **Experimental Run** | **$C_{L64}$ [w/w%]** | **$C_{Lecithin}$ [w/w%]** | **$C_{EtAc}$ [w/w%]** | **Solvent/water ratio [ml/ml]** | **Flowrate of $scCO_2$ [ml/min]** | **p [bar]** | **T [°C]** | **Density of $scCO_2$ medium [g/mL]** | **Slope** | **Residual EtAc [w/w%]** |
|---|---|---|---|---|---|---|---|---|---|---|
| *1* | *0.4* | *2.0* | *18.9* | *1/4* | *6.5* | *84.9* | *40.7* | *0.34* | | - |
| *2* | *0.4* | *2.0* | *18.9* | *1/4* | *6.5* | *85.0* | *40.6* | *0.34* | | - |
| ***3_C*** | ***0.8*** | ***2.0*** | ***18.8*** | ***1/4*** | ***9.9*** | ***100.0*** | ***40.8*** | ***0.61*** | ***-9.13E-03*** | **-** |
| ***4_C*** | ***0.8*** | ***2.0*** | ***18.8*** | ***1/4*** | ***6.5*** | ***99.8*** | ***40.2*** | ***0.62*** | ***-4.74E-03*** | **-** |
| ***5_C*** | ***0.8*** | ***2.0*** | ***18.8*** | ***1/4*** | ***6.5*** | ***99.9*** | ***40.7*** | ***0.61*** | ***-1.09E-02*** | **-** |
| ***6*** | **-** | ***3.4*** | ***18.7*** | ***1/4*** | ***6.5*** | ***99.5*** | ***40.3*** | ***0.62*** | ***-4.57E-03*** | ***3.6*** |
| ***7*** | **-** | ***2.0*** | ***29.7*** | ***1/2*** | ***6.5*** | ***99.9*** | ***40.2*** | ***0.62*** | ***-3.75E-03*** | **-** |
| *8* | - | *2.0* | *19.0* | *1/4* | *6.5* | *99.4* | *45.6* | *0.47* | *-5.49E-04* | - |
| 9 | - | 2.0 | 19.0 | 1/4 | 6.5 | 79.4 | 51.5 | 0.21 | | - |
| 10 | - | 2.0 | 19.0 | 1/4 | 6.5 | 79.7 | 50.0 | 0.22 | -6.46E-05 | - |
| 11 | - | 2.0 | 19.0 | 1/4 | 6.5 | 80.0 | 49.8 | 0.22 | -1.32E-03 | 1.7 |
| Only pressurized | - | 2.0 | 29.7 | 1/2 | 6.5 | | | | | 2.8 |

Table 8: Experimental plan for dynamic measurement with DCM prepared o/w emulsions: Runs for study the **effect of concentration of lecithin and DCM** marked by font type Bold; runs for study the *effect of temperature- and pressure change only* marked by font type Italic; Centrum point runs marked by "_C"; "Only pressurized": After sample was pressurize till 100 bar at 40°C, immediately depressurized

| **Experimental Run** | **$C_{L64}$ [w/w%]** | **$C_{Lecithin}$ [w/w%]** | **$C_{DCM}$ [w/w%]** | **Solvent/water ratio [ml/ml]** | **p [bar]** | **T [°C]** | **Density of $scCO_2$ medium [g/mL]** | **Flowrate of $scCO_2$ [ml/min]** | **Slope** | **Residual EtAc [w/w%]** |
|---|---|---|---|---|---|---|---|---|---|---|
| 1 | 0.4 | 1.8 | 25.5 | 1/4 | 85.4 | 37.5 | 0.51 | 6.5 | -1.23E-02 | 7.9 |
| ***2_C*** | ***0.7*** | ***1.8*** | ***25.4*** | ***1/4*** | ***100.0*** | ***41.3*** | ***0.60*** | ***6.5*** | ***-1.16E-02*** | **-** |
| ***3_C*** | **-** | ***1.8*** | ***25.6*** | ***1/4*** | ***99.9*** | ***40.7*** | ***0.61*** | ***4.5*** | ***-1.30E-02*** | ***11.3*** |
| ***4*** | **-** | ***3.2*** | ***25.2*** | ***1/4*** | ***99.9*** | ***40.5*** | ***0.62*** | ***6.5*** | ***-6.81E-03*** | **-** |
| ***5*** | **-** | ***1.8*** | ***38.3*** | ***1/2*** | ***99.9*** | ***40.6*** | ***0.61*** | ***6.5*** | ***-4.39E-03*** | **-** |
| *6* | - | *1.8* | *25.6* | *1/4* | *86.9* | *40.5* | *0.38* | *6.5* | | *7.2* |
| *7* | - | *1.8* | *25.6* | *1/4* | *99.6* | *46.0* | *0.46* | *6.5* | *-6.34E-03* | *6.1* |
| 8 | - | 1.8 | 25.6 | 1/4 | 79.8 | 50.8 | 0.22 | 6.5 | | 5.4 |
| 9 | - | 1.8 | 25.6 | 1/4 | 107.7 | 34.7 | 0.74 | 6.5 | | 15.1 |
| 10 | - | 1.8 | 25.6 | 1/4 | 80.0 | 35.4 | 0.39 | 6.5 | | 12.5 |
| 11 | - | 1.8 | 25.6 | 1/4 | 109.4 | 35.7 | 0.73 | 6.5 | -3.63E-02 | - |
| Only pressurized | - | 1.8 | 25.6 | 1/4 | | | | 6.5 | | 18.2 |

## 4. CONCLUSIONS

In this work mass transfer properties of o/w emulsions – $scCO_2$ system were measured by magnetic suspension balances, which let us measure the weight change profile of a sample contactlessly. EtAc and DCM based o/w emulsions were prepared, and the effect on mass transport properties of the initial organic/water proportion, the concentration of surfactant materials (soy-bean lecithin and additional Pluronic L64®), and the density of $scCO_2$ atmosphere were studied. In the static system the dissolution of $scCO_2$ by the sample and the extraction of organic phase was observed simultaneously, but each mechanism was dominant the process and hence the weight change profile of the o/w emulsions in different moments. In the case of EtAc/w emulsion - $scCO_2$ system, only the density of $scCO_2$ was significantly influencing the mass transfer in both – the $scCO_2$ dissolution, and the organic phase extraction – zones. In the case of DCM/w emulsion - $scCO_2$ system, the influence of density of the surrounding $scCO_2$ was also observed, but phase separation of DCM and water occurred immediately after the pressurization of the sample by $CO_2$, indicating that DCM based aqueous emulsions are might be not adequate for SFEE process. A five-parameters mass transfer model was developed for the measured results, and two parameters of them were fixed, indicating that three process steps are influencing significantly the whole behaviour of o/w emulsion – $scCO_2$ system: Dissolution of the $scCO_2$ and the organic solvent in the water phase, and the extraction of the organic phase by the $scCO_2$ through the water phase boundary. In the case of the of DCM/w emulsion system, experimental results could not be appropriately described by the mass transfer model, proving that phase separation occurs immediately upon pressurizing, and forming a water boundary between DCM and $scCO_2$, which acts as a diffusion limitation layer. According to dynamic measurements – done with MSB device, which let us measure the weight change of o/w emulsions which continuously contacted with a $scCO_2$ flow – is concluded, that the higher proportion of organic phase extraction during the SFEE process occurs, during the

pressurization of the system by $scCO_2$, as mixing effect between o/w emulsion - $scCO_2$ is more efficient during the pressurization process, and during the phase change of the supercritical solvent.

**Acknowledgement**

Authors gratefully acknowledge Jens Rother for support on use of the MSB device used in static measurements, and Gerrit Dresp for design and support with the MSB device used in dynamic measurements.

This research has been funded by the European Initial TrainingNetwork FP7-PEOPLE 2012 ITN 316959, "DoHip", by Junta de Castilla y León with project VA225U14. This research has been done in the framework of RESOLV (EXC 1069) funded by the Deutsche Forschungsgemeinschaft. Á. Martín thanks the Spanish Ministry of Economy and Competitiveness for a Ramón y Cajal research fellowship. S. Rodríguez-Rojo thanks the Spanish Ministry of Economy and Competitiveness for a Juan de la Cierva research fellowship.

## REFERENCES

[1] B.Y. Shekunov, P. Chattopadhyay, J. Seitzinger, R. Huff, Nanoparticles of poorly water-soluble drugs prepared by supercritical fluid extraction of emulsions, Pharm. Res. 23 (2006) 196–204. doi:10.1007/s11095-005-8635-4.

[2] A. Martín, A. Bouchard, G.W. Hofland, G.-J. Witkamp, M.J. Cocero, Mathematical modeling of the mass transfer from aqueous solutions in a supercritical fluid during particle formation, J. Supercrit. Fluids. 41 (2007) 126–137. doi:10.1016/j.supflu.2006.08.015.

[3] J.O. Werling, P.G. Debenedetti, Numerical modeling of mass transfer in the supercritical antisolvent process, J. Supercrit. Fluids. 16 (1999) 167–181. doi:10.1016/S0896-8446(99)00027-3.

[4] J.O. Werling, P.G. Debenedetti, Numerical modeling of mass transfer in the supercritical antisolvent process: Miscible conditions, J. Supercrit. Fluids. 18 (2000) 11–24. doi:10.1016/S0896-8446(00)00054-1.

[5] N. Elvassore, F. Cozzi, A. Bertucco, Mass Transport Modeling in a Gas Antisolvent Process, Ind. Eng. Chem. Res. 43 (2004) 4935–4943. doi:10.1021/ie034040y.

[6] M. Lora, A. Bertucco, I. Kikic, Simulation of the Semicontinuous Supercritical Antisolvent Recrystallization Process, Society. (2000) 1487–1496. doi:10.1021/ie990685f.

[7] Y. Pérez De Diego, F.E. Wubbolts, P.J. Jansens, Modelling mass transfer in the PCA process using the Maxwell-Stefan approach, J. Supercrit. Fluids. 37 (2006) 53–62. doi:10.1016/j.supflu.2005.07.002.

[8] B.Y. Shekunov, J. Baldyga, P. York, Particle formation by mixing with supercritical antisolvent at high Reynolds numbers, Chem. Eng. Sci. 56 (2001) 2421–2433. <Go to ISI>://000168599100018.

[9] M. Mukhopadhyay, S. V. Dalvi, Mass and heat transfer analysis of SAS: Effects of thermodynamic states and flow rates on droplet size, J. Supercrit. Fluids. 30 (2004) 333–348. doi:10.1016/j.supflu.2003.10.001.

[10] F. Mattea, A. Martin, A. Matias-Gago, M.J. Cocero, Supercritical antisolvent precipitation from an emulsion: beta-Carotene nanoparticle formation, J. Supercrit. Fluids. 51 (2009) 238–247. doi:10.1016/j.supflu.2009.08.013.

[11] F. Mattea, Á. Martín, C. Schulz, P. Jaeger, R. Eggers, M.J. Cocero, Behavior of an Organic Solvent Drop During the Supercritical Extraction of Emulsions, AIChE J. 56 (2010) 1184–1195. doi:0.1002/aic.12061.

[12] F. Bashforth, J.C. Adams, eds., An attempt to test the theories of capillary action by comparing the theoretical and measured forms of drops of fluid. With an explanation of the method of integration employed in constucting the tables which give the theoretical forms of such drops, Cambridge [Eng.] University Press, Cambridge, 1883. https://archive.org/details/attempttest00bashrich.

[13] M. Stievano, N. Elvassore, High-pressure density and vapor-liquid equilibrium for the binary systems carbon dioxide-ethanol, carbon dioxide-acetone and carbon dioxide-dichloromethane, J. Supercrit. Fluids. 33 (2005) 7–14. doi:10.1016/j.supflu.2004.04.003.

[14] A. Bamberger, G. Sieder, G. Maurer, High-pressure (vapor+liquid) equilibrium in binary mixtures of (carbon dioxide+water or acetic acid) at temperatures from 313 to 353 K, J. Supercrit. Fluids. 17 (2000) 97–110. doi:10.1016/S0896-8446(99)00054-6.

[15] S. Varona, Á. Martín, M.J. Cocero, Formulation of a natural biocide based on lavandin essential oil by emulsification using modified starches, Chem. Eng. Process. Process Intensif. 48 (2009) 1121–1128. doi:10.1016/j.cep.2009.03.002.

[16] G. Lévai, Á. Martín, E. De Paz, S. Rodríguez-Rojo, M.J. Cocero, Production of stabilized quercetin aqueous suspensions by supercritical fluid extraction of emulsions, J. Supercrit. Fluids. 100 (2015) 34–45. doi:10.1016/j.supflu.2015.02.019.

[17] T. Fieback, F. Dreisbach, M. Petermann, R. Span, E. Weidner, New sorption and solvation measuring methods: Forced flow through liquids and solid state fluidised bed sorbents in high pressure gravimetry, Fluid Phase Equilib. 301 (2011) 217–224. doi:10.1016/j.fluid.2010.11.027.

[18] J.P. Mata, P.R. Majhi, C. Guo, H.Z. Liu, P. Bahadur, Concentration, temperature, and salt-induced micellization of a triblock copolymer Pluronic L64 in aqueous media, J. Colloid Interface Sci. 292 (2005) 548–556. doi:10.1016/j.jcis.2005.06.013.

[19] J.A. Byers, No Title, Www.phenomenex.com. (2003) Phenomenex catalog. http://www.chemical-ecology.net/java/solvents.htm.

[20] J.T. Kennedy, G. Thodos, The transport properties of carbon dioxide, AIChE J. 7 (1961) 625–631. doi:10.1002/aic.690070419.

[21] P.R. Sassiat, P. Mourier, M.H. Caude, R.H. Rosset, Measurement of diffusion coefficients in supercritical carbon dioxide and correlation with the equation of Wilke and Chang, Anal. Chem. 59 (1987) 1164–1170. doi:10.1021/ac00135a020.

[22] Á. Martín, M.D. Bermejo, F.A. Mato, M.J. Cocero, Teaching advanced equations of state in applied thermodynamics courses using open source programs, Educ. Chem. Eng. 6 (2011) 114–121. doi:10.1016/j.ece.2011.08.003.

[23] R. Stryjek, J.H. Vera, PRSV - An improved peng-Robinson equation of state with new mixing rules for strongly nonideal mixtures, Can. J. Chem. Eng. 64 (1986) 334–340. doi:10.1002/cjce.5450640225.

[24] D.S.H. Wong, S.I. Sandler, A theoretically correct mixing rule for cubic equations of state, AIChE J. 38 (1992) 671–680. doi:10.1002/aic.690380505.

[25] K.M. Klincewicz, R.C. Reid, Estimation of critical properties with group contribution methods, AIChE J. 30 (1984) 137–142. doi:10.1002/aic.690300119.

[26] W.B. R., V.L. Gladdy, The Solubility of Carbon Dioxide in Water at Various Temperatures from 12 to 40°C and at Pressures to 500 Atmospheres, Critical Phenomena, Solubility of carbon dioxide in water, in: Contrib. from Bur. Agric. Chem. Eng. U.S. Dep. Agric. Washington, D.C, Washington, D.C., 1940: pp. 815–817.

[27] Y.H. Ji, X.Y. Ji, X. Feng, C. Liu, L.H. Lu, X.H. Lu, Progress in the study on the phase equilibria of the CO2-H2O and CO2-H2O-NaCl systems, Chinese J. Chem. Eng. 15 (2007) 439–448. doi:10.1016/s1004-9541(07)60105-0.

[28] C. Yang, Y. Gu, Accelerated mass transfer of CO2 in reservoir brine due to density-driven natural convection at high pressures and elevated temperatures, Ind. Eng. Chem. Res. 45 (2006) 2430–2436. doi:10.1021/ie050497r.

[29] B. Arendt, D. Dittmar, R. Eggers, Interaction of interfacial convection and mass transfer effects in the system CO2-water, Int. J. Heat Mass Transf. 47 (2004) 3649–3657. doi:10.1016/j.ijheatmasstransfer.2004.04.011.

# CHAPTER III

## PRODUCTION OF ENCAPSULATED QUERCETIN PARTICLES

## USING SUPERCRITICAL FLUID TECHNOLOGIES

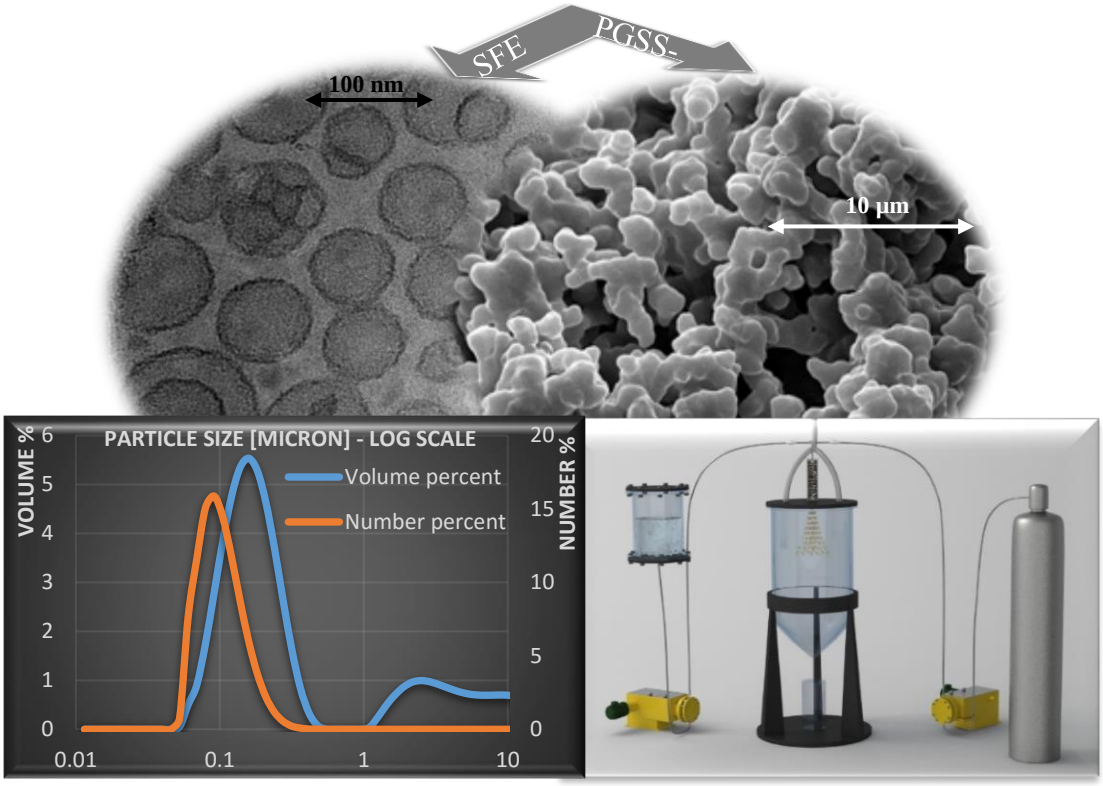
SFE
PGSS-
100 nm
10 µm
PARTICLE SIZE [MICRON] - LOG SCALE
Volume percent
Number percent
VOLUME %
NUMBER %
0
1
2
3
4
5
6
0
5
10
15
20
0.01
0.1
1
10

**ABSTRACT**

Quercetin is an antioxidant compound and it is a highly promising material against a wide variety of diseases, including cancer. A major limitation for the clinical application of quercetin is its low bioavailability, due to its low solubility in water. One way to increase the bioavailability of quercetin is to precipitate it in nanometric scale, encapsulated by a surfactant material, using Supercritical Fluid Extraction of Emulsions (SFEE) technology to obtain an aqueous suspension. This product is further treatable by Particles from Gas Saturated Solutions (PGSS)-drying technology, to obtain quercetin loaded dried particles in micrometric scale. In this work batch and semi-continuous SFEE, and PGSS drying processes are used, applying the mixture of soy-bean lecithin - Pluronic L64® as surfactant materials. Robustness study of a batch SFEE process is done, moreover is successfully scaled up to a semi-continuous process, in order to produce aqueous suspension product in higher scale, which is further used for PGSS-drying experiments. Lyophilization (assumed as a quercetin-degradation-free process) of two SFEE produced aqueous suspension mixtures is paralelly done with PGSS-drying, and encapsulation efficiency, and antioxidant activity of with PGSS drying and with lyophilization prepared dried products are measured and compared with each other. Franz-cell measurements are done for determine transdermal diffusion capacity of encapsulated quercetin product, prepared by supercritical and non-supercritical technology.

Key Words: Supercritical fluid extraction of emulsion, Scaling up, PGSS drying, Lyophilisation, Antioxidant activity, Franz cell

## 1. INTRODUCTION

Quercetin (3,3',4,4',5,7-pentahydroxyflavone) is a bioflavonoid, available in various fruits, vegetables oils and many other food components. Several studies show that it has strong antioxidant-, antiviral-, antibacterial-, antihistaminic- and anti-inflammatory effects. Moreover, it presents anti-proliferative effects in a wide range of human cancer cell lines [1]. Due to its ion chelating and iron stabilizing effect, it can scavenge reactive oxygen species, and down-regulate lipid peroxidation [2]. Due to these properties, quercetin is a highly promising active compound against a wide variety of diseases, including cancer. A major limitation for the clinical application of quercetin is its low bioavailability (17% in rats [3] and lower than 1% in humans [4]), which makes it necessary to administrate in high doses (50 mg/kg) [5]. One way to increase the bioavailability of quercetin is to produce encapsulated quercetin particles in nanometric scale. In this work, production of nanoencapsulated quercetin has been investigated using Supercritical Fluid Extraction of Emulsions (SFEE) and/or Particles from Gas Saturated Solutions (PGSS)-drying technology.

SFEE technology is used for producing aqueous suspensions, containing encapsulated valuable material (drug, bioactive compound etc.) in sub-micrometric scale. In SFEE process an initially prepared oil in water (o/w) emulsion (where the material of interest is dissolved in the organic phase) is contacted with a supercritical fluid, in order to extract rapidly the organic phase from the emulsion. Supercritical fluid must be chosen to have high affinity for the organic solvent, meanwhile negligible affinity for the active compound. Due to the rapid supersaturation of the active compound promote by the extraction of the solvent, it is precipitated in sub-micrometric scale, encapsulated by the surfactant material, used to prepare the emulsion. The product obtained by SFEE is therefore an aqueous suspension of the encapsulated material. To produce a dry product, water must be removed from this suspension. By PGSS-drying technology [6], water content of an aqueous solution is eliminated, and a micronized, encapsulated product is

obtained. For this, the aqueous solution is put into contact with supercritical carbon-dioxide ($scCO_2$) in the pressure- and temperature range of 10-15 MPa and 373-393 K, using a static mixer, and thus it becomes saturated with dissolved $CO_2$. Then this mixture is sprayed through a nozzle into a tower, which is operating at ambient pressure and temperature. Depressurization in the nozzle causes a sudden vaporization of the $CO_2$ dissolved in the liquid phase, which enhances atomization by an effervescent effect and, promotes the formation of particles with controlled particle size distribution in micrometric range [7] [8] [9]. In order to obtain a dry product, operating conditions in the spray tower must be chosen in order to operate above of the dew line of $CO_2$ - $H_2O$ mixtures [10].

In this work encapsulated quercetin particles were produced using SFEE technology as batch- and scaled-up semi-continuous process to obtain aqueous suspensions, and PGSS drying technology to obtain quercetin loaded dry particles in micrometric scale. On the basis of results obtained in a previous work at laboratory batch scale, process conditions for the scale-up of SFEE process were studied and validated analysing the characteristic of the product. Quercetin loaded dry particles were also obtained by conventional lyophilization, in order to compare and study the properties of the products, obtained by lyophilization and by PGSS-drying.

## 2. MATERIALS AND METHODS

### 2.1 Materials

Quercetin Hydrate ($C_{15}H_{10}O7xH_2O$, 95% purity, CAS: 849061-97-8) was obtained from Acros Organics (New Jersey, USA). The surfactant material poly-(ethylene glycol)- block –poly-(propylene glycol)- block -poly-(ethylene glycol) (Pluronic L64®, CAS: 9003-11-6) was obtained from Sigma Aldrich (St Louis, USA). Soy-bean lecithin was obtained from Glama-Sot (SOTYA, Madrid, Spain). Ethyl Acetate (EtAc, CAS: 141-78-6) and methanol (MeOH, CAS: 67-56-1), with a purity of 99% and 99.9 %, respectively, were obtained from Panreac Química (Barcelona, Spain). Acetonitrile (CAS: 75-05-8); acetic acid (reference number: 211008.1211) with a purity of 99.9% and 99.5 %, respectively, were obtained from Panreac Química (Barcelona, Spain). Carbon dioxide was provided by Carburos Metálicos (Barcelona, Spain). For intestinal fluid water milliQ, potassium phosphate dibasic trihydrate, >=99.0% ($KH_2PO_4$) (CAS: 16788-57-1; LOT: P5504-500G) obtained from Sigma Aldrich, and HCl 37% (M = 36.46 g/mol) obtained from Pronalab, Rua da Madalena, 161-1100 Lisbon, Portugal were used.

### 2.2 Emulsion preparation and supercritical extraction of the emulsion

The initial emulsion for SFEE experiments was prepared using an IKA LABOR-PILOT 2000/4 (IKA-WERKE GMBH&CO.KG) high frequency mixing device with a cooling jacket. For this, the required amount of quercetin was dissolved in the organic phase (ethyl acetate), meanwhile surfactant material was dissolved in water, purified by Millipore Elix. Separately prepared organic- and water based solutions were mixed together using a magnetic stirring with a minimum of 500 rpm mixing rate for 5 minutes. Then this dispersion was further treated with the high shear emulsifier device for 4 min at 70 Hz frequency. The optimal emulsification conditions were determined in previous works [11] [12].

In a previous work described a batch SFEE equipment [11] was used to extract the organic content of the o/w emulsion under the restrictions of FDAA [13], and to produce aqueous suspensions, containing quercetin loaded lecithin nanoparticles. The equipment consists of an extractor and a buffer vessel with a volume, which are located in a heated oven, and are separable from each other, using two valves. Temperature of the system was set to 40°C and pressurized with $CO_2$ till ca. 100 bar, and 25 mL of o/w emulsion was pumped into the extractor vessel using a GILSON 305 HPLC pump with a flowrate of 5 mL/min. $SCCO_2$ was continuously circulated between the extractor- and the buffer vessel, and emulsion was continuously mixed, using a magnetic stirrer (1500 rpm). $SCCO_2$ was drive into the bottom of the extractor vessel using an 1/16" tube and it was partially renewed several times in each experiment, in order to increase the efficiency of the extraction. To do so, the extraction vessel was isolated from the recirculation circuit, in order to maintain the extraction vessel at a constant pressure and temperature, meanwhile the $CO_2$ was renewed in the rest of the circuit, thus minimizing the disturbances and losses of emulsion, by entrapment in $CO_2$ during the repeated depressurization processes needed for each $CO_2$ renewal. According to preliminary experiments, five cycles with a total treatment duration of 575 min proved to be optimum, by decreasing the residual organic content under the restriction of the FDA [13], without significant degradation or agglomeration effect of the encapsulated quercetin particles [12]. Upon termination of the process, the complete system was slowly depressurized using a Milli-Mite® serie 1300 micrometric valve provide by HOKE, and produced aqueous suspension product was stored at 4-6°C, protected from light.

In this work a scaled-up, semi-continuous SFEE process was designed (**Fig 1**), in order to extract the organic content much faster, from a significantly higher amount of o/w emulsion, using continuously maintained $scCO_2$ flow. Scaled-up SFEE equipment consists of an electrically tempered extractor vessel with a Micromite® serie 1600 micrometric valve (provide

by HOKE) on its output, in order to maintain a controlled continuous $scCO_2$ flow, pumped by a Milroyal® Dosapro® Milton Roy membrane pump. Flowrate of liquid $CO_2$ was measured by a Micro Motion RFT 9739 coriolis flowmeter. Starting sequence of the scaled up system is very similar to the batch one: Temperature of the system was set 35-40°C and the system was pressurized with $CO_2$ till ca. 85 bar. Extractor vessel was then filled with approximately 168 mL of o/w emulsion, using a GILSON 305 HPLC pump with a flowrate of 20 mL/min. Then sc-$CO_2$ was continuously pumped into the bottom of the extractor vessel using a four-times perforated 1/16" tube. With this, $CO_2$ was continuously bubbled through on the emulsion, and emulsion was also stirred, using a magnetic stirrer with a mixing rate of 300 rpm. Due to the use of a continuous $CO_2$ flow, the efficiency of the extraction of organic solvent was increased, reaching a concentration below the restrictions of FDA [13], applying a treatment of only 80-90 min long. This process is so called semi-continuous, due to the continuos flow of $scCO_2$ over a fixed volume of emulsion for a predefined time. O/W emulsions are prepared in the same way as for the previously applied batch process.

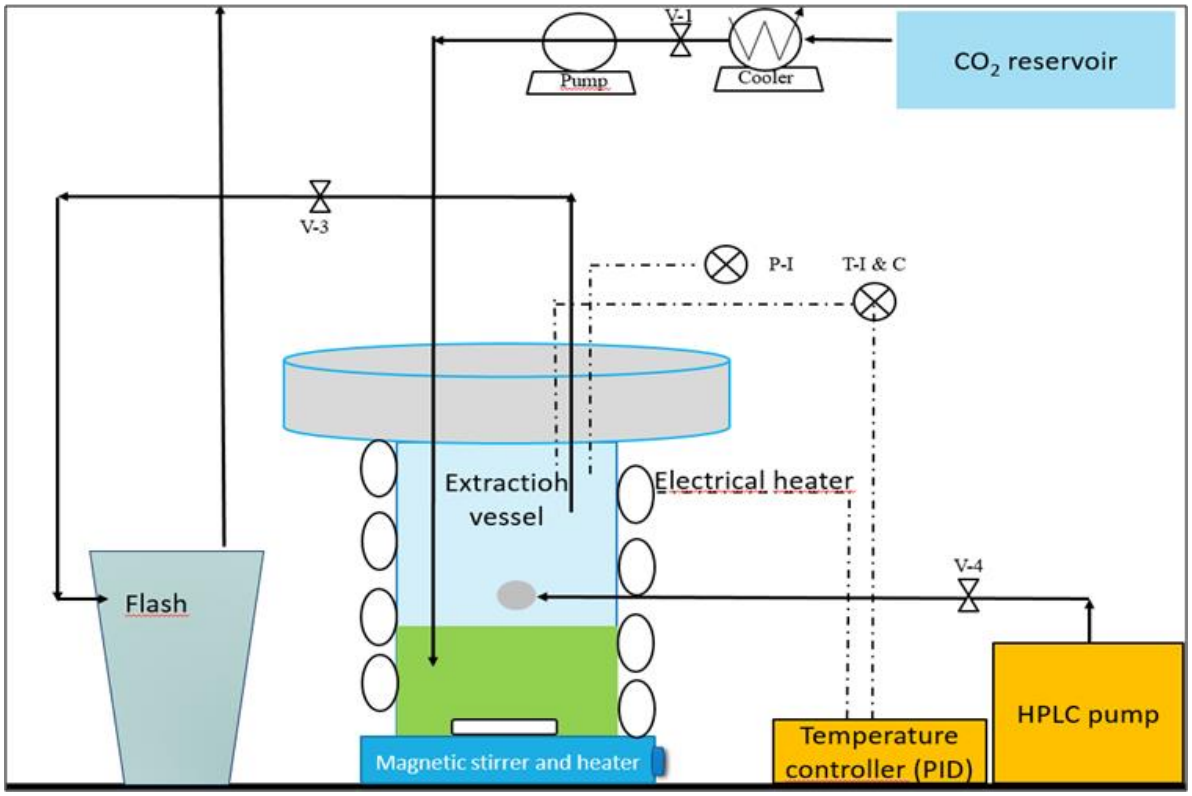


**Fig 1:** Scaled-up SFEE semi-continuous process

### 2.3 PGSS drying and lyophilization of SFEE produced aqueous suspensions

SFEE-produced aqueous suspensions were further treated by PGSS drying, in order to remove the water content, and to obtain a quercetin loaded solid product. With PGSS drying obtained solid product become available for long-term storage without significant degradation of quercetin, which is rapidly taking place in aqueous medium [14]. The PGSS drying equipment, presented on Fig 2, allows operation with a maximum of 15 kg $CO_2$ per hour, which is pumped by a piston pump, provide by LEWA Herbert Ott GmbH + Co. SFEE produced aqueous suspension is pumped by a Milroyal® Dosapro® Milton Roy membrane pump, and continuously mixed with $scCO_2$ in a static mixer, filled with glass beads of 4 mm of diameter. The so produced biphasic mixture is rapidly depressurized to atmospheric pressure through a capillary nozzle with a diameter of 500 µm (Spraying System, Co.), resulting a fine powder formulation of the product. Temperature in the spray tower must be kept above the dew line curve of the of $CO_2$ - $H_2O$ mixture phase equilibrium, in order to obtain dry powder [15] [16]. Influencing process conditions in terms of residual water content and quercetin encapsulation efficiency of the PGSS drying obtained product, such as gas to liquid ratio (GLR), pre-expansion pressure and temperature were studied already in previous works [17] [18].

Lyophilization of SFEE produced aqueous suspension products was also done, using a HT40 Beijer Electronics LyoQuest equipment, produced by Telstar. Two lyophilization runs were performed at conditions of 0.180 mbar and -51.5°C for 48 hours. Different pre-treatment processes were applied to each of these two samples: one sample was cooled down before lyophilization process at around -20°C for 6 hours, meanwhile the other sample was rapidly cooled down by liquid $N_2$, in order to avoid the formulation of huge water crystals, and to protect the morphological character of the sample. Characteristics of PGSS-dried and

lyophilized solid products were analysed and compared, in order to estimate the degradation effect of the samples, prepared with different methods.

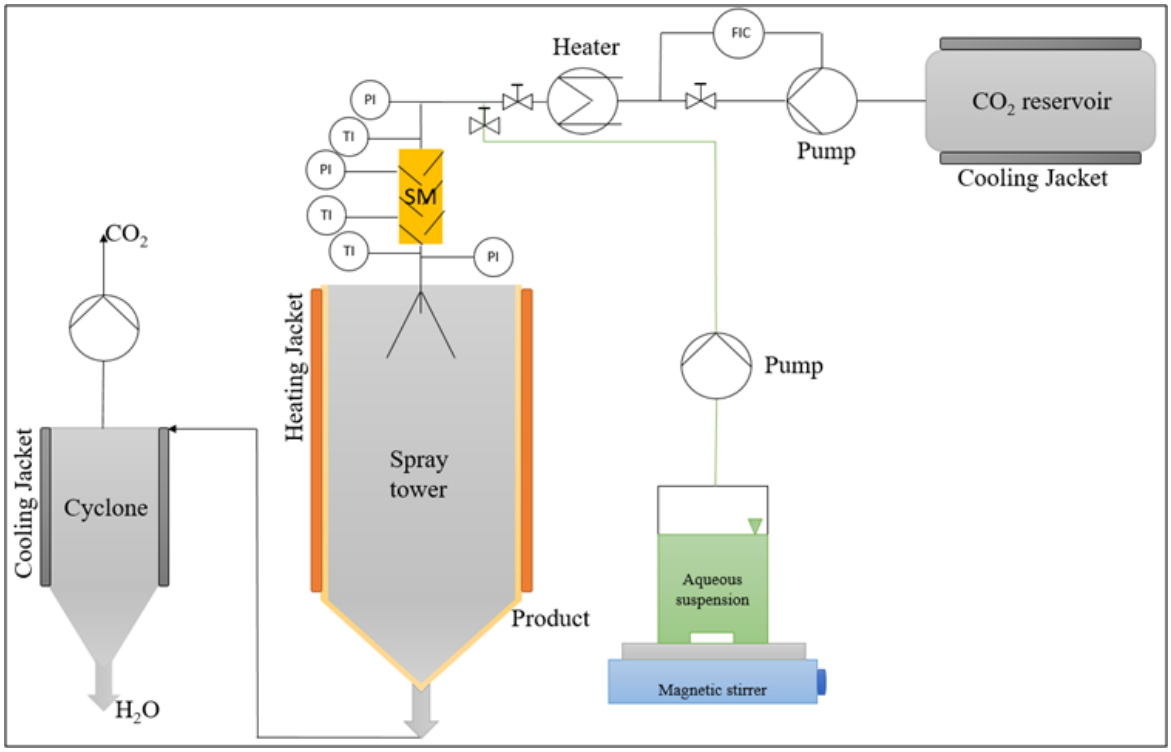


**Fig 2:** PGSS-drying equipment

## 2.4 Analytical methods

### 2.4.1 Particle size distribution measurement and morphological characterization

Particle size distribution of SFEE treated aqueous suspension products was measured using a Malvern Mastersizer 2000 Light Scattering device, provided by Malvern Instruments. The measurement range of the equipment is from 0.02 to 2000 µm. It uses a 4 mW diode laser with a dual – wavelength detection system (red light 633 nm, blue light 436 nm). The sample was diluted with deionized water in the dispersion unit (Hydro SM), in order to obtain an adequate level of laser obscuration, and prevent multiple scattering effects. Refractive index for the dispersed phase (water) is 1.331, meanwhile for quercetin particles is 1.823. Each measurement was performed in triplicate.

Optical microscopy, (Leica DM4000 B) was used for doing visual observations of SFEE-treated aqueous suspensions. Morphological observations of PGSS dried samples were done by Quanta 200F scanning electron microscopy provide by FEI. Samples were coated by 24 k gold with a width of approximately 10 nm, using an Emitech K575X device.

### 2.4.2 Structural characterization

Fourier Transform Infrared Spectroscopy (FTIR) measurements were done in an ALPHA PLATINUM – ATR device, equipped with a high throughput ZnSe ATR crystal, produced by BRUKER. Previously, aqueous suspension samples were dried in vacuum at 35°C over two days.

X-Ray diffraction (XRD) measurements were done by a BRUKER D8 DISCOVER A25 device, Generator 3KW, Ceramic cupper tube 2.2 KW type FFF. Aqueous SFEE samples were prepared the same way as for FTIR measurements, as detailed above.

Differential scanning calorimetry (DSC) profiles of particles produced by PGSS-drying were obtained using a DSC Q200 calorimeter (TA Instruments). Temperature range was -20 to 350°C with a heating rate of 10°C/min under N2 flow rate. Aluminium crucibles with perforated lid were used, in order to permit the evaporation of heat sensitive components or moisture content of samples during the measurement. An empty perforated crucible was used as reference. Instrument was calibrated with platinum.

### 2.4.3 Residual organic content of SFEE prepared samples, and residual water content of PGSS-drying prepared samples.

Remaining organic solvent in SFEE treated aqueous suspensions was measured by Head Space Gas Chromatography. Measurements were done twice, and calibration series are done in the range of 0 – 1000 mg/L EtAc concentration with an $R^2 = 0.999$. The method of GC analysis was detailed in previous work [11]. Briefly 4 mL of sample were introduced in a hermetically

closed vial with a volume of 10 mL, and vials were tempered before GC injection at 40°C. Sample for GC injection was taken using a Hamilton syringe with a volume of 1000 µL from the gas phase. Syringe was washed two times with the sample before sampling. GC equipment was an Agilent Technologies 7890A gas chromatograph with a flame ionization detector (FID), with a HP-5 5% phenyl-methyl-silicone 30 m x 32 m x 25 µm column. The operating conditions for the analysis were: injector temperature 200º C, detector temperature 200º C, column temperature 80 ºC, injector flow rate 24 mL/min, column flow rate 1 mL/min (He) and split (sample dilution) 70:1.

Residual water content of with PGSS-drying prepared samples were measured by weight measuring at heated oven, after keeping the samples for 48 hours at 80°C.

### 2.4.4 Quercetin concentration

Quercetin concentration was determined by HPLC, using a Waters 2487 chromatograph consisting of a Waters In-Line degasser, Waters 515 HPLC pump and Waters 717 Plus Autosampler device. The injection volume of samples was 20 µL. The mobile phase was acetonitrile / milliQ water containing acetic acid in 5 V/V% concentration with a flowrate of 1 mL/minute. Equipment included a pre-column Bio-Sil C18 HL90-5 30 X 4.6 mm with a pore size 5 µm, provided by BIO-RAD. A Waters Symmetry ® C18 150 X 4.6 mm with a pore size 5 µm column at 30°C was used. The detector was a Waters 2784 Dual λ absorbance detector set on the wavelength of 373 nm. Before the analysis, SFEE aqueous suspension samples were centrifuged for 30 min at 2.3 g using a Spectrafuge 240 centrifuge provided by Labnet International Inc., NJ, USA, in order to separate sediment crystals. Furthermore, samples were diluted 5 times in volume in MeOH and filtered with 0.45 µm pore size and 25 mm diameter PP filters, provide by FILTER – LAB®. Solid samples prepared by PGSS and lyophilization were dissolved in water MilliQ / MeOH = 0.6 / 9.4 (in volume) in adequate dilution, and filtered with 0.45 µm pore size and 25 mm diameter PP filters, provide by FILTER – LAB®. To

quantify the concentration of quercetin, a calibration line was developed from analysis of standard solutions of quercetin dissolved in a solution of methanol / water = 70 / 30 (V/V%), in the concentration range from 0 to 100 µg/mL, with $R^2 = 0.998$.

2.4.5 Antioxidant activity measurement

Oxygen radical absorbance capacity (ORAC) measurements were made determining the ability of the antioxidant species present in the sample to inhibit the oxidation of disodium fluorescein (FL) catalysed by peroxyl radicals generated from α, α'-Azodiisobutyramidine Dihydrochloride porum (AAPH). For this, in a 96-well micro plate 25 µL of the appropriate sample dilution were added together with 150 µL of disodium fluorescein (10 nM). The micro plate was put in a fluorescent reader that allowed incubating the samples at 37ºC for 30 minutes. The reaction was started with 25 µL of AAPH (240 mM). Fluorescence emitted by the reduced form FL was measured in an BMG LABTECH Fluostar OPTIMA fluorescent reader, and recorded every 1 min at the emission wavelength of 530±25 nm and excitation wavelength of 485±20 nm for a period of 90 min. Phosphate buffer (75 mM, pH=7.4) was used to prepare AAPH and FL solutions, and was also used as blank. Standards went from 13 till 200 µM Trolox, and additionally one independent control sample was also prepared. Samples and the independent control sample were analysed six times, while blank and standards were analysed three times. Final ORAC values were calculated by a regression equation between the Trolox concentration and the net area under the FL decay curve, and expressed as µM Trolox Equivalents per gram of quercetin (µM TE/g quercetin) [19]. SFEE samples were centrifuged by 2.3 g (Spectrafuge 240, Labnet International Inc., NJ, USA), diluted 50 times by water milliQ. Solid samples prepared by PGSS and lyophilization were dissolved in water MilliQ in adequate dilution. Antioxidant activity in case of with PGSS-drying prepared solid samples were corrected by the residual water content of the samples.

### 2.4.6 Transdermal diffusion measurements

With PGSS-drying and with lyophilization obtained solid products in-vitro permeability studies were done using 25 mm diameters membranes for Transdermal Diffusion Tests, provide by Strat-M$^{TM}$ (Made in Bedford, MA, USA, EMD Millipore Corporation, Ref n.: 800-645-5476). Unjacketed 20 mm Franz Cell with 15 mL receptor volume provided by PermeGear Inc. (3575 North Drive, Bethlehem, PA 18015, Ref n.: #6G-01-00-20-15). Dissolution medium was simulated intestinal fluid, prepared by adding 6.8 g of phosphate buffer to 1 L of water milliQ, and pH adjusted to 6.8 with HCl, using Methrom 827 pH lab device. Sample with around 12 mg/L quercetin content (around 80% of quercetin encapsulation efficiency was taking into account) was placed on the transdermal membrane, and Franz-cell was placed at 37°C water-bath, protected from light, for a duration minimum of 24 h. Liquid samples from Franz-cell in given time intervals were taken, and stored at -20°C, protected from light. Residual liquid content in Franz-cell after experiment has finished was diluted by MeOH in order to avoid quercetin precipitation due to temperature decrease, and stored at -20°C, protected from light, until the analyzation of all samples, using HPLC.

## 3. RESULTS AND DISCUSSION

### 3.1 Batch-SFEE experiments

As detailed in previous works, soy-bean lecithin proved to be a suitable material for encapsulating in nanometric scale precipitated quercetin [12]. Moreover, according to surface tension measurements, using a mixture of soy-bean lecithin with Pluronic L64® as additional surfactant, a significant reduction in surface tension is observed [Chapter II]. According to these results, in this work all o/w emulsions were prepared using the mixture of soy-bean lecithin – Pluronic L64® as surfactant material. A design of experimental plan with full resolution (three factors varied on two levels with two centrum point measurements) was established, in order to determine factors, which are significantly influencing the final particle size distribution and the quercetin recovery ratio in the SFEE treated aqueous suspensions. Factors varied were the concentration of quercetin, Pluronic L64® and soy-bean lecithin, as detailed in Table 1. All experiments were carried out with an initial ratio: EtAc / water = 1/4, as according to previous work [12], this parameter has no significant influence on final product. According to the statistical analysis, none of the studied factors in the examined range are influencing significantly the final particle size distribution, as presented on **Fig 3 (A)**, and the amount of encapsulated quercetin (**Fig 3 (B)**).

In all experimental runs a multimodal particle size distribution was obtained in terms of volume of the precipitated particles (an example is plotted on **Fig 5 (A)**. Comparing with the results obtained in a previous work in which only lecithin was used as surfactant [12], higher average values of particle size were obtained in current work using the mixture of lecithin and Pluronic L64® as surfactants (**Table 2**). This is the consequence of using a higher total concentration of surfactant materials, and might be the formation of bigger multi-layered lecithin vesicles of sizes above 1 μm range during SFEE treatment process

**Table 1:** Experimental plan for studying the effect of factors on final particle size distribution, quercetin recovery, Centrum point measurements marked by (C), In all experimental runs the initial ration of EtAc/$H_2O$ was 1 / 4 (mL/mL)

| Experi-mental Run | Quercetin concent-ration [w/w%] | Pluronic L64® concent-ration [w/w%] | Lecithin concent-ration [w/w%] | Pluronic L64® / Lecithin [w/w] | Quercetin in product [mg/L] | Quer-cetin recov-ery [%] | D (0.1) [µm] | Under 1 µm [V/V%] | Medium between 0.138-0.158 µm [V/V%] | ORAC [µmol TE / g of quercetin] | Residual EtAc [mg/L] |
|---|---|---|---|---|---|---|---|---|---|---|---|
| **1 (C)** | 0.02 | 0.4 | 2.0 | 0.2 | 234.6 | 98.2 | 0.125 | 29.4 | 2.23 | n/a | 1985 |
| **2 (C)** | 0.02 | 0.4 | 2.0 | 0.2 | 195.1 | 81.7 | 0.145 | 20.5 | 1.79 | 26218 | 322 |
| **3** | 0.01 | 0.2 | 1.6 | 0.1 | 127.4 | 88.0 | 0.108 | 35.4 | 2.93 | 28972 | 190 |
| **4** | 0.03 | 0.2 | 1.6 | 0.1 | 306.0 | 90.5 | 0.115 | 28.9 | 2.85 | 17805 | 350 |
| **5** | 0.01 | 0.6 | 1.6 | 0.4 | 120.3 | 83.4 | 0.116 | 27.2 | 3.13 | 28021 | 247 |
| **6** | 0.03 | 0.6 | 1.6 | 0.4 | 301.2 | 89.6 | 0.110 | 32.8 | 3.73 | 17915 | 229 |
| **7** | 0.01 | 0.2 | 2.4 | 0.1 | 108.1 | 75.8 | 0.097 | 40.7 | 3.81 | 33065 | 342 |
| **8** | 0.03 | 0.2 | 2.4 | 0.1 | 256.8 | 77.2 | 0.105 | 35.0 | 3.09 | 21872 | 309 |
| **9** | 0.01 | 0.6 | 2.4 | 0.3 | 117.7 | 82.9 | 0.104 | 40.4 | 4.68 | 35137 | 258 |
| **10** | 0.03 | 0.6 | 2.4 | 0.3 | 288.2 | 87.0 | 0.106 | 32.5 | 2.94 | 19651 | 264 |
| **11** | 0.01 | 0.6 | 2.4 | 0.3 | 114.5 | 80.7 | 0.103 | 34.0 | 3.30 | 32602 | 338 |

**Table 2:** Comparison of average results of aqueous suspensions obtained by batch SFEE process from o/w emulsions prepared by soy-bean lecithin only, and by the mixture of soy-bean lecithin – Pluronic L64®. Average results of with only soy-bean lecithin prepared o/w emulsions are taken from a previous work [12].

| Tpye of initial o/w emulsion | Droplet size in initial emulsion [µm] | Quer-cetin reco-very [%] | ORAC [µMTE / / g of quercetin] | D (0.1) [µm] | D (0.5) [µm] | Under 1 µm [V/V%] | Between 0.138 - 0.158 µm [V/V%] | Residual organic content [mg/L] |
|---|---|---|---|---|---|---|---|---|
| **Lecithin** | 1.63 | 58.8 | 36401 | 0.09 | 1.15 | 56.1 | 4.76 | 48 |
| **Lecithin + Pluronic L64®** | 1.84 | 83.7 | 26126 | 0.11 | 4.61 | 32.4 | 3.13 | 439 |

While as indicated, the use of Pluronic L64® as additional surfactant material did not allow the further reduction of final particle size distribution of the aqueous suspension product, with the use of this additional surfactant, the average encapsulation efficiency of quercetin was increased from 69.2% to 83.7% (**Table 2**). Encapsulation efficiency of quercetin in experimental run 1 is significantly higher than in case of the other runs, most probably due to the higher residual organic content, which contributes to maintain quercetin in the solution. Due to the high residual organic content, the quercetin encapsulation efficiency of experimental run 1 was not taken into account in the calculation of average value (83.7%).

According to the statistical analysis, antioxidant activity is influenced significantly by the concentration of quercetin, meanwhile it is almost independent on the concentration of soy-bean lecithin, as can be seen on **Fig 3 (C)**. Higher antioxidant activity (expressed as µMTE/g quercetin and therefore normalized by the amount of quercetin in the sample) is obtained, when the concentration of quercetin is decreased, meanwhile the influence of the concentration of surfactants are negligible, until they are above of their critical micelle concentrations. An average antioxidant activity 26126 µMTE / g of quercetin is measured, which is approximately

equal with the antioxidant activity measured in the case of aqueous suspensions produced only with soy-bean lecithin as surfactant material (**Table 2**), and significantly higher, than the antioxidant activity of pure quercetin: 6300±300 µMTE / g of quercetin. This result is due to an antioxidant synergism effect, which is resulting the formation of chain structures between quercetin and phosphatidyl-choline, linked by hydrogen bonds [20]. However, pure physical mixture has a higher ORAC value (as presented in previous work [12]) than SFEE produced sample, probably by the loss of the just mentioned chain structures between quercetin and phosphatidyl-choline during the $scCO_2$ extraction process

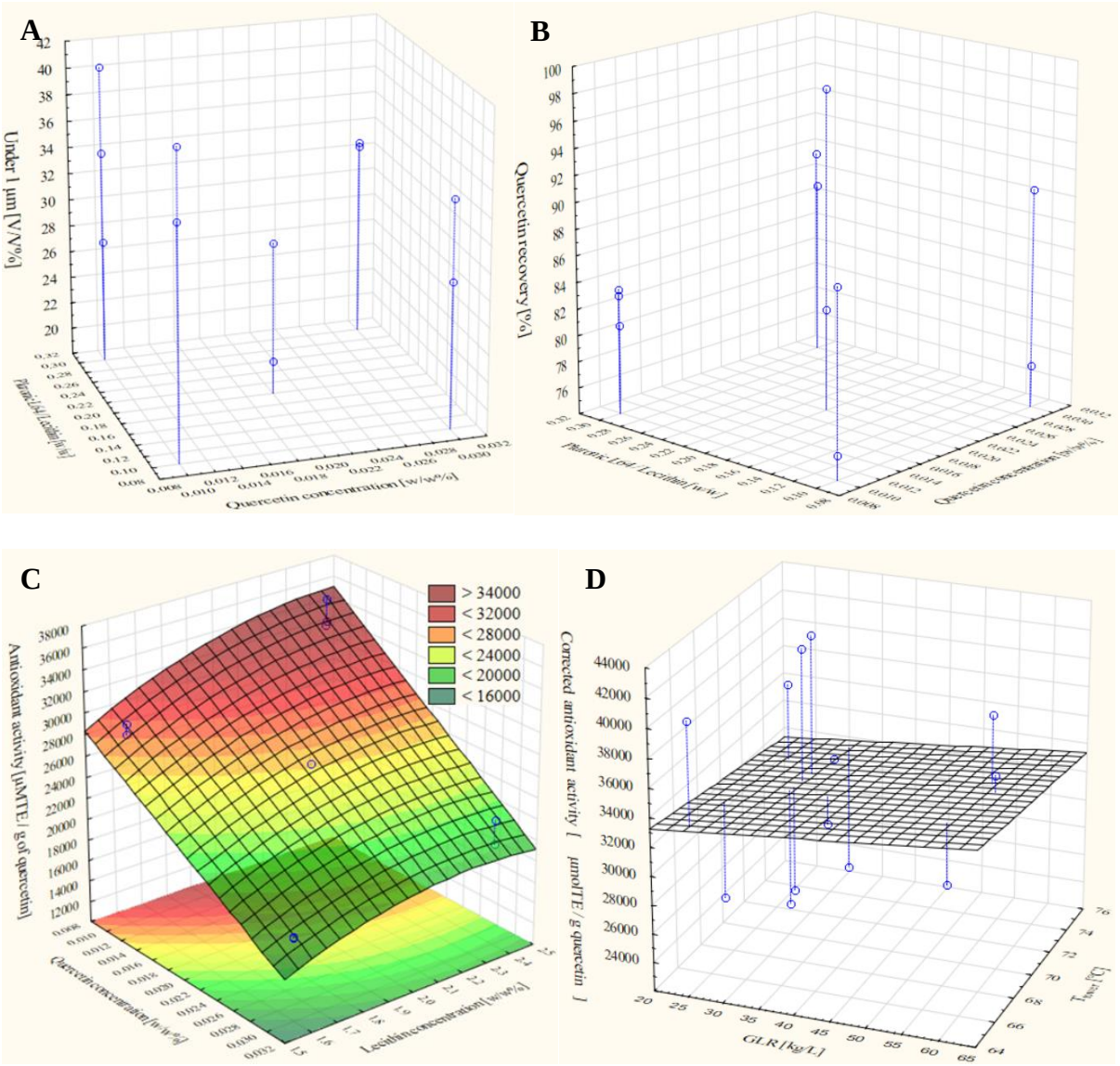

**Fig 3:** **A:** Dependency of particle size obtained by SFEE on the concentration of quercetin and on the ratio of Pluronic L64® / lecithin

**B:** Dependency of encapsulation efficiency obtained by SFEE on the concentration of quercetin and on the ratio of Pluronic L64® / lecithin

**C:** Factors significantly influencing the antioxidant activity of aqueous suspension products obtained by SFEE

**D:** Dependency of corrected antioxidant activity on GLR and temperature of the tower

### 3.2 Scaled-up, semi-continuous SFEE experimental runs

In this work a scaled-up, semi-continuous SFEE equipment was designed (presented in section 2.2), and used for producing aqueous suspensions in higher scale, which were then further treated by PGSS-drying. As the robustness of the products of SFEE process and independency of the conditions of emulsification was proved with the batch experiments reported in section 3.1, all experiments with the scaled-up system were performed, applying only the conditions of the initial emulsion, corresponding to the centrum point setting, detailed in **Table 1**.

For scaling-up of SFEE device, the ratio of the height- and the diameter of the o/w emulsion filled into the extractor vessel was chose as a scaling-up factor (**Fig 4**). This ratio was chose keeping considered, that the contact speed of $scCO_2$ – o/w emulsion as a key factor of SFEE process ([11], [21], [22]), and the speed of the evaporation of EtAc contained $scCO_2$, mainly depends on the available free surface area of the emulsion. This means, height of the emulsion column is limited by its diameter, as free surface area. Contact area of $scCO_2$ – emulsion was increased by the perforation of the $CO_2$ inlet tube in several axial positions, along the whole emulsion column. Value of scaling-up ratio was kept at approximate value of 0.8, and theoretically treatable volume of o/w emulsion increased from 25 to 196 mL.

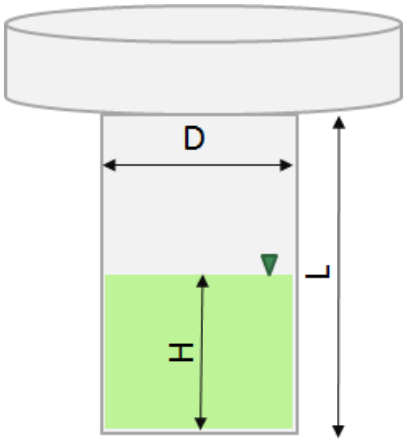


| Dimensions | Batch | Scaled-up |
|---|---|---|
| **H [mm]** | 29 | 56 |
| **L [mm]** | 100 | 121 |
| **D [mm]** | 35 | 67 |

**Fig 4:** Dimensions of extractor vessel in batch and scaled-up device

The main criteria of scaled-up system was to obtain batch SFEE obtained similar product characteristics (residual organic content under the restrictions of FDA [13], without the appearance of quercetin crystals, and without the aggregation of encapsulated quercetin nanoparticles). All SFEE products were observed by optical microscopy, in order to verify the lack of crystalline quercetin particles, which is a crucial process issue.

**Table 3:** Results of SFEE experiments with scaled-up system

| Mix-ture for PGSS run | T [°C] | p [bar] | Density of $CO_2$ [kg/L] | Dura-tion of SFEE [min] | Used $CO_2$/ / emulsion [kg/L] | $CO_2$ mass flow [kg/h] | Quer-cetin in pro-duct [mg/l] | Quer-cetin recov ery [%] | ORAC [µMTE/ /g of quer-cetin] | D (0.1) [µm] | D (0.2) [µm] | Under 1 µm [V/V%] | Between 0.138 - 0.158 µm [V/V%] | Resi-dual organic content [mg/L] |
|---|---|---|---|---|---|---|---|---|---|---|---|---|---|---|
| **1** | 35.1 | 80.0 | 0.41 | 90 | 6.83 | 1.56 | n/a | n/a | n/a | 0.105 | 0.138 | 44.5 | 5.54 | 484.7 |
| **2** | 35.2 | 80.0 | 0.40 | 87 | 6.59 | 1.53 | 208.0 | 87.1 | 34893 | n/a | n/a | n/a | n/a | 434.3 |
| **3** | 40.1 | 100.1 | 0.63 | 96 | 4.41 | 0.94 | 208.6 | 87.3 | 17209 | 0.101 | 0.151 | 37.2 | 3.54 | 328 |
| **4** | 35.0 | 80.0 | 0.42 | 89 | 7.23 | 1.66 | 219.7 | 92.0 | 29493 | 0.125 | 0.204 | 24.9 | 3.06 | n/a |
| **5** | 35.1 | 80.0 | 0.41 | 90 | 7.08 | 1.61 | 196.1 | 82.1 | 23592 | 0.085 | 0.118 | 51.9 | 4.80 | n/a |
| **6** | 35.4 | 80.0 | 0.38 | 90 | 6.54 | 1.51 | 211.3 | 88.4 | 20156 | 0.084 | 0.112 | 56.7 | 5.48 | n/a |
| **7** | 40.0 | 100.0 | 0.63 | 92 | 4.01 | 0.88 | 206.2 | 86.3 | 22989 | 0.117 | 0.585 | 36.4 | 3.72 | n/a |
| **8** | 36.1 | 79.1 | 0.33 | 88 | 6.90 | 1.48 | 185.8 | 78.9 | 18585 | 0.059 | 0.078 | 38.4 | 6.14 | 200 |
| **9** | 40.1 | 99.2 | 0.62 | 96 | 4.30 | 0.90 | 214.5 | 89.8 | 17434 | 0.101 | 0.151 | 37.2 | 3.56 | 561 |
| **10** | 40.3 | 100.0 | 0.62 | 90 | 4.10 | 0.93 | 191.5 | 80.1 | 21483 | 0.098 | 0.147 | 39.4 | 3.73 | n/a |
| **11** | 39.6 | 99.5 | 0.63 | 104 | 4.34 | 0.86 | 235.4 | 98.5 | n/a | 0.094 | 0.130 | 48.7 | 4.79 | n/a |
| **12** | 34.6 | 83.1 | 0.60 | 75 | 4.93 | 1.37 | 223.0 | 85.5 | 21867 | 0.092 | 0.125 | 52.3 | 5.31 | 356 |
| **13** | 34.7 | 80.6 | 0.50 | 81 | 5.22 | 1.30 | n/a | n/a | n/a | 0.103 | 0.135 | 47.9 | 5.65 | n/a |
| **14** | 35.2 | 104.8 | 0.73 | 87 | 5.41 | 1.29 | 247.0 | 90.4 | 10528 | 0.097 | 0.136 | 46.2 | 4.86 | 111 |

**Table 4:** Comparison of average results obtained by batch- and scaled-up, semi-continuous SFEE process

| Type of SFEE process | Treatment time [min] | Treated o/w emulsion [mL] | Quercetin recovery [%] | ORAC [µMTE/g of quercetin] | D (0.1) [µm] | D (0.2) [µm] | Under 1 µm [V/V%] | Between 0.138 - 0.158 µm [V/V%] | Residual organic content [mg/L] |
|---|---|---|---|---|---|---|---|---|---|
| **Batch** | 575 | 25 | 85.0 | 26126 | 0.112 | 0.226 | 32.4 | 3.13 | 439 |
| **Semi-continuous** | 89.5 | 168 | 87.2 | 21657 | 0.097 | 0.170 | 43.2 | 4.63 | 354 |

As presented in **Table 4**, using the scaled-up process, with a significantly shorter processing time, similar- or even better results were obtained in terms of particle size distribution, quercetin recovery and antioxidant activity, than in case of batch SFEE process. In particular, a similar particle size distribution was obtained with the scaled-up and the batch process, as presented in **Fig 5B**. Moreover, as presented in **Table 4**, repetition of experimental conditions yielded very similar results. Similarly, in the case of batch system, no connection was found between the conditions of SFEE process and the quercetin recovery and the particle size distribution of the final product.

According to these results, the robustness of scaled-up, semi-continuous SFEE system in the studied range of settings is demonstrated, and expectations detailed in the beginning of this section regarding the reduction of residual solvent content and the prevention of formation of quercetin crystals were fulfilled, by applying $scCO_2$ in the middle density range (80 -100 bar and 35ºC – 40°C), with an SFEE treatment time of 80-90 min, and using no more than 5 kg of $CO_2$ per 1 L of emulsion. Moreover, these mild temperature settings and the low treatment time reduce the possible degradation- and aggregation of encapsulated quercetin.

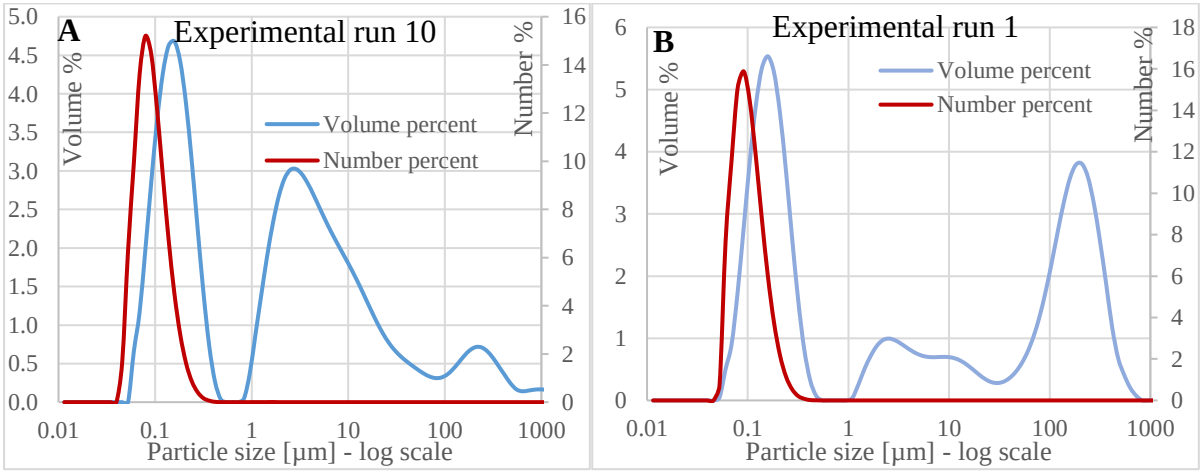


**Fig 5:** Particle size distribution result of bacth (A) and scaled-up (B) device

### 3.3 Results of with PGSS-drying and with lyophilization prepared products

SFEE obtained aqueous suspensions were further treated by PGSS-drying process, in order to extract water, and to obtain a dry powder, which is more suitable for long-term storage. Although in the work E. de Paz- and S. Varona et al [23], [17] the best process conditions of PGSS-drying have been studied, in this work an experimental study is also done in order to obtain best process conditions, regarding the highest possible antioxidant activity, and less possible quercetin degradation during PGSS-drying process. PGSS-drying process is considered as successful when a product with a residual moisture content below 10 w/w% is obtained. In the experimental study the effect of pre-expansion temperature in the range 109.4 – 132.5°C was studied, and the Gas/Liquid Ratio GLR (24.5 – 58.9 kg/L) was also varied, by varying the emulsion liquid flowrate (3 – 7 mL/min) and $CO_2$ flow rate (8 -12 kg/h). By varying GLR, pressure drop in the static mixer also changed, as detailed in **Table 5**. Quercetin recovery difference between SFEE obtained aqueous suspension mixtures and PGSS-drying obtained particles is defined as “quercetin loss during PGSS-drying process”, and analysed as main process parameter. Characteristics of collected SFEE samples, used for PGSS-experiments are detailed in **Table 3**.

**Table 5**: PGSS – drying experimental runs, *centrum point runs are* marked by font type Italic

| PGSS run | Pre-expansion temperature [°C] | Pre-expansion pressure [bar] | Density of $scCO_2$ in static mixture [kg/L] | Δp (static-mixture) [mbar] | $T_{tower}$ [°C] | Emulsion liquid flowrate [mL/min] | GLR [kg/L] | Quercetin content [mg/g of product] +/- 10% | Quercetin recovery of PGSS [%] | Quercetin loss during PGSS [%] | Corrected ORAC [µmol TE/ /g of quercetin] +/- 5% | Residual water content [%] |
|---|---|---|---|---|---|---|---|---|---|---|---|---|
| 1 | 109.4 | 92.2 | 0.16 | 96.8 | 64.7 | 7.0 | 24.5 | 7.0 | 84.6 | n/a | 40395 | 3.0 |
| 2 | 111.6 | 92.9 | 0.16 | 62.5 | 67.6 | 7.0 | 24.5 | 7.1 | 86.4 | 0.6 | 26070 | 3.4 |
| 3 | 110.4 | 96.4 | 0.17 | 109.2 | 66.8 | 3.0 | 57.2 | 5.5 | 67.0 | 20.3 | 30289 | 12.9 |
| 4 | 110.2 | 105.1 | 0.19 | 152.5 | 70.5 | 3.5 | 58.9 | 6.0 | 72.5 | 19.5 | 35126 | 31.9 |
| 5 | 132.5 | 76.8 | 0.12 | 95.9 | 73.2 | 5.5 | 25.0 | 6.6 | 79.3 | 2.8 | 37300 | 19.3 |
| 6 | 125.6 | 104.8 | 0.17 | 128.5 | 71.4 | 3.0 | 57.2 | 6.3 | 76.7 | 11.7 | 38526 | 12.3 |
| 7 | 125.7 | 117.7 | 0.20 | 82.4 | 68.9 | 5.5 | 37.5 | 6.0 | 72.2 | 14.1 | 31337 | 8.3 |
| 8 | 124.8 | 104.1 | 0.17 | 106.5 | 71.5 | 5.5 | 31.2 | 5.1 | 61.3 | 17.6 | 42227 | 2.3 |
| *9* | *125.6* | *99.9* | *0.16* | *54.3* | *69.8* | *5.5* | *31.2* | *6.4* | *78.0* | *11.8* | 25498 | *2.5* |
| *10* | *124.7* | *100.5* | *0.16* | *58.8* | *69.4* | *5.5* | *31.2* | *6.2* | *75.6* | *4.6* | 24832 | *8.9* |
| *11* | *125.4* | *98.8* | *0.16* | *48.8* | *71.1* | *5.5* | *31.2* | *6.9* | *83.4* | *15.1* | *n/a* | *n/a* |
| *12* | *125.4* | *99.1* | *0.16* | *39.6* | *73.6* | *5.5* | *31.2* | *6.0* | *72.3* | *13.2* | 32138 | *7.4* |
| *13* | *126.1* | *99.7* | *0.16* | *53.4* | *75.1* | *5.5* | *31.2* | *5.8* | *70.5* | *n/a* | 23077 | *7.4* |
| *14* | *124.2* | *98.5* | *0.16* | *75.8* | *70.6* | *5.5* | *31.2* | *7.4* | *81.3* | *9.1* | 41850 | *1.7* |

### 3.3.1 Process parameters, influencing on product quality

Antioxidant activity of PGSS-drying product shows high deviance for of all studied factors, – an example is shown on **Fig 3 (D)**–, as the antioxidant activity of the product is determined by the antioxidant activity of the original SFEE mixture.

As presented on **Fig 6 (A)** and **Fig 6 (B)**, quercetin loss during PGSS drying process is influenced by the GLR, the density of $CO_2$ contacted with the aqueous suspension SFEE product in the column, and slightly influenced by the temperature of the PGSS-drying tower: by increasing GLR and $scCO_2$ density in the static mixer, higher quercetin loss values were obtained, meanwhile higher temperatures than 70°C of the tower could also facilitate the degradation of quercetin.

However, according to **Fig 6 (C)** and **Fig 6 (D)**, the lowering of GLR value and the $scCO_2$ density, –which are favourable for reducing quercetin loss –, also cause an increase in the residual water content of the product. Therefore, compromised values of these settings need to be found, in order to keep residual moisture content under 10 w/w%. According to **Fig 6** (**A-D)**, in order to obtain the less possible quercetin loss during PGSS-drying process and the less possible residual moisture content, GLR value should be in the range of 31-35 kg/L, density of $CO_2$ in the column in the range 0.16 – 0.17 kg/L (which corresponds to ~125°C and ~100 bar of pre-expansion temperature and pre-expansion pressure, respectively), and tower temperature should be around 70°C.

Moreover, as visible on SEM pictures presented on **Fig 7**, GLR has a strong influence on the morphology of product: in all cases a fully encapsulation of quercetin by the surfactant material is obtained, but in case of experimental run 9 (**Fig 7 (A)**), by applying GLR in the adequate ratio, low quercetin loss, low residual water content, and micronized particles in generally smaller particle size are obtained. In case of experimental run 3 (**Fig 7 (B)**), applying higher GLR ratio (57.2 kg/L), quercetin loss is similar, but due to the higher residual water content,

agglomeration of particles took place. Moreover, as visible on **Fig 7 (C, D)**, using different GLR value than the adequate, not only the increase of the residual water content occurs, but also quercetin crystals are observed. From all cases, only in case of experimental run 9 (**Fig 7 (A)**, a free-flowing powder was obtained, due to adequate residual moisture content. Applying either lower or higher GLR value than the adequate range, higher residual moisture content, of the sample is increased: By applying lower GLR values then 31 kg/L, higher residual water content is obtained, as not sufficiently enough $scCO_2$ was contacted with the aqueous suspension. However, in case of higher GLR values applied than 35 kg/L, also higher residual water content is obtained, as the high amount of $CO_2$ contacted each L of suspension has a higher extracting effect for the water content in the static mixer, and therefore, the aqueous suspension of lecithin becomes more viscous and more residue is found in the static mixer, as shown on **Fig 6** (**E)**. This is an important detail in case of treating highly viscous materials due to safety reasons, as material could stuck in the column during treatment, and might causing plugging effect in the filled column, in where $scCO_2$ and aqueous mixtures are contacted with high flowrate and elevated pressure and temperature conditions.

**Fig 6:** **A:** Dependency of quercetin loss during PGSS-drying process on the GLR and on the tower temperature

**B:** Dependency of quercetin loss during PGSS-drying process on the GLR and on the density of $scCO_2$ in the column

**C:** Dependency of residual water content during PGSS-drying process on the GLR and on the tower temperature

**D:** Dependency of residual water content during PGSS-drying process on the GLR and on the density of $scCO_2$ in the column

**E:** Dependency of residuum of product in column during PGSS-drying process on the GLR and on the density residual water content

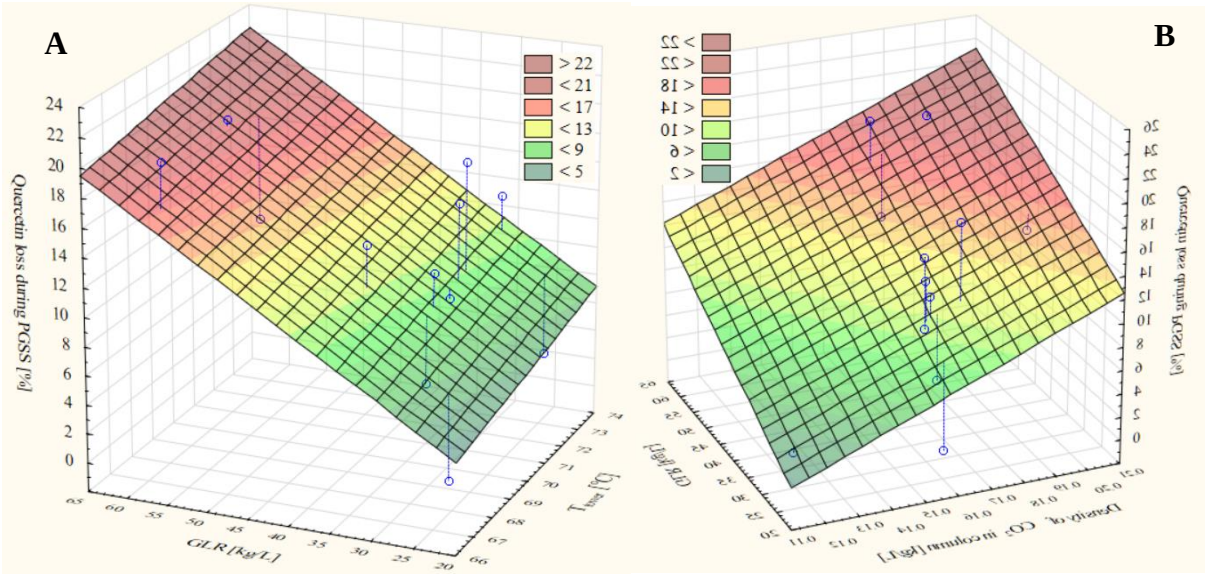
A
> 22
< 21
< 17
< 13
< 9
< 5
Quercetin loss during PGSS [%]
GLR [kg/L]
B
Quercetin loss during PGSS [%]

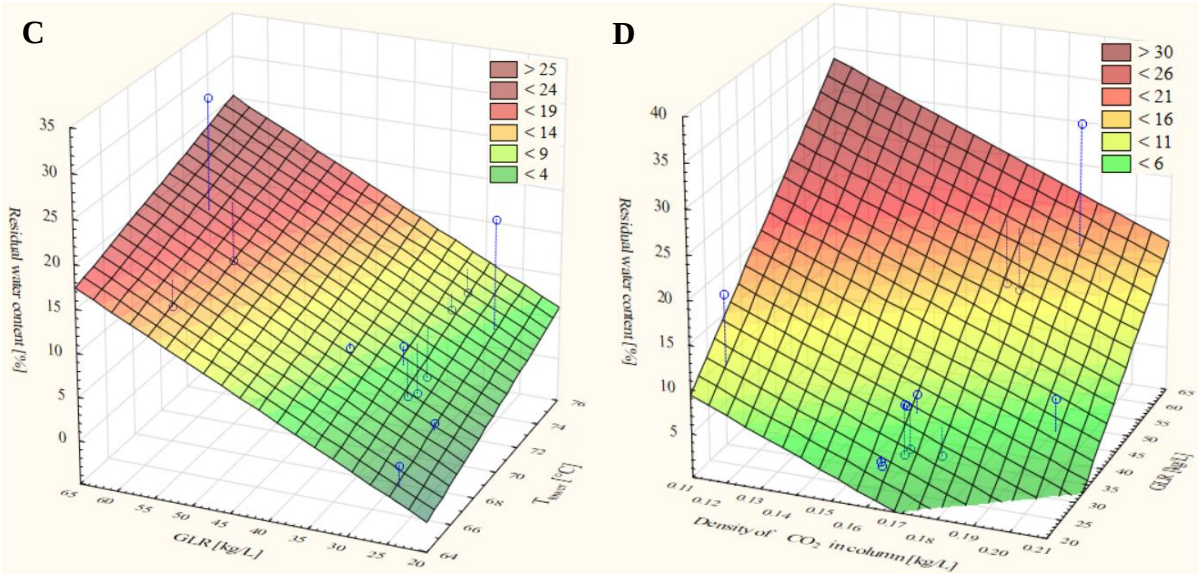
C
> 25
< 24
< 19
< 14
< 9
< 4
Residual water content [%]
GLR [kg/L]
D
> 30
< 26
< 21
< 16
< 11
< 6
Residual water content [%]
Density of CO2 in column [kg/L]

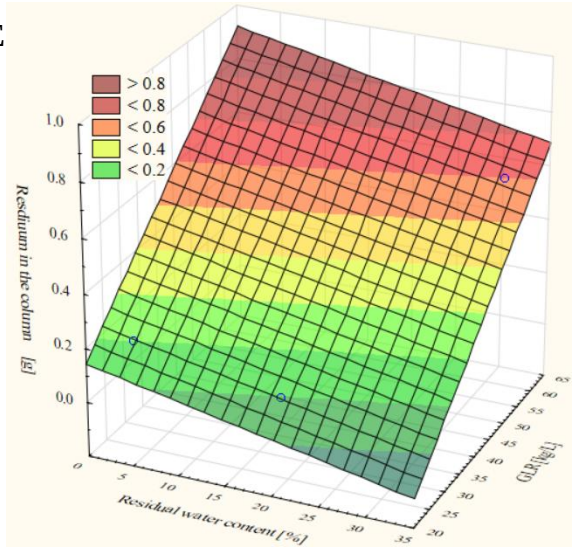
E
> 0.8
< 0.8
< 0.6
< 0.4
< 0.2
Residuum in the column [g]
Residual water content [%]

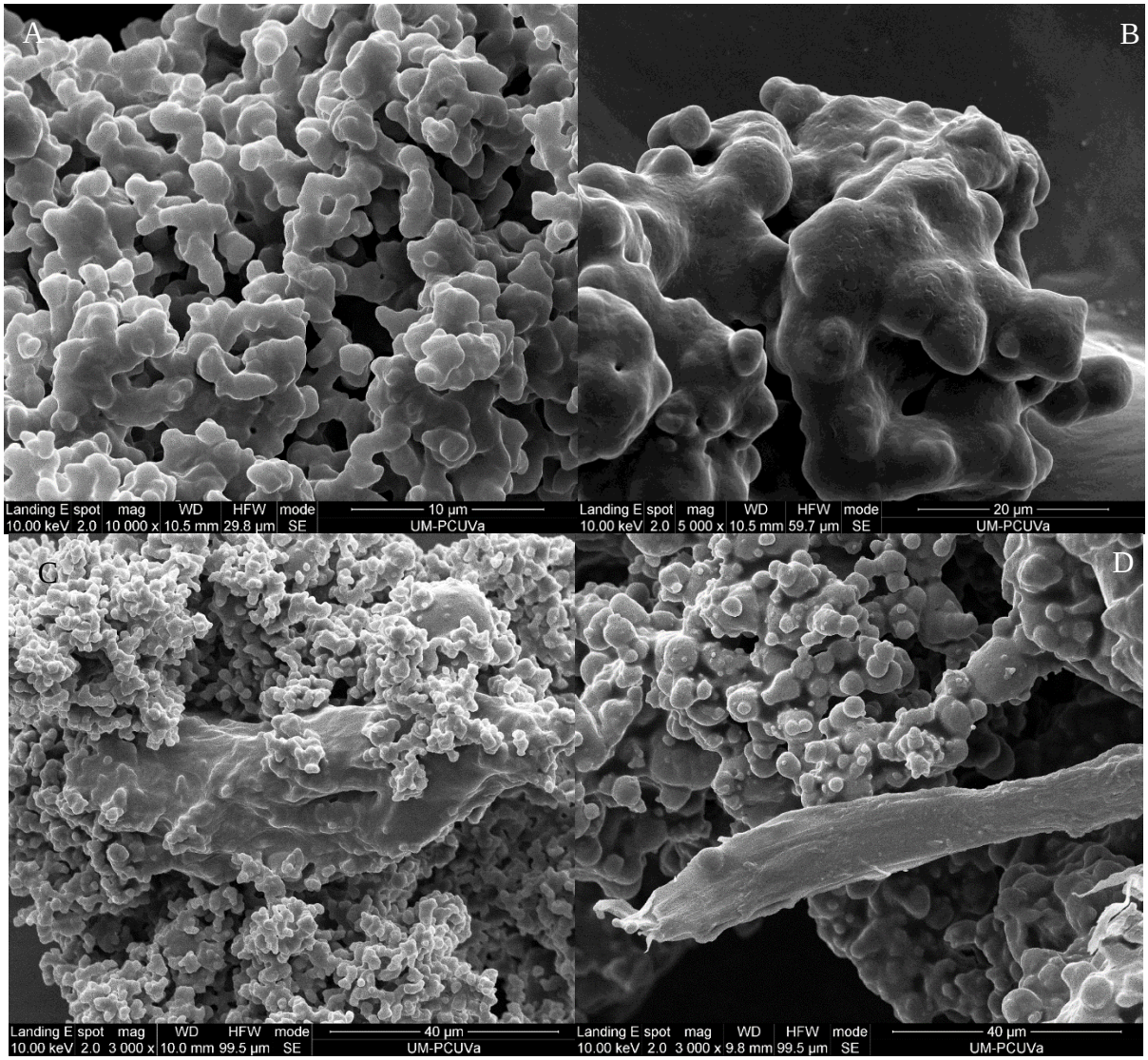


**Fig 7:** Scanning electron microscopy picture about PGSS - drying experimental runs 9 (A); 3 (B); 5 (C); 4 (D)

### 3.3.2 Structural characterization

As shown in FTIR spectra presented on **Fig 8**, the characteristic peaks of quercetin are neither present in the spectra of physical mixture of quercetin - lecithin - Pluronic L64®, nor in the spectra of PGSS-drying prepared samples. In contrast of that result, in previous work obtained spectra of the physical mixture of quercetin / lecithin = 1 / 75 (in mass) [12] showed the characteristic peaks of pure quercetin in the range of 1480-1380, 1200-1100, 880-750 and 600-400 $cm^{-1}$ [24]. This result could indicate, that although Pluronic L64® itself is not able to encapsulate quercetin particles, as presented in previous work [12], applying it with soy-bean lecithin as a mixture of encapsulating materials, encapsulation capacity would be stronger, which able to prevent more effectively the quercetin from degradation effect during SFEE treatment. This observation is consistent with the encapsulation efficiency observed in this work using the mixed surfactant material, discussed in section 3.1, which is significantly higher, than the average encapsulation efficiency of SFEE treatments done by using soy-bean lecithin only as surfactant material.

XRD spectres of physical mixture of quercetin/lecithin = 1/75 w/w, a lyophilised and two PGSS-dried samples are presented on **Fig 10**. Pure quercetin has high crystallinity and presents its characteristics peaks at 2θ values of 10.78°, 12.46°, 15.88°, and two more prominent peaks at 25.66°, and 27.4° [25] [26]. According to the XRD spectra, only a few peaks of pure quercetin are visible on the spectra of physical mixture at the 2θ values of 25.66 and 27.4, but none of the previously mentioned quercetin peaks are visible in the PGSS-dried and in the lyophilised samples, conforming that encapsulation and morphological change of quercetin to amorphous state is performed in both of the drying technology.

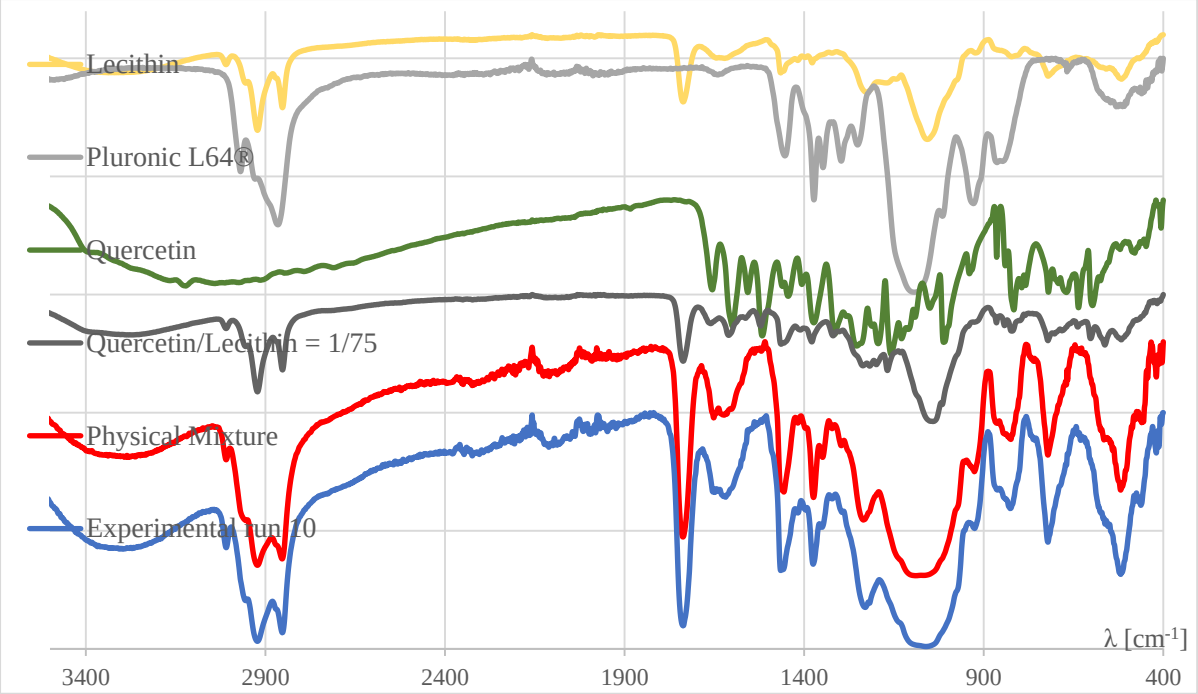


**Fig 8:** FTIR diagram of pure materials, quercetin - lecithin mixture, physical mixture and experimental runs 10

**Table 6:** Characteristics of lyophilized products done from SFEE mixtures detailed in **Table 3**

| SFEE mixture | Quercetin content [mg/g of product] +/-10% | Quercetin recovery [%] | Quercetin loss in lyophilization [%] | Antioxidant activity [µmol TE/g quercetin] +/-5% |
|---|---|---|---|---|
| **12** | 6.5 | 78.9 | 6.6 | 22848 |
| **13** | 8.8 | 100 | - | 19869 |

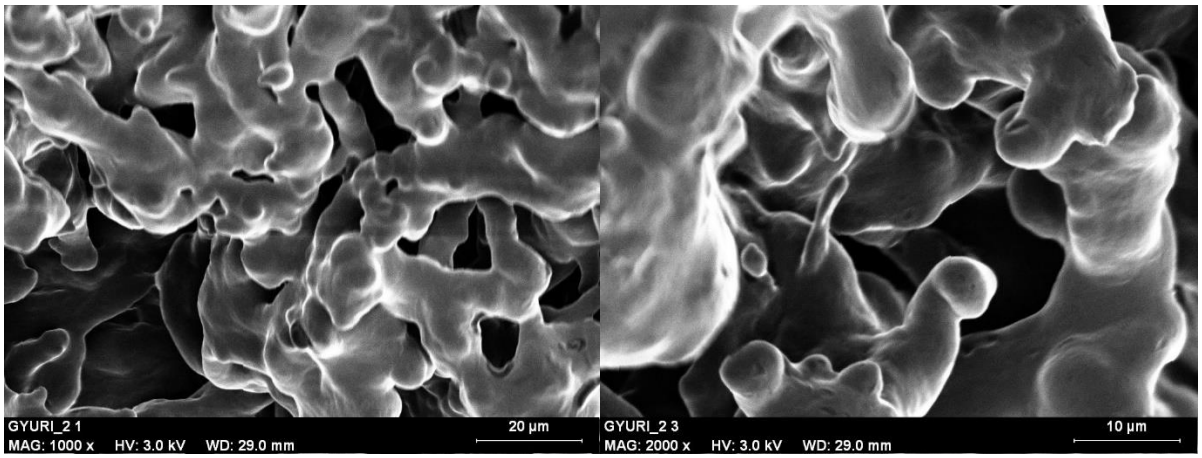


**Fig 9:** Scanning electron microscopy pictures about lyophilized SFEE mixture 13

The results of samples prepared by lyophilisation are presented on **Table 6**. Although significant degradation of quercetin does not occur during lyophilization, as samples are frozen and completely protected from light during the process, but more aggregated particles due to higher residual water content are visible, as shown on **Fig 9**. As detailed in **Table 5** and **Table 6**, PGSS-drying process operated at the optimal process conditions (previously described), yields are comparable with the yields of lyophilization, in terms of quercetin degradation and antioxidant activity. Moreover, SFEE mixture 13 after lyophilization process show a higher final quercetin encapsulation than SFEE mixture 12, most probably as precooling in case of mixture 13 was proceed by liquid nitrogen instead of commercial freezer, and a more efficient conservation of the physical structure was completed, due to the faster deep-cooling effect.

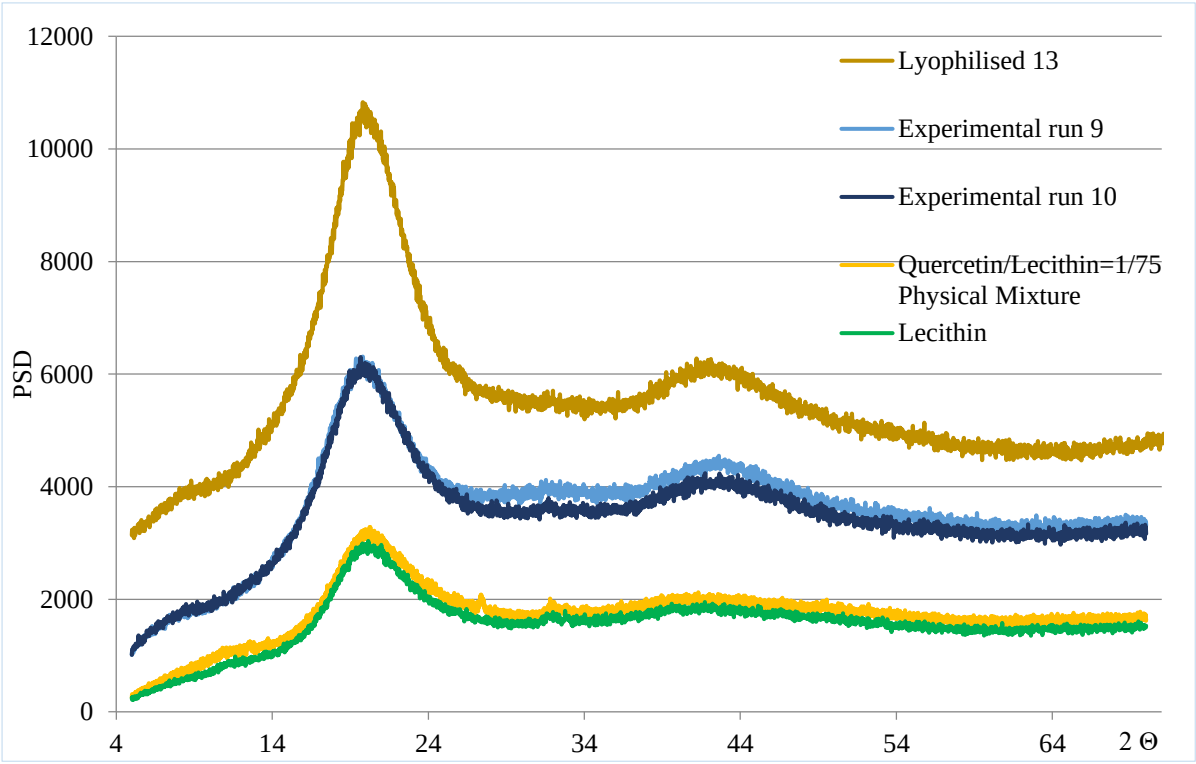


**Fig 10:** XRD diagram of pure materials, physical mixture, and a lyophilised and two PGSS--drying runs

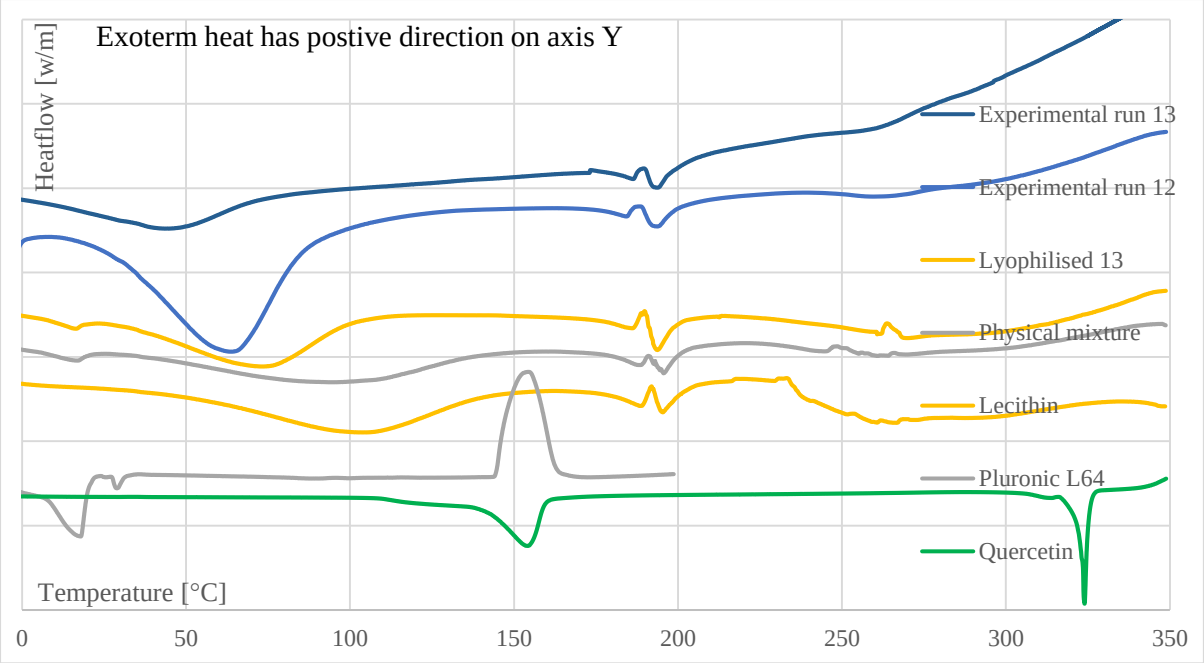


**Fig 11:** DSC diagram of pure materials, physical mixture and two experimental runs

Qualitative DSC curves of pure quercetin, Pluronic L64®, soy-bean lecithin, lyophilized and PGSS-dried samples are presented on **Fig 11**. Melting of pure Pluronic L64® in the temperature range of 8-18°C is visible in physical mixture and in samples prepared by PGSS - drying and lyophilization. Moreover, the melting of pure soy-bean lecithin in the temperature range of 150-170°C, followed by an exothermic peak of crystal transition at 193°C and a second melting peak at 195.5°C, are visible in physical mixture and samples prepared by PGSS - drying and by lyophilization, too. Crystal transition peaks of pure quercetin are neither visible in physical mixture, nor in the samples prepared by PGSS - drying and lyophilisation, thus, corroborating the amorphous state of the quercetin as indicated by the XRD analyses. Curves of samples containing lecithin above 250°C are not evaluable, due to thermal degradation effect of soy-bean lecithin.

### 3.3.3 Results of transdermal diffusion measurements

Quercetin permeability and aqueous stability of with SFEE and then PGSS-drying treated and micronized samples increased up to 9 times, comparing to pure physical mixture and by lyophilization obtained product, independently from the duration of measurement, indicated on the columns in hours (**Fig 12**). Pure physical mixture and with lyophilization prepared samples permeability and stability of quercetin is similar, and significantly lower, than with supercritical processes prepared samples, as micronization of encapsulated quercetin did not take place during the lyophilization due to the lack of the supercritical process, confirmed by the presence of more aggregated particles on **Fig 9**, than on **Fig 7**.

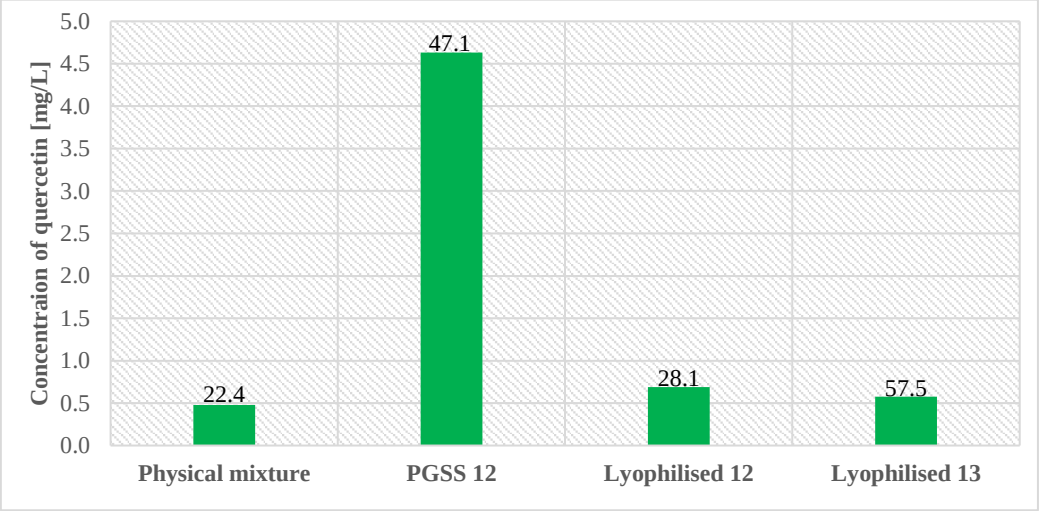


**Fig 12:** Franz cell measurement results (measurement time indicated in hours on columns)

## 4. CONCLUSIONS

By comparing the results of batch and scaled-up systems, robustness of scaled-up, semi-continuous SFEE process is proved. According to product quality considerations, $CO_2$ contacted with o/w emulsion should be slightly above its critical point, and no more than 5 kg $CO_2$ should be used for the treatment of 1 L emulsion, with a total 80-90 min of SFEE process time. SFEE products were treated by PGSS-drying, in order to obtain a dry quercetin loaded particles in micrometric range, and to increase long-term stability of product. Characteristics of products prepared by PGSS-drying and by lyophilization, regarding antioxidant activity and quercetin encapsulation efficiency are similar, proving that PGSS-drying is a suitable process to produce quercetin loaded particles in micrometric scale, without degradation of quercetin, or antioxidant activity loss. Quercetin permeability through transdermal membrane into simulated intestinal fluid is increased significantly, owing to the microencapsulation processes.

**Acknowledgement**

This research has been funded by the European Initial TrainingNetwork FP7-PEOPLE 2012 ITN 316959, “DoHip”, by Junta de Castilla y León with project VA225U14. Á. Martín thanks the Spanish Ministry of Economy and Competitiveness for a Ramón y Cajal research fellowship. S. Rodríguez-Rojo thanks the Spanish Ministry of Economy and Competitiveness and University of Valladolid for a Juan de la Cierva research fellowship (JCI-2012-14992).

## REFERENCES

[1] Y. Gao, Y. Wang, Y. Ma, A. Yu, F. Cai, W. Shao, G. Zhai, Formulation optimization and in situ absorption in rat intestinal tract of quercetin-loaded microemulsion, Colloids Surfaces B Biointerfaces. 71 (2009) 306–314. doi:10.1016/j.colsurfb.2009.03.005.

[2] S. Das, A.K. Mandal, A. Ghosh, S. Panda, N. Das, S. Sarkar, Nanoparticulated quercetin in combating age related cerebral oxidative injury, Curr Aging Sci. 1 (2008) 169–174. http://www.ncbi.nlm.nih.gov/entrez/query.fcgi?cmd=Retrieve&db=PubMed&dopt=Citation&list_uids=20021389.

[3] Khaled A. Khaled, Yousry M. El-Sayeda, Badr M. Al-Hadiyab, Disposition of the Flavonoid Quercetin in Rats After Single Intravenous and Oral Doses, Drug Dev. Ind. Pharm. 29 (2003) 397–403. doi:10.1081/DDC-120018375.

[4] R. Gugler, M. Leschik, H.J. Dengler, Disposition of quercetin in man after single oral and intravenous doses, Eur. J. Clin. Pharmacol. 9 (1975) 229–234. doi:10.1007/BF00614022.

[5] S. Chakraborty, S. Stalin, N. Das, S. Thakur Choudhury, S. Ghosh, S. Swarnakar, The use of nano-quercetin to arrest mitochondrial damage and MMP-9 upregulation during prevention of gastric inflammation induced by ethanol in rat, Biomaterials. 33 (2012) 2991–3001. doi:10.1016/j.biomaterials.2011.12.037.

[6] E. Weidner, Z. Knez, Z. Novak, A process and equipment for production and fractionation of fine particles from gas saturated solutions, World Patent, WO 95/21688, 1994.

[7] Á. Martín, E. Weidner, PGSS-drying: Mechanisms and modeling, J. Supercrit. Fluids. 55 (2010) 271–281. doi:10.1016/j.supflu.2010.08.008.

[8] E. Sher, T. Bar-Kohany, A. Rashkovan, Flash-boiling atomization, Prog. Energy Combust. Sci. 34 (2008) 417–439. doi:10.1016/j.pecs.2007.05.001.

[9] S.D. Sovani, P.E. Sojka, A.H. Lefebvre, Effervescent atomization, Prog. Energy Combust. Sci. 27 (2001) 483–521. doi:10.1016/S0360-1285(00)00029-0.

[10] Á. Martín, H.M. Pham, A. Kilzer, S. Kareth, E. Weidner, Phase equilibria of carbon dioxide+poly ethylene glycol+water mixtures at high pressure: Measurements and modelling, Fluid Phase Equilib. 286 (2009) 162–169. doi:http://dx.doi.org/10.1016/j.fluid.2009.08.010.

[11] S. Varona, Á. Martín, M.J. Cocero, Formulation of a natural biocide based on lavandin essential oil by emulsification using modified starches, Chem. Eng. Process. Process Intensif. 48 (2009) 1121–1128. doi:10.1016/j.cep.2009.03.002.

[12] G. Lévai, Á. Martín, E. De Paz, S. Rodríguez-Rojo, M.J. Cocero, Production of stabilized quercetin aqueous suspensions by supercritical fluid extraction of emulsions, J. Supercrit. Fluids. 100 (2015) 34–45. doi:10.1016/j.supflu.2015.02.019.

[13] Purdief, Guidance for Industry Q3C — Tables and List Guidance for Industry Q3C — Tables and List Guidance for Industry Q3C — Tables and List, 9765 (2012) 301–827. http://www.fda.gov/Drugs/GuidanceComplianceRegulatoryInformation/Guidances/default.htm\nhttp://www.fda.gov/BiologicsBloodVaccines/GuidanceComplianceRegulatoryInformation/Guidances/default.htm.

[14] D. Althans, P. Schrader, S. Enders, Solubilisation of quercetin: Comparison of hyperbranched polymer and hydrogel, J. Mol. Liq. 196 (2014) 86–93. doi:10.1016/j.molliq.2014.03.028.

[15] Á. Martín, H.M. Pham, A. Kilzer, S. Kareth, E. Weidner, Micronization of polyethylene glycol by PGSS (Particles from Gas Saturated Solutions)-drying of aqueous solutions, Chem. Eng. Process. Process Intensif. 49 (2010) 1259–1266. doi:10.1016/j.cep.2010.09.014.

[16] E. Badens, C. Magnan, G. Charbit, Microparticles of soy lecithin formed by supercritical processes, Biotechnol. Bioeng. 72 (2001) 194–204. doi:10.1002/1097-0290(20000120)72:2<194::AID-BIT8>3.0.CO;2-L.

[17] S. Varona, Á. Martín, M.J. Cocero, Liposomal incorporation of lavandin essential oil by a thin-film hydration method and by particles from gas-saturated solutions, Ind. Eng. Chem. Res. 50 (2011) 2088–2097. doi:10.1021/ie102016r.

[18] M. Salgado, S. Rodríguez-Rojo, F.M. Alves-Santos, M.J. Cocero, Encapsulation of resveratrol on lecithin and β-glucans to enhance its action against Botrytis cinerea, J. Food Eng. 165 (2015) 13–21. doi:10.1016/j.jfoodeng.2015.05.002.

[19] F. Ganske, B. Labtech, G.E.J. Offenburg, ORAC Assay on the FLUOstar OPTIMA to Determine Antioxidant Capacity, Bmglabtech.Com. (2006). http://www.bmglabtech.com/application-notes/fluorescence-intensity/orac-148.cfm.

[20] M.F. Ramadan, Antioxidant characteristics of phenolipids (quercetin-enriched lecithin) in lipid matrices, Ind. Crops Prod. 36 (2012) 363–369. doi:10.1016/j.indcrop.2011.10.008.

[21] F. Mattea, Á. Martín, C. Schulz, P. Jaeger, R. Eggers, M.J. Cocero, Behavior of an Organic Solvent Drop During the Supercritical Extraction of Emulsions, AIChE J. 56 (2010) 1184–1195. doi:0.1002/aic.12061.

[22] F. Mattea, A. Martin, A. Matias-Gago, M.J. Cocero, Supercritical antisolvent precipitation from an emulsion: beta-Carotene nanoparticle formation, J. Supercrit. Fluids. 51 (2009) 238–247. doi:10.1016/j.supflu.2009.08.013.

[23] E. de Paz, Á. Martín, C.M.M. Duarte, M.J. Cocero, Formulation of β-carotene with poly-(ε-caprolactones) by PGSS process, Powder Technol. 217 (2012) 77–83. doi:10.1016/j.powtec.2011.10.011.

[24] D. Bennet, M. Marimuthu, S. Kim, J. An, Dual drug-loaded nanoparticles on self-integrated scaffold for controlled delivery, Int. J. Nanomedicine. 7 (2012) 3399–3419. doi:10.2147/IJN.S32800.

[25] A. Shawky, M. Ghanem, H. Saleh, M. Ali, S.M. El-shanawany, E.A. Ibrahim, Solubility and dissolution enhancement of quercetin via preparation of spray dried microstructured solid dispersions Abstract :, 37 (2013) 12–24.

[26] S. Scalia, M. Haghi, V. Losi, V. Trotta, P.M. Young, D. Traini, Quercetin solid lipid microparticles: A flavonoid for inhalation lung delivery, Eur. J. Pharm. Sci. 49 (2013) 278–285. doi:10.1016/j.ejps.2013.03.009.

# CHAPTER IV

## QUERCETIN LOADED PARTICLES PRODUCTION BY MEANS OF SUPERCRITICAL FLUID EXTRACTION OF EMULSIONS: PROCESS SCALE-UP STUDY AND THERMO-ECONOMIC EVALUATION

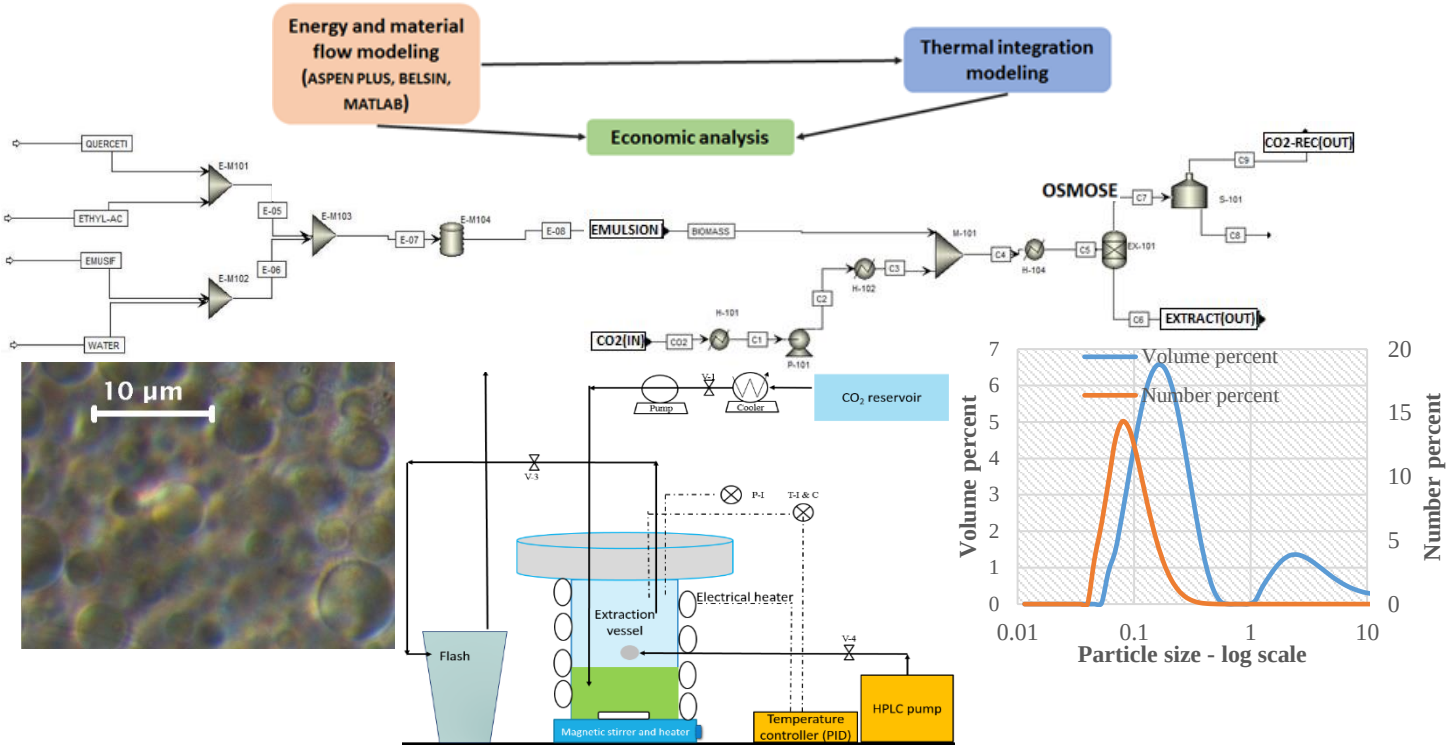
Energy and material flow modeling (ASPEN PLUS, BELSIN, MATLAB)
Thermal integration modeling
Economic analysis
QUERCETI
ETHYL-AC
EMUSIF
WATER
E-M101
E-M102
E-M103
E-M104
E-05
E-06
E-07
E-08
EMULSION
BIOMASS
M-101
H-101
H-102
H-104
P-101
CO2(IN)
CO2
C1
C2
C3
C4
C5
C6
C7
C8
C9
OSMOSE
S-101
EX-101
CO2-REC(OUT)
EXTRACT(OUT)
10 µm
Pump
Cooler
CO2 reservoir
V-1
V-3
V-4
P-1
T-I & C
Flash
Extraction vessel
Electrical heater
Magnetic stirrer and heater
Temperature controller (PID)
HPLC pump
Volume percent
Number percent
Particle size - log scale
0.01
0.1
1
10
0
1
2
3
4
5
6
7
0
5
10
15
20

**ABSTRACT**

Quercetin is an antioxidant compound, and it is a highly promising material against a wide variety of diseases, including cancer. A major limitation for the clinical application of quercetin is its low bioavailability, due to its low solubility in water. One way to increase the bioavailability of quercetin is to precipitate it in sub-micrometric scale, encapsulated by a surfactant material, using Supercritical Fluid Extraction of Emulsions (SFEE). The objective of the present work was to study the scale-up of semi-continuous SFEE process for quercetin loaded particles production. In addition, a themo-economic evaluation was done in order to identify bottlenecks and promote solutions. Soy-bean lecithin–Pluronic L64® encapsulated quercetin particle production was performed in order to obtain product characteristics significantly influenced factors, such as duration of SFEE, density of $CO_2$ medium, used $CO_2$ / L of emulsion (kg/L). The decrease of $CO_2$ flow demonstrated to be the main parameter to decrease the energy demand and cost of manufacturing of the SFEE process, thus further experimental studies should be done towards this optimization.

**Key-words**: Encapsulation, Supercritical $CO_2$, Semi-continuous SFEE technology, Economic evaluation, particle formation

## 1. INTRODUCTION

Quercetin (3,3',4,4',5,7-pentahydroxyflavone) is a bioflavonoid, available in various fruits, vegetable oils and many other food components. According to preliminary studies, it has strong antioxidant-, antiviral-, antibacterial-, antihistaminic- and anti-inflammatory effect. Moreover it presents anti-proliferative effects in a wide range of human cancer cell lines [1]. Due to its ion chelating and iron stabilizing effect it can scavenge reactive oxygen species, and down-regulate lipid peroxidation [2]. Furthermore, quercetin can promote the oxidation of $Fe^{2+}$ to $Fe^{3+}$, which become less effective by generating free radicals. Beneficial effects of quercetin might be explained by its o-diphenol B-ring structure [3], which has the ability of donating $\pi$ electrons from its benzene ring, meanwhile it is remaining relatively stable [4]. Moreover, in medical area is already demonstrated, that by applying only 150 mg quercetin/day, is able to downregulate the systolic pressure with an average value of 2.9 mmHg (3.7 mmHg in case of hypersensitive people) the range of age 25-50 [5]. Due to these properties, quercetin is a highly promising material against a wide variety of diseases, including cancer. A major limitation for the clinical application of quercetin is its low bioavailability (17% in rats [6] and lower than 1% in humans [7]), which makes it necessary to administrate in high doses (50 mg/kg) [8]. Applying supercritical fluid technologies as Supercritical Antisolvent- (SAS) [9] Gas Antisolvent- (GAS) [10] or Supercritical Fluid Extraction of Emulsion (SFEE) [11] methods are promising way to precipitate active compounds in sub-micrometric scale, and hence increase their specific surface area and their bioavailability. Moreover, by applying an adequate supercritical medium, as supercritical carbon-dioxide ($scCO_2$), thermal degradation of the bioactive compound is not taking place, due to low critical temperature of the supercritical solvent medium.

SFEE technology is used for producing aqueous suspensions, containing encapsulated valuable material (drug, bioactive compound etc.) in sub-micrometric scale. In SFEE process an initially

prepared oil in water (o/w) emulsion (material of interest is dissolved in the organic phase, which is separated by surfactant material from the continuous aqueous phase) is contacted with a supercritical fluid, in order to extract rapidly the organic phase from the emulsion. Supercritical fluid must be chosen to have high affinity for the organic solvent, meanwhile negligible affinity for the active compound. Due to the rapid supersaturation of the dissolution medium by the active compound, it is precipitating in sub-micrometric scale, encapsulated by the surfactant material. Principles of SFEE technology is shown on **Fig 1.**

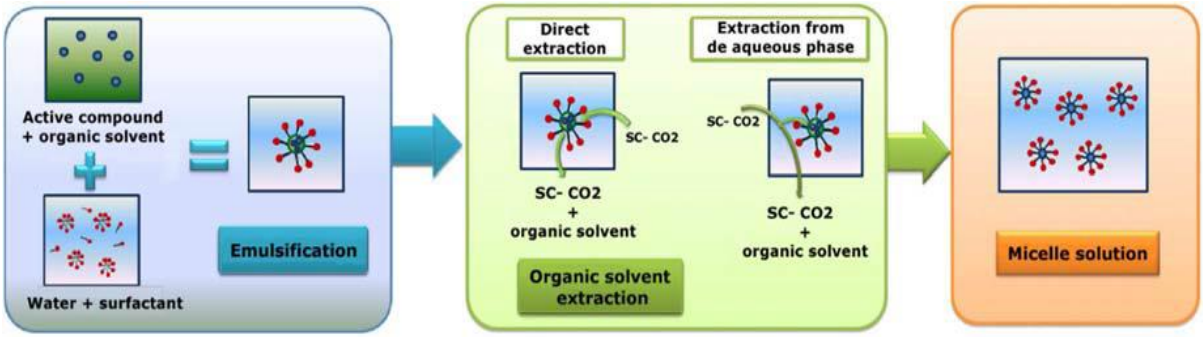


**Fig 1:** Principles of SFEE technology

Previously, we have demonstrated the technical feasibility to produce stabilized quercetin aqueous suspensions by supercritical fluid extraction of emulsions using batch SFEE equipment [11]. In this study our research group will do one step further, evaluating the scale-up of quercetin loaded particles in nanometric scale by semi-continuous SFEE technology. Encapsulation material was a combination of soybean lecithin and Pluronic L64®. An experimental plan was performed in order to obtain product characteristics significantly influenced factors, such as duration of SFEE, density of $CO_2$ medium, used $CO_2$ / L of emulsion (kg/L). Furthermore, thermo-economic perspectives of the proposed SFEE process were evaluated as an inevitable first-step to the conceptual process design for this quercetin encapsulation process. To the best of our knowledge, this is the first study regarding to the thermal demand and economic analysis of a SFEE process.

## 2. MATERIALS AND METHODS

### 2.1 Materials

Quercetin Hydrate ($C_{15}H_{10}O7xH_2O$, 95% purity, CAS: 849061-97-8) was obtained from Acros Organics (New Jersey, USA). The surfactant material poly-(ethylene glycol)- block –poly-(propylene glycol)- block -poly-(ethylene glycol) (Pluronic L64®, CAS: 9003-11-6) was obtained from Sigma Aldrich (St Louis, USA). Soy-bean lecithin was obtained from Glama-Sot (SOTYA, Madrid, Spain). Ethyl Acetate (EtAc, CAS: 141-78-6) and methanol (MeOH, CAS: 67-56-1), with a purity of 99% and 99.9 %, respectively, were obtained from Panreac Química (Barcelona, Spain). Acetonitrile (CAS: 75-05-8); acetic acid (reference number: 211008.1211) with a purity of 99.9% and 99.5 %, respectively, were obtained from Panreac Química (Barcelona, Spain). Carbon dioxide was provided by Carburos Metálicos (Barcelona, Spain).

### 2.2 Emulsion preparation and supercritical extraction of the emulsion

Preparation method of initial emulsion for SFEE process is described detailed in previous work [11]. Briefly an organic- and an aqueous based homogenous solution was prepared separately, the required amount of quercetin was dissolved in the organic phase (ethyl acetate), meanwhile surfactant material was dissolved in the water phase, purified by Millipore Elix. After homogenous solution had obtained, they were mixed together a minimum for 5 minutes with a minimum mixing rate of 500 rpm in order to obtain a homogeneous dispersion. Using Ultraturrax IKA LABOR-PILOT 2000/4 (IKA-WERKE GMBH&CO.KG) emulsifier device, emulsion was prepared with a frequency of 70 Hz for 4 min.

Experimental plan was done using a scaled-up semi-continuous SFEE device, presented on **Fig 2**, maintaining a continuous $scCO_2$ flow bubbled through the emulsion. Scaled-up SFEE equipment consist of on electrically tempered extractor vessel with a Micromite® serie 1600 micrometric valve (provide by HOKE) on its output, in order to maintain a controlled

continuous $scCO_2$ flow, pumped by a Milroyal® Dosapro® Milton Roy membrane pump. Flowrate of liquid $CO_2$ was measured by a Micro Motion RFT 9739 flowmeter. By starting the experiment, temperature of the system was set to the experimental plan designed value, and it was pressurized with $CO_2$ above the critical pressure, below the current experimental run designed vale, in order to leave margin for further pressure increase due to emulsion injection. Extractor vessel was than filled with approximately 168 mL of o/w emulsion using a GILSON 305 HPLC pump with a flowrate of 20 mL/min. Emulsion was introduced after pressurization of extractor vessel by $CO_2$ had been done, in order minimizing the disturbances and losses of liquid phase due to rapid initial pressure increase. Moreover, pumping through the emulsion on $scCO_2$ phase might have better phase contact than the other way around, by increasing this way the process efficiency, and hence decreasing the required process duration.

After HPLC pump had been separated from the system, liquid $CO_2$ was continuously pumped into the bottom of the extractor vessel using a four-times perforated 1/16" tube. Once the current experimental plan designed pressure was obtained, micrometric valve on the outer line was slightly opened, in order to maintain a controlled continuous $CO_2$ flow bubbling through on the emulsion, moreover emulsion was stirred using a magnetic stirrer with a mixing rate of 300 rpm. SFEE process was successfully efficient in case of the organic part was extracted below the restrictions of FDA [12]. This process is so called semi-continuous, due to only flowing of $scCO_2$, without flowing of emulsion is taking place in it.

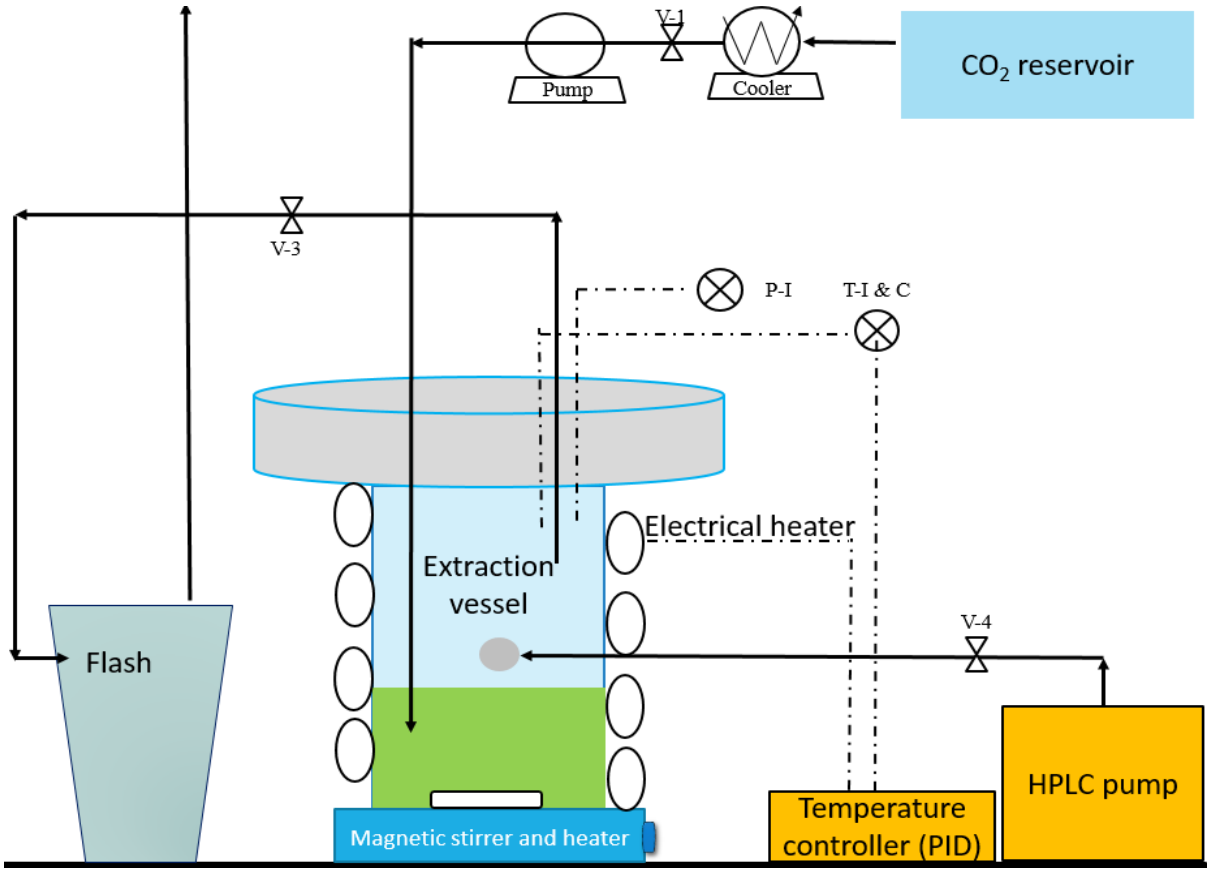


**Fig 2:** Scaled-up SFEE semi-continuous process

## 2.3 Analytical methods

### 2.3.1 Particle size distribution measurement and morphological characterization

Particle size distribution of SFEE treated aqueous suspension products was measured by Malvern Mastersizer 2000 Light Scattering device, provided by Malvern Instruments. The measurement range of the equipment is from 0.02 to 2000 µm using a diode laser 4 mW with a dual – wavelength detection system (red light 633 nm, blue light 436 nm). The sample was diluted by deionized water in the dispersion unit (Hydro SM), in order to obtain an adequate level of laser obscuration, and prevent multiple scattering effects. Refractive index for the dispersed phase (water) is 1.331, meanwhile for quercetin particles is 1.823. Each measurement was performed triplicate.

Optical microscopy, (Leica DM4000 B) was used for doing visual observations about initial o/w emulsions and SFEE-treated aqueous suspensions. Morphological observations about PGSS dried samples are done by Quanta 200F scanning electron microscopy provide by FEI. Samples were coated by 24 k gold with a width of approximately 10 nm using an Emitech K575X device.

### 2.3.2 Residual organic content

Remaining organic solvent of SFEE aqueous suspensions was measured by Head Space Gas Chromatography. Measurements were done two times, calibration series are done in the range of 0 – 1000 mg/L EtAc concentration with an $R^2 = 0.999$. Method of GC analysis detailed in previous work [13]. Briefly 4 mL of sample was introduced in a hermetically closed vial with a volume of 10 mL and vials were tempered before GC injection at 40°C. Sample for GC injection was taken by a Hamilton syringe with a volume of 1000 µL from the gas phase. Syringe was washed two times with the sample before sampling. GC equipment is provided by Agilent Technologies, 7890A gas chromatograph with a flame ionization detector (FID), with a HP-5 5% phenyl-methyl-silicone 30 m x 32 m x 25 µm column. The operating conditions for the analysis were: injector temperature 200º C, detector temperature 200º C, column temperature 80 ºC, injector flow rate 24 mL/min, column flow rate 1 mL/min (He) and split (sample dilution) 70:1.

### 2.3.3 Quercetin concentration

Due to interference of lecithin and quercetin in the absorption spectra [14], quercetin concentration was determined by HPLC, using a Waters 2487 chromatography system, consisting of a Waters In-Line degasser, Waters 515 HPLC pump and Waters 717 Plus Autosampler device. The injection volume of samples was 20 µL. The mobile phase was acetonitrile / milliQ water containing acetic acid in 5 V/V% concentration with a flowrate of 1

mL/minute. The method used a Pre-column, Guard cartridge package 2 from BIO-RAD: Bio-Sil C18 HL90-5 30 X 4.6 mm with a pore size 5 µm. The column was Waters Symmetry ® C18 150 X 4.6 mm with a pore size 5 µm, thermostated at 30°C. The detector was Waters 2784 Dual λ absorbance detector set on the wavelength of 373 nm, in order to determine the quercetin concentration with a retention time 8.32 min. SFEE aqueous suspension samples were centrifuged for 30 min with 2.3 g (equipment provided by Spectrafuge 240, Labnet International Inc., NJ, USA), in order to separate sediment crystals. Furthermore, samples were diluted 5 times in volume by MeOH and filtered by 0.45 µm pore size and 25 mm diameter PP filters provide by FILTER – LAB® (Cod. JPP045025N, Lot: 121022020), as according to UV-VIS measurements (Shimadzu UV-2550, 373 nm) polypropylene filters has the lowest absorbance for quercetin. To quantify the concentration of quercetin, a calibration line was developed from analysis of standard solutions of quercetin dissolved in a solution of methanol / water = 70 / 30 (V/V%), in the concentration range from 0 to 100 µg/mL with an $R^2 = 0.998$.

2.3.4 Antioxidant activity

Oxygen radical absorbance capacity (ORAC) measurements were also made in order to measure the ability of the antioxidant species, present in the sample to inhibit the oxidation of disodium fluorescein (FL) catalysed by peroxyl radicals generated from α, α'-Azodiisobutyramidine Dihydrochloride porum (AAPH). In a 96-well micro plate 25 µL of the appropriate sample dilution were added together with 150 µL of disodium fluorescein (10 nM). The micro plate was put in a fluorescent reader that allowed incubating the samples at 37ºC for 30 minutes. The reaction was started with 25 µL of AAPH (240 mM). Fluorescence emitted by the reduced form FL was measured in an BMG LABTECH Fluostar OPTIMA fluorescent reader, recorded every 1 min at the emission wavelength of 530±25 nm and excitation wavelength of 485±20 nm for a period of 90 min. Phosphate buffer (75 mM, pH=7.4) was used to prepare AAPH and FL solutions, and was also used as blank. Standards went from 13 till

200 µM Trolox, and additionally one independent control sample was also prepared. Samples and an independent control sample were analysed six times, blank and standards three times. Final ORAC values were calculated by a regression equation between the Trolox concentration and the net area under the FL decay curve and expressed as µM Trolox Equivalents per gram of quercetin (µM TE/g quercetin) [15]. SFEE samples were centrifuged by 2.3 g (Spectrafuge 240, Labnet International Inc., NJ, USA), diluted 50 times by water milliQ.

## 2.4 Process modelling and simulation description

A flowsheet model of SFEE process was developed using the commercial software Aspen Plus® and the process integration and the thermo-economic evaluation was carried out using Matlab. The thermodynamic model used to represent the process was RK-ASPEN model when supercritical fluid extraction of emulsion was considered and UNIQUAC model for low pressure processes. For more details about the modeling and simulation performed in Aspen Plus® v 8.4 see Appendix A. Matlab simulation software was used to perform thermal integration and economic analysis of the evaluated process using the developed platform OSMOSE. OSMOSE (OptimiSation Multi-Objectifs de Systemes Energetiques integres, which means “Multi-Objective OptimiZation of integrated Energy Systems”) is a computation platform that was built in MATLAB (MATrix LABoratory), developed and continuously improved at École Polytechnique Fédérale de Lausanne in Switzerland for the design and analysis of integrated energy systems, described in detail in Appendix B. In this study, the problem resolution was carried out following the steps:

1. Process data was gathered from the performed experiments
2. Aspen Plus® flowsheeting software was used to model mass and energy flows of the process. The model was used to calculate the associated heat and power balances

3. Pinch analysis methodology [16] was used to perform the thermal integration of the process aiming at the reduction of process steam requirements

4. An economic model was developed using data obtained from the flowsheeting software Aspen Plus® and the results obtained by the thermal integration model

The SFEE process was evaluated regarding productivity and economic process indicators.

The emulsification step of the process was simulated in Aspen Plus® considering 3 mixing tanks with external agitation and an ultrasonic homogenizer (also simulated as a mixing tank) to produce the final quercetin emulsion. The composition of the final emulsion was set according with experimental data using the design specification tool of Aspen Plus®.

The SFEE unit was simulated considering that the $CO_2$ sent to the process is initially cooled to -30°C and compressed to 200 bar. It is then heated to the extraction temperature, reaching the supercritical conditions. Later, the extraction vessel of 500 L, is filled with the emulsion and the supercritical fluid is passed through it. As the process was studied in a stationary regimen, it was considered 2 SFEE unities working in parallel to achieve a continuous inlet and outlet material flow. After the extraction process, the organic solvent diluted in supercritical $CO_2$ is sent to a depressurization tank to separation. At this stage, the pressure is reduced to 50 bar and temperature is set at 25°C. $CO_2$ is recycled to the process with a 5% loss.

## 2.5 Economic evaluation description

In order to accomplish an economic evaluation of the process viability at industrial scale, lab results were scaled-up considering that the same performance would be obtained. This criterion, which has been used by other authors for supercritical fluid-based processes [17], [18] assumes that the process will have identical performance with respect to yield at the laboratory and industrial scales if the same process conditions are used (temperature, pressure, extraction time, etc.). To calculate the total investment cost, the major process equipment was

roughly sized and their purchase cost were calculated and adjusted to account for specific process pressures and materials using correlations from literature [19], [20] and manufacturers[21]. The total investment cost was then calculated using multiplication factors to take into account indirect expenses like installation costs, contingencies and auxiliary facilities. All costs had been updated by using the Marshall and Swift Index.

Cost of manufacturing (COM) estimation for the proposed process was accomplished was based on the methodology of Turton et al. [19] in which variable cost (operational costs which are dependent on the production rate and consist in raw material costs, operational labour, utilities, among others), fixed costs (do not dependent on production rate and include territorial taxes, insurance, depreciation, etc.) and general expenses (cover business maintenance and include management, administrative sales, research and development costs) are calculated. These three components are estimated in terms of five main costs: fixed capital investment (FCI), cost of utilities (CUT), cost of operational labour (COL), cost of waste treatment (CWT) and cost of raw materials (CRM). The raw material cost is mainly related to the quercetin, ethyl acetate, the surfactant material and the extracting solvent lost during the process. Utility costs considered the electricity and the cooling requirements under 293 K. COM was calculated as presented in Eq 1.

$$COM = (VC + FC + GE)*(1 + 0.03COM + 0.11COM + 0.05COM), \quad (1)$$

In which 0.03COM represents the royalties; 0.11COM the distribution and selling and 0.05COM the research and development investments. **Table 1** shows the list of assumptions that support the economic assessment results.

**Table 1:** List of assumptions of the economic analysis of the proposed process

| **Economic data** | **Value** | **Unit** |
|---|---|---|
| Project lifetime | 25 | (years) |
| Construction and startup | 2 | (years) |
| Depreciation | 10 | (years) |
| Interest rate | 15 | (% per year) |
| Days worked in a year | 320 | (days/year) |
| **Price of raw materials** | | |
| Quercetin (purified) | 85.00[1] | (USD/kg) |
| Extract with 50% of quercetin | 12.00[1] | (USD/kg) |
| Extract with 5% of quercetin | 1.00[1] | (USD/kg) |
| Ethyl Acetate | 0.85 [2] | (USD/kg) |
| Soy Lecithin | 0.66 [1] | (USD/kg) |
| Polyethylene Glycol | 1.80 [1] | (USD/kg) |
| $CO_2$ | 0.30 [3] | (USD/kg) |
| Electricity | 0.05 [4] | (USD/kWh) |
| Cold demand under 293K | 0.028 [5] | (USD/kWh) |

[1] calculated based on a medium value from different manufactors; [2] data from[22]; [3] data from [23]; [4] data from [24]; [5] data from [17].

## 3. RESULTS AND DISCUSSION

### 3.1 Scaled-up, semi-continuous SFEE experimental runs

An experimental plan with scaled-up, semi-continuous SFEE experiment is done in this work in order to optimize the process conditions and increase its economic efficiency. As independence of product characteristics, obtained by batch SFEE process on the initial conditions of the initial emulsion and robustness of batch SFEE process was proved in a previous work, in the performed experimental plan only the effect of the following process

conditions were studied: $CO_2$ / emulsion ratio (3.64 – 7.50 kg/L), mass flow of $CO_2$ (0.8-1.8 kg/h), the average density of $scCO_2$ (0.22 – 0.74 g/mL) by chancing process pressure (77.3-108.5 bar) and temperature (34.0-50.3°C), and the duration of SFEE process (55-122 min). As using $scCO_2$ in a lower density region a faster organic extraction process was obtained, in two experimental runs *lower processing time* is applied (marked by font type Italic in **Table 2**), in order to examine the effect of shorter processing time for product degradation and antioxidant activity loose. Moreover, by applying shorter processing time, consumption of $CO_2$ and pumping- and heating energy is further reducible. As economic efficiency of the process mainly depends on the initial concentration- and the final recovery ratio of quercetin, the effect of a higher initial concentration of quercetin in o/w emulsion (0.03 w/w%) was also studied, and marked by font type Bold in **Table 2**. Major criteria of SFEE process are to decrease the residual organic content of the aqueous suspension products below 1000 mg/L without the appearance of quercetin crystals, and to decrease the particle size of encapsulated quercetin in sub-micrometric range. As visible on **Fig 4 (B)**, less than 1000 mg/L of residual content is easily obtainable only by applying a minimum of 80 min as processing time. Longer duration of SFEE treatment than 90 min is not economically favourable, as no better results are obtainable, however more $CO_2$ and heating and pumping energy is used and wasted.

**Table 2:** Experimental plan done by scaled-up, semi-continuous SFEE device, initial conditions of all o/w emulsions: $c_{quercetin}$ = 0.02 w/w%; $c_{lecithin}$ = 2.00 w/w%; $c_{PluronicL64®}$ = 0.4 w/w%; PlronicL64® / lecithin = 0.2 (w/w); solvent / water = 0.25 (V/V), **Experimental runs 2 and 8** (marked by font type **Bold) are done by** increased concentration of quercetin (0.03 w/w%), other settings are the same; *SFEE experimental runs with lower duration of SFEE* marked by font type *Italic*.

| SFEE run | T [°C] | p [bar] | Density of $CO_2$ [kg/L] | Dura-tion of SFEE [min] | Used $CO_2$ / emulsion [kg/L] | $CO_2$ mass flow [kg/h] | Quercetin recovery [%] | ORAC [µMTE / / g of quercetin] | D (0.1) [µm] | D (0.2) [µm] | Under 1 µm [V/V%] | Between 0.138 - 0.158 µm [V/V%] | Residual organic content [mg/L] |
|---|---|---|---|---|---|---|---|---|---|---|---|---|---|
| ***1*** | *50.3* | *80* | *0.22* | *61* | *5.26* | *1.77* | *89.6* | *n/a* | *0.105* | *0.146* | *39.0* | *4.37* | *2073* |
| ***2*** | ***50.0*** | ***80*** | ***0.22*** | ***60*** | ***4.65*** | ***1.60*** | ***35.6*** | ***n/a*** | ***0.098*** | ***0.128*** | ***52.4*** | ***6.05*** | *5734* |
| ***3*** | 37.6 | 81 | *0.33* | 80 | 7.14 | 1.35 | 92.0 | 23181 | 0.106 | 0.171 | 32.0 | 4.60 | 174 |
| ***4*** | 37.6 | 77 | *0.27* | 88 | 6.79 | 1.50 | 76.8 | 24043 | 0.092 | 0.121 | 53.3 | 5.71 | 295 |
| ***5*** | 35.3 | 80 | *0.39* | 87 | 7.50 | 1.45 | 70.3 | 16088 | 0.082 | 0.109 | 60.2 | 5.71 | 294.0 |
| ***6*** | 35.4 | 80 | *0.39* | 88 | 6.40 | 1.50 | 89.9 | 15171 | n/a | n/a | n/a | 7.05 | n/a |
| ***7*** | 35.0 | 101 | *0.72* | 90 | 6.63 | 1.47 | 79.6 | 18517 | 0.089 | 0.115 | 59.0 | 6.31 | 179 |
| ***8*** | **35.4** | **108** | ***0.74*** | **85** | **4.35** | **1.13** | **100.0** | **3519** | **0.104** | **0.154** | **34.9** | **3.58** | **53** |
| ***9*** | 34.7 | 80 | 0.46 | 89 | 5.17 | 1.21 | 81.2 | 28777 | 0.096 | 0.124 | 59.9 | 6.56 | 325 |
| ***10*** | 35.0 | 83 | 0.58 | n/a | 4.41 | 1.64 | 90.4 | 22636 | 0.085 | 0.116 | 55.9 | 5.14 | 379 |
| ***11*** | 34.7 | 83 | 0.59 | 75 | 4.46 | 1.20 | 82.9 | 22439 | 0.094 | 0.125 | 50.2 | 5.35 | 425 |
| ***12*** | 34.0 | 83 | 0.62 | 80 | 5.65 | 1.42 | 85.5 | 22183 | 0.094 | 0.134 | 43.4 | 4.19 | 282 |
| ***13*** | 39.9 | 98 | 0.62 | 85 | 3.64 | 0.85 | 89.7 | 19656 | 0.104 | 0.152 | 36.6 | 3.78 | 1153 |
| ***14*** | 40.1 | 100 | 0.63 | 93 | 4.44 | 0.97 | n/a | 11121 | 0.100 | 0.155 | 36.6 | 3.30 | 426 |
| ***15*** | 40.3 | 100 | 0.62 | 110 | 4.82 | 0.87 | 89.3 | 19133 | 0.098 | 0.146 | 38.5 | 3.61 | 343 |
| ***16*** | 40.4 | 100 | 0.62 | 89 | 3.85 | 0.88 | 77.5 | 22545 | 0.098 | 0.145 | 38.5 | 3.71 | 457 |
| ***17*** | 40.1 | 100 | 0.63 | 91 | 4.36 | 0.99 | 82.4 | 19499 | 0.098 | 0.149 | 40.2 | 3.74 | n/a |
| ***18*** | 40.2 | 100 | 0.62 | 90 | 4.17 | 0.93 | 85.8 | 32982 | 0.101 | 0.156 | 35.3 | 3.20 | 401 |
| ***19*** | 39.9 | 100 | 0.63 | 102 | 4.65 | 0.94 | 88.8 | 21143 | 0.100 | 0.146 | 39.1 | 3.88 | 277 |
| ***20*** | 40.2 | 100 | 0.62 | 91 | 3.87 | 0.86 | 90.3 | 22301 | 0.141 | 1.046 | 19.8 | 2.12 | 665 |
| ***21*** | 39.8 | 100 | 0.63 | 93 | 4.14 | 0.90 | 89.0 | 23984 | 0.092 | 0.124 | 52.9 | 5.32 | n/a |
| ***22*** | 39.3 | 99 | 0.64 | 99 | 3.85 | 0.79 | n/a | n/a | 0.097 | 0.135 | 46.6 | 4.57 | n/a |
| ***23*** | 39.2 | 99 | 0.64 | 101 | 4.71 | 0.95 | n/a | n/a | 0.093 | 0.129 | 47.7 | 4.71 | n/a |
| ***24*** | 39.8 | 100 | 0.63 | 122 | 4.71 | 0.79 | n/a | n/a | 0.090 | 0.126 | 49.4 | 4.60 | n/a |
| ***25*** | 40.2 | 100 | 0.63 | 92 | 4.12 | 0.91 | n/a | n/a | 0.095 | 0.128 | 50.9 | 5.29 | n/a |

Although results of samples with approximately 60 min as SFEE treatment time was also studied, results of these runs were not taken into account in the analysis, due to their significantly higher residual organic content than 1000 mg/L, according to **Fig 4 (A)**. Moreover, antioxidant activity is not depending on the duration of SFEE treatment, no increased degradation effect of product was obtained upon 80 – 90 min as treatment time instead of 60 min. Duration of SFEE treatment in the studied region neither has effect on quercetin recovery.

As visible on **Fig 4 (C)**, with increased initial concentration of quercetin, no more increase in the recovery ratio was obtained. However, as the fully dissolved state of quercetin in the initial o/w emulsion is a crucial process step, and the lack of the evaluation of a homogenous dissolution might cause the formation of quercetin crystals and phase destabilization of emulsion, and hence the failure of the SFEE process, which might have occurred in case of experimental run 2, as presented on **Fig 3 (A)**. All SFEE products were observed by optical microscopy, and were closed from further study in case of segregated quercetin crystal formation.

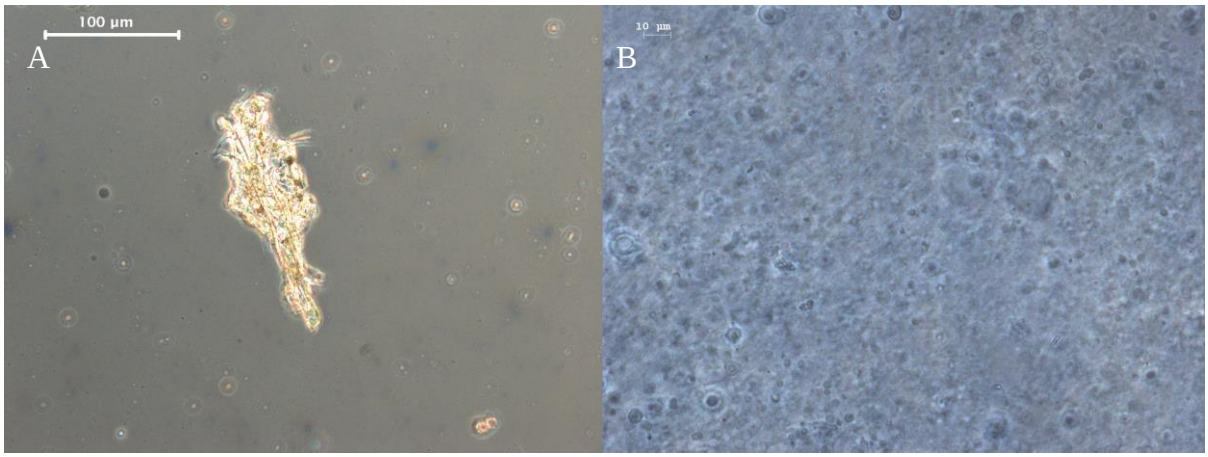


**Fig 3:** Optical microscopy pictures about experimental runs 2 (A) and experimental run 4 (B)

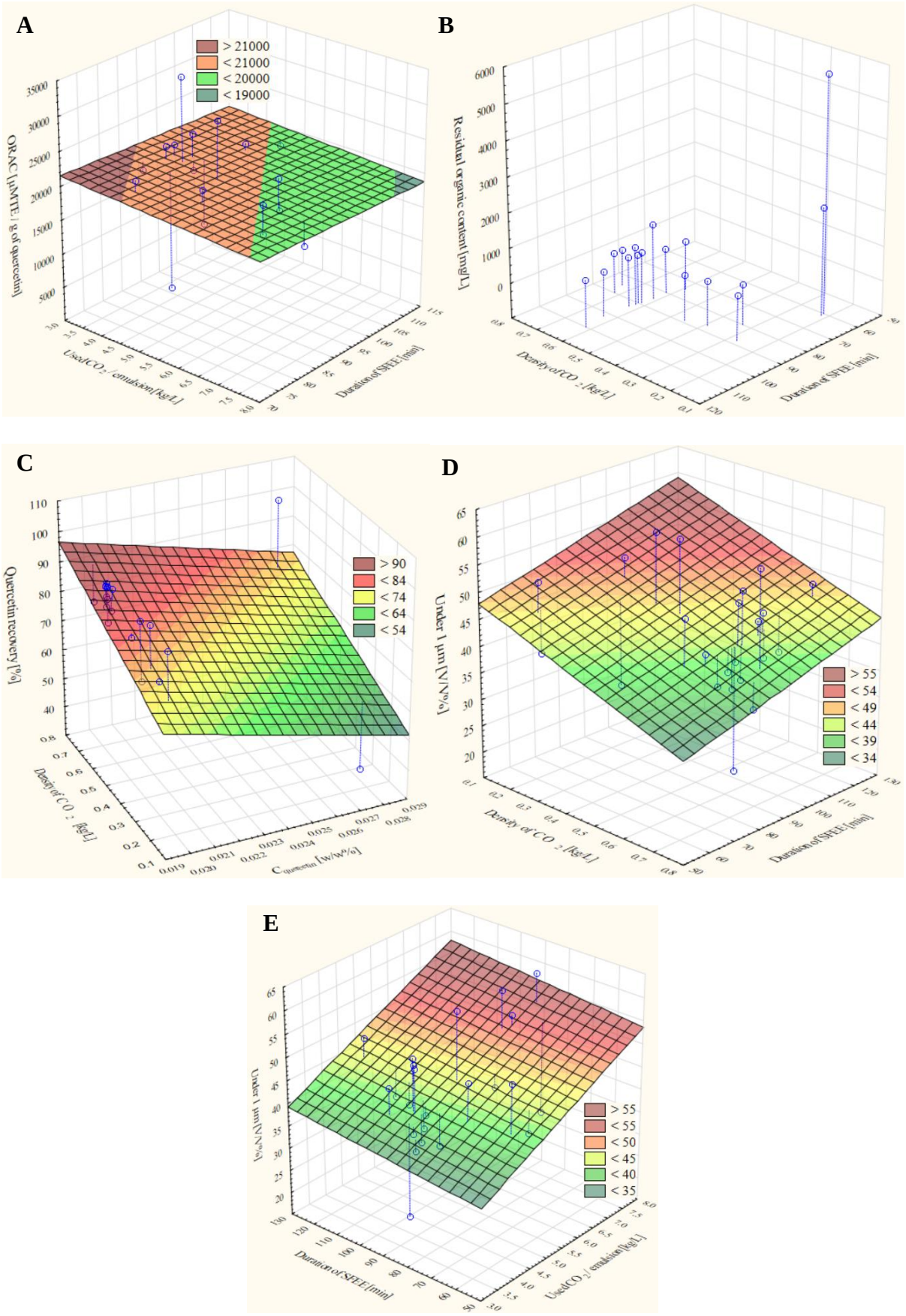
A
> 21000
< 21000
< 20000
< 19000
ORAC [µMTE / g of quercetin]
Used CO2 / emulsion [kg/L]
Duration of SFEE [min]
B
Residual organic content [mg/L]
Density of CO2 [kg/L]
Duration of SFEE [min]
C
> 90
< 84
< 74
< 64
< 54
Quercetin recovery [%]
Density of CO2 [kg/L]
Cquercetin [w/w%/s]
D
> 55
< 54
< 49
< 44
< 39
< 34
Under 1 µm [V/V%]
Density of CO2 [kg/L]
Duration of SFEE [min]
E
> 55
< 55
< 50
< 45
< 40
< 35
Under 1 µm [V/V%]
Duration of SFEE [min]
Used CO2 / emulsion [kg/L]

**Fig 4** **A:** Dependency of antioxidant activity on the duration of SFEE treatment and on used $CO_2$ / emulsion [kg/L]

**B:** Dependency of residual organic content on the duration of SFEE treatment and on the density of sample treated $scCO_2$

**C:** Dependency of quercetin recovery on the duration of SFEE treatment and on the density of sample treated $scCO_2$

**D:** Dependency of particle size of quercetin on the duration of SFEE treatment and on the density of sample treated $scCO_2$

**E:** Dependency of particle size of quercetin on the duration of SFEE treatment and on the used $scCO_2$ / L of emulsion [kg/L]

As visible on **Fig 4 (D)** and on **Fig 4 (E)**, higher part of particles were in nanometric range by applying $scCO_2$ in middle density region (slightly elevated pressure (80 bar) and temperature (35°C)), with an SFEE treatment time of around 80-90 min. Applying lower SFEE treatment time is not efficiency enough for organic extraction, meanwhile applying higher SFEE treatment duration than 90 min might lead to higher degradation range of quercetin, or particles agglomeration. However, in the studied range the SFEE duration and density of $scCO_2$ have no significant effect on the particle size distribution and antioxidant activity results, applying not highly elevated pressure and temperature is more favourable economically, as shorter processing time as well.

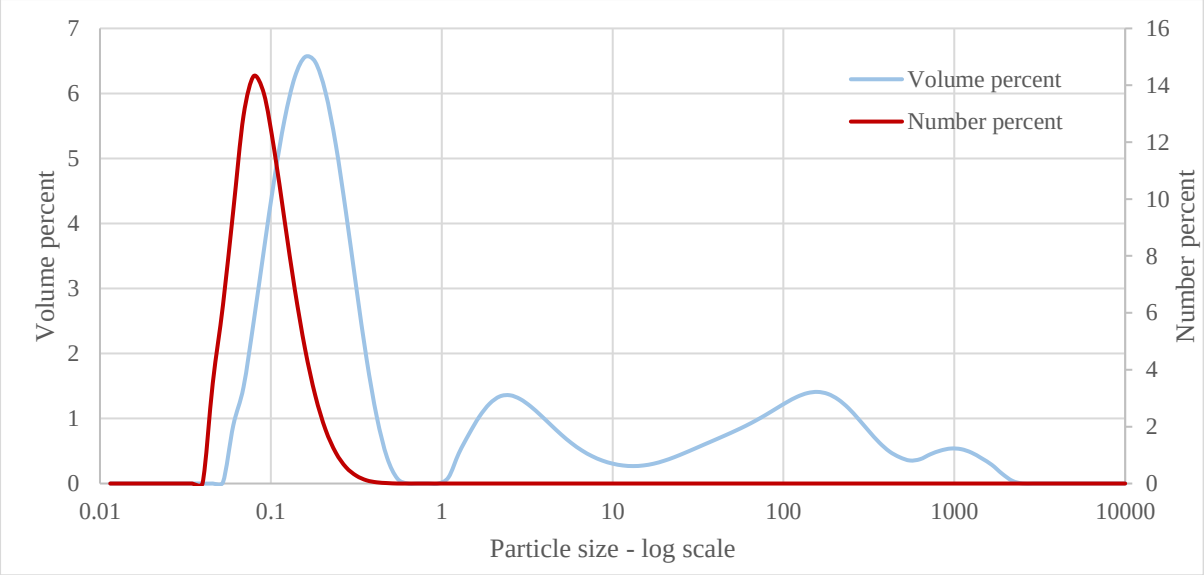


**Fig 5:** Particle size distribution result of experimental run 9

As visible on **Fig 5** using scaled-up SFEE process, obtained particle size distribution is similar to particle size distributions obtained with batch SFEE process presented in previous works: multimodal in terms of volume percent with a mean particle size distribution around 100 nm, meanwhile converting this result to number percent, monomodal particle size distribution is obtained.

According to the results detailed above, robustness of scaled-up, semi-continuous SFEE process is proved, and according to economical- and product quality considerations, $CO_2$ contacted with o/w emulsion should be slightly above its critical point, and no more than 5 kg $CO_2$ should be used for the treatment of 1 L emulsion, by applying an around 80-90 min of SFEE treatment time, and hence decrease the cost of producing 1 L of aqueous suspension, and possible degradation effects in products. In the following sections economical aspects of the developed SFEE process will be presented. To the best of our knowledge, this is the first study regarding to the thermal and economic evaluation of the SFEE process.

## 3.2 Process evaluation using simulation tools

### 3.2.1 Regarding productivity indicators

**Fig 6** shows the productivity based on encapsulated quercetin present in the final extract (aqueous suspension) and total final extract produced for the evaluated configurations (Runs 3-21). It was possible to achieve encapsulated quercetin production higher than 28 t/year for Runs 3, 6, 8, 10, 15, 20. Run 8 presented the final extract with the highest encapsulated quercetin concentration, 47.4 t/year, due to the higher initial quercetin concentration on the emulsion. Increasing in 50% the initial concentration of quercetin in the emulsion, from 0.02% to 0.03% w/w, it was possible to produce 1.6 times more quercetin encapsulated than the best production condition in low quercetin concentration in the emulsion, Run 3.

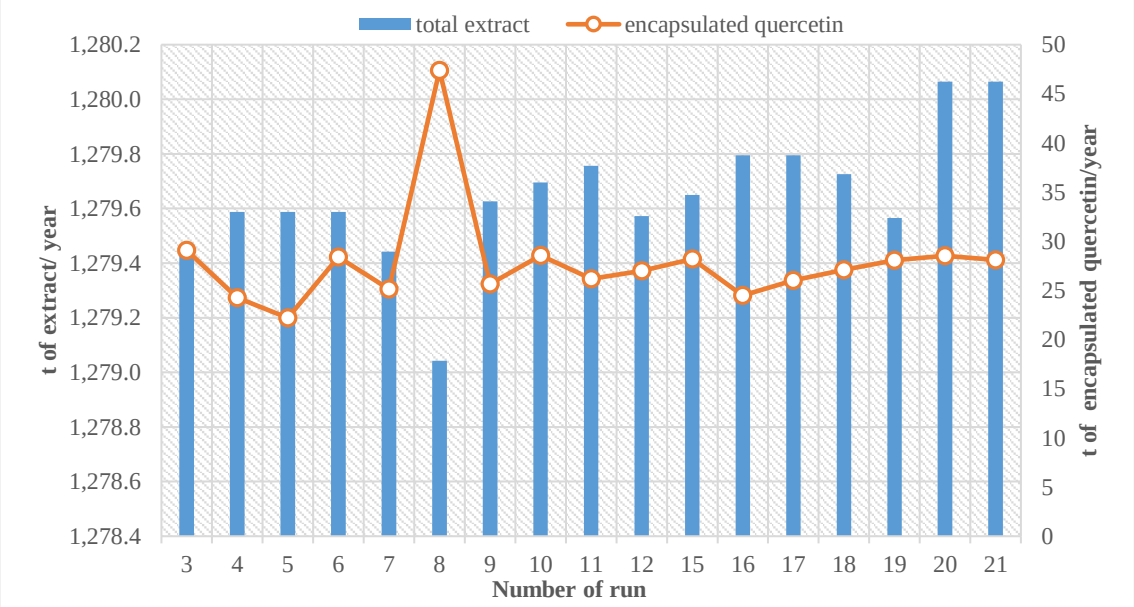


**Fig 6:** Process productivity based on encapsulated quercetin present in the final extract and total final extract produced for different evaluated configurations

### 3.2.2 Regarding thermal indicators

Regarding the thermal demand of the evaluated process, after thermal integration there was no need for heat supply to the process, only cooling of the streams was necessary. As evaluated

experimentally, the initial 5% of $CO_2$ removed contained the main part of the ethyl acetate present in the emulsion. It was considered that the initial 5% of $CO_2$ was removed from the system and the remaining $CO_2$ was recirculated to the process, adding fresh $CO_2$ to the process to maintain the $CO_2$ flow constant. Electricity consumption and the cooling demand for the process varied according with the configuration proposed, the higher the amount of $CO_2$ used in the process. The mean values were 51.67 MW and 575.91 MW. Run 7 presented the highest electricity consumption, increasing the mean value in 58%, while Run 5 presented the highest cooling demand, increasing the mean value in 44%. The lowest electricity consumption was found for Runs 10 and 11, 27% lower than the mean value, and the lowest cooling demand for Runs 16 and 20, 26% lower than the mean value.

### 3.2.3 Regarding economic indicators

The economic analysis of the process showed that all runs presented investment of approximately 571.20 thousand dollars. Being Run 7 the most expensive, 7% more expensive than the mean value, because of the high amount of $CO_2$ used and the high pressure employed. The cheapest runs were Run 10 and 11, both presenting investment 4.3% cheaper than the mean value.

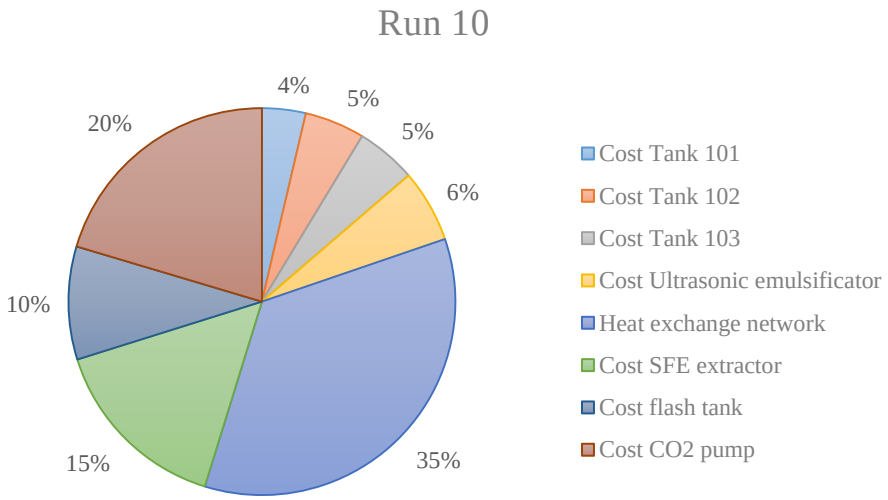


**Fig 7:** Component contribution in the investment cost

The amount of $CO_2$ also highly influenced the investment cost (**Fig 7**). In general, the extraction vessel is the main cost of a supercritical fluid extraction system[25]. Nevertheless, as the $CO_2$ flow employed in this process is much higher than the ones employed, for example, on Supercritical Fluid Extraction (SFE) process for extracting bioactive compounds from vegetable sources, around 100 times higher, both the $CO_2$ pump and the heat exchange network, which heated and cooled $CO_2$, presented the higher share of the investment. Together they represented 55% of the investment for Run 10, and 57%±2 as a mean value for all the runs.

Figure 8 shows the cost of manufacturing (COM) estimation for the evaluated alternatives based on the amount of extract or encapsulated quercetin. The mean value of the COM was 2.14 and 101.23 USD/kg, for the final extract and the encapsulated quercetin, respectively. The estimation of the COM for the encapsulated quercetin was performed by taking into account the fact that the percentage of encapsulated quercetin in the final extract can affect their specific cost, for this reason the specific cost for quercetin (COM encapsulated quercetin) is always higher than the COM extract. Calculated COM higher than the mean value were found for the runs with Used $CO_2$ / emulsion (kg/L) (**Table 2**) than 5.5 (Runs 3, 4, 5, 6, 7, 12), the higher the amount of $CO_2$ used the higher is the electricity and cooling requirements and also the investment cost for the process. The highest Used $CO_2$ / emulsion (kg/L), Run 5; presented the highest COM, 25% and 52% higher than the mean value, for the extract and the encapsulated quercetin, respectively. The lowest COM was found for Run 8, which considered the increase in 50% of quercetin in the emulsion preparation, presenting COM of the encapsulated quercetin 48% lower than the mean value. The increase in the quercetin concentration in the emulsion demonstrated to be an important aspect to decrease the cost of manufacture together with the decrease of $CO_2$ flow.

**Table 3:** Composition of the COM for the lowest values of COM found based on the quercetin amount in the final extract

| **Run** | **8** | **10** | **13** | **18** | **20** | **21** | |
|---|---|---|---|---|---|---|---|
| **Variable cost** | 1,778.21 | 1,777.01 | 1,720.37 | 1,646.44 | 1,712.98 | 1,778.21 | thousand USD |
| **Fixed cost** | 283.13 | 279.04 | 282.54 | 281.89 | 282.47 | 283.13 | thousand USD |
| **General production cost** | 51.95 | 51.73 | 51.92 | 51.89 | 51.92 | 51.95 | thousand USD |
| **COM** | 2,514.82 | 2,508.26 | 2,445.24 | 2,356.46 | 2,436.36 | 2,514.82 | thousand USD |
| **COM extract** | 1.97 | 1.96 | 1.91 | 1.84 | 1.90 | 1.97 | USD/kg |
| **COM encapsulated quercetin** | 53.07 | 87.83 | 90.21 | 82.60 | 86.65 | 53.07 | USD/kg |

**Table 3** presents the composition of the COM for the lowest values of COM found based on the quercetin amount in the final extract (aqueous suspension). Variable cost, i.e. operational costs which are dependent on the production rate and consist in raw material costs, operational labour, utilities, among others, is the highest share in the total COM, account for 71% of the COM.

From the evaluated alternatives, Run 8, that considered a higher quercetin concentration in the emulsion, presented the best economic indicators with the cheapest COM and investment cost equal to the mean investment cost calculated. Run 20 also seemed to be a good alternative presenting COM of encapsulated quercetin 18% cheaper than the mean value and investment cost 1% lower than mean investment cost.

This study considered the use of purified quercetin, nevertheless an interesting alternative to the process would be the use of quercetin extract directly in the encapsulation process. **Table 4** shows the results of evaluating the economic impact of using quercetin extracts in the process, considering no change on process yields. The use of a no purified quercetin extract could reduce the price of quercetin on 76% or 72%, when considering an extract with 5% or

50% quercetin content, respectively. Even though, the reduction in the cost is high, the impact on the final COM is less than 1%. The share for the quercetin cost in the total raw material cost is also of 1%, while the highest share is found for the fresh $CO_2$ consumption, varying from 43 to 88% of the total raw material cost.

**Table 4:** Economic impact of using quercetin-rich extracts in the SFEE process

| | | **COM EXTRACT** | **COM ENCAPSULATED QUERCETIN** |
|---|---|---|---|
| **RUN** | | **(USD/kg)** | **(USD/ kg of encapsulated quercetin)** |
| **8** | pure | 1.97 | 53.07 |
| | extract containing 50% of quercetin | 1.96 | 52.58 |
| | extract containing 5% of quercetin | 1.95 | 52.55 |
| **20** | pure | 1.84 | 82.60 |
| | extract containing 50% of quercetin | 1.82 | 81.80 |
| | extract containing 5% of quercetin | 1.82 | 81.75 |
| **21** | pure | 1.90 | 86.65 |
| | extract containing 50% of quercetin | 1.89 | 85.83 |
| | extract containing 5% of quercetin | 1.88 | 85.78 |

The different process configurations were analyzed considering that the total $CO_2$ amount used experimentally at each run for emulsion extraction was used in a period of 60 min. In this configuration there would have 2 reactors working in parallel, while one was working the other one was discharging the product, cleaning and being prepared for the next use. However, the runs analyzed were mainly conducted during 90 min. Therefore, the best 3 configurations

studied regarding the minimum COM and/or investment cost, Runs 8, 10 and 20, were evaluated considering a 90 min process. In this new configuration the mass flow of $CO_2$ used per hour would decrease 25%, but at the same time it would be necessary 3 extractors and 2 sets of $CO_2$ pumps and flash tanks. **Table 5** shows the results for this new configuration. The increase in the mean investment cost for this 3 configurations would be of 30% in comparison with a 60 min process. Concerning the COM, the increase would be of 22 and 21% for the extract and the encapsulated quercetin, respectively. Note that there is no change on the amount of extract produced, as the process is considered in stationary regime.

Run 8 was the best economic solution to quercetin encapsulation through SFEE. It presented the lowest COM for the encapsulated quercetin, investment cost similar to the mean value calculated for the evaluated configurations and even when a 90 min process was considered, the calculated COM for the encapsulated quercetin is lower than the other runs considering a 60 min process. The amount of $CO_2$ used was the main limiting factor for the process, its use in a proportion higher than 5.5 kg/L of emulsion resulted in the less attractive economic scenarios studied. Further investigation should be conducted in order to establish the minimum $CO_2$ use in the process with quercetin concentration in the emulsion of 0.03 % w/w (higher level).

**Table 5:** Economic impact of considering a 90 min SFEE process

| Run | 8 | 10 | 20 | |
|---|---|---|---|---|
| **Total extract** | 1,279.3 | 1,279.7 | 1,280.1 | t extract/ year |
| **Encapsulated quercetin** | 47.4 | 28.6 | 28.5 | t encapsulated quercetin/year |
| **Electricity consumption** | 72.0 | 48.7 | 63.3 | MW |
| **Cooling demand** | 642.7 | 651.5 | 571.7 | MW |
| **total investment** | 743.91 | 702.42 | 731.30 | thousand USD |
| **COM** | 3,236.97 | 2,983.17 | 2,782.60 | thousand USD |
| **COM extract** | 2.53 | 2.33 | 2.17 | USD/kg |
| **COM encapsulated quercetin** | 68.31 | 104.45 | 97.54 | USD/kg |

## 4. CONCLUSIONS

Robustness of scaled-up semi-continuous SFEE process soy-bean lecithin–Pluronic L64® encapsulated quercetin particles production is demonstrated, and according to thermal-economic- and product quality considerations, $CO_2$ contacted with o/w emulsion should be slightly above it's critical point, and no more than 5.5 kg $CO_2$ should be used for the treatment of 1 L emulsion, by around 80-90 min of SFEE process time, and hence decrease cost of production of 1 L of aqueous suspension and possible degradation effects of products. Regarding thermo-economic indicators the increase in the quercetin concentration in the emulsion together with the decrease of $CO_2$ flow demonstrated to be the main two important parameters to decrease the energy demand and cost of manufacturing. The higher the amount of $CO_2$ used the higher is the electricity and cooling requirements and also the investment cost for the process, thus further experimental studies should be done towards this optimization.

## Appendix A

In this appendix Aspen Plus® simulation details are described. The thermodynamic model used to represent the process was RK-ASPEN model when supercritical fluid extraction was considered and UNIQUAC model for low pressure processes. The RK-ASPEN model can be applied to the SFEE process as it is particularly suitable for modeling a mixture of light gases (such as $CO_2$) at medium to high pressures, with polar components. The RK-ASPEN property method distinguishes between the subcritical and supercritical components and applies either the Mathias alpha function or the Boston–Mathias extrapolation of the alpha function. The RK-ASPEN model is indicated by ASPEN PLUS user guide to this application due to the before mention characteristic, as well as the formulation of the mixing rules. This model was validated by [26]. For the simulation $CO_2$ was considered a Henry component. The thermodynamic model used to represent the low pressure processes was UNIQUAC model. Although the methods mentioned were the best available, it is recognized that for complex streams as present in our process the model will never be 100% accurate.

The flowcharts of the Aspen Plus® process simulation is presented in **FigA1**-**FigA3**.

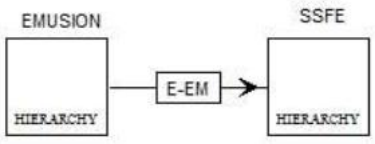


**FigA1 :** Overall SFEE process flowchart developed in Aspen Plus®

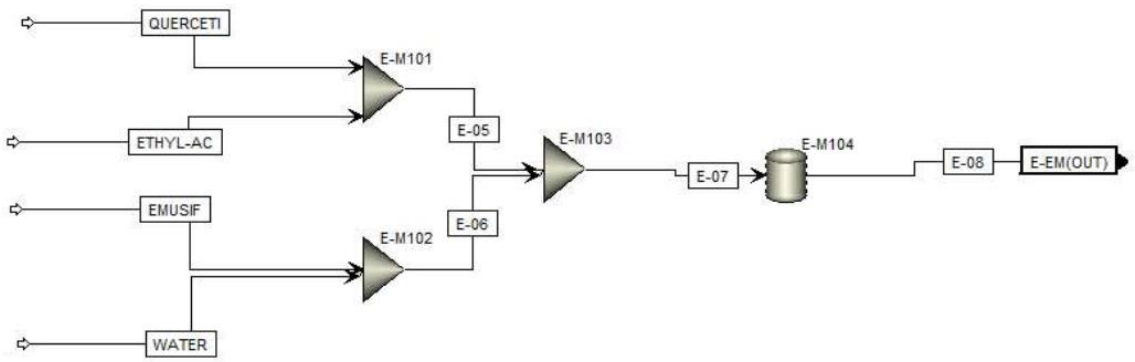


**FigA2 :** Emulsion preparation flowchart developed in Aspen Plus®.

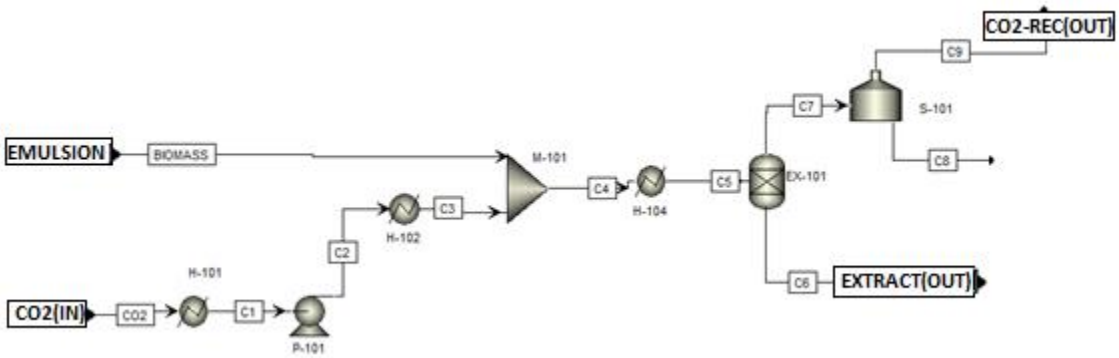


**FigA3 :** Flowchart of the supercritical fluid extraction of emulsions (SFEE) process developed in Aspen Plus®.

**Table A1** summarizes all the simulated equipment and the specification set in the Aspen Plus® simulator. Note that Aspen Plus® does not have a specific model for representing supercritical extraction with stationary bed, but this does not limit the use of the software to evaluate mass and energy balance of this unit operation. The extraction process was simulated in ASPEN Plus using the ASPEN models mixer, heat exchanger and separator. In the first model $CO_2$ and the emulsion was mixed at the desired pressure, than it was heated to extraction temperature and in the separator model the experimental SFEE results were inferred by a design specification calculation tool (flowsheeting options, Design Specs). Thermodynamic equilibrium was

calculated in the flash tank in which $CO_2$ is separated. In this way, simulation could represent the process successfully.

**Table A1 :** Equipment specification simulated in Aspen Plus®.

| Equipment | Description | ASPEN model | Parameters |
|---|---|---|---|
| *SFEE* | | | |
| H-101 | Solvent $CO_2$ cooling | Exchangers - Heater | 293 K |
| H-1101 | Solvent $CO_2$ cooling | Exchangers - Heater | 263 K |
| P-101 | Solvent $CO_2$ pumping | Pressure Changers – Pump | 20 MPa |
| H-102 | Solvent $CO_2$ heating | Exchangers - Heater | 313 K |
| M-101 | SFEE extractor | Mixers - Mixer | Set according to the experimental data |
| H-104 | | Exchangers - Heater | |
| EX-101 | | Separators - Sep | |
| S-101 | $CO_2$ separation tank | Separators - flash2 | 5 MPa<br>298 K |
| *Emulsification* | | | |
| E-M101 | Quercetin – ethyl acetate mixing tank | Mixers - Mixer | Pressure (set pressure constant) |
| E-M102 | Water-emulsificant mixing tank | Mixers - Mixer | Pressure (set pressure constant) |
| E-M103 | Emulsion mixing tank | Mixers - Mixer | Pressure (set pressure constant) |
| E-M104 | Ultrasonic homogenizer | Mixers - Mixer | Pressure (set pressure constant) |

The thermal demand required for cooling the Ultrasonic homogenizer was calculated considering that 50% of the electricity input in the process was lost in for of heat [27]. The electricity consumption at the ultrasonic homogenizer was calculated considering data from the manufacture, 1.4 kWh/m3 of solution [21]

## Appendix B

OSMOSE simulation details are described in this appendix. OSMOSE platform allows one to link several software such as Belsim Vali and Aspen Plus® for a complete suite of computation and result analysis tools (optimization, sensitivity analysis, Pareto curve analysis, etc.). In the present study energy and material flow modeling was done in Aspen Plus® as described previously and the thermal integration modeling and the economic modeling was performed in the OSMOSE platform. **FigB1** illustrates the involved modeling methodology when OSMOSE was used, where information is exchanged across the models using state and optimized variables based on the decision variables or performance indicators.

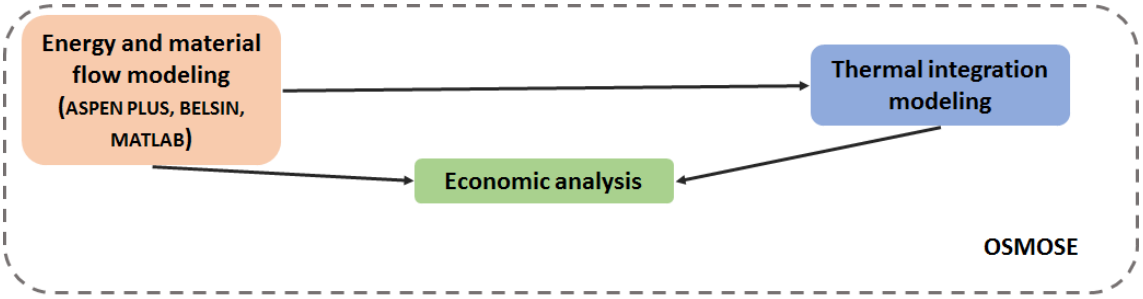


**FigB1 :** Modeling methodology possible in the OSMOSE (OptimiSation Multi-Objectifs de Systemes Energetiques integres) platform.

Based on the pinch analysis methodology [16], the optimal thermal process integration is computed in the OSMOSE platform after the maximum heat recovery potential between hot and cold streams is defined and a minimum approach temperature $\Delta T_{min}$, which represents the energy capital trade-off between the energy savings obtained by heat exchange and the required heat exchangers investment, is considered. The optimal utility integration is obtained when the combined production of fuel, power and heat are maximized, which minimizes the operating cost by solving a linear programming problem (i.e. mathematical method used in computer modeling to find the best possible solution representing the problem using linear relationships). In the thermal integration, the primary energy requirement must be satisfied in terms of hot and

cold utilities. The minimum energy requirement is computed from the hot and cold process streams using the heat cascade method, which accounts for the potential heat recovery. The potential fuels are assembled in a superstructure, which integrates different possibilities and computes the optimal solution by minimizing the operating cost using a linear programming model.

The thermal integration is declared in OSMOSE as follow. First the variables are extracted from Aspen Plus® simulation (as in the tag assignment example), then the thermal integration is performed (thermal integration modeling).

Tag assignment example in MATLAB

```
% SSFE extraction
% H-102
nt=nt+1;
technology.Tags(nt).TagName = {'t_c2_in'};
technology.Tags(nt).Unit = {'C'};
technology.Tags(nt).Aspen.Line_1 = {'Stream-Var Stream=SSFE.C2
Substream=MIXED'};
technology.Tags(nt).Aspen.Line_2 = {'Variable=TEMP'};
technology.Tags(nt).Status = {'off'};
```

Thermal integration modeling

```
% description of the flow
% type, unit, tag_name , T_in [K], h_in [kW], T_out [K], h_out[kW], deltaTmin
ns = 0;

% Cold streams () ----------------------------------------------------------  tout en kW
```

```
ns = ns+1;
 technology.EI.Streams(ns).Short                                                    =
{'qt','sfee','h102','@t_c2_in+273','0','@t_c2_out+273','@heat_h102*1163',5};



      % % Hot streams  () ------------------------------------------------------------


ns = ns+1;
 technology.EI.Streams(ns).Short
{'qt','sfee','h101','@t_co2+273.15','-1*@heat_h101*1163','@t_c1+273.15','0',5};


ns = ns+1;
 technology.EI.Streams(ns).Short
{'qt','sfee','h105','@t_c10+273.15','-1*@heat_h105*1163','@t_c11+273.15','0',5};


% emulsification - cooling of the ultrasonic emulsifier
ns = ns+1;
 technology.EI.Streams(ns).Short
 {'qt','sfee','eh101','25.5+273.15','-1*@heat_eh101*1163','24+273.15','0',5};
```

Using the data from the Aspen Plus® and thermal process integration models, the costs are estimated in OSMOSE based on the equipment sizing and cost correlations from the literature [19], [20]. **Table B1** gives the cost function and the necessary parameter for its calculation for the evaluated equipment.

**Table B1 :** Cost function for the evaluated equipment defined in the economic analysis simulated.

| Equipment | Cost function | Reference |
|---|---|---|
| *SFEE* | | |
| SFEE extractor | Jacketed reactor | [20] |
| $CO_2$ separation tank | Flash drum 2min | [19], [20] |
| Quercetin – ethyl acetate mixing tank | Vertical Vessels | [20] |
| Water-emulsificant mixing tank | Vertical Vessels | [20] |
| Emulsion mixing tank | Vertical Vessels | [20] |
| Ultrasonic homogenizer | Hielsher UIP1000hdT[a] | [21] |

[a] cost obtained from Hielsher 17,350.00 USD/equipment

The ultrasonic homogenizer equipment cost was obtained from the manufacturer [4]. It was considered 2 Hielsher UIP1000hdT working in parallel to achieve the necessary working flow as the capacity of each homogenizer is $5 m^3$/day.

The electricity consumption modeling developed is presented in the following.

```
%% Electricity consumption (kW)
%-----------------------------------------------------------------
% SFEE process
    power_sfee = power_pco2;

% Emulsion process
% Stirring in the extraction reactor 0.3 kWh/m3
    power_m101 = volum_em101 * 0.3;
    power_m102 = volum_em102 * 0.3;
```

```
    power_m103 = volum_em103 * 0.3;
% Ultrasonic emusification equipment 1.4 kWh/m3
% (info:www.hielscher.com/energy_efficiency_01.htm) accessed 08/08/2016
    power_emusfr = volum_em103 * 1.4;


    power_emusion = power_m101 + power_m102 + power_m103 + power_emusfr;


%----------------------------------------
%%% total electricity consumption
elec_consum = (power_sfee + power_emusion)*1.3; %kWh;power_pretreatment
```

## REFERENCES

[1] Y. Gao, Y. Wang, Y. Ma, A. Yu, F. Cai, W. Shao, G. Zhai, Formulation optimization and in situ absorption in rat intestinal tract of quercetin-loaded microemulsion, Colloids Surfaces B Biointerfaces. 71 (2009) 306–314. doi:10.1016/j.colsurfb.2009.03.005.

[2] S. Das, A.K. Mandal, A. Ghosh, S. Panda, N. Das, S. Sarkar, Nanoparticulated quercetin in combating age related cerebral oxidative injury, Curr Aging Sci. 1 (2008) 169–174. http://www.ncbi.nlm.nih.gov/entrez/query.fcgi?cmd=Retrieve&db=PubMed&dopt=Citation&list_uids=20021389.

[3] M.F. Ramadan, Antioxidant characteristics of phenolipids (quercetin-enriched lecithin) in lipid matrices, Ind. Crops Prod. 36 (2012) 363–369. doi:10.1016/j.indcrop.2011.10.008.

[4] A. Parmar, K. Singh, A. Bahadur, G. Marangoni, P. Bahadur, Interaction and solubilization of some phenolic antioxidants in Pluronic?? micelles, Colloids Surfaces B Biointerfaces. 86 (2011) 319–326. doi:10.1016/j.colsurfb.2011.04.015.

[5] S. Egert, A. Bosy-Westphal, J. Seiberl, C. Kürbitz, U. Settler, S. Plachta-Danielzik, A.E. Wagner, J. Frank, J. Schrezenmeir, G. Rimbach, S. Wolffram, M.J. Müller, Quercetin reduces systolic blood pressure and plasma oxidised low-density lipoprotein concentrations in overweight subjects with a high-cardiovascular disease risk phenotype: a double-blinded, placebo-controlled cross-over study., Br. J. Nutr. 102 (2009) 1065–1074. doi:10.1017/S0007114509359127.

[6] Khaled A. Khaled, Yousry M. El-Sayeda, Badr M. Al-Hadiyab, Disposition of the Flavonoid Quercetin in Rats After Single Intravenous and Oral Doses, Drug Dev. Ind. Pharm. 29 (2003) 397–403. doi:10.1081/DDC-120018375.

[7] R. Gugler, M. Leschik, H.J. Dengler, Disposition of quercetin in man after single oral and intravenous doses, Eur. J. Clin. Pharmacol. 9 (1975) 229–234. doi:10.1007/BF00614022.

[8] S. Chakraborty, S. Stalin, N. Das, S. Thakur Choudhury, S. Ghosh, S. Swarnakar, The use of nano-quercetin to arrest mitochondrial damage and MMP-9 upregulation during prevention of gastric inflammation induced by ethanol in rat, Biomaterials. 33 (2012) 2991–3001. doi:10.1016/j.biomaterials.2011.12.037.

[9] M. Fraile, R. Buratto, B. Gómez, Á. Martín, M.J. Cocero, Enhanced delivery of quercetin by encapsulation in poloxamers by supercritical antisolvent process, Ind. Eng. Chem. Res. 53 (2014) 4318–4327. doi:10.1021/ie5001136.

[10] F. Mattea, ??ngel Mart??n, A. Mat??as-Gago, M.J. Cocero, Supercritical antisolvent precipitation from an emulsion: ??-Carotene nanoparticle formation, J. Supercrit. Fluids. 51 (2009) 238–247. doi:10.1016/j.supflu.2009.08.013.

[11] G. Lévai, Á. Martín, E. De Paz, S. Rodríguez-Rojo, M.J. Cocero, Production of stabilized quercetin aqueous suspensions by supercritical fluid extraction of emulsions, J. Supercrit. Fluids. 100 (2015) 34–45. doi:10.1016/j.supflu.2015.02.019.

[12] Purdief, Guidance for Industry Q3C — Tables and List Guidance for Industry Q3C — Tables and List Guidance for Industry Q3C — Tables and List, 9765 (2012) 301–827. http://www.fda.gov/Drugs/GuidanceComplianceRegulatoryInformation/Guidances/default.htm\nhttp://www.fda.gov/BiologicsBloodVaccines/GuidanceComplianceRegulatoryInformation/Guidances/default.htm.

[13] S. Varona, Á. Martín, M.J. Cocero, Formulation of a natural biocide based on lavandin essential oil by emulsification using modified starches, Chem. Eng. Process. Process Intensif. 48 (2009) 1121–1128. doi:10.1016/j.cep.2009.03.002.

[14] N.S. Acharya, G. V. Parihar, S.R. Acharay, PHYTOSOMES: NOVEL APPROACH FOR DELIVERING HERBAL EXTRACT WITH IMPROVED BIOAVAILABILITY, Pharma Sci. Monit. An Int. J. Pharm. Sci. 2 (2011) 144–160.

[15] F. Ganske, B. Labtech, G.E.J. Offenburg, ORAC Assay on the FLUOstar OPTIMA to Determine Antioxidant Capacity, Bmglabtech.Com. (2006). http://www.bmglabtech.com/application-notes/fluorescence-intensity/orac-148.cfm.

[16] B. Linnhoff, D.W. Towsend, D. Boland, G.F. Hewitt, B.E.A. Thomas, A.R. Guy, R.H. Marsland, A user guide on process integration for the efficient use of energyitle, The Institution of Chemical Engineers: Rugby, United Kingdom, 1982.

[17] C.G. Pereira, M.A.A. Meireles, Supercritical fluid extraction of bioactive compounds: Fundamentals, applications and economic perspectives, Food Bioprocess Technol. 3 (2010) 340–372. doi:10.1007/s11947-009-0263-2.

[18] M.M.R. De Melo, H.M.A. Barbosa, C.P. Passos, C.M. Silva, Supercritical fluid extraction of spent coffee grounds: Measurement of extraction curves, oil characterization and economic analysis, J. Supercrit. Fluids. 86 (2014) 150–159. doi:10.1016/j.supflu.2013.12.016.

[19] R.B. Turton, B. Wallace, J.S. Whiting, D. Bhattacharyya, Analysis, synthesis and design of chemical processes, 3rd ed., Prentice Hall: Upper Saddle River, United States of America, 2009.

[20] G. Ulrich, P. Vasudevan, A guide to chemical engineering process design and economics a practical guide, 2nd ed., Boca Raton, United States of America, 2003.

[21] Hielsher UIP1000hdT, 08/08/2016. (2016). https://www.hielscher.com/i1000_p.htm.

[22] J. Pitches, Ethylene Europe prices, markets & analysis, 2016.07.25. (2016). http://www.icis.com/chemicals/ethylene/europe.

[23] D.T. Santos, J.Q. Albarelli, M.A. Rostagno, A. V Ensinas, F. Maréchal, M.A.A. Meireles, New proposal for production of bioactive compounds by supercritical technology integrated to a sugarcane biorefinery, Clean Technol. Environ. Policy. 16 (2014) 1455–1468. doi:10.1007/s10098-014-0760-5.

[24] J.Q. Albarelli, A. V Ensinas, M.A. Silva, Product diversification to enhance economic viability of second generation ethanol production in Brazil: The case of the sugar and ethanol joint production, Chem. Eng. Res. Des. 92 (2016) 1470–1481. doi:10.1016/j.cherd.2013.11.016.

[25] J. Albarelli, D. Santos, M. Cocero, M. Meireles, Economic Analysis of an Integrated Annatto Seeds-Sugarcane Biorefinery Using Supercritical CO2 Extraction as a First Step, Materials (Basel). 9 (2016) 494. doi:10.3390/ma9060494.

[26] C.S. Lim, Z.A. Manan, M.R. Sarmidi, Simulation modeling of the phase behavior of palm oil-supercritical carbon dioxide, J. Am. Oil Chem. Soc. 80 (2003) 1147–1156. doi:10.1007/s11746-003-0834-6.

[27] V. Karcher, F.A. Perrechil, A.C. Bannwart, Interfacial Energy During the Emulsification of Water-in-Heavy Crude Oil Emulsions, Brazilian J. Chem. Eng. 32 (2015) 127–137. doi:10.1590/0104-6632.20150321s00002696.

# CONCLUSIONS

## BIOPRODUCTS PROCESSING BY SFEE:

## APPLICATION FOR LIQUID AND SOLID

## QUERCETIN FORMULATIONS

Although quercetin is a highly promising active compound in biomedical applications [1], clinical application of it is limited due to its low bioavailability (lower than 1% in humans [2]), and its low water solubility, which makes it necessary to administrate it in high doses (50 mg/kg [3]). The main aim of this thesis is to increase the bioavailability and stability of quercetin, by encapsulating it in biopolymers, using the Supercritical Fluid Extraction of Emulsion (SFEE) technology, and precipitating the biopolymer-quercetin compound, using the Particles from Gas Saturated Solutions (PGSS)-drying technology.

**ENCAPSULATION OF QUERCETIN BY BATCH SFEE PROCESS**

First, SFEE as a batch process was applied to produce quercetin nanoparticles encapsulated by Pluronic L64® polaxomers, but needle like quercetin crystals in aqueous suspension were obtained, indicating that Pluronic L64® is not a suitable material for the encapsulation of quercetin in aqueous system. In further experiments soy-bean lecithin as surfactant material was used, and with a total SFEE treatment duration of 575 min (divided in five cycles), quercetin loaded lecithin multivesicules with multimodal particle size distributions were obtained. Robustness of the results of batch SFEE process was proved, as a successful encapsulation was achieved in a range of conditions of the oil in water (o/w) emulsion, such as the concentration of lecithin and quercetin, and the organic to water ratio. 58.8% as an average encapsulation efficiency of quercetin (corresponding to 0.16 g quercetin / L of suspension) was achieved, in a suspension that was stable up to 14 days. Residual organic content in all final suspensions was below the restriction of the FDA [4], without the presence of quercetin crystals. According to antioxidant activity measurement, SFEE produced aqueous suspensions presenting an increased antioxidant activity than pure quercetin, most probably due to the formation of hydrogen bonds between quercetin and phosphatidylcholine, resulting an antioxidant synergism effect [5]. However, these bonds could be partially broken by the $scCO_2$

treatment process, resulting lower antioxidant activity in SFEE produced samples, than in a physical mixture.

As applied concentration of soy-bean lecithin in batch SFEE experiments was above its critical micelle concentration (CMC), further increase of lecithin content has no effect on the characteristics of aqueous suspension, as no more reduction of interfacial tension between the organic and the aqueous phase of the o/w emulsion was obtained. However, by applying the mixture of soy-bean lecithin and Pluronic L64® (above its CMC) as surfactants, a higher encapsulation efficiency of quercetin (83.7%, corresponding to 0.19 g quercetin / L of suspension) is reached.

**MASS TRANSFER STUDY OF SFEE**

To assist in the optimization and scale-up of the process, mass transfer of compounds during the SFEE process was studied. EtAc and DCM based o/w emulsions were prepared and contacted with $scCO_2$, and mass transfer processes were measured in static and dynamic (in where $scCO_2$ flow was continuously maintained through the emulsion) systems, using Magnetic Suspension Balances (MSB), which provide an on-line, contactless weight monitoring method of sample, placed in a closed system. In case of DCM/w emulsions stabilized with lecithin or Pluronic L64®, phase separation occurred immediately upon pressurizing them with $scCO_2$, indicating that these emulsions are not appropriate for SFEE process, as it is not working in DCM/w emulsions, as emulsion stability is a crucial issue of SFEE, as each emulsion droplet behaves as a miniature gas antisolvent (GAS) precipitator [6]. In case of EtAc/w emulsions the dissolution of $scCO_2$ by the sample, and the extraction of organic phase was observed simultaneously, but each mechanism was dominating the mass change of o/w emulsions in different part of the whole process. A five parameter model was fitted on experimental results.

Analysis of the model parameters revealed, that only three process steps has significant influence on the mass transport properties: the dissolution of $scCO_2$- and organic solvent in the water phase, and the extraction of organic phase by $scCO_2$. Mass transport velocity is only influenced by the density of sample surrounded $scCO_2$, and was independent of the initial conditions of the o/w emulsions, such as the ratio- and the total concentration of surfactants, and the organic to water ratio, confirming the robustness of results, observed in batch SFEE experiments.

According to dynamic measurements, a high proportion of the organic phase is already extracted during the pressurization process of emulsions with $scCO_2$, and with a significantly shorter processing time, a similar residual organic content result is obtained, than in case of static measurements, with an around 20 hours of measurement time. F. Mattea et al. also found a rapid initial organic extraction, most probably due to water phase became rapidly saturated by $scCO_2$, due to the stirring effect, caused by the pressurization and the phase change of $CO_2$, [6]. Another possible reason is the natural convection of streams and interfacial turbulence due to the so-called Marangoni effect, which can occur in $CO_2$ - $H_2O$ systems, as $CO_2$ saturated water has higher density than pure water [7], [8].

**SCALED-UP SFEE**

According to mass transfer measurement and modelling results, a successful scaling-up of SFEE process was done. For this, a semi-continuous equipment was designed, maintaining a continuous $scCO_2$ flow through the emulsion during the whole treatment process, keeping into account the importance of available contact surface of $scCO_2$ and o/w emulsion, and the speed of the organic extraction process. Robustness of scaled-up SFEE process on the initial conditions of the o/w emulsions, such as the ratio- and the total concentration of surfactants, the concentration of quercetin and the organic to water ratio was proved, and with a significantly shorter processing time, a significantly higher amount of aqueous suspension was produced, with a similar quercetin encapsulation efficiency and stability, antioxidant activity, residual organic content and particle size distribution results, than in case of batch SFEE process. Moreover, according to economic evaluation, in order to obtain quercetin loaded aqueous suspensions in nanometric scale with high quercetin encapsulation efficiency and low residual organic content results, process temperature and pressure should be chosen to obtain $scCO_2$ slightly above its critical point, and no more than 5 kg $CO_2$ should be used for the treatment of 1 L emulsion, with a total SFEE processing time of 80-90 min. Moreover, keeping these moderate temperature and pressure conditions and applying a $CO_2$ / emulsion ratio as low as possible on lowest possible temperature and treatment duration, not only the investment price and thermo-economic operational expanses of the SFEE process can be maintained on its minimum, but also the probability of possible quercetin degradation and aggregation of encapsulated sub-micrometric particles can be decreased.

## EXPERIMENTAL RUNS PERFORMED BY PGSS-DRYING TECHNOLOGY

In this thesis PGSS-drying technology was used, in order to extract water content of the SFEE produced aqueous suspensions, and to obtained quercetin loaded dry-product with a controlled, micrometric particle size distribution. Product characteristics significantly influencing process parameters, such as the Gas/Liquid Ratio (GLR) and the density of with aqueous suspension contacted $scCO_2$ (changing the pre-expansion pressure and temperature) was observed, and the optimal value of these process parameters was obtained, keeping the residual moisture content of product under 10 w/w%, with the lowest quercetin loss as possible. GLR was obtained the most important process parameter, as applying lower or higher value than the adequate, higher residual moisture content is obtainable, due to the insufficient-, or the too high amount of $scCO_2$, contacted by the aqueous suspension in the extraction column: The former cause an insufficient water evaporation, meanwhile the latter cause a too high amount of water evaporation, leading to a partial plugging of the glass-balls filled extractor column by the highly viscous lecithin. Upon applying adequate process settings of PGSS-drying, no segregated quercetin crystals are formed, conforming the encapsulation and morphological change of quercetin to amorphous state. Quercetin permeability of PGSS-drying micronized quercetin through transdermal membrane – comparing to lyophilized product and unprocessed physical mixture –, is proved.

## FUTURE WORK

As moderate aqueous solubility and antioxidant activity increase of by SFEE- and by PGSS-drying produced quercetin loaded particles are obtained and proved using HPLC, ORAC and in-vitro tests, the so-produced particles need to be analysed by in-vivo measurements, in order to prove bioavailability increase clearly. Further experiments for the concentration of quercetin are required, by trying higher initial quercetin concentration, trying other organic phase as initial solubility agent, or by applying different kinds of encapsulation materials. New design need to be extablished, in order to decrease $CO_2$ consumption, wich is a key factor in cost of operation.

**REFERENCES**

[1] Y. Gao, Y. Wang, Y. Ma, A. Yu, F. Cai, W. Shao, G. Zhai, Formulation optimization and in situ absorption in rat intestinal tract of quercetin-loaded microemulsion, Colloids Surfaces B Biointerfaces. 71 (2009) 306–314. doi:10.1016/j.colsurfb.2009.03.005.

[2] Khaled A. Khaled, Yousry M. El-Sayeda, Badr M. Al-Hadiyab, Disposition of the Flavonoid Quercetin in Rats After Single Intravenous and Oral Doses, Drug Dev. Ind. Pharm. 29 (2003) 397–403. doi:10.1081/DDC-120018375.

[3] S. Chakraborty, S. Stalin, N. Das, S. Thakur Choudhury, S. Ghosh, S. Swarnakar, The use of nano-quercetin to arrest mitochondrial damage and MMP-9 upregulation during prevention of gastric inflammation induced by ethanol in rat, Biomaterials. 33 (2012) 2991–3001. doi:10.1016/j.biomaterials.2011.12.037.

[4] U.S.D. of H. and H. Services, F. and D. Administration, C. for D.E. and R. (CDER), C. for B.E. and R. (CBER), Guidance for Industry Q3C — Tables and List Revision 2, Febr. 2012. (2012). http://www.google.es/url?sa=t&rct=j&q=&esrc=s&source=web&cd=1&ved=0ahUKEwiU_eLSrrTMAhWFgYMKHTx0DWwQFggpMAA&url=http://www.fda.gov/downloads/drugs/guidancecomplianceregulatoryinformation/guidances/ucm073395.pdf&usg=AFQjCNFMtH0rXC962u9xqiKZO.

[5] M.F. Ramadan, Antioxidant characteristics of phenolipids (quercetin-enriched lecithin) in lipid matrices, Ind. Crops Prod. 36 (2012) 363–369. doi:10.1016/j.indcrop.2011.10.008.

[6] F. Mattea, Á. Martín, C. Schulz, P. Jaeger, R. Eggers, M.J. Cocero, Behavior of an Organic Solvent Drop During the Supercritical Extraction of Emulsions, AIChE J. 56 (2010) 1184–1195. doi:0.1002/aic.12061.

[7] C. Yang, Y. Gu, Accelerated mass transfer of CO2 in reservoir brine due to density-driven natural convection at high pressures and elevated temperatures, Ind. Eng. Chem. Res. 45 (2006) 2430–2436. doi:10.1021/ie050497r.

[8] B. Arendt, D. Dittmar, R. Eggers, Interaction of interfacial convection and mass transfer effects in the system CO2-water, Int. J. Heat Mass Transf. 47 (2004) 3649–3657. doi:10.1016/j.ijheatmasstransfer.2004.04.011.

# RESUMEN

## DESARROLLO DE BIOPRODUCTOS MEDIANTE EXTRACCION SUPERCRITICA DE EMULSIONES: APLICACIÓN A LA OBTENCION DE FORMULACIONES SOLIDAS Y LIQUIDAS DE QUERCITINA

## 1. INTRODUCCIÓN

Los polifenoles son muy utilizados por la industria farmacéutica y cosmética debido a sus efectos beneficiosos asociados a sus propiedades antioxidantes, antivirales y antiestaminicas. La quercitina (**Figura 1**) es un flavonoide, que constituyen el mayor grupo de los polifenoles. Se encuentra en algunas frutas, en los vegetales y en algunos aceites. Es un compuesto antioxidante bastante estable debido a su estructura química de o-diphenol B-anillo [8], que permite ser donor de electrones de niveles π de su anillo bencénico, sin perder su estabilidad [1], aportando también un efecto "antimultiplicador" en bastantes células cancerígenas humanas [10]. Ademas es abundante en muchos subproductos de industria agroalimentaria, como residuos de la producción de vino, frutas, aceites vegetales entre otros. En esta tesis se va a estudiar la obtención de productos activos de quercitina utilizando tecnologias con fluidos supercriticos. La utilización de quercitina en aplicaciones clinicas esta limitada por su baja biodisponibilidad (17% en ratas [2] y aún menor del 1% in humanos [3]), lo que hace necesario suministrar dosis de hasta 50 mg/kg [4].

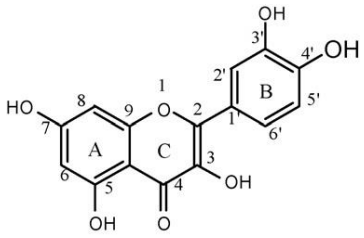


**Figura 1:** Estructura química de la quercitina. [5]

Se han estudiado diferentes vías de mejorar la biodisponibilidad de la quercitina, Mulholland y col. [6] han sintetizado un derivado soluble en agua, pero solo han conseguido aumentar su biodisponibilidad un 20%. Otras alternativas son la utilización de partículas lipídicas cargadas con la quercitina o la formación de complejos de quercetina con lecitina y ciclodestrinas en disolución acuosa [7] [8]. Li y col. [9] han obtenido quercitina encapsulada en lecitina, mediante emulsificación y solidificación a baja temperatura, obteniendo partículas esféricas con un diámetro de 155 nm y con una eficacia de encapsulamiento del 90%. También se han estudiado la obtención de otras morfologías, estructuras coloidales como micelas, liposomas, formulados obtenidos mediante moldeados por enfriamiento y nanopartículas.

La utilización de tecnologías basadas en el uso de fluidos supercríticos es una vía innovadora para obtención de productos bioactivos, como formulados de quercitina. Las tecnologías basadas en la utilización de dióxido de carbono en condiciones supercríticas ($scCO_2$), permiten obtener formulados de compuestos bioactivos a temperaturas próximas a la ambiente en atmosfera inerte, evitando la degradación térmica del producto y su oxidación; y la posible contaminación debida al uso de disolventes orgánicos. Varios autores han estudiado la obtención de bioproductos mediante el uso de tecnologías con fluidos supercríticos. La extremadamente baja solubilidad de la quercitina en $scCO_2$ [10], hace que la tecnología de utilizar el dióxido de carbono en condiciones supercríticas como antidisolvente (SAS) haya obtenido buenos resultados. Mediante tecnología de SAS, quercitina pura se ha obtenido quercitina cristalina de tamaño entre 1 – 6 µm [11], [12], [13]. Fraile y col. [14] han obtenido quercetina encapsulada en Pluronic F127 mediante tecnología de SAS obteniendo partículas esféricas con tamaño de micras. Este formulado ha permitido aumentar la solubilidad de la quercitina en un simulado fluido intestinal, en 8 veces.

## 2. OBJETIVOS

El objetivo de este trabajo es obtener formulados de quercitina, en fase liquida y sólida, para aumentar su solubilidad en agua y su biodisponibilidad. Se pretende obtener quercitina con tamaño de partículas submicrometricas, y el empleo de surfactante que actúen como agentes encapsulantes para obtener los formulados. La tecnología seleccionada es la extracción supercrítica de emulsiones (SFEE), para obtener formulados de quercitina en suspensiones acuosas, y PGSS-drying (secado de disoluciones saturadas de gas) para obtener formulados sólidos de partículas de quercitina con tamaño micrométrico.

Este objetivo global se desarrolla a través de los siguientes objetivos

1 Obtener suspensiones acuosas de quercitina a partir de emulsiones orgánico/agua utilizando lecitina de soja y polaxameros, o sus mezclas como surfactantes. Estudiar el efecto de las variables de operación de la SFEE, presión, temperatura, concentraciones de surfactante y quercitina, y orgánico y agua en la emulsión inicial. Determinar cómo afectan a la atomización, difusión, precipitación de partículas y aglomeración de la suspensión producida.

2 Estudiar experimentalmente y modelar la transferencia de materia entre las emulsiones EtAc y DCM en agua (o/w) y el $scCO_2$ mediante una balanza de suspensión magnética, (MSB) tanto en un sistema estático como en un sistema dinámico. Las variables a estudiar son, presión y temperatura, y características de la emulsión inicial. La transferencia de materia en un sistema dinámico se estudiará mediante un aporte continuo de scCO2 a la emulsión, para estudiar cómo afectará la mejora del contacto CO2/emulsión al proceso.

3 A partir del modelado de la transferencia de materia, se propone determinar las etapas controlantes del proceso, y realizar el escalado del mismo. El proceso en semicontinuo se realizará haciendo circular un flujo continuo de $CO_2$ sobre la emulsión, para extraer el disolvente orgánico. Se pretende reducir el tiempo de operación actuando sobre las etapas controlantes del proceso.

4 Obtener formulados solidos de quercitina encapsulada en los surfactantes seleccionados, lecitina y polaxerameros, mediante el secado de las suspensiones obtenidas utilizando la tecnología de secado a partir de disoluciones saturadas de gas (PGSS-drying). Estudiar el efecto de las variables de operación del proceso PGSS-drying, como son la relación entre los flujos de suspensión y $CO_2$, presión y temperatura de pre-expansión, sobre las características del producto.

5 Utilizar un proceso convencional de liofilización para obtener formulados sólidos, y compara con los productos obtenidos mediante la tecnología supercrítica.

## 3. RESULTADOS Y DISCUSION

### CAPÍTULO I

La tecnología de SFEE se utiliza para obtener suspensiones acuosas de compuestos no solubles en agua. El proceso consiste en formar una emulsión aceite/agua (o/w), conteniendo la quercetina en la fase orgánica. El disolvente orgánico se extrae de esta emulsión utilizando $scCO_2$, que es un buen disolvente del orgánico pero no del compuesto activo. El orgánico se transfiere desde la gota de la emulsión a la fase acuosa y el $CO_2$ se transfiere a la gota disolviéndose en la fase orgánica. La rápida disolución del $CO_2$, hace que la concentración de $CO_2$ en la gota aumenta rápidamente y el compuesto activo precipita por el efecto antisolvente del $CO_2$. La precipitación del compuesto activo en el interior de la gota hace que el tamaño de las partículas del compuesto activo sea nanométrico. El fundamento de la SFEE se representa en la **Figura 2**.

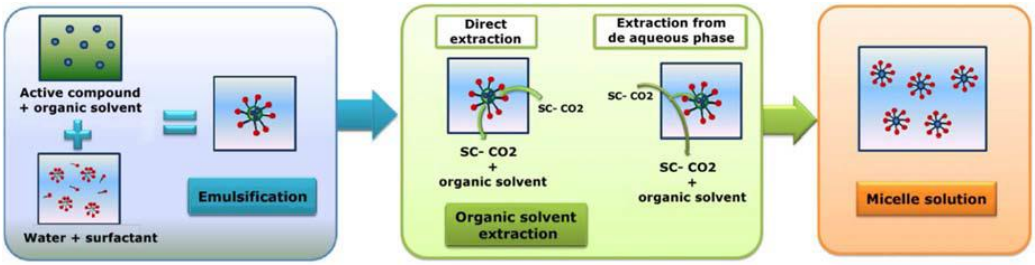


**Figura 2:** Fundamento de la tecnología de SFEE.

La quercitina se encapsula en un surfactante que ayuda a formar y estabilizar la emulsión, y hace de agente encapsulante cuando ha precipitado la quercitina en la gota, de esta forma se obtiene el formulado formando una suspensión acuosa [15]. Como surfactantes se han utilizado los biopolímeros Pluronic L64® y lecitina de soja.

La emulsión es sometida al proceso de extracción utilizando un equipo de SFEE que opera en batch y se presenta en la **Figura 3**. El extractor contiene la emulsión y el $CO_2$, y el deposito-buffer contiene el $CO_2$. Experimentalmente se determina el número de ciclos

que hay que dar así como la duración de los mismos, para reducir la concentración de orgánico en la suspensión acuosa hasta valores por debajo de la normativa de la FDA [17], sin que se produzca la degradación ni la aglomeración de la quercitina encapsulada.

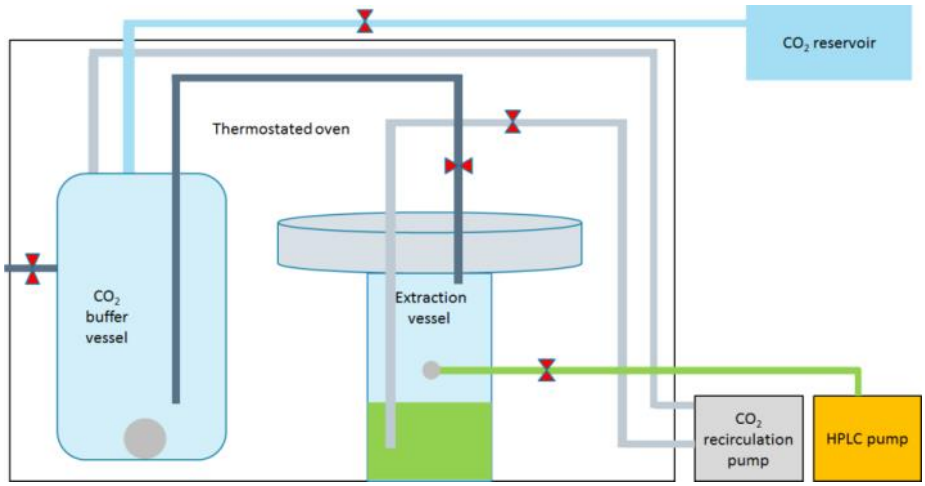


**Figura 3:** Diagrama del equipo batch de SFEE.

La formulación en Pluronic L64® permite obtener partículas con forma de agujas de un tamaño de 1 µm y baja eficacia de encapsulación. La formulación con lecitina de soja permite obtener liposomas multivesiculares (**Figura 4** A), con partículas de tamaño medio de 100 nm ((**Figura 4** B) con una eficacia de encapsulación del 70%, sin que se produzcan cristales de quercitina fuera del formulado. Además, con la formulación se aumenta la actividad antioxidante del compuesto.

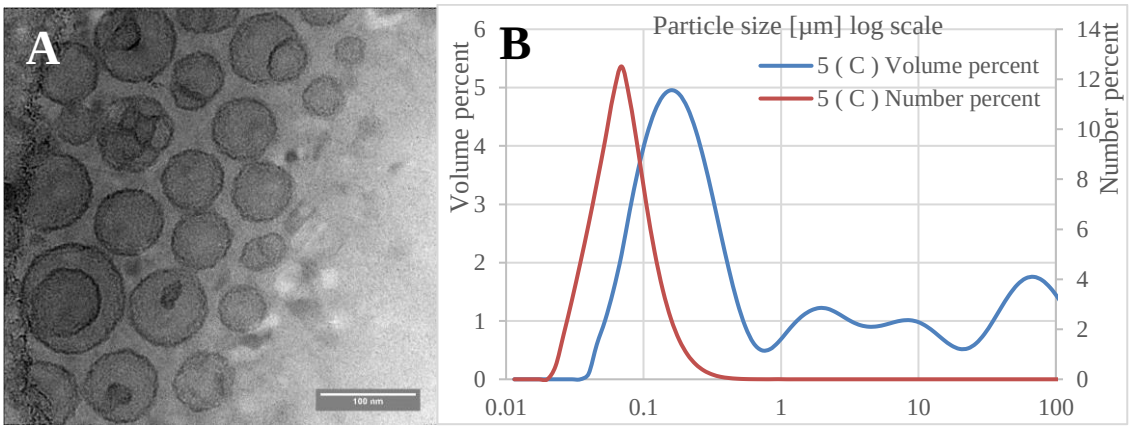


**Figura 4:** A: Cryo-TEM fotos sobre liposomas multivesiculares obtenidos con lecitina de soja; B: general distribución de partículas obtenido con SFEE

**CAPÍTULO II**

En este capítulo se ha utilizado una balanza de suspensión magnética (MSB, **Figura 5**) para estudiar la transferencia de materia en los sistemas acetato de etilo y DCM emulsiones orgánico/agua – $scCO_2$. La MSB se permite el seguimiento en continuo del efecto del $CO_2$ sobre la emulsión mediante la variación del peso que experimenta.

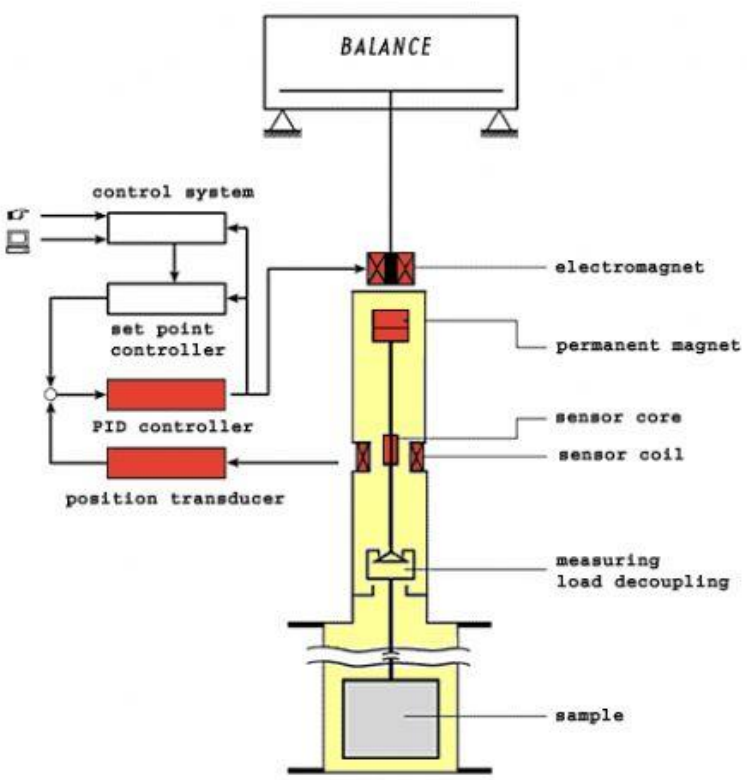


**Figura 5:** Diagrama del equipo balanza de suspensión magnética

Se han realizado medidas en estático y en dinámico aplicando un flujo en continuo del $CO_2$. Se ha estudiado el efecto de la concentración orgánico/agua, concentración de surfactante (lecitina de soja y Pluronic L64®) y la densidad del $CO_2$, sobre la transferencia de materia en la emulsión. En la operación en estático se ha seguido la disolución del $CO_2$ en la emulsión, y la extracción del orgánico. (**Figura 6**).

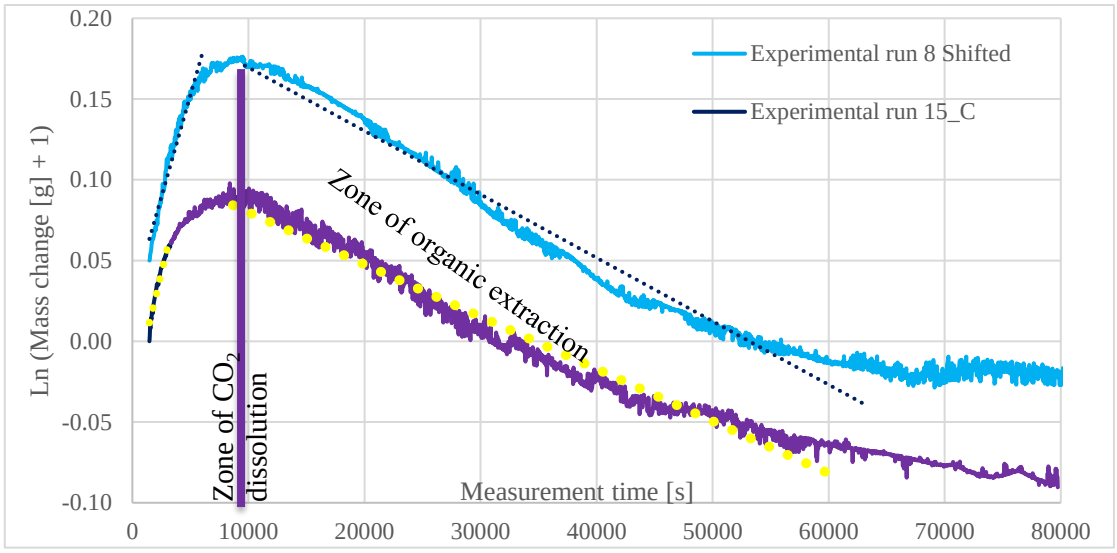


**Figura 6:** Evolución de la masa de la emulsión a lo largo del proceso de extracción, determinada con la balanza de suspensión magnética

Se ha desarrollado un modelo de 5 parámetros que describe el transporte, dos parámetros fijos y 3 calculados que describen como afectan las 3 etapas del proceso: la difusión en el sistema o/w emulsion - $scCO_2$, la disolución del $CO_2$ y del disolvente orgánico en la fase acuosa, y la extracción del orgánico mediante el $CO_2$ a través de la capa limite en la interfase con el agua.

Los resultados muestran que la emulsión DCM/w no es adecuada para el proceso de SFEE. Debido a la alta tensión interfacial entre la fase orgánica y acuosa, la separación de las fases tiene lugar inmediatamente después de la presurización. En el caso del sistema EtAc/w - $scCO_2$, solo la densidad del $scCO_2$ afecta significativamente la transferencia de materia de los compuestos que intervienen. De acuerdo con el estudio dinámico, una elevada proporción de orgánico se extrae con la presurización del sistema por el $CO_2$. Este efecto puede justificarse por el efecto Marangoni, que se da en el sistema $CO_2$ - $H_2O$ debido a la elevada diferencia de densidades ([16] [17]), o debido al efecto de la mezcla en el sistema durante el proceso de presurización y el cambio de fase del $CO_2$.

**CAPÍTULO III**

Partiendo de los resultados del capítulo I, donde se presenta el estudio de la precipitación de la quercitina con tamaño nanométrico y su encapsulación en lecitina de soja; en el capítulo **III** se estudia la mejora de la eficacia de la encapsulación mediante la combinación de dos surfactantes, lecitina de soja y Pluronic L64®, sin que se produzcan cambios en las propiedades de la quercitina formulada obtenida. Se realiza un estudio experimental operando en batch estudiando el efecto de las variables de operación, concentraciones de quercitina y surfactantes, relación entre la concentración de Pluronic L64® y lecitina sobre la eficacia de la encapsulación y sobre la distribución de tamaño de las partículas obtenida en la suspensión acuosa. Al comparar con los resultados obtenidos en el capítulo I, se observa un aumento significativo sobre la eficacia de la encapsulación, pasando del 58.8% al 83.7%.

Se estudia el paso del proceso desde operación en batch a semicontinuo, en un equipo de SFEE que permite bombear un flujo continuo de $scCO_2$ sobre la emulsión, cuyo esquema se presenta en la **Figura 7**. Con la operación en semicontinuo se llega a reducir significativamente el tiempo y producir mayor cantidad de suspensión acuosa de quercitina formulada. Se demuestra así que la SFEE es una tecnología robusta y escalable para obtener los formulados de quercitina. Este proceso ha permitido producir suficiente cantidad de suspensión de quercitina para obtener el formulado sólido, secando la suspensión mediante un proceso de PGSS-drying.

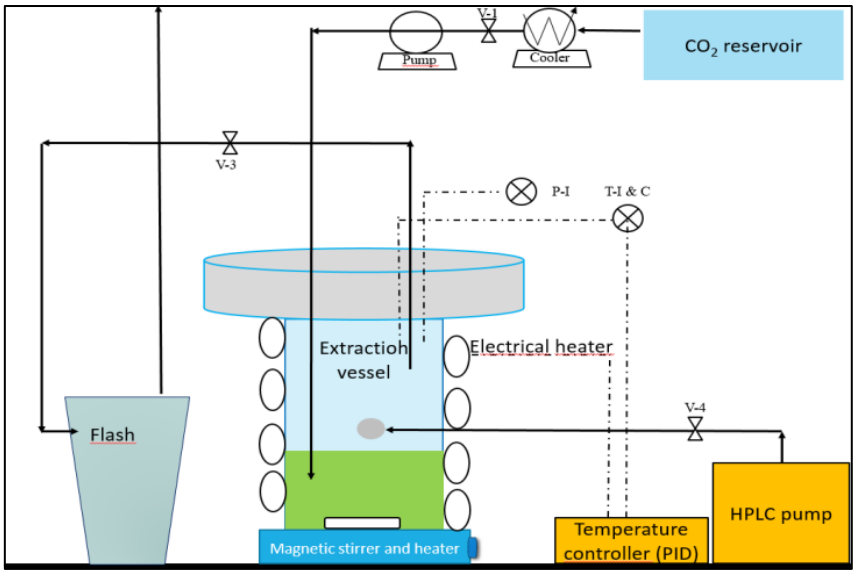


**Figura 7:** Proceso semicontinuo de SFEE

La tecnología de obtención de partículas a partir del secado de disoluciones saturadas de gas (PGSS)-drying, se presenta en la **Figura 8**. Se ha realizado un estudio experimental para determinar el efecto de las variables de operación, como son la relación entre los flujos de suspensión acuosa y $CO_2$ (GLR), temperatura y presión de pre-expansión, y minimizar la degradación de la quercitina obtenida y el minimizar el contenido de humedad del formulado solido obtenido.

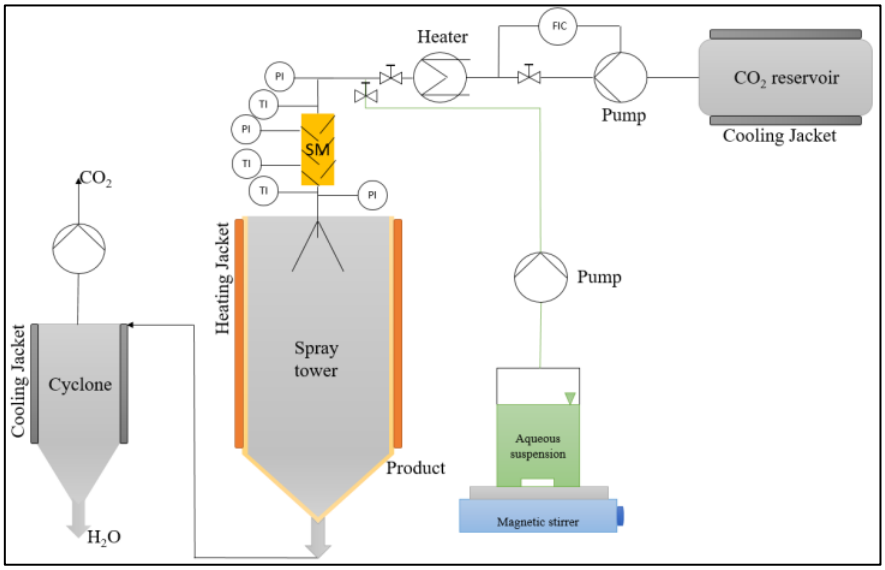


**Figura 8:** Equipo de PGSS-drying

La figura **Figura 9** presenta los resultados obtenidos operando con mayor y menor GLR que la óptima (30 – 35 kg/L). Se observa que se puede producir un formulado en polvo con una humedad inferior al 10% w/w%.

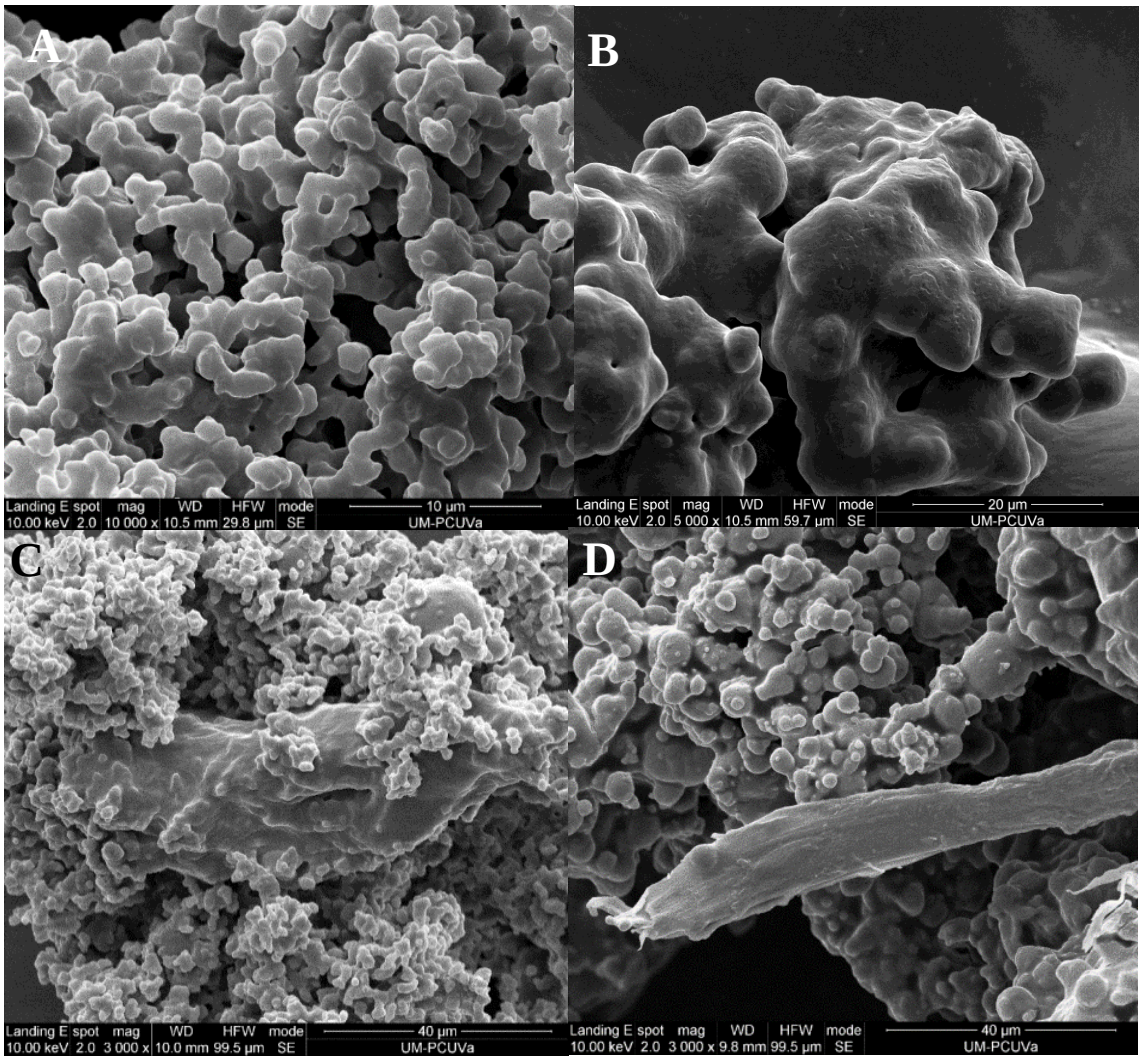


**Figura 9:** Scanning electron microscopy picture about PGSS-drying experimental runs applying different GLR-s [kg/L]:31.2 (A); 57.2 (B); 25 (C); 58.9 (D)

El proceso de secado mediante PGSS-drying se compara secando las mismas muestras de las suspensiones obtenidas mediante liofilización. Se determina la actividad antioxidante y la eficacia de encapsulación, resultando que las muestras secadas mediante PGSS-drying presentan un poder antioxidante máxima 41268 µMTE / g quercitina y que la eficacia máxima de encapsulación es 86.4%,

**CAPÍTULO IV**

En el capítulo **IV** se estudia el escalado del proceso para obtener las condiciones de operación de un proceso escalada (**Figura 10**). Los experimentos se han realizados en el equipo presentada en **Figura 7**. Se ha determinado la concentración de quercitina en la emulsión, relación entre los flujos de $CO_2$/emulsión, densidad del sc$CO_2$ (presión y temperatura para operar a una determinada densidad), y tiempo de operación del proceso de SFEE. Con estos parámetros se realiza una evaluación de los costes de operación de este proceso, y se determinan las condiciones de operación que marcan un óptimo económico para obtener el producto con las mejores propiedades.

El producto producido se compara con el obtenido mediante la tecnología de fluidos supercríticos desarrollado en esta tesis. Los resultados muestran que la operación más cara del proceso es el enfriamiento y bombeo del $CO_2$ supercrítico. El proceso necesita 5.5 kg $CO_2$ supercrítico / L emulsión para obtener quercetina encapsulada tanto como 28 toneladas / año en tamaño nanómetrico (D(0.1=98nm), con residuo orgánico tan bajo, como 332 ppm. El extractor es el equipo más caro, pero la eficiencia mejora significativamente empleando dos extractores usados paralelamente, de forma que mientras uno está en uso en el proceso de extracción, el otro estaría en parada para su limpieza. En el proceso, el 95% de $CO_2$ fue recirculado.

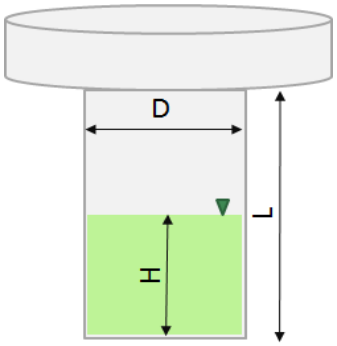


| Dimensiones | Batch | emicontinuo |
|---|---|---|
| **H [mm]** | 29 | 56 |
| **L [mm]** | 100 | 121 |
| **D [mm]** | 35 | 67 |

**Figura 10:** Diferencia de los tamaños entre de los extractores aplicados en proceso batch y en el escalado en semicontinuo

## 4. CONCLUSIONES Y TRABAJO FUTURO

En esta tesis se ha estudiado el desarrollo de productos con base de quercitina para mejorar su solubilidad en agua y su biodisponibilidad utilizando tecnologías con fluidos supercríticos. El estudio realizado permite aportar las siguientes conclusiones:

1 La extracción supercrítica de emulsiones se ha utilizado para obtener suspensiones acuosas de quercitina de tamaño nanometrico. El $CO_2$ se transfiere a la gota de la emulsión disolviéndose en el disolvente orgánico, a la vez que este se transfiere a la fase acuosa. El $CO_2$ disuelto en el interior de la gota hace de antidisolvente, consiguiendo la rápida precipitación de la quercitina dentro de la gota, lo que controla su tamaño. Emulsiones de quercitina disuelta en acetato de etilo utilizando lecitina de soja como surfactante, han permitido obtener suspensiones acuosas de quercitina encapsulada en liposomas multivesiculares, con una eficacia del 58%. La combinación de la lecitina con Pluronic L64®, se ha permitido aumentar la eficacia de la encapsulación hasta el 83.7%, (0.19 mg quercetina / L of suspensión). La capacidad antioxidante de la quercitina encapsulada aumenta, debido al efecto sinérgico de la lecitina sobre la actividad antioxidante de la quercetina.

2 El modelado de la trasferencia de materia pone de manifiesto que las etapas claves del proceso son la disolución del $CO_2$ y del disolvente orgánico en la fase acuosa, y la extracción del disolvente orgánico por el $CO_2$. Las medidas realizadas al estudiar la transferencia de materia cuando se hace circular el $CO_2$ sobre la emulsión, indica que la mayor parte del disolvente se extrae durante la presurización de la emulsión por el $CO_2$, debido a que se mejora la mezcla y al efecto Marangoni, que se da entre el $CO_2$ y $H_2O$ debida a la diferencia entre sus densidades. El principal parámetro que influye sobre la transferencia de materia, es la densidad del $CO_2$.

3 A partir de los resultados del modelado, se ha llevado el proceso desde operación en batch a semicontinuo, lo que ha permitido reducir el tiempo de operación y obtener una abundante suspensión acuosa. El factor considerado para el cambio de escala ha sido la relación entre la altura y el diámetro en el extractor. El volumen de la emulsión tratada ha aumentado desde 25 a 168 mL-ros, mientras que el tiempo se ha reducido desde 575 hasta 89.5 minutos, consiguiendo mantener la misma eficacia de encapsulación, actividad antioxidante y características morfológicas de la suspensión obtenida en la operación en semicontinuo, que la obtenida en la operación en batch.

3 Teniendo en cuenta los resultados sobre la influencia de los parámetros en el proceso en semicontinuo, y su previsible influencia en los costes, puede establecerse las variables de operación, temperatura y presión deben de ser ligeramente superiores a las críticas del $CO_2$, y se requieren 5 kg de $CO_2$ por L de emulsión.

4 La obtención de formulados solidos de quercitina se ha realizado mediante secado de la suspensión obtenida por PGSS-drying, secado mediante disoluciones saturadas de gas. Los resultados indican que el parámetro que controla el proceso es la relación entre los flujos de suspensión acuosa y $CO_2$ (GLR), que debe de estar entre 31-35 kg/L, para que la humedad residual sea inferior al 10 w/w%, la degradación de la quercitina menor del 10%, y se obtenga la menor pérdida de actividad antioxidante.

5 La utilización de tecnologías supercríticas para micronizar y encapsular quercitina, permite poder operar con concentraciones de quercitina de 4.6 mg/L, mientras que con el producto obtenido por liofilización, no se han conseguido concentraciones superiores a 0.7 mg/L.

Estos resultados ponen de manifiesto las ventajas de utilizar la SFEE y el PGSS-drying en la micronización y encapsulación de partículas de bioproductos, tecnologías que operan a temperaturas y presiones moderadas sin que se degrade o se produzca una pérdida significativa de actividad antioxidante.

La SFEE seguida del secado por PGSS-Drying permite obtener formulados de quercitina con mejor solubilidad en agua, mayor actividad antioxidante y mayor permeabilidad, como se presenta en esta tesis mediante los análisis HPLC, ORAC y test in-vitro en celda de Franz, respectactivamente. Las formulaciones obtenidas necesitan análisis in-vitro con líneas celulares específicas para demostrar la mejora en la biodisponibilidad que se espera conseguir con estos formulados. Como trabajo de futuro se propone aumentar la concentración de quercitina en la emulsión o/w, o utilizando otros agentes encapsulantes o mediante otros métodos de emulsificación como la técnica de emulsiones presurizadas. Estos nuevos formulados se utilizaran en la SFEE para aumentar la concentración de quercitina en el producto final.

## 5. REFERENCIAS

[1] A. Parmar, K. Singh, A. Bahadur, G. Marangoni, P. Bahadur, Interaction and solubilization of some phenolic antioxidants in Pluronic?? micelles, Colloids Surfaces B Biointerfaces. 86 (2011) 319–326. doi:10.1016/j.colsurfb.2011.04.015.

[2] Khaled A. Khaled, Yousry M. El-Sayeda, Badr M. Al-Hadiyab, Disposition of the Flavonoid Quercetin in Rats After Single Intravenous and Oral Doses, Drug Dev. Ind. Pharm. 29 (2003) 397–403. doi:10.1081/DDC-120018375.

[3] R. Gugler, M. Leschik, H.J. Dengler, Disposition of quercetin in man after single oral and intravenous doses, Eur. J. Clin. Pharmacol. 9 (1975) 229–234. doi:10.1007/BF00614022.

[4] S. Chakraborty, S. Stalin, N. Das, S. Thakur Choudhury, S. Ghosh, S. Swarnakar, The use of nano-quercetin to arrest mitochondrial damage and MMP-9 upregulation during prevention of gastric inflammation induced by ethanol in rat, Biomaterials. 33 (2012) 2991–3001. doi:10.1016/j.biomaterials.2011.12.037.

[5] T.-H. Wu, F.-L. Yen, L.-T. Lin, T.-R. Tsai, C.-C. Lin, T.-M. Cham, Preparation, physicochemical characterization, and antioxidant effects of quercetin nanoparticles., Int. J. Pharm. 346 (2008) 160–8. doi:10.1016/j.ijpharm.2007.06.036.

[6] P.J. Mulholland, D.R. Ferry, D. Anderson, S.A. Hussain, A.M. Young, J.E. Cook, E. Hodgkin, L.W. Seymour, D.J. Kerr, Pre-clinical and clinical study of QC12, a water-soluble, pro-drug of quercetin., Ann. Oncol. 12 (2001) 245–248.

[7] T. Pralhad, K. Rajendrakumar, Study of freeze-dried quercetin-cyclodextrin binary systems by DSC, FT-IR, X-ray diffraction and SEM analysis, J. Pharm. Biomed. Anal. 34 (2004) 333–339. doi:10.1016/S0731-7085(03)00529-6.

[8] Z.P. Yuan, L.J. Chen, L.Y. Fan, M.H. Tang, G.L. Yang, H.S. Yang, X.B. Du, G.Q. Wang, W.X. Yao, Q.M. Zhao, B. Ye, R. Wang, P. Diao, W. Zhang, H. Bin Wu, X. Zhao, Y.Q. Wei, Liposomal quercetin efficiently suppresses growth of solid tumors in murine models, Clin. Cancer Res. 12 (2006) 3193–3199. doi:10.1158/1078-0432.CCR-05-2365.

[9] H. Li, X. Zhao, Y. Ma, G. Zhai, L. Li, H. Lou, Enhancement of gastrointestinal absorption of quercetin by solid lipid nanoparticles, J. Control. Release. 133 (2009) 238–244. doi:10.1016/j.jconrel.2008.10.002.

[10] A. Chafer, T. Fornari, A. Berna, R.P. Stateva, Solubility of quercetin in supercritical CO2 + ethanol as a modifier: Measurements and thermodynamic modelling, J. Supercrit. Fluids. 32 (2004) 89–96. doi:10.1016/j.supflu.2004.02.005.

[11] X. Liu, Z. Li, B. Han, T. Yuan, Supercritical Antisolvent Precipitation of Microparticles of Quercetin, Chinese J. Chem. Eng. 13 (2005) 128–130. http://www.cjche.com.cn/EN/abstract/abstract474.shtml#.

[12] D.T. Santos, M.A.A. Meireles, Micronization and encapsulation of functional pigments using supercritical carbon dioxide, J. Food Process Eng. 36 (2013) 36–49. doi:10.1111/j.1745-4530.2011.00651.x.

[13] P. Alessi, A. Cortesi, N. De Zordi, T. Gamse, I. Kikic, M. Moneghini, D. Solinas, Supercritical Antisolvent Precipitation of Quercetin Systems: Preliminary Experiments, Chem. Biochem. Eng. Q. 26 (2012) 391–398. <Go to ISI>://WOS:000314256800010.

[14] M. Fraile, R. Buratto, B. Gómez, Á. Martín, M.J. Cocero, Enhanced delivery of quercetin by encapsulation in poloxamers by supercritical antisolvent process, Ind. Eng. Chem. Res. 53 (2014) 4318–4327. doi:10.1021/ie5001136.

[15] F. Mattea, Á. Martín, C. Schulz, P. Jaeger, R. Eggers, M.J. Cocero, Behavior of an Organic Solvent Drop During the Supercritical Extraction of Emulsions, AIChE J. 56 (2010) 1184–1195. doi:0.1002/aic.12061.

[16] C. Yang, Y. Gu, Accelerated mass transfer of CO2 in reservoir brine due to density-driven natural convection at high pressures and elevated temperatures, Ind. Eng. Chem. Res. 45 (2006) 2430–2436. doi:10.1021/ie050497r.

[17] B. Arendt, D. Dittmar, R. Eggers, Interaction of interfacial convection and mass transfer effects in the system CO2-water, Int. J. Heat Mass Transf. 47 (2004) 3649–3657. doi:10.1016/j.ijheatmasstransfer.2004.04.011.

## ACKNOWLEDGEMENT

This thesis and all research work included has been funded by the European Initial Training Network FP7-PEOPLE 2012 ITN 316959, “DoHip”, and by Junta de Castilla y León with project VA225U14.

I would like to give my acknowledgement to Prof María José Cocero, Prof. Ángel Martín, Soraya Rodríguez-Rojo PhD. for giving me the opportunity to be a member of the High Pressure Research Group in University of Valladolid, and providing me appropriate guidance in the professional work. Also thank for Ester de Paz Barragán for the temporary supervision.

I am gratefully acknowledged for Prof. Edit Székely and Prof Béla Simándi, whose realized my abilities in academic career, and guided me to obtain a Marie Curie PhD position.

I would thank the possibility of Prof. Dr.-Ing. Tobias Fieback, for the possibility of a three-month stay at University of Bochum, Germany, and establish a great part of this thesis using MSB-s. Moreover, I’m very grateful to Jens Rother PhD for support on the use of the MSB device used in static measurements, and Gerrit Dresp for the design and supporting me using MSB device in dynamic measurements.

Many thanks for Dr. Catarina M.M. Duarte and Dr. Ana Matias (Instituto de Biologia Experimental e Tecnológia (IBET), Portugal) for the opportunity to collaborate in their research group as well as their valuable guidance, help and advices during my stay.

Without the support of my family and Hungarian friend thesis would not be established.

Finally, I would like to thank all of my friends in Valladolid and in Lisbon, respectively (in alphabetical order): **Alberto Romero**, Álvaro Cabeza Sánchez, **Ana Álvarez**, Ana Inés Paninho, Andrea Natolino, **Celia Martínez**, Gerardo Tita, **Gianluca Gallina**, Joana Lopes, **Luis Miguel Sanz**, **María Pinilla**, **Marta Salgado**, Miriam Rueda, **Nerea Abad Fernández**, **Nuria Sánchez**, Reinaldo Vallejo, Ricardo Ferraz de Oliveira, **Rut Romero Díez**, **Sergio Muñoz Palacios**, **Vanessa Gonçalves**, Victoria Pazo, **Yoana García**, Ana Nunes Nunes, Daniel Deodato Lopes, Joana Poejo.

## ABOUT THE AUTHOR

György Lévai was born at 31 of March, 1988 in Békéscsaba, Hungary. He finished his university education at 2013 at the Budapest University of Technology and Economics (BUTE), Faculty of Chemical Technology and Biotechnology, as a Chemical Engineer MSc, with a diploma qualification Suma Cum Laude. During his studies he joined to the Supercritical Fluid Extraction Group, headed by Edit Székely PhD. Under the supervision of Edit Székely PhD., György Lévai obtained a second prize on the Scientific Students' Conference, organized by the Faculty of Chemical Technology and Biotechnology, BUTE. During his master studies he spent a semester at Aalto University, School of Chemical Technology, Finland, in founded by the Erasmus Exchange Program. Moreover, he obtained the Presidential Scholarship, Ministry of Human Resources, Hungary.

After obtained his Master Diploma, he obtained a Marie Curie PhD scholarship at University of Valladolid, Spain. In the frame of the DoHip program, supported by the People Programme (Marie Curie Actions), he finished his PhD work in the scheduled timescale (three years), in the topic of Development of novel nanocarriers for drug delivery, supervised by Prof. María José Cocero, Prof. Ángel Martín and Soraya Rodríguez-Rojo PhD. During his PhD program, he fulfilled internships and secondments at Ruhr University of Bochum, Germany, and at Instituto de Biologia Experimental e Tecnológia, Portugal.

## LIST OF SCIENTIFIC RESULTS

**Articles:**

G. Lévai, A. Moro, Á. Martín, S. Rodríguez, M. Cocero, production of encapsulated quercetin particles using supercritical fluid technologies, Submitted to Journal on the Science and Technology of Wet and Dry Particulate Systems

G. Lévai, Á. Martín, S. Rodríguez, M. Cocero, T.M. Fieback, Measurement and modelling of mass transport properties in supercritical carbon-dioxide – (EtAc/DCM based) oil in water emulsion systems, Submitted to J. of Supercritical Fluids

G. Lévai, Á. Martín, E. de Paz, S. Rodríguez, M. Cocero Production of stabilized quercetin aqueous suspensions by supercritical fluid extraction of emulsions, J. of Supercritical Fluids 100 p.: 34–45, 2015, doi:10.1016/j.supflu.2015.02.19

**Oral communications:**

G. Lévai, S. Rodríguez, Martín, M. Cocéro, Efficient production of soy-bean lecithin – Pluronic L64® encapsulated quercetin particles in nanometric scale using SFEE and PGSS drying processes, GPE 2016, Mont Tremblant, Quebec, Canada, 19-24.06.2016

G. Lévai, Á. Martín, S. R. Rojo, M. J. Cocero, T. M. Fieback, J. Rother, G. Dresp, Experimental Determination of Mass Transport In Supercritical Fluid Extraction of Emulsions Technology, EMSF 2016, Essen, Germany, 8.05.2016 – 11.05.2016

G. Lévai, S. Rodríguez, Á. Martín, M. Cocéro, Increasing bioavailability of quercetin by producing encapsulated nanonparticles using SFEE- and PGSS drying process, ECCE10+ECAB3+EPIC5, Nice, France, 27.09.2015 – 01.10.2015

G. Lévai, S. Rodríguez, Á. Martín, M. Cocéro, Production of encapsulated quercetin nanoparticles by SFEE, Hungarian National Conference on Supercritical Fluids, 21.05.2015. Budapest, Hungary

G. Lévai, S. Rodríguez, Á. Martín, M. Cocéro, Quercetin loaded nanopartciles created by supercritical fluid extraction of emulsions, 14th European Meeting on Supercritical Fluids, Marseille, France, 18-21. May 2014